Lectures in Theoretical Biophysics

K. Schulten and I. Kosztin

Department of Physics and Beckman Institute
University of Illinois at Urbana–Champaign
405 N. Mathews Street, Urbana, IL 61801 USA

(April 23, 2000)

VISIT…

Contents

1 Introduction **1**

2 Dynamics under the Influence of Stochastic Forces **3**
2.1 Newton's Equation and Langevin's Equation 3
2.2 Stochastic Differential Equations 4
2.3 How to Describe Noise 5
2.4 Ito calculus 21
2.5 Fokker-Planck Equations 29
2.6 Stratonovich Calculus 31
2.7 Appendix: Normal Distribution Approximation 34
2.7.1 Stirling's Formula 34
2.7.2 Binomial Distribution 34

3 Einstein Diffusion Equation **37**
3.1 Derivation and Boundary Conditions 37
3.2 Free Diffusion in One-dimensional Half-Space 40
3.3 Fluorescence Microphotolysis 44
3.4 Free Diffusion around a Spherical Object 48
3.5 Free Diffusion in a Finite Domain 57
3.6 Rotational Diffusion 60

4 Smoluchowski Diffusion Equation **63**
4.1 Derivation of the Smoluchoswki Diffusion Equation for Potential Fields 64
4.2 One-Dimensional Diffuson in a Linear Potential 67
4.2.1 Diffusion in an infinite space $\Omega_\infty =]-\infty, \infty[$ 67
4.2.2 Diffusion in a Half-Space $\Omega_\infty = [0, \infty[$ 70
4.3 Diffusion in a One-Dimensional Harmonic Potential 74

5 Random Numbers **79**
5.1 Randomness 80
5.2 Random Number Generators 83
5.2.1 Homogeneous Distribution 83
5.2.2 Gaussian Distribution 86
5.3 Monte Carlo integration 88

6 Brownian Dynamics **91**
6.1 Discretization of Time . . . 91
6.2 Monte Carlo Integration of Stochastic Processes . . . 93
6.3 Ito Calculus and Brownian Dynamics . . . 95
6.4 Free Diffusion . . . 96
6.5 Reflective Boundary Conditions . . . 100

7 The Brownian Dynamics Method Applied **103**
7.1 Diffusion in a Linear Potential . . . 103
7.2 Diffusion in a Harmonic Potential . . . 104
7.3 Harmonic Potential with a Reactive Center . . . 107
7.4 Free Diffusion in a Finite Domain . . . 107
7.5 Hysteresis in a Harmonic Potential . . . 108
7.6 Hysteresis in a Bistable Potential . . . 112

8 Noise-Induced Limit Cycles **119**
8.1 The Bonhoeffer–van der Pol Equations . . . 119
8.2 Analysis . . . 121
8.2.1 Derivation of Canonical Model . . . 121
8.2.2 Linear Analysis of Canonical Model . . . 122
8.2.3 Hopf Bifurcation Analysis . . . 124
8.2.4 Systems of Coupled Bonhoeffer–van der Pol Neurons . . . 126
8.3 Alternative Neuron Models . . . 128
8.3.1 Standard Oscillators . . . 128
8.3.2 Active Rotators . . . 129
8.3.3 Integrate-and-Fire Neurons . . . 129
8.3.4 Conclusions . . . 130

9 Adjoint Smoluchowski Equation **131**
9.1 The Adjoint Smoluchowski Equation . . . 131
9.2 Correlation Functions . . . 135

10 Rates of Diffusion-Controlled Reactions **137**
10.1 Relative Diffusion of two Free Particles . . . 137
10.2 Diffusion-Controlled Reactions under Stationary Conditions . . . 139
10.2.1 Examples . . . 141

11 Ohmic Resistance and Irreversible Work **143**

12 Smoluchowski Equation for Potentials: Extremum Principle and Spectral Expansion **145**
12.1 Minimum Principle for the Smoluchowski Equation . . . 146
12.2 Similarity to Self-Adjoint Operator . . . 149
12.3 Eigenfunctions and Eigenvalues of the Smoluchowski Operator . . . 151
12.4 Brownian Oscillator . . . 155

13 The Brownian Oscillator **161**
13.1 One-Dimensional Diffusion in a Harmonic Potential . . . 162

14 Fokker-Planck Equation in x and v for Harmonic Oscillator **167**

15 Velocity Replacement Echoes **169**

16 Rate Equations for Discrete Processes **171**

17 Generalized Moment Expansion **173**

18 Curve Crossing in a Protein: Coupling of the Elementary Quantum Process to Motions of the Protein **175**
18.1 Introduction 175
18.2 The Generic Model: Two-State Quantum System Coupled to an Oscillator 177
18.3 Two-State System Coupled to a Classical Medium 179
18.4 Two State System Coupled to a Stochastic Medium 182
18.5 Two State System Coupled to a Single Quantum Mechanical Oscillator 184
18.6 Two State System Coupled to a Multi-Modal Bath of Quantum Mechanical Oscillators 189
18.7 From the Energy Gap Correlation Function $\Delta E[\mathbf{R}(t)]$ to the Spectral Density $J(\omega)$. 192
18.8 Evaluating the Transfer Rate 196
18.9 Appendix: Numerical Evaluation of the Line Shape Function 200

Bibliography **203**

Chapter 1

Introduction

Chapter 2

Dynamics under the Influence of Stochastic Forces

Contents

2.1 Newton's Equation and Langevin's Equation 3
2.2 Stochastic Differential Equations 4
2.3 How to Describe Noise 5
2.4 Ito calculus 21
2.5 Fokker-Planck Equations 29
2.6 Stratonovich Calculus 31
2.7 Appendix: Normal Distribution Approximation 34
2.7.1 Stirling's Formula 34
2.7.2 Binomial Distribution 34

2.1 Newton's Equation and Langevin's Equation

In this section we assume that the constituents of matter can be described classically. We are interested in reaction processes occuring in the bulk, either in physiological liquids, membranes or proteins. The atomic motion of these materials is described by the Newtonian equation of motion

$$m_i \frac{d^2}{dt^2} r_i = -\frac{\partial}{\partial r_i} V(r_1, \ldots, r_N) \tag{2.1}$$

where $r_i \quad (i = 1, 2, \ldots, N)$ describes the position of the i-th atom. The number N of atoms is, of course, so large that solutions of Eq. (2.1) for macroscopic systems are impossible. In microscopic systems like proteins the number of atoms ranges between 10^3 to 10^5, i.e., even in this case the solution is extremely time consuming.
However, most often only a few of the degrees of freedom are involved in a particular biochemical reaction and warrant an explicit theoretical description or observation. For example, in the case of transport one is solely interested in the position of the center of mass of a molecule. It is well known that molecular transport in condensed media can be described by phenomenological equations much simpler than Eq. (2.1), e.g., by the Einstein diffusion equation. The same holds true for reaction

processes in condensed media. In this case one likes to focus onto the reaction coordinate, e.g., on a torsional angle.
In fact, there exist successful descriptions of a small subset of degrees of freedom by means of Newtonian equations of motion with effective force fields and added frictional as well as (time dependent) fluctuating forces. Let us assume we like to consider motion along a small subset of the whole coordinate space defined by the coordinates $q_1, \ldots, q_M$ for $M \ll N$. The equations which model the dynamics in this subspace are then ($j = 1, 2, \ldots, M$)

$$\mu_j \frac{d^2}{dt^2} q_j \;=\; -\frac{\partial}{\partial q_j} W(q_1, \ldots, q_M) \;-\; \gamma_j \frac{d}{dt} q_j \;+\; \sigma_j \xi_j(t). \tag{2.2}$$

The first term on the r.h.s. of this equation describes the force field derived from an effective potential $W(q_1, \ldots, q_M)$, the second term describes the velocity ($\frac{d}{dt} q_j$) dependent frictional forces, and the third term the fluctuating forces $\xi_j(t)$ with coupling constants σ_j. $W(q_1, \ldots, q_M)$ includes the effect of the thermal motion of the remaining $n - M$ degrees of freedom on the motion along the coordinates $q_1, \ldots, q_M$.
Equations of type (2.2) will be studied in detail further below. We will not "derive" these equations from the Newtonian equations (2.1) of the bulk material, but rather show by comparision of the predictions of Eq. (2.1) and Eq. (2.2) to what extent the suggested phenomenological descriptions apply. To do so and also to study further the consequences of Eq. (2.2) we need to investigate systematically the solutions of stochastic differential equations.

2.2 Stochastic Differential Equations

We consider stochastic differential equations in the form of a first order differential equation

$$\partial_t \boldsymbol{x}(t) \;=\; \boldsymbol{A}[\boldsymbol{x}(t), t] \;+\; \mathbf{B}[\boldsymbol{x}(\mathbf{t}), \mathbf{t}] \cdot \boldsymbol{\eta}(\mathbf{t}) \tag{2.3}$$

subject to the initial condition

$$\boldsymbol{x}(0) \;=\; \boldsymbol{x}_0. \tag{2.4}$$

In this equation $\boldsymbol{A}[\boldsymbol{x}(t), t]$ represents the so-called drift term and $\mathbf{B}[\boldsymbol{x}(\mathbf{t}), \mathbf{t}] \cdot \boldsymbol{\eta}(\mathbf{t})$ the noise term which will be properly characterized further below. Without the noise term, the resulting equation

$$\partial_t \boldsymbol{x}(t) \;=\; \boldsymbol{A}[\boldsymbol{x}(t), t]. \tag{2.5}$$

describes a deterministic drift of particles along the field $\boldsymbol{A}[\boldsymbol{x}(t), t]$.
Equations like (2.5) can actually describe a wide variety of phenomena, like chemical kinetics or the firing of neurons. Since such systems are often subject to random perturbations, noise is added to the deterministic equations to yield associated stochastic differential equations. In such cases as well as in the case of classical Brownian particles, the noise term $\mathbf{B}[\boldsymbol{x}(\mathbf{t}), \mathbf{t}] \cdot \boldsymbol{\eta}(\mathbf{t})$ needs to be specified on the basis of the underlying origins of noise. We will introduce further below several mathematical models of noise and will consider the issue of constructing suitable noise terms throughout this book. For this purpose, one often adopts a heuristic approach, analysing the noise from observation or from a numerical simulation and selecting a noise model with matching characteristics. These characteristics are introduced below.
Before we consider characteristics of the noise term $\boldsymbol{\eta}(t)$ in (2.3) we like to demonstrate that the one-dimensional Langevin equation (2.2) of a classical particle, written here in the form

$$\mu \ddot{q} \;=\; f(q) \;-\; \gamma \dot{q} \;+\; \sigma \xi(t) \tag{2.6}$$

is a special case of (2.3). In fact, defining $\boldsymbol{x} \in \mathbb{R}^2$ with components $x_1 = m$, and $\dot{q}$, $x_2 = m\,q$ reproduces Eq. (2.3) if one defines

$$\boldsymbol{A}[\boldsymbol{x}(t),t] \;=\; \begin{pmatrix} f(x_2/m) - \gamma\, x_1/m \\ x_1 \end{pmatrix}, \quad \mathbf{B}[\boldsymbol{x}(\mathbf{t}),\mathbf{t}] \;=\; \begin{pmatrix} \sigma & 0 \\ 0 & 0 \end{pmatrix}, \text{ and } \quad \boldsymbol{\eta}(\mathbf{t}) \;=\; \begin{pmatrix} \xi(t) \\ 0 \end{pmatrix}. \tag{2.7}$$

The noise term represents a stochastic process. We consider only the factor $\boldsymbol{\eta}(t)$ which describes the essential time dependence of the noise source in the different degrees of freedom. The matrix $\mathbf{B}[\boldsymbol{x}(\mathbf{t}),\mathbf{t}]$ describes the amplitude and the correlation of noise between the different degrees of freedom.

2.3 How to Describe Noise

We are now embarking on an essential aspect of our description, namely, how stochastic aspects of noise $\boldsymbol{\eta}(t)$ are properly accounted for. Obviously, a particular realization of the time-dependent process $\boldsymbol{\eta}(t)$ does not provide much information. Rather, one needs to consider the *probability* of observing a certain sequence of noise values $\boldsymbol{\eta}_1, \boldsymbol{\eta}_2, \ldots$ at times $t_1, t_2, \ldots$. The essential information is entailed in the *conditional probabilities*

$$p(\boldsymbol{\eta}_1, t_1; \boldsymbol{\eta}_2, t_2; \ldots | \boldsymbol{\eta}_0, t_0; \boldsymbol{\eta}_{-1}, t_{-1}; \ldots) \tag{2.8}$$

when the process is assumed to generate noise at fixed times t_i, $\quad t_i < t_j$ for $i < j$. Here $p(\ |\ )$ is the probability that the random variable $\boldsymbol{\eta}(t)$ assumes the values $\boldsymbol{\eta}_1, \boldsymbol{\eta}_2, \ldots$ at times $t_1, t_2, \ldots$, *if* it had previously assumed the values $\boldsymbol{\eta}_0, \boldsymbol{\eta}_{-1}, \ldots$ at times $t_0, t_{-1}, \ldots$.
An important class of random processes are so-called *Markov processes* for which the conditional probabilities depend only on $\boldsymbol{\eta}_0$ and t_0 and not on earlier occurrences of noise values. In this case holds

$$p(\boldsymbol{\eta}_1, t_1; \boldsymbol{\eta}_2, t_2; \ldots | \boldsymbol{\eta}_0, t_0; \boldsymbol{\eta}_{-1}, t_{-1}; \ldots) \;=\; p(\boldsymbol{\eta}_1, t_1; \boldsymbol{\eta}_2, t_2; \ldots | \boldsymbol{\eta}_0, t_0)\,. \tag{2.9}$$

This property allows one to factorize $p(\ |\ )$ into a sequence of consecutive conditional probabilities.

$$\begin{aligned} p(\boldsymbol{\eta}_1, t_1; \boldsymbol{\eta}_2, t_2; \ldots | \boldsymbol{\eta}_0, t_0) \;&=\; p(\boldsymbol{\eta}_2, t_2; \boldsymbol{\eta}_3, t_3; \ldots | \boldsymbol{\eta}_1, t_1)\; p(\boldsymbol{\eta}_1, t_1 | \boldsymbol{\eta}_0, t_0) \\ &=\; p(\boldsymbol{\eta}_3, t_3; \boldsymbol{\eta}_4, t_4; \ldots | \boldsymbol{\eta}_2, t_2)\; p(\boldsymbol{\eta}_2, t_2 | \boldsymbol{\eta}_1, t_1)\; p(\boldsymbol{\eta}_1, t_1 | \boldsymbol{\eta}_0, t_0) \\ &\;\;\vdots \end{aligned} \tag{2.10}$$

The unconditional probability for the realization of $\boldsymbol{\eta}_1, \boldsymbol{\eta}_2, \ldots$ at times $t_1, t_2, \ldots$ is

$$p(\boldsymbol{\eta}_1, t_1; \boldsymbol{\eta}_2, t_2; \ldots) \;=\; \sum_{\boldsymbol{\eta}_0} p(\boldsymbol{\eta}_0, t_0) \quad p(\boldsymbol{\eta}_1, t_1 | \boldsymbol{\eta}_0, t_0) \quad p(\boldsymbol{\eta}_2, t_2 | \boldsymbol{\eta}_1, t_1) \;\cdots \tag{2.11}$$

where $p(\boldsymbol{\eta}_0, t_0)$ is the unconditional probability for the appearence of $\boldsymbol{\eta}_0$ at time t_0. One can conclude from Eq. (2.11) that a knowledge of $p(\boldsymbol{\eta}_0, t_0)$ and $p(\boldsymbol{\eta}_i, t_i | \boldsymbol{\eta}_{i-1}, t_{i-1})$ is sufficient for a complete characterization of a Markov process.
Before we proceed with three important examples of Markov processes we will take a short detour and give a quick introduction on mathematical tools that will be useful in handling probability distributions like $p(\boldsymbol{\eta}_0, t_0)$ and $p(\boldsymbol{\eta}_i, t_i | \boldsymbol{\eta}_{i-1}, t_{i-1})$.

Characteristics of Probability Distributions

In case of a one-dimensional random process $\boldsymbol{\eta}$, denoted by $\eta(t)$, $p(\eta,t)\,d\eta$ gives the probability that $\eta(t)$ assumes a value in the interval $[\eta, \eta + d\eta]$ at time t.
Let $f[\eta(t)]$ denote some function of $\eta(t)$. $f[\eta(t)]$ could represent some observable of interest, e.g., $f[\eta(t)] = \eta^2(t)$. The average value measured for this observable at time t is then

$$\left\langle f[\eta(t)] \right\rangle \;=\; \int_\Omega d\eta\; f[\eta]\; p(\eta,t)\;. \tag{2.12}$$

Here Ω denotes the interval in which random values of $\eta(t)$ arise. The notation $\langle\cdots\rangle$ on the left side of (2.12) representing the average value is slightly problematic. The notation of the average should include the probability distribution $p(\eta,t)$ that is used to obtain the average. Misunderstandings can occur,

- if $f[\eta(t)] = 1$ and hence any reference to η and $p(\eta,t)$ is lost,
- if dealing with more than one random variable, and if thus it becomes unclear over which variable the average is taken and,
- if more than one probability distribution $p(\eta,t)$ are under consideration and have to be distinguished.

We will circumvent all of these ambiguities by attaching an index to the average $\langle\cdots\rangle$ denoting the corresponding random variable(s) and probability distribution(s), if needed. In general however, the simple notation adopted poses no danger since in most contexts the random variable and distribution underlying the average are self-evident.
For simplicity we now deal with a one-dimensional random variable η with values on the complete real axis, hence $\Omega = \mathbb{R}$. In probability theory the Fourier-transform $G(s,t)$ of $p(\eta,t)$ is referred to as the *characteristic function* of $p(\eta,t)$.

$$G(s,t) \;=\; \int_{-\infty}^{+\infty} d\eta\; p(\eta,t)\, e^{i\,s\,\eta}\;. \tag{2.13}$$

Since the Fourier transform can be inverted to yield $p(\tilde\eta,t)$

$$p(\tilde\eta,t) \;=\; \frac{1}{2\pi}\int_{-\infty}^{+\infty} ds\; G(s,t)\; e^{-i\,s\,\tilde\eta}\;, \tag{2.14}$$

$G(s,t)$ contains all information on $p(\eta,t)$.
The characteristic function can be interpreted as an average of $f[\eta(t)] = e^{i\,s\,\eta(t)}$, and denoted by

$$G(s,t) \;=\; \left\langle e^{i\,s\,\eta(t)} \right\rangle\;. \tag{2.15}$$

Equation (2.15) prompts one to consider the Taylor expansion of (2.15) for (is) around 0:

$$G(s,t) \;=\; \sum_{n=0}^{\infty} \left\langle \eta^n(t) \right\rangle \frac{(i\,s)^n}{n!} \tag{2.16}$$

where

$$\left\langle \eta^n(t) \right\rangle \;=\; \int d\eta\; \eta^n\; p(\eta,t) \tag{2.17}$$

are the so-called *moments* of $p(\eta, t)$. One can conclude from (2.14, 2.16, 2.17) that the moments $\langle \eta^n(t) \rangle$ completely characterize $p(\eta, t)$.
The moments $\langle \eta^n(t) \rangle$ can be gathered in a statistical analysis as averages of powers of the stochastic variable $\eta(t)$. Obviously, it is of interest to employ averages which characterize a distribution $p(\eta, t)$ as succinctly as possible, i.e., through the smallest number of averages. Unfortunately moments $\langle \eta^n(t) \rangle$ of all orders of n contain significant information about $p(\eta, t)$.
There is another, similar, but more useful scheme to describe probability distributions $p(\eta, t)$; the *cumulants* $\langle\!\langle \eta^n(t) \rangle\!\rangle$. As moments are generated by the characteristic function $G(s, t)$, cumulants are generated by the logarithm of the characteristic function $\log [G(s, t)]$

$$\log[G(s,t)] \;=\; \sum_{n=1}^{\infty} \langle\!\langle \eta^n(t) \rangle\!\rangle \, \frac{(i\,s)^n}{n!} \; . \tag{2.18}$$

Cumulants can be expressed in terms of $\langle \eta^n(t) \rangle$ by taking the logarithm of equation (2.16) and comparing the result with (2.18). The first three cumulants are

$$\langle\!\langle \eta^1(t) \rangle\!\rangle \;=\; \langle \eta^1(t) \rangle \; , \tag{2.19}$$

$$\langle\!\langle \eta^2(t) \rangle\!\rangle \;=\; \langle \eta^2(t) \rangle \;-\; \langle \eta^1(t) \rangle^2 \; , \tag{2.20}$$

$$\langle\!\langle \eta^3(t) \rangle\!\rangle \;=\; \langle \eta^3(t) \rangle \;-\; 3 \langle \eta^2(t) \rangle \langle \eta^1(t) \rangle \;+\; 2 \langle \eta^1(t) \rangle^3 \; . \tag{2.21}$$

These expressions reveal that the first cumulant is equal to the average of the stochastic variable and the second cumulant is equal to the variance[1] . The higher orders of cumulants contain less information about $p(\eta, t)$ than lower ones. In fact it can be shown, that in the frequently arising case of probabilities described by *Gaussian* distributions (the corresponding random processes are called Gaussian) all, but the first and second-order cumulants vanish. For non-Gaussian distributions, though, all cumulants are non-zero as stated in the theorem of Marcienkiewicz [24]). Nevertheless, cumulants give a more succint description of $p(\eta, t)$ than moments do, dramatically so in case of Gaussian processes. This is not the only benefit as we will see considering scenarios with more than one random variable $\eta(t)$.
We now proceed to probability distributions involving two random variables as they arise in case of $\boldsymbol{\eta}(t) \in \mathbb{R}^2$ or if one looks at single random process $\eta(t) \in \mathbb{R}$ at two different times. Both cases are treated by the same tools, however, names and notation differ. We will adopt a notation suitable for a single random process $\eta(t)$ observed at two different times t_0 and t_1, and governed by the unconditional probability distribution $p(\eta_0, t_0; \eta_1, t_1)$. $p(\eta_1, t_1; \eta_0, t_0)\, d\eta_1 d\eta_0$ gives the probability that $\eta(t)$ assumes a value in the interval $[\eta_0, \eta_0 + d\eta_0]$ at time t_0, and a value $[\eta_1, \eta_1 + d\eta_1]$ at time t_1.
As stated in equation (2.11) $p(\eta_0, t_0; \eta_1, t_1)$ can be factorized into the unconditional probability $p(\eta_0, t_0)$ and the conditional probability $p(\eta_0, t_0 | \eta_1, t_1)$. Finding η_0 *and* η_1 is just as probable as first obtaining η_0 and then finding η_1 under the conditition of having found η_0 already. The probability of the later is given by the conditional probability $p(\eta_1, t_1 | \eta_0, t_0)$. Hence one can write,

$$p(\eta_0, t_0; \eta_1, t_1) \;=\; p(\eta_1, t_1 | \eta_0, t_0)\; p(\eta_0, t_0) \; . \tag{2.22}$$

In the case that η_1 is statistically independent of η_0 the conditional probability $p(\eta_1, t_1 | \eta_0, t_0)$ does not depend on η_0 or t_0 and we obtain

$$p(\eta_1, t_1 | \eta_0, t_0) \;=\; p(\eta_1, t_1) \; , \tag{2.23}$$

[1]The variance is often written as the average square deviation from the mean $\langle (\eta(t) - \langle \eta(t) \rangle)^2 \rangle$ which is equivalent to $\langle \eta^2(t) \rangle - \langle \eta(t) \rangle^2$.

and, hence,

$$p(\eta_0, t_0; \eta_1, t_1) \;=\; p(\eta_1, t_1)\; p(\eta_0, t_0)\;. \tag{2.24}$$

In order to characterize $p(\eta_0, t_0; \eta_1, t_1)$ and $p(\eta_0, t_0|\eta_1, t_1)$ one can adopt tools similar to those introduced to characterize $p(\eta_0, t_0)$. Again one basic tool is the average, now the average of a function $g[\eta(t_0), \eta(t_1)]$ with two random variables. Note, that $g[\eta(t_0), \eta(t_1)]$ depends on two random values η_0 and η_1 rendered by a single random process $\eta(t)$ at times t_0 and t_1.

$$\begin{aligned}\Big\langle g[\eta(t_0)\,\eta(t_1)]\Big\rangle \;&=\; \int_\Omega d\eta_1 \int_\Omega d\eta_0\; g[\eta_1, \eta_0]\, p(\eta_0, t_0; \eta_1, t_1) \\ &=\; \int d\eta_0\; p(\eta_0, t_0) \int d\eta_1\; g[\eta_1, \eta_0]\, p(\eta_1, t_1|\eta_0, t_0)\;.\end{aligned} \tag{2.25}$$

The same advise of caution as for the average of one random variable applies here aswell.
The characteristic function is the Fourier-transform of $p(\eta_0, t_0; \eta_1, t_1)$ in η_0 and η_1.

$$\begin{aligned}G(s_0, t_0; s_1, t_1) \;&=\; \int d\eta_0\; p(\eta_0, t_0) \int d\eta_1\; p(\eta_1, t_1|\eta_0, t_0)\; \exp\big[i\,(s_0\,\eta_0 \,+\, s_1\,\eta_1)\big] \\ &=\; \Big\langle e^{i\,(s_0\eta(t_0) + s_1\eta(t_1))}\Big\rangle\;.\end{aligned} \tag{2.26}$$

This can be written as the average [c.f. Eq. (2.25)]

$$G(s_0, t_0; s_1, t_1) \;=\; \Big\langle e^{i(s_0\eta(t_0)+s_1\eta(t_1))}\Big\rangle\;. \tag{2.27}$$

The coefficients of a Taylor expansion of $G(s_0, t_0; s_1, t_1)$ in (is_0) and (is_1), defined through

$$G(s_0, t_0; s_1, t_1) \;=\; \sum_{n_0, n_1 = 0}^{\infty} \Big\langle \eta^{n_0}(t_0)\; \eta^{n_1}(t_1)\Big\rangle\; \frac{(i\,s_0)^{n_0}}{n_0!}\; \frac{(i\,s_1)^{n_1}}{n_1!} \tag{2.28}$$

$$\Big\langle \eta^{n_0}(t_0)\; \eta^{n_1}(t_1)\Big\rangle \;=\; \int d\eta_0\; \eta_0^{n_0}\, p(\eta_0, t_0) \int d\eta_1\; \eta_1^{n_1}\, p(\eta_1, t_1|\eta_0, t_0)\;. \tag{2.29}$$

are called *correlations* or *correlation functions*; the later if one is interested in the time dependency. Cumulants are defined through the expansion

$$\log\big[G(s_0, t_0; s_1, t_1)\big] \;=\; \sum_{n_0, n_1 = 0}^{\infty} \Big\langle\!\!\Big\langle \eta^{n_0}(t_0)\; \eta^{n_1}(t_1)\Big\rangle\!\!\Big\rangle\; \frac{(i\,s_0)^{n_0}}{n_0!}\; \frac{(i\,s_1)^{n_1}}{n_1!}\;. \tag{2.30}$$

These multi-dimensional cumulants can also be expressed in terms of correlation functions and moments. For example, one can show

$$\Big\langle\!\!\Big\langle \eta(t_0)\,\eta(t_1)\Big\rangle\!\!\Big\rangle \;=\; \Big\langle \eta(t_0)\,\eta(t_1)\Big\rangle \;-\; \Big\langle \eta(t_0)\Big\rangle \Big\langle \eta(t_1)\Big\rangle\;. \tag{2.31}$$

Cumulants are particularly useful if one has to consider the sum of statistically independent random values, for example the sum

$$\sigma \;=\; \eta_0 + \eta_1\;. \tag{2.32}$$

The probability $p(\sigma, t_0, t_1)$ for a certain value σ to occur is associated with the characteristic function

$$G_\sigma(r, t_0, t_1) \;=\; \int d\sigma\; p(\sigma, t_0, t_1)\; e^{i\,r\sigma}\;. \tag{2.33}$$

$p(\sigma, t_0, t_1)$ can be expressed as

$$p(\sigma, t_0, t_1) \;=\; \iint d\eta_0\, d\eta_1\; p(\eta_0, t_0; \eta_1, t_1)\; \delta(\eta_0 + \eta_1 - \sigma)\;. \tag{2.34}$$

Accordingly, one can write

$$G_\sigma(r, t_0, t_1) \;=\; \int d\sigma \iint d\eta_0\, d\eta_1\; p(\eta_0, t_0; \eta_1, t_1)\; \delta(\eta_0 + \eta_1 - \sigma)\; e^{i\,r\sigma}\;. \tag{2.35}$$

Integrating over σ results in

$$G_\sigma(r, t_0, t_1) \;=\; \iint d\eta_0\, d\eta_1\; p(\eta_0, t_0; \eta_1, t_1)\; e^{i\,r(\eta_0+\eta_1)}\;. \tag{2.36}$$

This expression can be equated to the characteristic function $G_{\eta_0\eta_1}(r, t_0; r, t_1)$ of the two summands η_0 and η_1, where

$$G_{\eta_0\eta_1}(s_0, t_0; s_1, t_1) \;=\; \iint d\eta_0\, d\eta_1\; p(\eta_0, t_0; \eta_1, t_1)\; e^{i\,(s_0\eta_0 + s_1\eta_1)}\;. \tag{2.37}$$

The statistical independence of η_0 and η_1 in (2.32) is expressed by equation (2.24) as $p(\eta_0, t_0; \eta_1, t_1) = p(\eta_0, t_0)\, p(\eta_1, t_1)$ and one can write

$$G_{\eta_0\eta_1}(s_0, t_0; s_1, t_1) \;=\; \int d\eta_0\; p(\eta_0, t_0)\; e^{i\,s_0\eta_0} \int d\eta_1\; p(\eta_1, t_1)\; e^{i\,s_1\eta_1} \tag{2.38}$$

from which follows

$$G_{\eta_0\eta_1}(s_0, t_0; s_1, t_1) \;=\; G_{\eta_0}(s_0, t_0)\; G_{\eta_1}(s_1, t_1)\;, \tag{2.39}$$

and, hence,

$$\log[G_{\eta_0\eta_1}(s_0, t_0; s_1, t_1)] \;=\; \log[G_{\eta_0}(s_0, t_0)] \;+\; \log[G_{\eta_1}(s_1, t_1)]\;. \tag{2.40}$$

Taylor-expansion leads to the cumulant identity

$$\Big\langle\!\Big\langle \eta^{n_0}(t_0)\; \eta^{n_1}(t_1) \Big\rangle\!\Big\rangle \;=\; 0\;, \quad \forall\; n_0, n_1 \geq 1\;. \tag{2.41}$$

One can finally apply $G_\sigma(r, t_0, t_1) = G_{\eta_0\eta_1}(r, t_0; r, t_1)$, see (2.36) and (2.37) and compare the Taylor coefficients.

$$\Big\langle\!\Big\langle \big(\eta(t_0) + \eta(t_1)\big)^n \Big\rangle\!\Big\rangle \;=\; \sum_{n_0, n_1} \Big\langle\!\Big\langle \eta^{n_0}(t_0)\; \eta^{n_1}(t_1) \Big\rangle\!\Big\rangle\; \frac{n!}{n_0!\, n_1!}\; \delta(n_0 + n_1 - n)\;. \tag{2.42}$$

According to equation (2.41) all but the two summands with $(n_0 = n, n_1 = 0)$ and $(n_0 = 0, n_1 = n)$ disappear and we deduce

$$\Big\langle\!\Big\langle \big(\eta(t_0) + \eta(t_1)\big)^n \Big\rangle\!\Big\rangle \;=\; \Big\langle\!\Big\langle \eta^n(t_0) \Big\rangle\!\Big\rangle \;+\; \Big\langle\!\Big\langle \eta^n(t_1) \Big\rangle\!\Big\rangle\;. \tag{2.43}$$

This result implies that cumulants of any order are simply added if one accumulates the corresponding statistically independent random variables, hence the name *cumulant*. For an arbitrary number of statistically independent random variables η_j or even continuously many $\eta(t)$ one can write

$$\Big\langle\!\Big\langle \Big(\sum_j\; \eta_j\Big)^n \Big\rangle\!\Big\rangle \;=\; \sum_j \Big\langle\!\Big\langle \eta_j^n \Big\rangle\!\Big\rangle \qquad \text{and} \tag{2.44}$$

$$\Big\langle\!\Big\langle \Big(\int dt\; \eta(t)\Big)^n \Big\rangle\!\Big\rangle \;=\; \int dt\; \Big\langle\!\Big\langle \eta^n(t) \Big\rangle\!\Big\rangle\;, \tag{2.45}$$

properties, which will be utilized below.

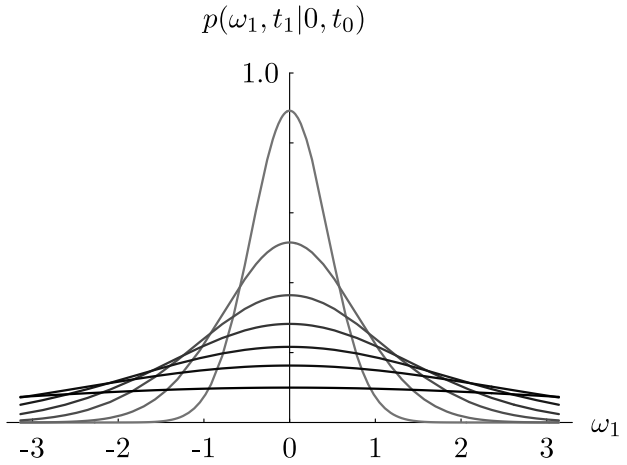

Figure 2.1: The probability density distribution (2.47) of a Wiener process for $D = 1$ in arbitrary temporal and spatial units. The distribution (2.47) is shown for $\omega_0 = 0$ and $(t_1 - t_0) = 0.1, 0.3, 0.6, 1.0, 1.7, 3.0$, and 8.0.

Wiener Process

We will now furnish concrete, analytical expressions for the probabilities characterizing three important Markov processes. We begin with the so-called *Wiener process*. This process, described by $\omega(t)$ for $t \geq 0$, is characterized by the probability distributions

$$p(\omega_0, t_0) = \frac{1}{\sqrt{4\pi D t_0}} \exp\left(-\frac{\omega_0^2}{4D t_0} \right) , \tag{2.46}$$

$$p(\omega_1, t_1|\omega_0, t_0) = \frac{1}{\sqrt{4\pi D\,\Delta t}} \exp\left(-\frac{(\Delta\omega)^2}{4D\,\Delta t} \right) , \tag{2.47}$$

$$\text{with} \quad \Delta\omega = (\omega_1 - \omega_0) ,$$
$$\Delta t = t_1 - t_0 .$$

The probabilities (see Figure 2.1) are parameterized through the constant D, referred to as the diffusion constant, since the probability distributions $p(\omega_0, t_0)$ and $p(\omega_1, t_1|\omega_0, t_0)$ are solutions of the diffusion equation (3.13) discussed extensively below. The Wiener process is homogeneous in time and space, which implies that the conditional transition probability $p(\omega_1, t_1|\omega_0, t_0)$ depends only on the relative variables $\Delta\omega$ and Δt. Put differently, the probability $p(\Delta\omega, \Delta t)$ for an increment $\Delta\omega$ to occur is independent of the current state of the Wiener process $\omega(t)$. The probability is

$$p(\Delta\omega, \Delta t) = p(\omega_0 + \Delta\omega, t_0 + \Delta t|\omega_0, t_0) = \frac{1}{\sqrt{4\pi D\,\Delta t}} \exp\left(-\frac{(\Delta\omega)^2}{4D\,\Delta t} \right) . \tag{2.48}$$

Characteristic Functions, Moments, Correlation Functions and Cumulants for the Wiener Process

In case of the Wiener process simple expressions can be provided for the characteristics introduced above, i.e., for the characteristic function, moments and cumulants. Combining (2.48) and (2.13) one obtains for the characteristic function

$$G(s, t) = e^{-D\,t\,s^2} . \tag{2.49}$$

A Taylor expansion allows one to identify the moments[2]

$$\left\langle \omega^n(t) \right\rangle = \begin{cases} 0 & \text{for odd } n, \\ (n-1)!!\ (2\,D\,t)^{n/2} & \text{for even } n, \end{cases} \tag{2.50}$$

The definition (2.18) and (2.49) leads to the expression for the cumulants

$$\left\langle\!\left\langle \omega^n(t) \right\rangle\!\right\rangle = \begin{cases} 2\,D\,t & \text{for } n = 2, \\ 0 & \text{otherwise .} \end{cases} \tag{2.51}$$

For the two-dimensional characteristic functions one can derive, using (2.47) and (2.26)

$$G(s_0, t_0; s_1, t_1) = \exp\left[-D\,\left(s_0^2\, t_0 + s_1^2\, t_1 + 2\, s_0\, s_1\, \min\left(t_0, t_1\right)\right)\right] . \tag{2.52}$$

From this follow the correlation functions

$$\left\langle \omega^{n_1}(t_1)\, \omega^{n_0}(t_0) \right\rangle = \begin{cases} 0 & \text{for odd } (n_0 + n_1), \\ 2\,D\ \min(t_1, t_0) & \text{for } n_0 = 1 \text{ and } n_1 = 1, \\ 12\,D^2\, t_0\ \min(t_1, t_0) & \text{for } n_0 = 1 \text{ and } n_1 = 3, \\ 4\,D^2\ \left(t_0\, t_1 + 2\ \min^2(t_1, t_0)\right) & \text{for } n_0 = 2 \text{ and } n_1 = 2, \\ \dots & \end{cases} \tag{2.53}$$

and, using the definition (2.30), the cumulants

$$\left\langle\!\left\langle \omega^{n_1}(t_1)\, \omega^{n_0}(t_0) \right\rangle\!\right\rangle = \begin{cases} 2\,D\ \min(t_1, t_0) & \text{for } n_0 = n_1 = 1, \\ 0 & \text{otherwise for } n_0, n_1 \neq 0 . \end{cases} \tag{2.54}$$

The Wiener Process as the Continuum Limit of a Random Walk on a Lattice

The Wiener process is closely related to a *random walk* on a one-dimensional lattice with lattice constant a. A n-step walk on a lattice is performed in discrete times steps $t_j = j\tau$, with $j = 0, 1, 2, \dots, n$. The walk may start at an arbitrary lattice site x_0. One can choose this starting position as the origin of the coordinate system so that one can set $x_0 = 0$. The lattice sites are then located at $x_i = ia$, $i \in \mathbb{Z}$.
At each time step the random walker moves with equal probability to the neighboring right or left lattice site. Thus, after the first step with $t = \tau$ one will find the random walker at $x = \pm a$, i.e. at site $x_{\pm 1}$ with probabitlity $P(\pm a, \tau) = \frac{1}{2}$. For a two-step walk the following pathes are possible:

path 1 : two steps to the left,
path 2 : one step to the left and then one step to the right,
path 3 : one step to the right and then one step to the left,
path 4 : two steps to the right.

Each path has a probability of $\frac{1}{4}$, a factor $\frac{1}{2}$ for each step. Pathes 2 and 3 both terminate at lattice site x_0. The probability to find a random walker after two step at position $x_0 = 0$ is therefore $P(0, 2\tau) = \frac{1}{2}$. The probabilities for lattice sites $x_{\pm 2}$ reached via path 1 and 4 respectively are simply $P(\pm 2a, 2\tau) = \frac{1}{4}$.

[2]The double factorial $n!!$ for positive $n \in \mathbb{N}$ denotes the product $n(n-2)(n-4)\dots 1$ for odd n and $n(n-2)(n-4)\dots 2$ for even n.

For an n-step walk one can proceed like this suming over all possible pathes that terminate at a given lattice site x_i. Such a summation yields the probability $P(ia, n\tau)$. However, to do so effectively a more elegant mathematical description is appropriate. We denote a step to the right by an operator $\mathcal{R}$, and a step to the left by an operator $\mathcal{L}$. Consequently a single step of a random walker is given by $\frac{1}{2}(\mathcal{L}+\mathcal{R})$, the factor $\frac{1}{2}$ denoting the probabilty for each direction. To obtain a n-step walk the above operator $\frac{1}{2}(\mathcal{L}+\mathcal{R})$ has to be iterated n times. For a two-step walk one gets $\frac{1}{4}\,(\mathcal{L}+\mathcal{R})\circ(\mathcal{L}+\mathcal{R})$. Expanding this expression results in $\frac{1}{4}\,(\mathcal{L}^2+\mathcal{L}\circ\mathcal{R}+\mathcal{R}\circ\mathcal{L}+\mathcal{R}^2)$. Since a step to the right and then to the left amounts to the same as a step first to the left and then to the right, it is safe to assume that $\mathcal{R}$ and $\mathcal{L}$ commute. Hence one can write $\frac{1}{4}\,\mathcal{L}^2+\frac{1}{2}\,\mathcal{L}\circ\mathcal{R}+\frac{1}{4}\,\mathcal{R}^2$. As the operator expression $\mathcal{L}^p\circ\mathcal{R}^q$ stands for p steps to the left and q steps to the right one can deduce that $\mathcal{L}^p\circ\mathcal{R}^q$ represents the lattice site x_{q-p}. The coefficients are the corresponding probabilties $P\big((q-p)\,a, (q+p)\,\tau\big)$.
The algebraic approach above proofs useful, since one can utilize the well known binomial formula

$$(x+y)^n \;=\; \sum_{k=0}^{n} \binom{n}{k}\, x^k\; y^{n-k}\;. \tag{2.55}$$

One can write

$$\left[\frac{1}{2}\;(\mathcal{L}\;+\;\mathcal{R})\right]^n \;=\; \left(\frac{1}{2}\right)^n \sum_{k=0}^{n} \binom{n}{k}\; \underbrace{\mathcal{L}^k\,\mathcal{R}^{n-k}}_{=x_{2k-n}}\,, \tag{2.56}$$

and obtains as coefficients of x_i the probabilities

$$P(i\,a, n\,\tau) \;=\; \frac{1}{2^n}\,\binom{n}{\frac{n+i}{2}}\;. \tag{2.57}$$

One can express (2.57) as

$$P(x,t) \;=\; \frac{1}{2^{t/\tau}}\,\binom{t/\tau}{\frac{t}{2\tau}+\frac{x}{2a}}\;. \tag{2.58}$$

The moments of the discrete probability distribution $P(x,t)$ are

$$\begin{aligned}\Big\langle x^n(t)\Big\rangle \;&=\; \sum_{x=-\infty}^{\infty} x^n\; P(x,t)\\ &=\; \begin{cases} 0 & \text{for odd } n,\\ a^2\;\frac{t}{\tau} & \text{for } n=2,\\ a^4\;\frac{t}{\tau}\;\left(3\,\frac{t}{\tau}-2\right) & \text{for } n=4,\\ a^6\;\frac{t}{\tau}\;\left(15\;\left(\frac{t}{\tau}\right)^2-30\,\frac{t}{\tau}+16\right) & \text{for } n=6,\\ \cdots\;. \end{cases}\end{aligned} \tag{2.59}$$

We now want to demonstrate that in the continuum limit a random walk reproduces a Wiener process. For this purpose we show that the unconditional probability distributions of both processes match. We do not consider conditional probabilities $p(x_1,t_1|x_0,t_0)$ as they equal unconditional probabilities $p(x_1-x_0,t_1-t_0)$ in both cases; in a Wiener process aswell as in a random walk.
To turn the discrete probability distribution (2.58) into a continuous probability density distribution one considers adjacent bins centered on every lattice site that may be occupied by a random walker.

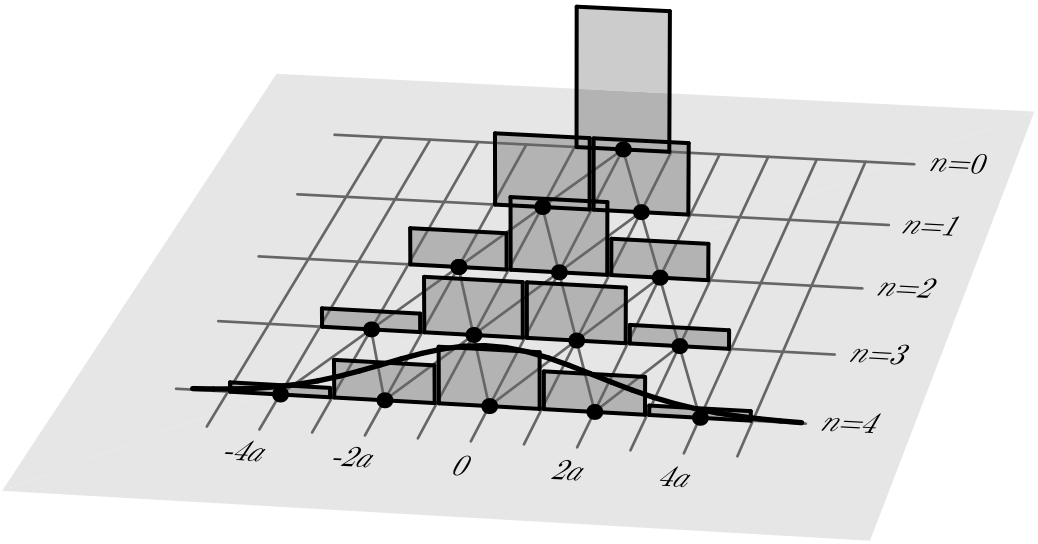

Figure 2.2: The probability density distributions (2.60) for the first four steps of a random walk on a discrete lattice with lattice constant a are shown. In the fourth step the continuous approximation (2.63) is superimposed.

Note, that only every second lattice site can be reached after a particular number of steps. Thus, these adjacent bins have a base length of $2a$ by which we have to divide $P(x,t)$ to obtain the probability density distribution $p(x,t)$ in these bins (see Figure 2.2).

$$p(x,t)\,dx \;=\; \frac{1}{2a}\,\frac{1}{2^{t/\tau}}\,\binom{t/\tau}{\frac{t}{2\tau}+\frac{x}{2a}}\,dx\;. \tag{2.60}$$

We then rescale the lattice constant a and the length τ of the time intervals to obtain a continuous description in time and space. However, τ and a need to be rescaled differently, since the spatial extension of the probability distribution $p(x,t)$, characterized by it's standard deviation

$$\sqrt{\left\langle\!\left\langle x^2(t)\right\rangle\!\right\rangle} \;=\; \sqrt{\left\langle x^2(t)\right\rangle \;-\; \left\langle x(t)\right\rangle^2} \;=\; a\sqrt{\frac{t}{\tau}}\,, \tag{2.61}$$

is not proportional to t, but to $\sqrt{t}$. This is a profound fact and a common feature for all processes accumulating uncorrelated values of random variables in time. Thus, to conserve the temporal-spatial proportions of the Wiener process one rescales the time step τ by a factor ε and the lattice constant a by a factor $\sqrt{\varepsilon}$:

$$\tau \;\longmapsto\; \varepsilon\,\tau \quad \text{and} \quad a \;\longmapsto\; \sqrt{\varepsilon}\,a\;. \tag{2.62}$$

A continuous description of the binomial density distribution (2.60) is then approached by taking the limit $\varepsilon \to 0$. When ε approaches 0 the number of steps $n = \frac{t}{\tau\varepsilon}$ in the random walk goes to

infinity and one observes the following identity derived in appendix 2.7 of this chapter.

$$\begin{aligned} p(x,t)\,dx &= \frac{1}{2\,\varepsilon\,a}\;2^{-\frac{t}{\varepsilon\tau}}\;\binom{\frac{t}{\varepsilon\tau}}{\frac{t}{2\varepsilon\tau}+\frac{x}{2\sqrt{\varepsilon}a}}\,dx \\ &= \sqrt{\frac{n\tau}{4\,a^2\,t}}\;2^{-n}\;\binom{n}{\frac{n}{2}+\frac{x}{a}\sqrt{\frac{n\,\tau}{4t}}}\,dx \\ &\overset{(2.165)}{=} \sqrt{\frac{\tau}{2\pi\,a^2\,t}}\;\exp\!\left(-\frac{x^2\,\tau}{2\,a^2\,t}\right)\,dx\;\left(1+\mathcal{O}\!\left(\frac{1}{n}\right)\right)\;. \end{aligned} \tag{2.63}$$

The fraction τ/a^2 is invariant under rescaling (2.62) and, hence, this quantity remains in the continuous description (2.63) of the probability density distribution $p(x,t)$. Comparing equations (2.63) and (2.48) one identifies $D = a^2/2\tau$. The relation between random step length a and time unit τ obviously determines the rate of diffusion embodied in the diffusion constant D: the larger the steps a and the more rapidly these are performed, i.e., the smaller τ, the quicker the diffusion process and the faster the broadening of the probability density distribution $p(x,t)$. According to (2.61) this broadening is then $\sqrt{2Dt}$ as expected for a diffusion process.

Computer Simulation of a Wiener Process

The random walk on a lattice can be readily simulated on a computer. For this purpose one considers an ensemble of particles labeled by k, $k = 1, 2, \ldots N$, the positions $x^{(k)}(j\tau)$ of which are generated at time steps $j = 1, 2, \ldots$ by means of a random number generator. The latter is a routine that produces quasi-random numbers r, $r \in [0,1]$ which are homogenously distributed in the stated interval. The particles are assumed to all start at position $x^{(k)}(0) = 0$. Before every displacement one generates a new r. One then executes a displacement to the left in case of $r < \frac{1}{2}$ and a displacement to the right in case of $r \geq \frac{1}{2}$.
In order to characterize the resulting displacements $x^{(k)}(t)$ one can determine the mean, i.e. the first moment or first cumulant,

$$\left\langle x(t)\right\rangle \;=\; \frac{1}{N}\sum_{k=1}^{N} x^{(k)}(t) \tag{2.64}$$

and the variance, i.e. the second cumulant,

$$\left\langle\!\left\langle x^2(t)\right\rangle\!\right\rangle \;=\; \left\langle x^2(t)\right\rangle - \left\langle x(t)\right\rangle^2 \;=\; \frac{1}{N}\sum_{k=1}^{N}\left(x^{(k)}(t)\right)^2 \;-\; \left\langle x(t)\right\rangle^2 \tag{2.65}$$

for $t = \tau, 2\tau, \ldots$. In case of $x^{(k)}(0) = 0$ one obtains $\langle x(t)\rangle \approx 0$. The resulting variance (2.65) is presented for an actual simulation of 1000 walkers in Figure 6.1.

A Wiener Process can be Integrated, but not Differentiated

We want to demonstrate that the path of a Wiener process cannot be differentiated. For this purpose we consider the differential defined through the limit

$$\frac{d\omega(t)}{dt} \;:=\; \lim_{\Delta t\to 0}\frac{\omega(t+\Delta t)-\omega(t)}{\Delta t} \;=\; \lim_{\Delta t\to 0}\frac{\Delta\omega(t)}{\Delta t}\;. \tag{2.66}$$

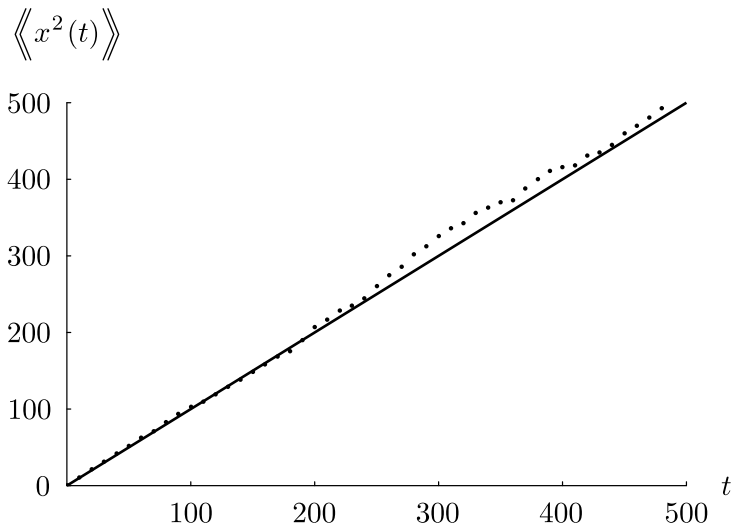

Figure 2.3: $\langle\langle x^2(t)\rangle\rangle$ resulting from a simulated random walk of 1000 particles on a lattice for $\tau = 1$ and $a = 1$. The simulation is represented by dots, the expected [c.f., Eq. (2.61)] result $\langle\langle x^2(t)\rangle\rangle = t$ is represented by a solid line.

What is the probability for the above limit to render a finite absolute value for the derivative smaller or equal an arbitrary constant v? For this to be the case $|\Delta\omega(t)|$ has to be smaller or equal $v\,\Delta t$. The probability for that is

$$\begin{aligned}\int_{-v\,\Delta t}^{v\,\Delta t} d(\Delta\omega)\; p(\Delta\omega,\Delta t) &= \frac{1}{\sqrt{4\pi D\,\Delta t}}\int_{-v\,\Delta t}^{v\,\Delta t} d(\Delta\omega)\;\exp\left[-\frac{(\Delta\omega)^2}{4D\,\Delta t}\right] \\ &= \operatorname{erf}\left[\sqrt{\frac{\Delta t}{D}}\,\frac{v}{2}\right]. \end{aligned} \tag{2.67}$$

The above expression vanishes for $\Delta t \to 0$. Hence, taking the differential as proposed in equation (2.66) we would almost never obtain a finite value for the derivative. This implies that the velocity corresponding to a Wiener process is almost always plus or minus infinity.
It is instructive to consider this calamity for the random walk on a lattice as well. The scaling (2.62) renders the associated velocities like $\pm\frac{a}{\tau}$ infinite and the random walker seems to be infinitely fast as well. Nevertheless, for the random walk on a lattice with non-zero ϵ one can describe the velocity through a discrete stochastic process $\dot{x}(t)$ with the two possible values $\pm\frac{a}{\tau}$ for each time interval $]j\,\tau,(j+1)\,\tau]$, $j \in \mathbb{N}$. Since every random step is completely independent of the previous one, $\dot{x}_i = \dot{x}(t_i)$ with $t_i \in]i\,\tau,(i+1)\,\tau]$ is completely uncorrelated to $\dot{x}_{i-1} = \dot{x}(t_{i-1})$ with $t_{i-1} \in [(i-1)\,\tau, i\,\tau]$, and $x(t)$ with $t \le i\,\tau$. Thus, we have

$$P(\dot{x}_i,t_i) = \begin{cases} \frac{1}{2} & \text{for } \dot{x}_i = \pm\frac{a}{\tau}\,, \\ 0 & \text{otherwise,}\end{cases} \tag{2.68}$$

$$P(\dot{x}_j,t_j|\dot{x}_i,t_i) = \begin{cases} \begin{cases} 1 & \text{for } \dot{x}_j = \dot{x}_i \\ 0 & \text{for } \dot{x}_j \neq \dot{x}_i \end{cases} & \text{, for } i = j\,, \\ P(\dot{x}_j,t_j) & \text{, for } i \neq j\,. \end{cases} \tag{2.69}$$

The velocity of a random walk on a lattice is characterized by the following statistical moments

$$\left\langle \dot{x}^n(t) \right\rangle \;=\; \begin{cases} \left(\frac{a}{\tau}\right)^n & \text{, for even } n \text{ ,} \\ 0 & \text{, for odd } n \text{ ,} \end{cases} \tag{2.70}$$

and correlation functions

$$\left\langle \dot{x}^n(t_j)\, \dot{x}^m(t_i) \right\rangle \;=\; \begin{cases} \begin{cases} \left(\frac{a}{\tau}\right)^{m+n} & \text{for even } (m+n) \\ 0 & \text{otherwise} \end{cases} & \text{for } i = j \text{ ,} \\ \begin{cases} \left(\frac{a}{\tau}\right)^{m+n} & \text{for even } m \text{ and even } n \\ 0 & \text{otherwise} \end{cases} & \text{for } i \neq j \text{ .} \end{cases} \tag{2.71}$$

If we proceed to a continuous description with probability density distributions as in equation (2.60), we obtain

$$p(\dot{x}_i, t_i) \;=\; \frac{1}{2}\left(\delta\Big(\dot{x}_i + \frac{a}{\tau}\Big) \,+\, \delta\Big(\dot{x}_i - \frac{a}{\tau}\Big) \right) , \tag{2.72}$$

$$p(\dot{x}_j, t_j | \dot{x}_i, t_i) \;=\; \begin{cases} \delta\big(\dot{x}_j - \dot{x}_i\big) & \text{, for } i = j \text{ ,} \\ p(\dot{x}_j, t_j) & \text{, for } i \neq j \text{ ,} \end{cases} \tag{2.73}$$

and we derive the same statistical momtents

$$\left\langle \dot{x}^n(t) \right\rangle \;=\; \begin{cases} \left(\frac{a}{\tau}\right)^n & \text{, for even } n \text{ ,} \\ 0 & \text{, for odd } n \text{ ,} \end{cases} \tag{2.74}$$

and correlation functions defined for continuous $\dot{x}$ range

$$\left\langle \dot{x}^n(t_j)\, \dot{x}^m(t_i) \right\rangle \;=\; \begin{cases} \begin{cases} \left(\frac{a}{\tau}\right)^{m+n} & \text{, for even } (m+n), \\ 0 & \text{, otherwise.} \end{cases} & \text{, for } i = j, \\ \begin{cases} \left(\frac{a}{\tau}\right)^{m+n} & \text{, for even } m \text{ and even } n, \\ 0 & \text{, otherwise,} \end{cases} & \text{, for } i \neq j \text{ .} \end{cases} \tag{2.75}$$

One encounters difficulties when trying to rescale the discrete stochastic process $\dot{x}(t_i)$ according to (2.62). The positions of the delta-functions $\pm\frac{a}{\tau}$ in the probability density distributions (2.72) wander to $\pm\infty$. Accordingly, the statistical moments and correlation functions of even powers move to infinity as well. Nevertheless, these correlation functions can still be treated as distributions in time. If one views the correlation function $\langle \dot{x}(t_1)\, \dot{x}(t_0) \rangle$ as a rectangle distribution in time t_1 (see Figure 2.4), one obtains for the limit $\varepsilon \to 0$

$$\begin{aligned} \left\langle \dot{x}(t_1)\, \dot{x}(t_0) \right\rangle dt_1 \;&=\; \lim_{\varepsilon \to 0} \left(\frac{\sqrt{\varepsilon}\, a}{\varepsilon \tau} \right)^2 \varepsilon \, dt_1 \\ &=\; \frac{a^2}{\tau} \; \delta(t_1 - t_0) \; dt_1 \; . \end{aligned} \tag{2.76}$$

Even though the probability distributions of the stochastic process $\dot{x}(t)$ exhibit some unusual features, $\dot{x}(t)$ is still an admissable Markov process. Thus, one has a paradox. Since

$$x(t_j) \;=\; \sum_{i=0}^{j} \tau\, \dot{x}(t_i) \; , \tag{2.77}$$

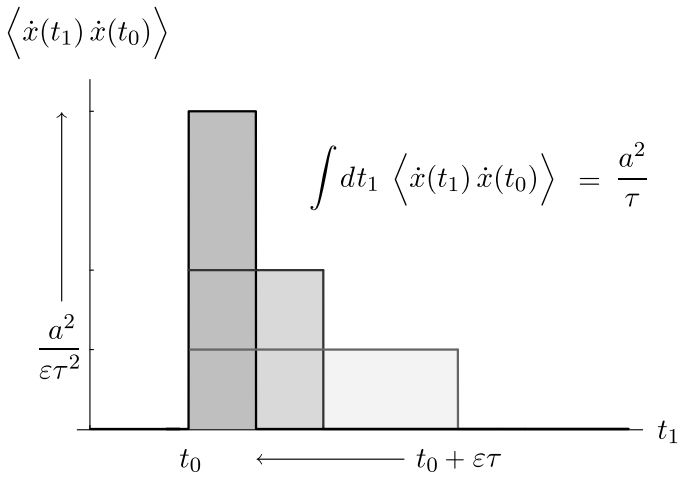

Figure 2.4: Cumulant (2.76) shown as a function of t_1. As ε is chosen smaller and smaller (2.76) approaches a Dirca delta distribution at t_0, since the area under the graph remains $\tau\,\frac{a^2}{\tau^2}$.

it is fair to claim that for the limit $\varepsilon \to 0$ the following integral equation holds.

$$x(t) \;=\; \int dt\; \dot{x}(t)\;. \tag{2.78}$$

The converse, however,

$$\frac{dx(t)}{dt} \;=\; \dot{x}(t) \tag{2.79}$$

is ill-defined as has been shown in equation (2.66).

Two questions come to mind. First, do stochastic equations like (2.3) and (2.79) make any sense? Second, is $\dot{x}(t)$ unique or are there other stochastic processes that sum up to $x(t)$?

The first question is quickly answered. Stochastic differential equations are only well defined by the integral equations they imply. Even then the integrals in these integral equations have to be handled carefully as will be shown below. Therefore, equation (2.79) should be read as equation (2.78).

We answer the second question by simply introducing another stochastic processes, the Ornstein-Uhlenbeck process, the integral over which also yields the Wiener process. Nevertheless, all processes that yield the Wiener process by integration over time do exhibit certain common properties that are used to define one encompassing, idealized Markov processes, the so-called Gaussian white noise. This process may be viewed as the time-derivative of the Wiener process. Gaussian white noise will be our third example of a stochastic process.

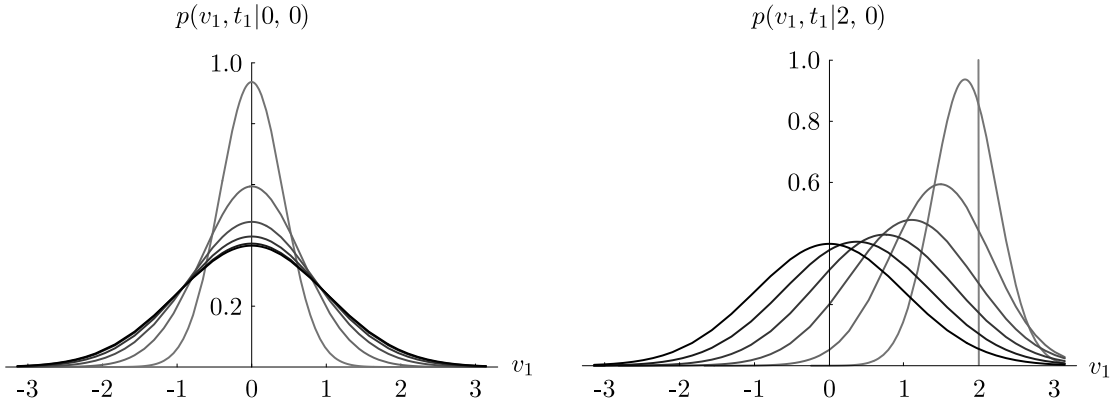

Figure 2.5: The probability density distribution (2.81) of a Ornstein-Uhlenbeck process for $\sigma = \sqrt{2}$ and $\gamma = 1$ in arbitrary temporal and spatial units. The distribution (2.81) is shown for $v_0 = 0$ and $v_0 = 2$ for $t_1 = 0.0, 0.1, 0.3, 0.6, 1.0, 1.7$, and ∞.

Ornstein-Uhlenbeck Process

Our second example for a Markov process is the *Ornstein-Uhlenbeck process*. The *Ornstein-Uhlenbeck process*, describing a random variable $v(t)$, is defined through the probabilities

$$p(v_0, t_0) = \frac{1}{\sqrt{\pi\,\gamma\,\sigma^2}}\,\exp\!\left(-\frac{v_0^2}{\gamma\,\sigma^2}\right) \tag{2.80}$$

$$p(v_1, t_1|v_0, t_0) = \frac{1}{\sqrt{\pi\,S}}\,\exp\!\left(-\frac{1}{S}\left(v_1 - v_0\; e^{-\gamma\,\Delta\,t}\right)^2\right)\,, \tag{2.81}$$

$$\text{with}\quad \Delta t = |\,t_1 - t_0\,|\,, \tag{2.82}$$
$$S = \gamma\,\sigma^2\,\left(1 - e^{-2\,\gamma\,\Delta\,t}\right)\,.$$

The probabilities (see Figure 2.5) are characterized through two parameters σ and γ. Their significance will be explained further below. The process is homogeneous in time, since (2.81) depends solely on Δt, but is not homogeneous in v. Furthermore, the Ornstein-Uhlenbeck Process is stationary, i.e., $p(v_0, t_0)$ does not change in time.
The characteristic function, associated with the unconditional probability distribution $p(v_0, t_0)$ in (2.80) is also independent of time and given by

$$G(s) = e^{-\gamma\left(\frac{\sigma\,s^2}{2}\right)}\,. \tag{2.83}$$

The associated moments and cumulants are

$$\left\langle v^n(t)\right\rangle = \begin{cases} 0 & \text{for odd } n, \\ (n-1)!!\;\left(\frac{1}{2}\,\gamma\,\sigma^2\right)^{n/2} & \text{for even } n, \end{cases} \tag{2.84}$$

and

$$\left\langle\!\left\langle v^n(t)\right\rangle\!\right\rangle = \begin{cases} \frac{\gamma\,\sigma^2}{2} & \text{for } n = 2, \\ 0 & \text{otherwise}\,. \end{cases} \tag{2.85}$$

The characteristic function for the conditional probability (2.81) is

$$G_v(s_0, t_0; s_1, t_1) = \exp\left[-\frac{1}{4}\,\gamma\,\sigma^2\,\left(s_0^2 + s_1^2 + 2\,s_0\,s_1\,e^{-\gamma\,|t_1 - t_0|}\right)\right]\,. \tag{2.86}$$

The corresponding correlation functions, defined according to (2.28, 2.29) are

$$\left\langle v_1^{n_1}(t_1)\, v_0^{n_0}(t_0)\right\rangle = \int dv_0\; v_0^{n_0}\; p(v_0,t_0) \int dv_1\; v_1^{n_1}\; p(v_1,t_1|v_0,t_0) \tag{2.87}$$

$$= \begin{cases} 0 & \text{, for odd } (n_0+n_1), \\ \frac{1}{2}\,\gamma\,\sigma^2\; e^{-\gamma\,|t_1-t_0|} & \text{, for } n_0=1 \text{ and } n_1=1, \\ \frac{3}{4}\,\gamma^2\sigma^4\; e^{-\gamma\,|t_1-t_0|} & \text{, for } n_0=1 \text{ and } n_1=3, \\ \frac{1}{4}\,\gamma^2\sigma^4\; \left(1\,+\,2\,e^{-2\gamma\,|t_1-t_0|}\right) & \text{, for } n_0=2 \text{ and } n_1=2, \\ \cdots & \end{cases} \tag{2.88}$$

This implies that the correlation of $v(t_1)$ and $v(t_0)$ decays exponentially. As for the Wiener process, the most compact description of the unconditional probability is given by the cumulants

$$\left\langle\!\left\langle v^{n_1}(t_1)\, v^{n_0}(t_0)\right\rangle\!\right\rangle = \begin{cases} \frac{\gamma\,\sigma^2}{2}\, e^{-\gamma\,|t_1-t_0|} & \text{for } n_0=n_1=1, \\ 0 & \text{otherwise, for } n_0 \text{ and } n_1 \neq 0\ . \end{cases} \tag{2.89}$$

We want to demonstrate now that integration of the Ornstein-Uhlenbeck process $v(t)$ yields the Wiener process. One expects the formal relationship

$$\tilde{\omega}(t) = \int_0^t ds\; v(s) \tag{2.90}$$

to hold where $\tilde{\omega}(t)$ is a Wiener process. In order to test this supposition one needs to relate the cumulants (2.51, 2.54) and (2.85, 2.89) for these processes according to

$$\left\langle\!\left\langle \tilde{\omega}(t)\,\tilde{\omega}(t')\right\rangle\!\right\rangle = \left\langle\!\left\langle \int_0^t ds\, v(s) \int_0^{t'} ds'\; v(s')\right\rangle\!\right\rangle = \int_0^t ds \int_0^{t'} ds' \left\langle\!\left\langle v(s)\; v(s')\right\rangle\!\right\rangle \tag{2.91}$$

assuming $t \geq t'$. By means of (2.89) and according to the integration depicted in Figure 2.6 follows

$$\begin{aligned} &\left\langle\!\left\langle \tilde{\omega}(t)\,\tilde{\omega}(t')\right\rangle\!\right\rangle \\ &= \frac{1}{2}\,\gamma\,\sigma^2 \left[\underbrace{\int_0^{t'} ds' \int_0^{s'} ds\; e^{-\gamma\,(s'-s)}}_{①} + \underbrace{\int_0^{t'} ds \int_0^{s} ds'\, e^{-\gamma\,(s-s')}}_{②} + \underbrace{\int_{t'}^{t} ds \int_0^{t'} ds'\, e^{-\gamma\,(s-s')}}_{③} \right] \\ &= \sigma^2\, t' \;+\; \frac{\sigma^2}{2\,\gamma}\left[-1 + e^{-\gamma\,t'} + e^{-\gamma\,t} - e^{-\gamma\,(t-t')}\right]\ . \end{aligned} \tag{2.92}$$

For times long compared to the time scale of velocity relaxation γ^{-1} one reproduces Eq. (2.54) (we don't treat explicitly the case $t \leq t'$), and for $t = t'$ Eq. (2.54), where $D = \sigma^2/2$.
The relationship between the Ornstein-Uhlenbeck and Wiener processes defined through (2.90) holds for all cumulants, not just for the cumulants of second order. We only had to proof relation (2.90), since all other cumulants of both processes are simply 0. This allows one to state for $D = \sigma^2/2$

$$\omega(t) \;=\; \lim_{\gamma\to\infty} \int dt\; v(t)\ . \tag{2.93}$$

With respect to their probability distributions the Ornstein-Uhlenbeck process $v(t)$ and the velocity of a random walker $\dot{x}(t)$ are different stochastic processes. However, in the limit $\gamma \to \infty$ and $\varepsilon \to 0$

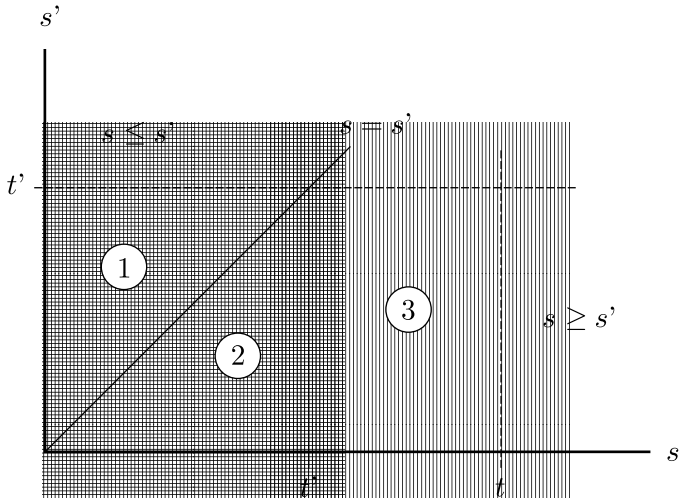

Figure 2.6: The three areas of integration as used in equation 2.92 are shown in the coordinate plane of the two integration variables s and s'.

the following moment and correlation function turn out to be the same for both processes, if $D = \frac{\sigma^2}{2} = \frac{a^2}{2\tau}$.

$$\left\langle v(t) \right\rangle = \left\langle \dot{x}(t) \right\rangle = 0 \,, \tag{2.94}$$

$$\lim_{\gamma\to\infty} \left\langle v(t_1)\, v(t_0) \right\rangle = \lim_{\varepsilon\to 0} \left\langle \dot{x}(t_1)\, \dot{x}(t_0) \right\rangle = 2\,D\;\delta(t_1 - t_0) \,. \tag{2.95}$$

Hence, one uses these later properties to define an idealized Markov process, the so-called *Gaussian white noise*.

White Noise Process

An important idealized stochastic process is the so-called '*Gaussian white noise*'. This process, denoted by $\xi(t)$, is not characterized through conditional and unconditional probabilities, but through the following statistical moment and correlation function

$$\left\langle \xi(t) \right\rangle = 0 \,, \tag{2.96}$$

$$\left\langle \xi(t_1)\, \xi(t_0) \right\rangle = \zeta^2\;\delta(t_1 - t_0) \,. \tag{2.97}$$

The attribute *Gaussian* implies that all cumulants higher than of second order are 0.

$$\left\langle\!\!\left\langle \xi^{n_1}(t_1)\, \xi^{n_0}(t_0) \right\rangle\!\!\right\rangle = \begin{cases} \zeta^2\;\delta(t_1 - t_0) & \text{, for } n_0, n_1 = 1 \,, \\ 0 & \text{, otherwise .} \end{cases} \tag{2.98}$$

The reason why this process is termed 'white' is connected with its correlation function (2.97), the Fourier transform of which is constant, i.e., entails all frequencies with equal amplitude just as white radiation. The importance of the process $\xi(t)$ stems from the fact that many other stochastic processes are described through stochastic differential equations with a (white) noise term $\xi(t)$. We will show this for the Wiener process below and for the Ornstein-Uhlenbeck processes later in the script.

As hinted by the examples in this section we can show that the integral of Gaussian white noise happens to be a Wiener process. We prove this in the same fashion as above by deriving the cumulants for $\int dt\, \xi(t)$. Again the task is simplified by the fact that only one cumulant is non-zero, namely,

$$\begin{aligned} \left\langle\!\!\left\langle \int_0^{t_1} ds_1\, \xi(s_1) \int_0^{t_0} ds_0\, v(s_0) \right\rangle\!\!\right\rangle &= \int_0^{t_1} ds_1 \int_0^{t_0} ds_0 \left\langle\!\!\left\langle v(s_1)\, v(s_0) \right\rangle\!\!\right\rangle \\ &= \int_0^{t_1} ds_1 \int_0^{t_0} ds_0\, \zeta^2\, \delta(s_1 - s_0) \\ &= \zeta^2\, \min(t_1, t_0)\ . \end{aligned} \tag{2.99}$$

We demonstrated, thereby, the important relationship between white noise $\xi(t)$ and the Wiener process $\omega(t)$.

$$\omega(t) = \int_0^t ds\, \xi(s)\ , \tag{2.100}$$

for $2D = \zeta^2 = 1$.

2.4 Ito calculus

The introduction to Ito's calculus in this section is based on [13] which we recommend for further reading as well as [30, 33].
We return to the stochastic differential equation of section 2.2, which we will now express as an integral equation. We will model the noise term $\boldsymbol{\eta}(t)$ by a tupel of normalized Gaussian white noise processes $\boldsymbol{\xi}(t)$ with $\zeta = 1$.

$$\mathbf{x}(t) = \int_0^t ds\, \boldsymbol{A}\left[\mathbf{x}(s), s\right] + \int_0^t ds\, \boldsymbol{\xi}(s) \cdot \mathbf{B}^T\left[\mathbf{x}(s), s\right]\ . \tag{2.101}$$

Since $\mathbf{x}(t)$ is continuous, the first integral on the r.h.s. is well defined, e.g., in the sense of a Riemann integral. However, the second integral poses problems. Let us consider the simple one-dimensional case with an arbitrary function or stochastic process $G[t]$.

$$I(t) = \int_0^t ds\, \xi(s)\, G[s]\ . \tag{2.102}$$

One can rewrite the integral (2.102) in terms of a normalized Wiener process $\omega(t)$ with $D = 1/2$. One subsitutes $d\omega(s)$ for $ds\xi(s)$, since $\int_0^t ds\xi(s) = \omega(t) = \int_0^t d\omega(s)$ and obtains

$$I(t) = \int_0^t d\omega(s)\, G[s]\ . \tag{2.103}$$

The kind of Riemann-Stieltjes integral (2.103) can be approximated by the sums $I_n^{(\alpha)}(t)$ which evaluate the integral at n discrete times steps $t_j = j\frac{t}{n}$.

$$I^{(\alpha)} = \operatorname*{ms\text{-}lim}_{n\to\infty} I_n^{(\alpha)}(t)\ , \text{ with} \tag{2.104}$$

$$I_n^{(\alpha)}(t) = \sum_{j=1}^{n} G\left[(1-\alpha)\, t_{j-1} + \alpha\, t_j\right] \left(\omega(t_j) - \omega(t_{j-1})\right)\ . \tag{2.105}$$

Two remarks about equation (2.104) and (2.105) are due. First, one has to specify the meaning of approximation, since one is dealing with random variables. To approximate the integral $I^{(\alpha)}$ one takes the so-called *mean square limit*. Such a limt has to satisfy the following condition of convergence.

$$X = \underset{n\to\infty}{\text{ms-lim}}\ X_n \text{ , if} \tag{2.106}$$

$$\lim_{n\to\infty} \left\langle (X_n - X)^2 \right\rangle = 0 \,. \tag{2.107}$$

Second, note that the sum $I_n^{(\alpha)}(t)$ is parameterized by α. This allows one to choose the position where to evaluated $G[t]$ within the time step intervals $[t_{j-1}, t_j]$. In the limit $n \to \infty$ as the intervals $[t_{j-1}, t_j]$ become infinitely small, non-stochastic integrals become independent of α, not so $I_n^{(\alpha)}(t)$!
We will demonstrate the dependence of $I^{(\alpha)}$ on α in two ways. We first derive a closed form of a simple stochastic integral and thereby put forward an explicit example of α-dependence. In addition we will determine an estimates for $I_n^{(\alpha)}(t)$ on the orders of $\mathcal{O}\left(\frac{1}{n}\right)$ and demonstrate the persistence of the α-dependence as n goes to infinity.
The simple integral we want to solve explicitly is $G[t] = \omega(t)$.

$$\begin{aligned}
&\int_0^t d\omega(s)\ \omega(s) \qquad (2.108)\\
&= \underset{n\to\infty}{\text{ms-lim}} \sum_{j=1}^{n} \omega(\tau)\ \big(\omega(t_j) - \omega(t_{j-1})\big) \qquad \text{, with } \tau = (1-\alpha)\, t_{j-1} + \alpha\, t_j \\
&= \underset{n\to\infty}{\text{ms-lim}} \sum_{j=1}^{n} \Big[\omega(\tau)\ \big(\omega(\tau) - \omega(t_{j-1})\big)\ +\ \omega(\tau)\ \big(\omega(t_j) - \omega(\tau)\big)\Big] \\
&= \underset{n\to\infty}{\text{ms-lim}} \sum_{j=1}^{n} \frac{1}{2}\Big[-\Big[\omega(\tau) - \big(\omega(\tau) - \omega(t_{j-1})\big)\Big]^2 + \ \omega^2(\tau)\ +\ \big(\omega(\tau) - \omega(t_{j-1})\big)^2 \\
&\qquad\qquad + \Big[\omega(\tau) + \big(\omega(t_j) - \omega(\tau)\big)\Big]^2 - \ \omega^2(\tau)\ -\ \big(\omega(t_j) - \omega(\tau)\big)^2\Big] \\
&= \underset{n\to\infty}{\text{ms-lim}} \sum_{j=1}^{n} \frac{1}{2}\Big[\omega^2(t_j)\ -\ \omega^2(t_{j-1})\ +\ \big(\omega(\tau) - \omega(t_{j-1})\big)^2 - \ \big(\omega(t_j) - \omega(\tau)\big)^2\Big] \,.
\end{aligned}$$

The first term of the j^{th} summand cancels the second term in the $(j+1)^{\text{th}}$ summand, hence only $\omega^2(t)$ and $-\omega^2(0)$ remain.

$$\begin{aligned}
&\int_0^t d\omega(s)\ \omega(s) \qquad (2.109)\\
&= \frac{1}{2}\Big[\omega^2(t)\ -\ \omega^2(0)\ +\ \underset{n\to\infty}{\text{ms-lim}} \sum_{j=1}^{n} \Big[\big(\omega(\tau) - \omega(t_{j-1})\big)^2 - \ \big(\omega(t_j) - \omega(\tau)\big)^2\Big]\Big] \,.
\end{aligned}$$

To determine the mean square limit of a sequence one can first calculate the limit of the average sequence and than verify if the result satisfies the mean square convergence condition (2.107). For the first step the average of the summands in (2.109) has to be derived. These summands consist of two squared increments of the normailzed Wiener process. These increments, we refer to both of

them with $\Delta\omega(\Delta t)$, exhibit the same unconditional probability distribution (2.48) as the Wiener process $\omega(t)$ itself und thus have the same statistical moments as displayed in (2.50), namely

$$\Big\langle \Delta\omega^n(\Delta t)\Big\rangle \;=\; \begin{cases} 0 & \text{for odd } n, \\ (n-1)!!\;(2D\,\Delta t)^{n/2} & \text{for even } n, \text{ with } D=\frac{1}{2}\;. \end{cases} \tag{2.110}$$

These moments applied to the increments $\omega(\tau)-\omega(t_{j-1})$ and $\omega(t_j)-\omega(\tau)$ resolve the limit in equation (2.109).

$$\begin{aligned} &\lim_{n\to\infty}\left\langle \sum_{j=1}^{n}\Big[\big(\omega(\tau)-\omega(t_{j-1})\big)^2-\big(\omega(t_j)-\omega(\tau)\big)^2\Big]\right\rangle \\ &\quad=\lim_{n\to\infty}\sum_{j=1}^{n}\Big[\Big\langle\big(\omega(\tau)-\omega(t_{j-1})\big)^2\Big\rangle-\Big\langle\big(\omega(t_j)-\omega(\tau)\big)^2\Big\rangle\Big] \\ &\quad=\lim_{n\to\infty}\sum_{j=1}^{n}\Big[\big(\tau-t_{j-1}\big)-\big(t_j-\tau\big)\Big] \\ &\quad=\lim_{n\to\infty}\sum_{j=1}^{n}\Big[\big(2\,\alpha-1\big)\;\big(t_j-t_{j-1}\big)\Big] \\ &\quad=\big(2\,\alpha-1\big)\;\big(t-0\big)\;. \end{aligned} \tag{2.111}$$

Now the mean square convergence of the limit (2.111) has to be checked.

$$\lim_{n\to\infty}\left\langle\Big[\sum_{j=1}^{n}\Big[\underbrace{\big(\omega(\tau)-\omega(t_{j-1})\big)^2}_{=:\,\Delta\omega^2_{1-\alpha}(t_j)}-\underbrace{\big(\omega(t_j)-\omega(\tau)\big)^2}_{=:\,\Delta\omega^2_{\alpha}(t_j)}\Big]\;-\;\big(2\,\alpha-1\big)\;t\Big]^2\right\rangle \tag{2.112}$$

$$\begin{aligned} &=\lim_{n\to\infty}\left\langle\sum_{j=1}^{n}\Big[\Delta\omega^4_{1-\alpha}(t_j)\;-\;2\,\Delta\omega^2_{1-\alpha}(t_j)\;\Delta\omega^2_{\alpha}(t_j)\;+\;\Delta\omega^4_{\alpha}(t_j)\Big]\right. \\ &\quad+\;2\sum_{j>k=1}^{n}\Big[\Delta\omega^2_{1-\alpha}(t_j)\;-\;\Delta\omega^2_{\alpha}(t_j)\Big]\;\Big[\Delta\omega^2_{1-\alpha}(t_k)\;-\;\Delta\omega^2_{\alpha}(t_k)\Big] \\ &\quad\left.-\;2\,\big(2\,\alpha-1\big)\;t\;\sum_{j=1}^{n}\Big[\Delta\omega^2_{1-\alpha}(t_j)\;-\;\Delta\omega^2_{\alpha}(t_j)\Big]\;+\;\big(2\,\alpha-1\big)^2\;t^2\right\rangle. \end{aligned}$$

For a Wiener process one can verify that increments $\Delta\omega(t)$ of non-over lapping time intervals $[t,t+\Delta t]$ are statistically independent. Hence we can spread the moment brakets $\langle\ldots\rangle$ as follows

$$\begin{aligned} &=\lim_{n\to\infty}\left(\sum_{j=1}^{n}\Big[\Big\langle\Delta\omega^4_{1-\alpha}(t_j)\Big\rangle-2\Big\langle\Delta\omega^2_{1-\alpha}(t_j)\Big\rangle\Big\langle\Delta\omega^2_{\alpha}(t_j)\Big\rangle+\Big\langle\Delta\omega^4_{\alpha}(t_j)\Big\rangle\Big]\right. \\ &\quad+\;2\sum_{j>k=1}^{n}\Big[\Big\langle\Delta\omega^2_{1-\alpha}(t_j)\Big\rangle-\Big\langle\Delta\omega^2_{\alpha}(t_j)\Big\rangle\Big]\;\Big[\Big\langle\Delta\omega^2_{1-\alpha}(t_k)\Big\rangle-\Big\langle\Delta\omega^2_{\alpha}(t_k)\Big\rangle\Big] \\ &\quad\left.-\;2\,\big(2\,\alpha-1\big)\;t\;\sum_{j=1}^{n}\Big[\Big\langle\Delta\omega^2_{1-\alpha}(t_j)\Big\rangle-\Big\langle\Delta\omega^2_{\alpha}(t_j)\Big\rangle\Big]\;+\;\big(2\,\alpha-1\big)^2\;t^2\right). \end{aligned}$$

Applying equation (2.110) to every moment and then splitting the first sum gives

$$
\begin{aligned}
&= \lim_{n\to\infty} \Bigg(\sum_{j=1}^{n} \Big[3\,(\tau - t_{j-1})^2 \;-\; 2\,(\tau - t_{j-1})\;(t_j - \tau) \;+\; 3\,(t_j - \tau)^2 \Big] \\
&\quad +\; 2 \sum_{j>k=1}^{n} \Big[(\tau - t_{j-1}) \;-\; (t_j - \tau) \Big] \Big[(\tau - t_{k-1}) \;-\; (t_k - \tau) \Big] \\
&\quad -\; 2\,(2\,\alpha - 1)\; t \sum_{j=1}^{n} \Big[(\tau - t_{j-1}) \;-\; (t_j - \tau) \Big] \;+\; (2\,\alpha - 1)^2\; t^2 \Bigg) \\
&= \lim_{n\to\infty} \Bigg(\sum_{j=1}^{n} \Big[2\,(\tau - t_{j-1})^2 \;+\; 2\,(t_j - \tau)^2 \Big] \\
&\quad +\; \sum_{j=1}^{n} \Big[(\tau - t_{j-1}) \;-\; (t_j - \tau) \Big] \Big[(\tau - t_{j-1}) \;-\; (t_j - \tau) \Big] \\
&\quad +\; 2 \sum_{j>k=1}^{n} \Big[(\tau - t_{j-1}) \;-\; (t_j - \tau) \Big] \Big[(\tau - t_{k-1}) \;-\; (t_k - \tau) \Big] \\
&\quad -\; 2\,(2\,\alpha - 1)\; t \sum_{j=1}^{n} \Big[(\tau - t_{j-1}) \;-\; (t_j - \tau) \Big] \;+\; (2\,\alpha - 1)^2\; t^2 \Bigg).
\end{aligned}
$$

The first sum is of order $\mathcal{O}(\frac{1}{n})$ and apporaches 0 for $n \to \infty$, since each summand is proportional to a time interval length squared and thus is of order $\mathcal{O}(\frac{1}{n^2})$. The second sum and the following double sum combine to a single double sum without the limitation $j > k$. This resulting double sum can then be written as a product of two sums.

$$
\begin{aligned}
&= \lim_{n\to\infty} \Bigg(\sum_{j,k=1}^{n} \Big[(\tau - t_{j-1}) \;-\; (t_j - \tau) \Big] \Big[(\tau - t_{k-1}) \;-\; (t_k - \tau) \Big] \\
&\quad -\; 2\,(2\,\alpha - 1)\; t \sum_{j=1}^{n} \Big[(\tau - t_{j-1}) \;-\; (t_j - \tau) \Big] \;+\; (2\,\alpha - 1)^2\; t^2 \Bigg). \\
&= \lim_{n\to\infty} \Bigg(\Big[\sum_{j=1}^{n} \Big[(\tau - t_{j-1}) \;-\; (t_j - \tau) \Big] \Big] \Big[\sum_{k=1}^{n} \Big[(\tau - t_{k-1}) \;-\; (t_k - \tau) \Big] \Big] \\
&\quad -\; 2\,(2\,\alpha - 1)\; t \sum_{j=1}^{n} \Big[(\tau - t_{j-1}) \;-\; (t_j - \tau) \Big] \;+\; (2\,\alpha - 1)^2\; t^2 \Bigg).
\end{aligned}
$$

All sums are now equivalent to the one in equation (2.111) and one finally obtains

$$
\begin{aligned}
&= \lim_{n\to\infty} \Big((2\,\alpha - 1)^2\; t^2 - \; 2\,(2\,\alpha - 1)\; t\; (2\,\alpha - 1)\; t \;+\; (2\,\alpha - 1)^2\; t^2 \Big) \\
&= \quad 0\,. \qquad (2.113)
\end{aligned}
$$

It is thus proven that the defining mean square limit of the stochastic integral (2.108) renders

$$
\int_0^t d\omega(s)\; \omega(s) \;\;=\;\; \frac{1}{2} \Big[\omega^2(t) \;-\; \omega^2(0) \;+\; (2\,\alpha - 1)\; t \Big]\,. \qquad (2.114)
$$

The observed dependence on α can be made plausible. Consider a time interval $[t_{i-1}, t_i]$ in the summation $I_n^{(\alpha)}(t)$ for $G(t) = \omega(t)$. The mean absolute difference of the Wiener process $\omega(t)$ at the left and the right side of the interval $[t_{i-1}, t_i]$ is given by the standard deviation of the difference $\omega(t_i) - \omega(t_{i-1})$

$$\sqrt{\left\langle (\omega(t_i) \, - \, \omega(t_{i-1}))^2 \right\rangle} \;\; = \;\; \sqrt{t_i - t_{i-1}} \; . \tag{2.115}$$

The difference in summing over all values on the left side of the intervals as opposed to the right side is then on average given by

$$\sum_{i=1}^{n} \underbrace{\sqrt{t_i - t_{i-1}}}_{\mathcal{O}\left(\sqrt{1/n}\right)} \underbrace{\left(\omega(t_i) \, - \, \omega(t_{i-1})\right)}_{\mathcal{O}\left(\sqrt{1/n}\right)} \; . \tag{2.116}$$

If we sum over all terms we obtain n-times an expression of order $\mathcal{O}(1/n)$ and consequently a finite value; a finite difference!
If we compare this observation with ordinary calculus we see the essential discrepancy. Consider the integral $\int_0^t dt f(t)$. The difference between evaluating the left and right side of interval $[t_{i-1}, t_i]$ is given by $f'(t_{i-1})\,(t_i - t_{i-1})$. Again the difference of summing over all values $f(t)$ on the left side of the intervals as opposed to the right side is

$$\sum_{i=1}^{n} \underbrace{f'(t_{i-1})\,(t_i - t_{i-1})}_{\mathcal{O}(1/n)} \underbrace{\left(t_i \, - \, t_{i-1}\right)}_{\mathcal{O}(1/n)} \; . \tag{2.117}$$

This sum is of order $\mathcal{O}(1/n)$ and approaches 0 for $n \to \infty$. It is consequently irrelvant which side of the interval $[t_{i-1}, t_i]$ we choose to evaluate $f(t)$.
The underlying cause for the α-dependence of stochastic integrals is evident. It is the $\sqrt{1/n}$-scaling property of stochastic processes! The α-dependence is here to stay. Before we proceed we return once more to our random walker example to gain more insight in the derivations given above.

Gambling on a Random Walk

As in section 2.3 we begin with a random walk on a lattice, this time with $a = \tau^2$ for simplicity. The random walker will be joined by a gambler. Due to his nature the gambler will make a bet at each step trying to forecast the direction the random walker will take. The gambler's strategy is the following. At time t_{j-1} he will take the distance $x(t_{j-1})$ from the origin $x(0)$ as an indication for the direction in which the random walker will proceed. He will bet an amount proportional to $|x(t_{j-1})|$ and claim that the random walker will further increase the distance from the starting point. The investment for each bet will be proportional to the step size $x(t_j) - x(t_{j-1})$; the smaller the steps, the more bets to make, the smaller the amount available for each bet. The pay off or loss $dF(t_j)$ will be proportional to the amount put forward. Hence, $dF(t_{j-1}) \propto (x(t_j) - x(t_{j-1})\, x(t_{j-1})$. Note, that $dF(t_{j-1})$ is positive or negative, if the forecast is true or false respectively. To see if this strategy pays we derive the total loss or gain of the gambler by suming over all bets and taking the mean square limit of $n \to \infty$. One determines

$$F(t) \;\; \propto \;\; \underset{n\to\infty}{\text{ms-lim}} \sum_{j=1}^{n} \left(x(t_j) - x(t_{j-1})\right) \, x(t_{j-1}) \tag{2.118}$$

As the random walk $x(t)$ describes a Wiener process $\omega(t)$ in the limit $n \to \infty$, we can write the above as a stochastic integral with $\alpha = 0$ and obtain

$$\begin{aligned} F(t) &\propto \int_0^t d\omega(s)\ \omega(s) \qquad \text{, with } \alpha = 0 \\ &\propto \frac{1}{2}\Big(x^2(t) - x^2(0) - t\Big) . \end{aligned} \tag{2.119}$$

Except for the extra term t, Eq. (2.119) resembles the result of ordinary calculus. The term t, however, is essential. It prevents the gambler to run a winning strategy. The mean for the overall loss or gain $F(t)$ is

$$\Big\langle F(t)\Big\rangle \ \propto\ \left\langle \frac{1}{2}\Big(x^2(t) - x^2(0) - t\Big)\right\rangle \ =\ \frac{1}{2}\Big(\langle x^2(t)\rangle - t\Big) \ =\ 0 . \tag{2.120}$$

as one might have expected all along.
To consider a case for which the above integral exhibits $\alpha = 1$ we turn to a cheating gambler. Assume that the cheating gambler has a way to tell which direction the random walker will turn next. Thus, at time t_{j-1} he will base his bet on the subsequent position $x(t_j)$ and not on $x(t_{j-1})$, a small, but decisive advantage. If he obeys the same strategy $d\tilde{F}(t_{j-1}) \propto (x(t_j) - x(t_{j-1})\, x(t_j)$ as above, however based on $x(t_j)$ and not $x(t_{j-1})$, he will mimic a similar betting behavior as the honest gambler, especially, when τ goes to 0. Then his insight into the future seems to vanish. Surprisingly as time goes by he will win a fortune $\tilde{F}(t)$ as the following result shows.

$$\begin{aligned} \tilde{F}(t) &\propto \operatorname*{ms\text{-}lim}_{n\to\infty} \sum_{j=1}^{n} \big(x(t_j) - x(t_{j-1})\big)\ x(t_j) \\ &\propto \int_0^t d\omega(s)\ \omega(s) \qquad \text{, with } \alpha = 1 \\ &\propto \frac{1}{2}\Big(x^2(t) - x^2(0) + t\Big) . \end{aligned} \tag{2.121}$$

The mean gain is

$$\Big\langle \tilde{F}(t)\Big\rangle \ \propto\ \left\langle \frac{1}{2}\Big(x^2(t) - x^2(0) + t\Big)\right\rangle \ =\ t . \tag{2.122}$$

A statistical analysis can detect the cheating gambler. The correlation between a random step $d\omega(t) = x(t_j) - x(t_{j-1})$ and the integrand functions $G[t] = x(t_{j-1})$ and $G[t] = x(t_j)$ reveals for the honest gambler

$$\begin{aligned} \Big\langle x(t_{j-1})\ \big(x(t_j) - x(t_{j-1})\big)\Big\rangle &= \Big\langle x(t_{j-1})\Big\rangle \Big\langle x(t_j) - x(t_{j-1})\Big\rangle \\ &= 0 , \end{aligned} \tag{2.123}$$

and for the cheating colleague

$$\begin{aligned} \Big\langle x(t_j)\ \big(x(t_j) - x(t_{j-1})\big)\Big\rangle &= \Big\langle \big(x(t_{j-1}) + x(t_j) - x(t_{j-1})\big)\ \big(x(t_j) - x(t_{j-1})\big)\Big\rangle \\ &= \Big\langle x(t_{j-1})\ \big(x(t_j) - x(t_{j-1})\big)\Big\rangle \ +\ \Big\langle \big(x(t_j) - x(t_{j-1})\big)^2\Big\rangle \\ &= \big(t_j - t_{j-1}\big). \end{aligned} \tag{2.124}$$

The honest gambling scheme is not correlated to the imminent random step, the cheating scheme however is. One therefore distinguishes between so-called *non-anticipating* and *anticipating* functions. It is obvious that correlations between an integrand $G(t)$ and the integration steps $d\omega(t)$ accumulate and that they have an overall effect on the integral as seen in this example.
We will no longer pursuit this exciting money making scheme, since it has one unfortunate draw back; one has to bet infinitely fast!

Ito's Rules

We have seen that it is not admissable to neglect the α-dependence. Nevertheless it is possible to develope a consistent calculus by assuming a fixed value for parameter α. There are two popular approaches, each with distinct benefits and disadvantages:

$$\begin{aligned} \alpha &= 0 \quad \text{Ito calculus,} \\ \alpha &= \frac{1}{2} \quad \text{Stratonovich calculus.} \end{aligned}$$

The Stratonovich calculus with $\alpha = 1/2$ exhibits the same integration rules as ordinary calculus. It also models processes with finite correlation time correctly. However, the rules for the Ito calculus are easier to derive. In many instances corresponding derivations are impossible in the Stratonovich case. Hence we begin with an introduction to Ito calculus. Later, in section 2.6 we will compare the Ito and Stratonovich approach. In any case, we have to keep in mind, that the choice of $\alpha = 0$ or $\alpha = 1/2$ is not arbitrary and has to be justified when modeling physical processes with stochastic differential and corresponding integral equations. For now we set $\alpha = 0$.
The foundation of Ito calculus are the four rules

$$d\omega_i(t)\; d\omega_j(t) = \delta_{ij}\; dt\;, \tag{2.125}$$

$$[d\omega(t)]^N = 0\;, \text{for } N > 2\;, \tag{2.126}$$

$$d\omega(t)^N\; dt = 0\;, \text{for } N \geq 1\;, \tag{2.127}$$

$$dt^N = 0\;, \text{for } N > 1\;. \tag{2.128}$$

As with distributions, like the Dirac delta function $\delta(x)$, these rules (2.125-2.128) have to be seen in the context of integration. Furthermore the integration has to be over so-called non-anticipating functions or processes $G(t)$. This will become clear as we proof rule (2.125) for the one-dimensional case.
Rules (2.125) and (2.126) have to be read as

$$\int_0^t [d\omega(s)]^N\; G(s) = \underset{n\to\infty}{\text{ms-lim}} \sum_{i=1}^{n} G(t_{i-1})\; [\Delta\omega(t_i)]^N \tag{2.129}$$

$$= \begin{cases} \displaystyle\int_0^t ds\; G(s) & \text{, for } N = 2 \\ 0 & \text{, for } N > 2\;, \end{cases} \tag{2.130}$$

for a non-anticipating function $G(t)$ that is statistcally independent of $(\omega(s) - \omega(t))$ for any $s > t$.

$$\Big\langle G[t]\; \big(\omega(s) - \omega(t)\big) \Big\rangle = 0\;, \quad \text{for } t < s\;. \tag{2.131}$$

To prove rule (2.125) we have to show that the following mean square limit vanishes:

$$\left\langle \left[\int_0^t [d\omega(s)]^2 \; G(s) \; - \int_0^t ds \; G(s) \right]^2 \right\rangle \tag{2.132}$$

$$= \underset{n\to\infty}{\text{ms-lim}} \left\langle \left[\sum_{i=1}^{n} \left(\Delta\omega^2(\Delta t_i) \; - \; \Delta t_i \right) \; G(t_{i-1}) \right]^2 \right\rangle$$

$$= \underset{n\to\infty}{\text{ms-lim}} \left\langle \sum_{i=1}^{n} \underbrace{G^2(t_{i-1})}_{\text{stat. indep.}} \; \underbrace{\left(\Delta\omega^2(\Delta t_i) - \Delta t_i \right)^2}_{\text{stat. independent}} \right\rangle$$

$$+ \underset{n\to\infty}{\text{ms-lim}} \left\langle \sum_{i>j=1}^{n} \underbrace{G(t_{i-1})\, G(t_{j-1}) \; \left(\Delta\omega^2(\Delta t_j) - \Delta t_j \right)}_{\text{stat. independent}} \; \underbrace{\left(\Delta\omega^2(\Delta t_i) - \Delta t_i \right)}_{\text{stat. independent}} \right\rangle \; . \tag{2.133}$$

Each of the above underbraced terms is statistically independent of the other underbraced factor. Here the non-anticipation property (2.131) of $G(t)$ comes into play! We obtain

$$I = \underset{n\to\infty}{\text{ms-lim}} \sum_{i=1}^{n} \left\langle G^2(t_{i-1}) \right\rangle \; \underbrace{\left\langle \left(\Delta\omega^2(\Delta t_i) - \Delta t_i \right)^2 \right\rangle}_{= 2\Delta t_i^2, \text{ due to (2.110)}}$$

$$+ \underset{n\to\infty}{\text{ms-lim}} \sum_{i>j=1}^{n} \left\langle G(t_{i-1})\, G(t_{j-1}) \; \left(\Delta\omega^2(\Delta t_j) - \Delta t_j \right) \right\rangle \; \underbrace{\left\langle \left(\Delta\omega^2(\Delta t_i) - \Delta t_i \right) \right\rangle}_{= 0, \text{ due to (2.110)}}$$

$$= \underset{n\to\infty}{\text{ms-lim}} \; 2 \sum_{i>j=1}^{n} \left\langle G^2(t_{i-1}) \right\rangle \; \Delta t_i^2 \; . \tag{2.134}$$

As Δt_i^2 is of order $\mathcal{O}(1/n^2)$ and as long as $G(s)$ is a bounded function, the above sum vanishes as $n \to \infty$. Thus, we have proven Ito's first rule (2.125). All the other rules are shown in a similar fashion.

Ito's Formula

Combining the stochastic differential equation (2.3) and Ito's rules we can derive another important equation, the so-called Ito's formula. Let $f[x(t)]$ be an arbitrary function of a process $x(t)$ that satisfies the one-dimensional sochastic differential equation

$$dx(t) \;\; = \;\; \Big(a[x(t),t] \; + \; b[x(t),t] \; \xi(t) \Big) \; dt \;\; = \;\; a[x(t),t] \; dt \; + \; b[x(t),t] \; d\omega(t) \; . \tag{2.135}$$

To determine the change of $f[x(t)]$ with respect to dx and dt we perform a Taylor expansion

$$\begin{aligned} df[x(t)] = \;& f[x(t) + dx(t)] \; - \; f[x(t)] \\ = \;& f'[x(t)] \; dx(t) \; + \; \frac{1}{2} f''[x(t)] \; dx^2(t) \; + \; \mathcal{O}\big(dx^3(t)\big) \; . \end{aligned}$$

Substituting equation (2.135) for dx we can write

$$\begin{aligned} df[x(t)] = \;& f'[x(t)] \; a[x(t),t] \; dt \; + \; f'[x(t)] \; b[x(t),t] \; d\omega(t) \\ & + \; \frac{1}{2} f''[x(t)] \; \Big(b[x(t),t] \; d\omega(t) \Big)^2 \; + \; \mathcal{O}\big(d\omega^3(t)\big) \; \mathcal{O}\big(dt^2\big) \; . \end{aligned}$$

We can neglect higher orders of $d\omega(t)$ and dt due to Ito's rules (2.126 - 2.128). We can also substitute $d\omega^2(t)$ by dt due to (2.125) and obatin

$$\begin{aligned} df[x(t)] = \;& f'[x(t)]\; a[x(t),t]\; dt \;+\; f'[x(t)]\; b[x(t),t]\; d\omega(t) \\ & +\; \frac{1}{2}\, f''[x(t)]\; \Big(b[x(t),t]\Big)^2\; dt\;. \end{aligned} \tag{2.136}$$

The resulting Ito's formula, now in more than one-dimension, reads

$$\begin{aligned} df[\mathbf{x}(t)] \;=\; & \sum_i\; A_i\Big(\partial_i\, f[\mathbf{x}(t)]\Big)\; dt \;+\; \sum_{i,j}\; \mathsf{B_{ij}}\Big(\partial_\mathsf{i}\, \mathsf{f}[\mathbf{x}(\mathsf{t})]\Big)\; \mathsf{d}\omega_\mathsf{j}(\mathsf{t}) \\ & +\; \frac{1}{2}\sum_{i,j,k}\; \mathsf{B_{ik}}\; \mathsf{B_{jk}}\Big(\partial_\mathsf{i}\partial_\mathsf{j}\, \mathsf{f}[\mathbf{x}(\mathsf{t})]\Big)\; \mathsf{dt}\;. \end{aligned} \tag{2.137}$$

This formula is most helpful when one has to find a relation between the stochastic differential equation (2.3) of $\mathbf{x}(t)$ and a distribution function $f[\mathbf{x}(t)]$. We will utilize Ito's formula in the next section where we will derive the Fokker-Planck equation.

2.5 Fokker-Planck Equations

Again we consider the stochastic differential equation (2.3) with a noise term characterized through white noise, i.e., Eq. (2.97)

$$\partial_t\, \boldsymbol{x}(t) = \boldsymbol{A}[\boldsymbol{x}(t),t] + \mathbf{B}[\boldsymbol{x}(\mathbf{t}),\mathbf{t}]\cdot\boldsymbol{\eta}(\mathbf{t}) \tag{2.138}$$

assuming $\boldsymbol{\eta}(t) = \boldsymbol{\xi}(t)$ with

$$\Big\langle \xi_i(t) \Big\rangle \;=\; 0 \tag{2.139}$$

$$\Big\langle \xi_i(t_1)\, \xi_j(t_0) \Big\rangle\; (dt)^2 \;=\; \delta_{ij}\; \delta(t_1 - t_0)\; dt\;. \tag{2.140}$$

For the sake of Ito's calculus one has to assume that coefficient $\mathbf{B}[\boldsymbol{x}(\mathbf{t}),\mathbf{t}]$ is a non-anticipating function. With this in mind we neglect the arguments $\boldsymbol{x}(t)$ and t of $\boldsymbol{A}$ and $\mathbf{B}$ for easier reading in the rest of this section.
We utilize the result of the section 2.4 and exploit the properties of white noise (2.96, 2.97) by considering the average of Ito's formula (2.137).

$$\begin{aligned} \Big\langle df[\boldsymbol{x}(t)] \Big\rangle \;=\; & \sum_i\; \Big\langle A_i\,\big(\partial_i\, f[\boldsymbol{x}(t)]\big)\; dt \Big\rangle \;+\; \sum_{i,j}\; \Big\langle \mathsf{B_{ij}}\,\big(\partial_\mathsf{i}\, \mathsf{f}[\boldsymbol{x}(\mathsf{t})]\big)\; \mathsf{d}\omega_\mathsf{j}(\mathsf{t}) \Big\rangle \\ & +\; \frac{1}{2}\sum_{i,j,k}\; \Big\langle \mathsf{B_{ik}}\, \mathsf{B_{jk}}\,\big(\partial_\mathsf{i}\partial_\mathsf{j}\, \mathsf{f}[\boldsymbol{x}(\mathsf{t})]\big)\; \mathsf{dt} \Big\rangle\;. \end{aligned} \tag{2.141}$$

The second sum on the r.h.s. vanishes, since $\mathbf{B}[\boldsymbol{x}(\mathbf{t}),\mathbf{t}]$ and $\partial_i f[\boldsymbol{x}(t)]$ are non-anticipating functions and therefore statistically independent of $d\omega_j(t)$, and because of equation (2.139) considering that $d\omega_j(t) = \xi_j(t)\, dt$.

$$\Big\langle \mathsf{B_{ij}}\,\big(\partial_\mathsf{i}\, \mathsf{f}[\boldsymbol{x}(\mathsf{t})]\big)\; \mathsf{d}\omega_\mathsf{j}(\mathsf{t}) \Big\rangle \;=\; \Big\langle \mathsf{B_{ij}}\,\big(\partial_\mathsf{i}\, \mathsf{f}[\boldsymbol{x}(\mathsf{t})]\big) \Big\rangle\; \underbrace{\Big\langle \xi_j(t) \Big\rangle}_{=\,0}\; \mathsf{dt} \;=\; 0\;. \tag{2.142}$$

One is left with equation

$$\left\langle \frac{d}{dt} f[\boldsymbol{x}(t)] \right\rangle \;=\; \sum_i \left\langle A_i\big(\partial_i f[\boldsymbol{x}(t)]\big)\right\rangle \;+\; \frac{1}{2}\sum_{i,j}\left\langle [\mathbf{B}\cdot\mathbf{B^T}]_{\mathbf{ij}}\left(\partial_{\mathbf{i}}\partial_{\mathbf{j}}\,\mathbf{f}[\boldsymbol{x}(\mathbf{t})]\right)\right\rangle . \tag{2.143}$$

According to definition (2.12) $\langle f[\boldsymbol{x}(t)]\rangle$ can be expressed as

$$\left\langle f[\boldsymbol{x}(t)]\right\rangle \;=\; \int d\boldsymbol{x}\; f[\boldsymbol{x}]\; p(\boldsymbol{x},t|\boldsymbol{x}_0,t_0)\;. \tag{2.144}$$

The reader should note that the initial value of $\langle f[\boldsymbol{x}(t)]\rangle$ defined through (2.144) is $f[\boldsymbol{x}_0]$ in accordance with the initial condition assumed for Eq. (2.3). Applying the time derivative to the r.h.s. of (2.144) and comparing with (2.143) yields

$$\begin{aligned}&\int d\boldsymbol{x}\; f[\boldsymbol{x}]\;\partial_t\, p(\boldsymbol{x},t|\boldsymbol{x}_0,t_0) \;= \qquad\qquad (2.145)\\ &\qquad \int d\boldsymbol{x}\left(\sum_i A_i\left(\partial_i f[\boldsymbol{x}]\right) \;+\; \frac{1}{2}\sum_{i,j}[\mathbf{B}\cdot\mathbf{B^T}]_{\mathbf{ij}}\left(\partial_{\mathbf{i}}\partial_{\mathbf{j}}\,\mathbf{f}[\boldsymbol{x}]\right)\right)\mathbf{p}(\boldsymbol{x},\mathbf{t}|\boldsymbol{x_0},\mathbf{t_0})\;.\end{aligned}$$

Partial integration assuming a volume Ω with a surface $\partial\Omega$ allows one to change the order of the partial differential operators. For example, the first sum becomes

$$\begin{aligned}\int_\Omega d\boldsymbol{x}\;\sum_i A_i\left(\partial_i f[\boldsymbol{x}]\right) p(\boldsymbol{x},t|\boldsymbol{x}_0,t_0) \;&=\; -\int_\Omega d\boldsymbol{x}\; f[\boldsymbol{x}]\left(\sum_i \partial_i A_i\; p(\boldsymbol{x},t|\boldsymbol{x}_0,t_0)\right)\\ &\quad +\int_\Omega d\boldsymbol{x}\left(\sum_i \partial_i\; A_i\; f[\boldsymbol{x}]\; p(\boldsymbol{x},t|\boldsymbol{x}_0,t_0)\right)\\ &=\; -\int_\Omega d\boldsymbol{x}\; f[\boldsymbol{x}]\left(\sum_i \partial_i A_i\; p(\boldsymbol{x},t|\boldsymbol{x}_0,t_0)\right)\\ &\quad +\int_{\partial\Omega} d\boldsymbol{a}\cdot\boldsymbol{A}\; f[\boldsymbol{x}]\; p(\boldsymbol{x},t|\boldsymbol{x}_0,t_0)\;. \qquad (2.146)\end{aligned}$$

Assuming a $p(\boldsymbol{x},t|\boldsymbol{x}_0,t_0)$ of finite spatial extent, such that it vanishes on the boundary $\partial\Omega$, we can neglect the surface term. Applying the same calculation twice to the second term in (2.145) leads to

$$\begin{aligned}&\int d\boldsymbol{x}\; f[\boldsymbol{x}]\;\partial_t\, p(\boldsymbol{x},t|\boldsymbol{x}_0,t_0) \;= \qquad\qquad (2.147)\\ &\qquad \int d\boldsymbol{x}\; f[\boldsymbol{x}]\left(-\sum_i \partial_i A_i\; p(\boldsymbol{x},t|\boldsymbol{x}_0,t_0) \;+\; \frac{1}{2}\sum_{i,j}\partial_i\partial_j\,[\mathbf{B}\cdot\mathbf{B^T}]_{\mathbf{ij}}\;\mathbf{p}(\boldsymbol{x},\mathbf{t}|\boldsymbol{x_0},\mathbf{t_0})\right).\end{aligned}$$

Since $f[\boldsymbol{x}(t)]$ is arbitrary we can conclude

$$\partial_t\, p(\boldsymbol{x},t|\boldsymbol{x}_0,t_0) \;=\; -\sum_i \partial_i A_i\; p(\boldsymbol{x},t|\boldsymbol{x}_0,t_0) \;+\; \frac{1}{2}\sum_{i,j}\partial_i\partial_j\,[\mathbf{B}\cdot\mathbf{B^T}]_{\mathbf{ij}}\;\mathbf{p}(\boldsymbol{x},\mathbf{t}|\boldsymbol{x_0},\mathbf{t_0})\;. \tag{2.148}$$

This is the celebrated Fokker-Planck equation which describes the time evolution of the probability that the stochastic process determined by (2.3) assumes the value $\boldsymbol{x}$ at time t when it had assumed the value $\boldsymbol{x}_o$ at time t_0.
Note, that the above Fokker-Planck equation holds for the stochastic differential equation (2.3) only within the framework of Ito calculus. The relation between SDE (2.3) and the Fokker-Planck equation (2.148) is slightly different when Stratonovitch calculus is applied!

2.6 Stratonovich Calculus

We take a quick look at Stratonovich calculus mentioned in section 2.4. We want to clarify the α-dependence of our results in sections 2.4 and 2.5. For this purpose it is sufficient to focus on processes satisfying the stochastic differential equation (2.3).
It is possible to show that a solution $\boldsymbol{x}(t)$ of the stochastic differential equation

$$\text{Ito } \alpha = 0: \qquad \partial_t \boldsymbol{x}(t) \;=\; \boldsymbol{A}[\boldsymbol{x}(t),t] \;+\; \mathbf{B}[\boldsymbol{x}(\mathbf{t}),\mathbf{t}] \cdot \boldsymbol{\xi}(\mathbf{t}) \tag{2.149}$$

solves a stochastic differential equation of the same form with different coefficients, this time however according to Stratonovich's calculus.

$$\text{Stratonovich } \alpha = \frac{1}{2}: \qquad \partial_t \boldsymbol{x}(t) \;=\; \overset{\mathcal{S}}{\boldsymbol{A}}[\boldsymbol{x}(t),t] \;+\; \overset{\mathcal{S}}{\mathbf{B}}[\boldsymbol{x}(t),t] \cdot \boldsymbol{\xi}(t)\ . \tag{2.150}$$

We give a derivation for $\overset{\mathcal{S}}{\boldsymbol{A}}[\boldsymbol{x}(t),t]$ and $\overset{\mathcal{S}}{\mathbf{B}}[\boldsymbol{x}(t),t]$ in the one-dimensional case as the lower case coefficients $\overset{\mathcal{S}}{a}[x(t),t]$ and $\overset{\mathcal{S}}{b}[x(t),t]$ indicate. As a first step we solve the integral corresponding to equation (2.150).

$$x(t) \;=\; x(t_0) \;+\; \int_{t_0}^{t} ds\ \overset{\mathcal{S}}{a}[x(s),s] \;+\; \oint_{t_0}^{t} d\omega(s)\ \overset{\mathcal{S}}{b}[x(s),s]\ . \tag{2.151}$$

The $\mathcal{S}$ on the second integral sign denotes a Stratonovich integral which has to be solved like a Riemann-Stieltjes integral as in equation (2.105) with $\alpha = 1/2$. The last term of equation (2.151) is the only one that differs from Ito's calculus and thus it is the only term that needs to be investigated. One can rewrite the last term as an Ito integral. We do so neglecting the mean square limit notation in the defintion of a Stratonovich integral and write

$$\begin{aligned}\oint_{t_0}^{t} d\omega(s)\ \overset{\mathcal{S}}{b}[x(s),s] \;&\simeq\; \sum_i \Big(\omega(t_i)-\omega(t_{i-1})\Big)\ \overset{\mathcal{S}}{b}[x(\tau),\tau]\ , \qquad \text{with } \tau := \frac{1}{2}(t_i+t_{i-1}) \\ &=\; \sum_i \Big(\omega(t_i)-\omega(\tau)\Big)\ \overset{\mathcal{S}}{b}[x(\tau),\tau] \;+\; \sum_i \Big(\omega(\tau)-\omega(t_{i-1})\Big)\ \overset{\mathcal{S}}{b}[x(\tau),\tau]\,. \end{aligned} \tag{2.152}$$

$\overset{\mathcal{S}}{b}[x(\tau),\tau]$ can be approximated by extrapolation starting with $\overset{\mathcal{S}}{b}[x(t_{i-1}),t_{i-1}]$ at the left side of interval $[t_{i-1},t_i]$.

$$\begin{aligned}\overset{\mathcal{S}}{b}[x(\tau),\tau] \;=\; \overset{\mathcal{S}}{b}[x(t_{i-1}),t_{i-1}] \;&+\; \Big(\partial_x\ \overset{\mathcal{S}}{b}[x(t_{i-1}),t_{i-1}]\Big)\ \big(x(\tau)-x(t_{i-1})\big) \\ &+\; \Big(\partial_t\ \overset{\mathcal{S}}{b}[x(t_{i-1}),t_{i-1}]\Big)\ \big(\tau-t_{i-1}\big) \\ &+\; \frac{1}{2}\Big(\partial_x^2\ \overset{\mathcal{S}}{b}[x(t_{i-1}),t_{i-1}]\Big)\ \big(x(\tau)-x(t_{i-1})\big)^2 \;+\; \ldots .\end{aligned} \tag{2.153}$$

Since $x(t)$ is a solution of Ito's stochastic equation (2.149) one can apply (2.149) to determine the infinitesimal displacement $x(\tau)-x(t_{i-1})$.

$$x(\tau)-x(t_{i-1}) \;=\; a[x(t_{i-1}),t_{i-1}]\ \big(\tau-t_{i-1}\big) \;+\; b[x(t_{i-1}),t_{i-1}]\ \big(\omega(\tau)-\omega(t_{i-1})\big)\ . \tag{2.154}$$

Filling equation (2.154) into (2.153) and applying Ito's rules (2.128) to the infinitesimal displacements $dt = (\tau - t_{i-1})$ and $d\omega(t) = \big(\omega(\tau) - \omega(t_{i-1})\big)$ one obtains

$$\begin{aligned}
\overset{s}{b}[x(\tau),\tau] &= \overset{s}{b}[x(t_{i-1}),t_{i-1}] + \Big(\partial_t\, \overset{s}{b}[x(t_{i-1}),t_{i-1}]\Big)\,(\tau - t_{i-1}) \\
&+ a[x(t_{i-1}),t_{i-1}]\,\Big(\partial_x\, \overset{s}{b}[x(t_{i-1}),t_{i-1}]\Big)\,(\tau - t_{i-1}) \\
&+ b[x(t_{i-1}),t_{i-1}]\,\Big(\partial_x\, \overset{s}{b}[x(t_{i-1}),t_{i-1}]\Big)\,\Big(\omega(\tau) - \omega(t_{i-1})\Big) \\
&+ \frac{1}{2}\, b^2[x(t_{i-1}),t_{i-1}]\,\Big(\partial_x^2\, \overset{s}{b}[x(t_{i-1}),t_{i-1}]\Big)\,(\tau - t_{i-1}) \qquad (2.155)
\end{aligned}$$

Substituting the above result (2.155) into the second sum of equation (2.152) one derives

$$\begin{aligned}
\oint_{t_0}^{t} d\omega(s)\; \overset{s}{b}[x(s),s] &\simeq \sum_i \Big(\omega(t_i) - \omega(\tau)\Big)\; \overset{s}{b}[x(\tau),\tau] \\
&+ \sum_i \Big(\omega(\tau) - \omega(t_{i-1})\Big)\; \overset{s}{b}[x(t_{i-1}),t_{i-1}] \\
&+ \sum_i \underbrace{\Big(\omega(\tau) - \omega(t_{i-1})\Big)\,(\tau - t_{i-1})}_{=0,\text{ due to (2.127)}}\,\Big(\partial_t\, \overset{s}{b}[x(t_{i-1}),t_{i-1}]\Big) \\
&+ \sum_i \underbrace{\Big(\omega(\tau) - \omega(t_{i-1})\Big)\,(\tau - t_{i-1})}_{=0,\text{ due to (2.127)}}\; a[x(t_{i-1})]\,\Big(\partial_x\, \overset{s}{b}[x(t_{i-1}),t_{i-1}]\Big) \\
&+ \sum_i \underbrace{\Big(\omega(\tau) - \omega(t_{i-1})\Big)^2}_{=(\tau - t_{i-1}),\text{ due to (2.125)}}\; b[x(t_{i-1}),t_{i-1}]\,\Big(\partial_x\, \overset{s}{b}[x(t_{i-1}),t_{i-1}]\Big) \\
&+ \frac{1}{2}\sum_i \underbrace{\Big(\omega(\tau) - \omega(t_{i-1})\Big)\,(\tau - t_{i-1})}_{=0,\text{ due to (2.127)}}\; b^2[x(t_{i-1}),t_{i-1}]\,\Big(\partial_x^2\, \overset{s}{b}[x(t_{i-1}),t_{i-1}]\Big)\,. \qquad (2.156)
\end{aligned}$$

The first two terms on the r.h.s. of equation (2.156) make up a sum that approximates an Ito integral with time steps just half the size. In the fifth term one can replace $(\tau - t_{i-1})$ by $\frac{1}{2}(t_i - t_{i-1})$. The result, again written for the multi-dimensional case, is

$$\oint_{t_0}^{t} d\boldsymbol{\omega}(s)\cdot \overset{s}{\mathbf{B}}{}^{T}[\boldsymbol{x}(s),s] = \int_{t_0}^{t} d\boldsymbol{\omega}(s)\cdot \overset{s}{\mathbf{B}}{}^{T}[\boldsymbol{x}(s),s] + \frac{1}{2}\int_{t_0}^{t} ds \sum_{i,j} \mathsf{B}_{\mathsf{ij}}[\boldsymbol{x}(\mathsf{s}),\mathsf{s}]\,\Big(\partial_{\mathsf{i}}\, \overset{s}{\mathsf{B}}{}^{\mathsf{T}}_{\mathsf{jk}}[\boldsymbol{x}(\mathsf{s}),\mathsf{s}]\Big). \qquad (2.157)$$

Note, that the above connection (2.157) between Ito and Stratonovich integrals only holds for $\boldsymbol{x}(t)$ satisfying Ito's SDE (2.149) or Stratonovich's SDE (2.150). There is no *general* connection between Ito and Stratonovich integrals!

Substituting (2.157) into Stratonovich's integral equation (2.151) and comparing the coefficients with the integral solving Ito's stochastic differential equation (2.149) we obtain the following relations

$$A_k = \overset{s}{A}_k + \frac{1}{2}\sum_{i,j} \overset{s}{\mathsf{B}}_{ij}\,\Big(\partial_i\, \overset{s}{\mathsf{B}}_{kj}\Big)\,, \qquad (2.158)$$

$$\mathsf{B}_{jk} = \overset{s}{\mathsf{B}}_{jk}\,, \qquad (2.159)$$

and conversely

$$\overset{S}{A}_k = A_k - \frac{1}{2}\sum_{i,j} \mathsf{B}_{ij}\left(\partial_i \mathsf{B}_{kj}\right) , \tag{2.160}$$

$$\overset{S}{\mathsf{B}}_{jk} = \mathsf{B}_{jk} . \tag{2.161}$$

We see that a difference between Ito and Stratonovich calculus only occurs, if $\mathbf{B}$ depends on $\boldsymbol{x}(t)$, that is if $\partial_i \mathsf{B}_{kj} \neq 0$.
To conclude this section we write down the Fokker-Planck equation in Stratonovich's terms. One simply substitutes the coefficients $\boldsymbol{A}$ and $\mathbf{B}$ according to equations (2.158) and (2.159), and applies the product rule for differential operations to simplify the expression.

$$\partial_t\, p(\boldsymbol{x},t|\boldsymbol{x}_0,t_0) = -\sum_i \partial_i \overset{S}{A}_i\; p(\boldsymbol{x},t|\boldsymbol{x}_0,t_0) + \frac{1}{2}\sum_{i,j,k} \partial_i \overset{S}{\mathsf{B}}_{ik}\Big(\partial_j \overset{S}{\mathsf{B}}_{jk}\; p(\boldsymbol{x},t|\boldsymbol{x}_0,t_0)\Big) . \tag{2.162}$$

2.7 Appendix: Normal Distribution Approximation

2.7.1 Stirling's Formula

We need Stirling's formula (2.163, 2.164) to prove Gauß's asymptotic approximation (2.165) of the binomial distribution. A derivation of Stirling's formula is outside the scope of this book. See [43] for a derivation based on Euler's summation formula.

$$n! \;=\; \sqrt{2\pi n}\,\left(\frac{n}{e}\right)^n\,\left(1+\mathcal{O}\left(\frac{1}{n}\right)\right) \tag{2.163}$$

$$\begin{aligned}\ln n! \;&=\; \ln\!\left(\sqrt{2\pi n}\,\left(\frac{n}{e}\right)^n\right) \;+\; \ln\!\left(1+\mathcal{O}\left(\frac{1}{n}\right)\right)\\ \ln n! \;&=\; \frac{1}{2}\ln(2\pi) \;+\; (n+\frac{1}{2})\ln n \;-\; n \;+\; \mathcal{O}\left(\frac{1}{n}\right)\end{aligned} \tag{2.164}$$

2.7.2 Binomial Distribution

We set forth to prove Eq. (2.165), i.e.,

$$\sqrt{\frac{n}{2}}\,2^{-n}\,\binom{n}{\frac{n}{2}+x\sqrt{\frac{n}{2}}} \;=\; \frac{1}{\sqrt{\pi}}\,\exp -x^2\,\left(1+\mathcal{O}\left(\frac{1}{n}\right)\right)\;. \tag{2.165}$$

Applying the natural logarithm on both sides of this equation we obtain

$$\begin{aligned}\ln\!\left[\sqrt{\frac{n}{2}}\,2^{-n}\,\binom{n}{\frac{n}{2}+x\sqrt{\frac{n}{2}}}\right] \;&=\; \ln\!\left(\frac{1}{\sqrt{\pi}}\,\exp -x^2\right) \;+\; \ln\!\left(1+\mathcal{O}\left(\frac{1}{n}\right)\right)\\ \ln\!\left[\sqrt{\frac{n}{2}}\,2^{-n}\,\binom{n}{\frac{n}{2}+x\sqrt{\frac{n}{2}}}\right] \;&=\; -\frac{1}{2}\ln\pi \;-\; x^2 \;+\; \mathcal{O}\left(\frac{1}{n}\right)\;.\end{aligned} \tag{2.166}$$

We will prove equation (2.166) by transforming the left hand side step by step. First, we utilize the formula $\binom{n}{k}=\frac{n!}{k!(n-k)!}$ for binomial coefficients.

$$\begin{aligned}&\ln\!\left(\sqrt{\frac{n}{2}}\,2^{-n}\,\binom{n}{\frac{n}{2}+x\sqrt{\frac{n}{2}}}\right) \qquad (2.167)\\ &=\; \frac{1}{2}\,(\ln n-\ln 2) \;-\; n\ln 2 \;+\; \ln\!\left(\frac{n!}{(\frac{n}{2}+x\sqrt{\frac{n}{2}})!\,(\frac{n}{2}-x\sqrt{\frac{n}{2}})!}\right)\\ &=\; \frac{1}{2}\ln n \;-\; \left(n+\frac{1}{2}\right)\ln 2 \;+\; \ln n! \;-\; \ln\!\left[\left(\frac{n}{2}+x\sqrt{\frac{n}{2}}\right)!\right] \;-\; \ln\!\left[\left(\frac{n}{2}-x\sqrt{\frac{n}{2}}\right)!\right]\;.\end{aligned}$$

Applying Stirling's formula (2.164) we derive furthermore

$$\begin{aligned}&=\; \frac{1}{2}\ln n \;-\; \left(n+\frac{1}{2}\right)\ln 2 \;+\; \frac{1}{2}\ln(2\pi) \;+\; (n+\frac{1}{2})\ln n \;-\; n \;+\\ &\quad-\; \frac{1}{2}\ln(2\pi) \;-\; \left(\frac{n}{2}+x\sqrt{\frac{n}{2}}+\frac{1}{2}\right)\ln\!\left(\frac{n}{2}+x\sqrt{\frac{n}{2}}\right) \;+\; \frac{n}{2} \;+\; x\sqrt{\frac{n}{2}} \;+\\ &\quad-\; \frac{1}{2}\ln(2\pi) \;-\; \left(\frac{n}{2}-x\sqrt{\frac{n}{2}}+\frac{1}{2}\right)\ln\!\left(\frac{n}{2}-x\sqrt{\frac{n}{2}}\right) \;+\; \frac{n}{2} \;-\; x\sqrt{\frac{n}{2}}\end{aligned}$$

$$
\begin{aligned}
&= \frac{1}{2}\ln n \;-\; \left(n+\frac{1}{2}\right)\ln 2 \;-\; \frac{1}{2}\ln(2\pi) \;+\; (n+\frac{1}{2})\ln n \;+ \\
&\quad -\; \left(\frac{n}{2} + x\sqrt{\frac{n}{2}}+\frac{1}{2}\right)\ln\left[\frac{n}{2}\left(1+x\sqrt{\frac{2}{n}}\right)\right] \;+ \\
&\quad -\; \left(\frac{n}{2} - x\sqrt{\frac{n}{2}}+\frac{1}{2}\right)\ln\left[\frac{n}{2}\left(1-x\sqrt{\frac{2}{n}}\right)\right] \\
&= (n+1)\ln n \;-\; \left(n+\frac{1}{2}\right)\ln 2 \;-\; \frac{1}{2}\ln 2 \;-\; \frac{1}{2}\ln\pi \;+ \\
&\quad -\; \left(\frac{n}{2} + x\sqrt{\frac{n}{2}}+\frac{1}{2}\right)\left(\ln\frac{n}{2} + \ln\left(1+x\sqrt{\frac{2}{n}}\right)\right) \;+ \\
&\quad -\; \left(\frac{n}{2} - x\sqrt{\frac{n}{2}}+\frac{1}{2}\right)\left(\ln\frac{n}{2} + \ln\left(1-x\sqrt{\frac{2}{n}}\right)\right) \;.
\end{aligned}
$$

Performing a Taylor expansion of $\ln(1 \pm z)$ with respect to z we obtain,

$$
\begin{aligned}
&= (n+1)\ln n \;-\; (n+1)\ln 2 \;-\; \frac{1}{2}\ln\pi \;+ \\
&\quad -\; \left(\frac{n}{2} + x\sqrt{\frac{n}{2}}+\frac{1}{2}\right)\left(\ln\frac{n}{2} + x\sqrt{\frac{2}{n}} - \frac{x^2}{n} + \frac{x^3}{3}\sqrt{\frac{8}{n^3}} + \mathcal{O}\left(\frac{1}{n^2}\right)\right) \;+ \\
&\quad -\; \left(\frac{n}{2} - x\sqrt{\frac{n}{2}}+\frac{1}{2}\right)\left(\ln\frac{n}{2} - x\sqrt{\frac{2}{n}} - \frac{x^2}{n} - \frac{x^3}{3}\sqrt{\frac{8}{n^3}} + \mathcal{O}\left(\frac{1}{n^2}\right)\right) \;,
\end{aligned}
$$

and expanding the products up to order $\mathcal{O}(1/n)$ we acquire the result, the right hand side of equation (2.166), results in

$$
\begin{aligned}
&= (n+1)(\ln n - \ln 2) \;-\; \frac{1}{2}\ln\pi \;+ \\
&\quad -\; \frac{n}{2}\ln\frac{n}{2} \;-\; x\sqrt{\frac{n}{2}} \;+\; \frac{x^2}{2} \;-\; \frac{x^3}{3}\sqrt{\frac{2}{n}} \;-\; x\sqrt{\frac{n}{2}}\ln\frac{n}{2} \;+ \\
&\qquad -\; x^2 \;+\; \frac{x^3}{\sqrt{2n}} \;-\; \frac{1}{2}\ln\frac{n}{2} \;-\; \frac{x}{\sqrt{2n}} \;+\; \mathcal{O}\left(\frac{1}{n}\right) \;+ \\
&\quad -\; \frac{n}{2}\ln\frac{n}{2} \;+\; x\sqrt{\frac{n}{2}} \;+\; \frac{x^2}{2} \;+\; \frac{x^3}{3}\sqrt{\frac{2}{n}} \;+\; x\sqrt{\frac{n}{2}}\ln\frac{n}{2} \;+ \\
&\qquad -\; x^2 \;-\; \frac{x^3}{\sqrt{2n}} \;-\; \frac{1}{2}\ln\frac{n}{2} \;+\; \frac{x}{\sqrt{2n}} \;+\; \mathcal{O}\left(\frac{1}{n}\right) \\
&= (n+1)\ln\frac{n}{2} \;-\; \frac{1}{2}\ln\pi \;+ \\
&\quad -\; n\ln\frac{n}{2} \;-\; x^2 \;-\; \ln\frac{n}{2} \;+\; \mathcal{O}\left(\frac{1}{n}\right) \\
&= -\frac{1}{2}\ln\pi \;-\; x^2 \;+\; \mathcal{O}\left(\frac{1}{n}\right) \qquad \text{q.e.d.}
\end{aligned}
$$

Chapter 3

Einstein Diffusion Equation

Contents

3.1 Derivation and Boundary Conditions 37
3.2 Free Diffusion in One-dimensional Half-Space 40
3.3 Fluorescence Microphotolysis 44
3.4 Free Diffusion around a Spherical Object 48
3.5 Free Diffusion in a Finite Domain 57
3.6 Rotational Diffusion 60

In this chapter we want to consider the theory of the Fokker-Planck equation for molecules moving under the influence of random forces in force-free environments. Examples are molecules involved in Brownian motion in a fluid. Obviously, this situation applies to many chemical and biochemical system and, therefore, is of great general interest. Actually, we will assume that the fluids considered are viscous in the sense that we will neglect the effects of inertia. The resulting description, referred to as Brownian motion in the *limit of strong friction*, applies to molecular systems except if one considers very brief time intervals of a picosecond or less. The general case of Brownian motion for arbitrary friction will be covered further below.

3.1 Derivation and Boundary Conditions

Particles moving in a liquid without forces acting on the particles, other than forces due to random collisions with liquid molecules, are governed by the Langevin equation

$$m\,\ddot{\boldsymbol{r}} \;=\; -\gamma\,\dot{\boldsymbol{r}} \;+\; \sigma\,\boldsymbol{\xi}(t) \tag{3.1}$$

In the *limit of strong friction* holds

$$|\gamma\,\dot{\boldsymbol{r}}| \;\gg\; |m\,\ddot{\boldsymbol{r}}| \tag{3.2}$$

and, (3.1) becomes

$$\gamma\,\dot{\boldsymbol{r}} \;=\; \sigma\,\boldsymbol{\xi}(t)\;. \tag{3.3}$$

To this stochastic differential equation corresponds the Fokker-Planck equation [c.f. (2.138) and (2.148)]

$$\partial_t\, p(\boldsymbol{r},t|\boldsymbol{r}_0,t_0) \;=\; \nabla^2\,\frac{\sigma^2}{2\gamma^2}\; p(\boldsymbol{r},t|\boldsymbol{r}_0,t_0)\;. \tag{3.4}$$

We assume in this chapter that σ and γ are spatially independent such that we can write

$$\partial_t\, p(\boldsymbol{r},t|\boldsymbol{r}_0,t_0) \;=\; \frac{\sigma^2}{2\gamma^2}\;\nabla^2\, p(\boldsymbol{r},t|\boldsymbol{r}_0,t_0)\;. \tag{3.5}$$

This is the celebrated *Einstein diffusion equation* which describes microscopic transport of material and heat.
In order to show that the Einstein diffusion equation (3.5) reproduces the well-known diffusive behaviour of particles we consider the mean square displacement of a particle described by this equation, i.e., $\left\langle (\,\boldsymbol{r}(t)-\boldsymbol{r}(t_0)\,)^2\right\rangle \sim t$. We first note that the mean square displacement can be expressed by means of the solution of (3.5) as follows

$$\left\langle \big(\,\boldsymbol{r}(t)-\boldsymbol{r}(t_0)\,\big)^2\right\rangle \;=\; \int_{\Omega_\infty} d^3r\;\big(\,\boldsymbol{r}(t)-\boldsymbol{r}(t_0)\,\big)^2\; p(\boldsymbol{r},t|\boldsymbol{r}_0,t_0)\;. \tag{3.6}$$

Integration over Eq. (3.5) in a similar manner yields

$$\frac{d}{dt}\left\langle \big(\,\boldsymbol{r}(t)-\boldsymbol{r}(t_0)\,\big)^2\right\rangle \;=\; \frac{\sigma^2}{2\gamma^2}\;\int_{\Omega_\infty} d^3r\;\big(\,\boldsymbol{r}(t)-\boldsymbol{r}(t_0)\,\big)^2\;\nabla^2\, p(\boldsymbol{r},t|\boldsymbol{r}_0,t_0)\;. \tag{3.7}$$

Applying Green's theorem for two functions $u(\boldsymbol{r})$ and $v(\boldsymbol{r})$

$$\int_{\Omega_\infty} d^3r\;\big(\,u\nabla^2 v\;-\;v\nabla^2 u\,\big) \;=\; \int_{\partial\Omega_\infty} d\boldsymbol{a}\cdot\big(\,u\boldsymbol{\nabla}v\;-\;v\boldsymbol{\nabla}u\,\big) \tag{3.8}$$

for an infinite volume Ω and considering the fact that $p(\boldsymbol{r},t|\boldsymbol{r}_0,t_0)$ must vanish at infinity we obtain

$$\frac{d}{dt}\,\left\langle \big(\,\boldsymbol{r}(t)-\boldsymbol{r}(t_0)\,\big)^2\right\rangle \;=\; \frac{\sigma^2}{2\gamma^2}\;\int_{\Omega_\infty} d^3r\; p(\boldsymbol{r},t|\boldsymbol{r}_0,t_0)\;\nabla^2\,\big(\,\boldsymbol{r}-\boldsymbol{r}_0\,\big)^2\;. \tag{3.9}$$

With $\nabla^2\,(\,\boldsymbol{r}-\boldsymbol{r}_0\,)^2 = 6$ this is

$$\frac{d}{dt}\,\left\langle \big(\,\boldsymbol{r}(t)-\boldsymbol{r}(t_0)\,\big)^2\right\rangle \;=\; 6\,\frac{\sigma^2}{2\gamma^2}\;\int_{\Omega_\infty} d^3r\; p(\boldsymbol{r},t|\boldsymbol{r}_0,t_0)\;. \tag{3.10}$$

We will show below that the integral on the r.h.s. remains constant as long as one does not assume the existence of chemical reactions. Hence, for a reaction free case we can conclude

$$\left\langle \big(\,\boldsymbol{r}(t)-\boldsymbol{r}(t_0)\,\big)^2\right\rangle \;=\; 6\,\frac{\sigma^2}{2\,\gamma^2}\;t\;. \tag{3.11}$$

For diffusing particles one expects for this quantity a behaviour $6D(t-t_0)$ where D is the diffusion coefficient. Hence, the calculated dependence describes a diffusion process with diffusion coefficient

$$D = \frac{\sigma^2}{2\,\gamma^2}\;. \tag{3.12}$$

One can write the *Einstein diffusion equation* accordingly

$$\partial_t\, p(\boldsymbol{r},t|\boldsymbol{r}_0,t_0) \;=\; D\;\nabla^2\, p(\boldsymbol{r},t|\boldsymbol{r}_0,t_0)\;. \tag{3.13}$$

We have stated before that the Wiener process describes a diffusing particle as well. In fact, the three-dimensional generalization of (2.47)

$$p(\boldsymbol{r},t|\boldsymbol{r}_0,t_0) \;=\; \big(4\pi\, D\,(t-t_0)\big)^{-\frac{3}{2}}\;\exp\!\left[-\frac{(\boldsymbol{r}-\boldsymbol{r}_0)^2}{4\,D\,(t-t_0)}\right] \tag{3.14}$$

is the solution of (3.13) for the initial and boundary conditions

$$p(\boldsymbol{r},t\to t_0|\boldsymbol{r}_0,t_0) \;=\; \delta(\boldsymbol{r}-\boldsymbol{r}_0)\;,\qquad p(|\boldsymbol{r}|\to\infty,t|\boldsymbol{r}_0,t_0) \;=\; 0\;. \tag{3.15}$$

One refers to the solution (3.14) as the *Green's function*. The Green's function is only uniquely defined if one specifies spatial boundary conditions on the surface $\partial\Omega$ surrounding the diffusion space Ω. Once the Green's function is available one can obtain the solution $p(\boldsymbol{r},t)$ for the system for any initial condition, e.g. for $p(\boldsymbol{r},t\to 0)=f(\boldsymbol{r})$

$$p(\boldsymbol{r},t) \;=\; \int_{\Omega_\infty} d^3r_0\; p(\boldsymbol{r},t|\boldsymbol{r}_0,t_0)\, f(\boldsymbol{r}_0)\;. \tag{3.16}$$

We will show below that one can also express the observables of the system in terms of the Green's function. We will also introduce Green's functions for different spatial boundary conditions. Once a Green's function happens to be known, it is invaluable. However, because the Green's function entails complete information about the time evolution of a system it is correspondingly difficult to obtain and its usefulness is confined often to formal manipulations. In this regard we will make extensive use of Green's functions later on.
The system described by the Einstein diffusion equation (3.13) may either be closed at the surface of the diffusion space Ω or open, i.e., $\partial\Omega$ either may be impenetrable for particles or may allow passage of particles. In the latter case $\partial\Omega$ describes a reactive surface. These properties of Ω are specified through the boundary conditions on $\partial\Omega$. In order to formulate these boundary conditions we consider the flux of particles through consideration of the total number of particles diffusing in Ω defined through

$$N_\Omega(t|\boldsymbol{r}_0,t_0) \;=\; \int_\Omega d^3r\; p(\boldsymbol{r},t|\boldsymbol{r}_0,t_0)\;. \tag{3.17}$$

Since there are no terms in the diffusion equation (3.13) which affect the number of particles (we will introduce such terms later on) the particle number is conserved and any change of $N_\Omega(t|\boldsymbol{r}_0,t_0)$ must be due to particle flux at the surface of Ω. In fact, taking the time derivative of (3.17) yields, using (3.13) and $\nabla^2 = \boldsymbol{\nabla}\cdot\boldsymbol{\nabla}$,

$$\partial_t N_\Omega(t|\boldsymbol{r}_0,t_0) \;=\; \int_\Omega d^3r\; D\;\boldsymbol{\nabla}\cdot\boldsymbol{\nabla}\, p(\boldsymbol{r},t|\boldsymbol{r}_0,t_0)\;. \tag{3.18}$$

Gauss' theorem

$$\int_\Omega d^3r\;\boldsymbol{\nabla}\cdot\boldsymbol{v}(\boldsymbol{r}) \;=\; \int_{\partial\Omega} d\boldsymbol{a}\cdot\boldsymbol{v}(\boldsymbol{r}) \tag{3.19}$$

for some vector-valued function $\boldsymbol{v}(\boldsymbol{r})$, allows one to write (3.18)

$$\partial_t\, N_\Omega(t|\boldsymbol{r}_0,t_0) \;=\; \int_{\partial\Omega} d\boldsymbol{a}\cdot D\,\boldsymbol{\nabla}\, p(\boldsymbol{r},t|\boldsymbol{r}_0,t_0)\;. \tag{3.20}$$

Here

$$\boldsymbol{j}(\boldsymbol{r},t|\boldsymbol{r}_0,t_0) \;=\; D\;\boldsymbol{\nabla}\,p(\boldsymbol{r},t|\boldsymbol{r}_0,t_0) \tag{3.21}$$

must be interpreted as the flux of particles which leads to changes of the total number of particles in case the flux does not vanish at the surface $\partial\Omega$ of the diffusion space Ω. Equation (3.21) is also known as Fick's law. We will refer to

$$\boldsymbol{\mathcal{J}}_0(\boldsymbol{r}) \;=\; D(\boldsymbol{r})\,\boldsymbol{\nabla} \tag{3.22}$$

as the flux operator. This operator, when acting on a solution of the Einstein diffusion equation, yields the local flux of particles (probability) in the system.
The flux operator $\boldsymbol{\mathcal{J}}_0(\boldsymbol{r})$ governs the spatial boundary conditions since it allows one to measure particle (probability) exchange at the surface of the diffusion space Ω. There are three types of boundary conditions possible. These types can be enforced simultaneously in disconnected areas of the surface $\partial\Omega$. Let us denote by $\partial\Omega_1, \partial\Omega_2$ two disconnected parts of $\partial\Omega$ such that $\partial\Omega = \partial\Omega_1 \cup \partial\Omega_2$. An example is a volume Ω lying between a sphere of radius R_1 ($\partial\Omega_1$) and of radius R_2 ($\partial\Omega_2$). The separation of the surfaces $\partial\Omega_i$ with different boundary conditions is necessary in order to assure that a continuous solution of the diffusion equation exists. Such solution cannot exist if it has to satisfy in an infinitesimal neighbourhood entailing $\partial\Omega$ two different boundary conditions.
The first type of boundary condition is specified by

$$\hat{\boldsymbol{a}}(\boldsymbol{r}) \cdot \boldsymbol{\mathcal{J}}_0(\boldsymbol{r})\; p(\boldsymbol{r},t|\boldsymbol{r}_0,t_0) \;=\; 0\;, \quad \boldsymbol{r} \in \partial\Omega_i\;, \tag{3.23}$$

which obviously implies that particles do not cross the boundary, i.e., are reflected. Here $\hat{\boldsymbol{a}}(\boldsymbol{r})$ denotes a unit vector normal to the surface $\partial\Omega_i$ at $\boldsymbol{r}$ (see Figure 3.1). We will refer to (3.23) as the *reflection boundary condition*.
The second type of boundary condition is

$$p(\boldsymbol{r},t|\boldsymbol{r}_0,t_0) \;=\; 0\;, \quad \boldsymbol{r} \in \partial\Omega_i\;. \tag{3.24}$$

This condition implies that all particles arriving at the surface $\partial\Omega_i$ are taken away such that the probability on $\partial\Omega_i$ vanishes. This boundary condition describes a reactive surface with the highest degree of reactivity possible, i.e., that *every* particle on $\partial\Omega_i$ reacts. We will refer to (3.24) as the *reaction boundary condition*.
The third type of boundary condition,

$$\hat{\boldsymbol{a}}(\boldsymbol{r}) \cdot \boldsymbol{\mathcal{J}}_0\; p(\boldsymbol{r},t|\boldsymbol{r}_0,t_0) \;=\; w\,p(\boldsymbol{r},t|\boldsymbol{r}_0,t_0)\;, \quad \boldsymbol{r} \text{ on } \partial\Omega_i\;, \tag{3.25}$$

describes the case of intermediate reactivity at the boundary. The reactivity is measured by the parameter w. For $w = 0$ in (3.25) $\partial\Omega_i$ corresponds to a non-reactive, i.e., reflective boundary. For $w \to \infty$ the condition (3.25) can only be satisfied for $p(\boldsymbol{r},t|\boldsymbol{r}_0,t_0) = 0$, i.e., every particle impinging onto $\partial\Omega_i$ is consumed in this case. We will refer to (3.25) as the *radiation boundary condition*.
In the following we want to investigate some exemplary instances of the Einstein diffusion equation for which analytical solutions are available.

3.2 Free Diffusion in One-dimensional Half-Space

As a first example we consider a particle diffusing freely in a one-dimensional half-space $x \geq 0$. This situation is governed by the Einstein diffusion equation (3.13) in one dimension

$$\partial_t\, p(x,t|x_0,t_0) \;=\; D\;\partial_x^2\, p(x,t|x_0,t_0)\;, \tag{3.26}$$

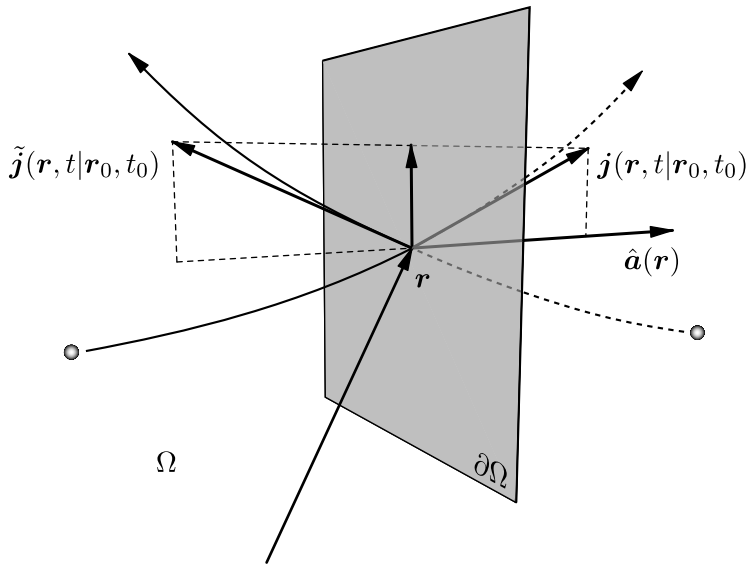

Figure 3.1: depicts the reflection of a partilcle at $\partial\Omega$. After the reflection the particle proceeds on the trajectory of it's mirror image. The probability flux $\boldsymbol{j}(\boldsymbol{r}, t|\boldsymbol{r}_0, t_0)$ of the particle prior to relfection and the probability flux $\tilde{\boldsymbol{j}}(\boldsymbol{r}, t|\boldsymbol{r}_0, t_0)$ of it's mirror image amount to a total flux vector parallel to the surface $\partial\Omega$ and normal to the normalized surface vector $\hat{\boldsymbol{a}}(\boldsymbol{r})$ which results in the boundary condition (3.23).

where the solution considered is the Green's function, i.e., satisfies the initial condition

$$p(x, t \to 0|x_0, t_0) \quad = \quad \delta(x - x_0) \ . \tag{3.27}$$

One-Dimensional Half-Space with Reflective Wall

The transport space is limited at $x = 0$ by a reflective wall. This wall is represented by the boundary condition

$$\partial_x \, p(x, t|x_0, t_0) \quad = \quad 0 \ . \tag{3.28}$$

The other boundary is situated at $x \to \infty$. Assuming that the particle started diffusion at some finite x_0 we can postulate the second boundary condition

$$p(x \to \infty, t|x_0, t_0) \quad = \quad 0 \ . \tag{3.29}$$

Without the wall at $x = 0$, i.e., if (3.28) would be replaced by $p(x \to -\infty, t|x_0, t_0) = 0$, the solution would be the one-dimensional equivalent of (3.14), i.e.,

$$p(x, t|x_0, t_0) \quad = \quad \frac{1}{\sqrt{4\pi \, D \, (t - t_0)}} \ \exp\left[-\frac{(x - x_0)^2}{4 \, D \, (t - t_0)} \right] \ . \tag{3.30}$$

In order to satisfy the boundary condition one can add a second term to this solution, the Green's function of an imaginary particle starting diffusion at position $-x_0$ behind the boundary. One

obtains

$$p(x,t|x_0,t_0) = \frac{1}{\sqrt{4\pi\, D\,(t-t_0)}}\ \exp\left[-\frac{(x-x_0)^2}{4\,D\,(t-t_0)}\right] + \frac{1}{\sqrt{4\pi\, D\,(t-t_0)}}\ \exp\left[-\frac{(x+x_0)^2}{4\,D\,(t-t_0)}\right]\ , \quad x \geq 0\ , \tag{3.31}$$

which, as stated, holds only in the available half-space $x \geq 0$. Obviously, this function is a solution of (3.26) since both terms satisfy this equation. This solution also satisfies the boundary condition (3.29). One can easily convince oneself either on account of the reflection symmetry with respect to $x = 0$ of (3.31) or by differentiation, that (3.31) does satisfy the boundary condition at $x = 0$. The solution (3.31) bears a simple interpretation. The first term of this solution describes a diffusion process which is unaware of the presence of the wall at $x = 0$. In fact, the term extends with non-vanishing values into the unavailable half-space $x \leq 0$. This "loss" of probability is corrected by the second term which, with its tail for $x \geq 0$, balances the missing probability. In fact, the $x \geq 0$ tail of the second term is exactly the mirror image of the "missing" $x \leq 0$ tail of the first term. One can envision that the second term reflects at $x = 0$ that fraction of the first term of (3.31) which describes a freely diffusing particle without the wall.

One-Dimensional Half-Space with Absorbing Wall

We consider now a one-dimensional particle which diffuses freely in the presence of an absorbing wall at $x = 0$. The diffusion equation to solve is again (3.26) with initial condition (3.27) and boundary condition (3.29) at $x \to \infty$. Assuming that the absorbing wall, i.e., a wall which consumes every particle impinging on it, is located at $x = 0$ we have to replace the boundary condition (3.28) of the previous problem by

$$p(x=0,t|x_0,t_0) = 0\ . \tag{3.32}$$

One can readily convince oneself, on the ground of a symmetry argument similar to the one employed above, that

$$p(x,t|x_0,t_0) = \frac{1}{\sqrt{4\pi\, D\,(t-t_0)}}\ \exp\left[-\frac{(x-x_0)^2}{4\,D\,(t-t_0)}\right] - \frac{1}{\sqrt{4\pi\, D\,(t-t_0)}}\ \exp\left[-\frac{(x+x_0)^2}{4\,D\,(t-t_0)}\right]\ , \quad x \geq 0 \tag{3.33}$$

is the solution sought. In this case the $x \leq 0$ tail of the first term which describes barrierless free diffusion is not replaced by the second term, but rather the second term describes a *further* particle loss. This contribution is not at all obvious and we strongly encourage the reader to consider the issue. Actually it may seem "natural" that the solution for an absorbing wall would be obtained if one just left out the $x \leq 0$ tail of the first term in (3.33) corresponding to particle removal by the wall. It appears that (3.33) removes particles also at $x \geq 0$ which did not have reached the absorbing wall yet. This, however, is not true. Some of the probability of a freely diffusing particle in a barrierless space for $t > 0$ at $x > 0$ involves Brownian trajectories of that particle which had visited the half-space $x \leq 0$ at earlier times. These instances of the Brownian processes are removed by the second term in (3.33) (see Figure 3.2).

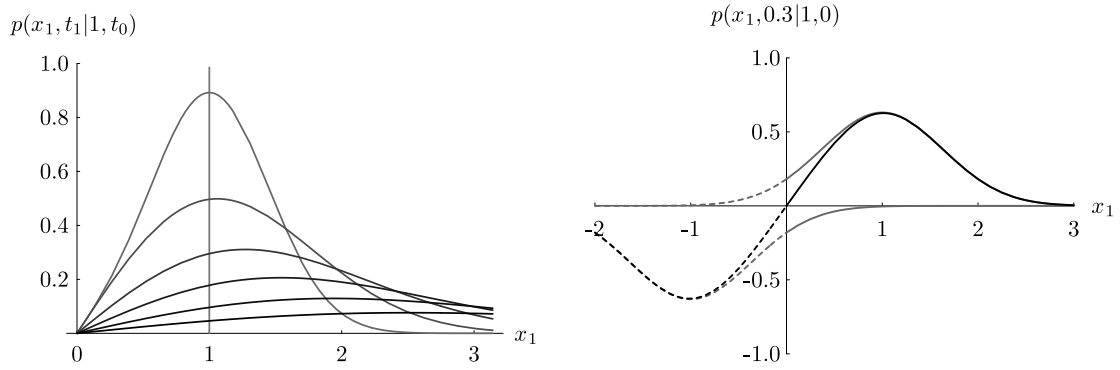

Figure 3.2: Probability density distribution of a freely diffusing particle in half-space with an absobing boundary at $x = 0$. The left plot shows the time evolution of equation (3.33) with $x_0 = 1$ and $(t_1 - t_0) = 0.0, 0.1, 0.3, 0.6, 1.0, 1.7$, and 3.0 for $D = 1$ in arbitrary temporal and spatial units. The right plot depicts the assembly of solution (3.33) with two Gaussian distributions at $(t_1 - t_0) = 0.3$.

Because of particle removal by the wall at $x = 0$ the total number of particles is not conserved. The particle number corresponding to the Greens function $p(x, t|x_0, t_0)$ is

$$N(t|x_0, t_0) \;=\; \int_0^\infty dx\; p(x, t|x_0, t_0)\;. \tag{3.34}$$

Introducing the integration variable

$$y \;=\; \frac{x}{\sqrt{4\,D\,(t - t_0)}} \tag{3.35}$$

(3.34) can be written

$$\begin{aligned} N(t|x_0, t_0) &= \frac{1}{\sqrt{\pi}} \int_0^\infty dy\; \exp\big[-(y - y_0)^2\big] \;-\; \frac{1}{\sqrt{\pi}} \int_0^\infty dy\; \exp\big[-(y - y_0)^2\big] \\ &= \frac{1}{\sqrt{\pi}} \int_{-y_0}^\infty dy\; \exp\big[-y^2\big] \;-\; \frac{1}{\sqrt{\pi}} \int_{y_0}^\infty dy\; \exp\big[-y^2\big] \\ &= \frac{1}{\sqrt{\pi}} \int_{-y_0}^{y_0} dy\; \exp\big[-y^2\big] \qquad (3.36) \\ &= \frac{2}{\sqrt{\pi}} \int_0^{y_0} dy\; \exp\big[-y^2\big]\;. \qquad (3.37) \end{aligned}$$

Employing the definition of the so-called error function

$$\mathrm{erf}(z) \;=\; \frac{2}{\sqrt{\pi}} \int_0^z dy\; \exp\big[-y^2\big] \tag{3.38}$$

leads to the final expression, using (3.35),

$$N(t|x_0, t_0) \;=\; \mathrm{erf}\left[\frac{x_0}{\sqrt{4\,D\,(t - t_0)}}\right]\;. \tag{3.39}$$

The particle number decays to zero asymptotically. In fact, the functional property of $\mathrm{erf}(z)$ reveal

$$N(t|x_0,t_0) \quad \sim \quad \frac{x_0}{\sqrt{\pi D(t-t_0)}} \quad \text{for } t \to \infty \; . \tag{3.40}$$

This decay is actually a consequence of the ergodic theorem which states that one-dimensional Brownian motion with certainty will visit every point of the space, i.e., also the absorbing wall. We will see below that for three-dimensional Brownian motion not all particles, even after arbitrary long time, will encounter a reactive boundary of finite size.
The rate of particle decay, according to (3.39), is

$$\partial_t \, N(t|x_0,t_0) \quad = \quad -\frac{x_0}{\sqrt{2\pi \, D \, (t-t_0)} \, (t-t_0)} \; \exp\left[-\frac{x_0^2}{4 \, D \, (t-t_0)} \right] \; . \tag{3.41}$$

An alternative route to determine the decay rate follows from (3.21) which reads for the case considered here,

$$\partial_t \, N(t|x_0,t_0) \quad = \quad -D \; \partial_x \, p(x,t|x_0,t_0)\Big|_{x=0} \; . \tag{3.42}$$

Evaluation of this expression yields the same result as Eq. (3.41). This illustrates how useful the relationship (3.21) can be.

3.3 Fluorescence Microphotolysis

Fluorescence microphotolysis is a method to measure the diffusion of molecular components (lipids or proteins) in biological membranes. For the purpose of measurement one labels the particular molecular species to be investigated, a membrane protein for example, with a fluorescent marker. This marker is a molecular group which exhibits strong fluorescence when irradiated; in the method the marker is chosen such that there exists a significant probability that the marker is irreversibly degraded through irradiation into a non-fluorescent form.
The diffusion measurement of the labelled molecular species proceeds then in two steps. In the first step at time t_o , a small, circular membrane area of diameter a (some μm) is irradiated by a short, intensive laser pulse of 1-100 mW, causing the irreversible change (photolysis) of the fluorescent markers within the illuminated area. For all practical purposes, this implies that no fluorescent markers are left in that area and a corresponding distribution $w(x,y,t_o)$ is prepared.
In the second step, the power of the laser beam is reduced to a level of 10-1000 nW at which photolysis is negligible. The fluorescence signal evoked by the attenuated laser beam,

$$N(t|t_o) \quad = \quad c_o \int_{\Omega_{\mathrm{laser}}} dx \, dy \; w(x,y,t) \tag{3.43}$$

is then a measure for the number of labelled molecules in the irradiated area at time t. Here Ω_{laser} denotes the irradiated area (assuming an idealized, homogenous irradiation profile) and c_o is a suitable normalization constant. $N(t|t_o)$ is found to increase rapidly in experiments due diffusion of unphotolysed markers into the area. Accordingly, the fluorescence recovery can be used to determine the diffusion constant D of the marked molecules.
In the following, we will assume that the irradiated area is a stripe of thickness $2a$, rather than a circular disk. This geometry will simplify the description, but does not affect the behaviour of the system in principle.

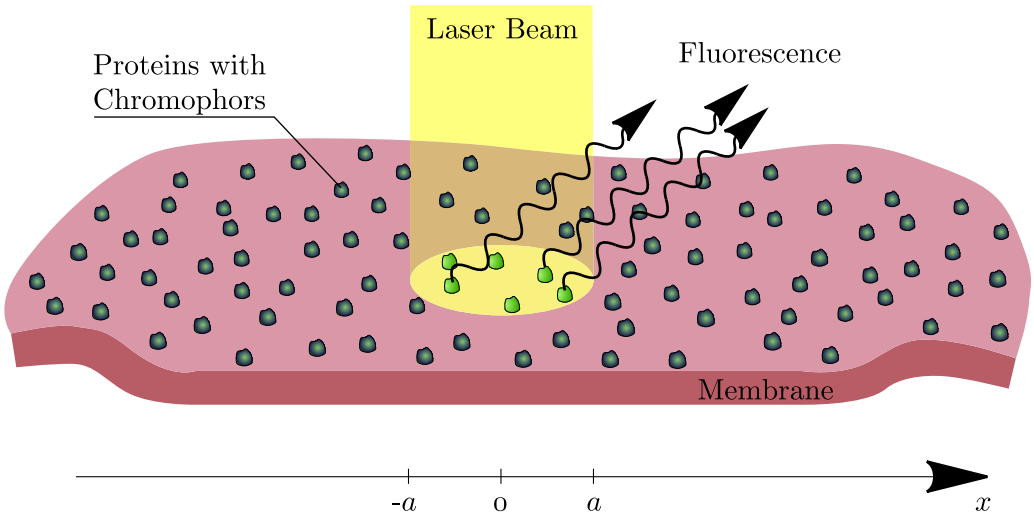

Figure 3.3: Schematic drawing of a fluorescence microphotolysis experiment.

For $t < t_0$ the molecular species under consideration, to be referred to as particles, is homogeneously distributed as described by $w(x,t) = 1$. At $t = t_0$ photolysis in the segment $-a < x < a$ eradicates all particles, resulting in the distribution

$$w(x,t_0) \quad = \quad \theta(a-x) \; + \; \theta(x-a) \; , \tag{3.44}$$

where θ is the Heavisides step function

$$\theta(x) \quad = \quad \begin{cases} 0 & \text{for } x \; < \; 0 \\ 1 & \text{for} x \; \geq \; 0 \end{cases} \; . \tag{3.45}$$

The subsequent evolution of $w(x,y,t)$ is determined by the two-dimensional diffusion equation

$$\partial_t \, w(x,y,t) \quad = \quad D \, \left(\partial_x^2 \, + \, \partial_y^2 \right) \, w(x,y,t) \; . \tag{3.46}$$

For the sake of simplicity, one may assume that the membrane is infinite, i.e., large compared to the length scale a. Since the initial distribution (3.44) does not depend on y, once can assume that $w(x,y,t)$ remains independent of y since distribution, in fact, is a solution of (3.46). However, one can eliminate consideration of y and describe teh ensuing distribution $w(x,t)$ by means of the one-dimensional diffusion equation

$$\partial_t \, w(x,t) \quad = \quad D \, \partial_x^2 \, w(x,t) \; . \tag{3.47}$$

with boundary condition

$$\lim_{|x| \to \infty} \, w(x,t) \quad = \quad 0 \; . \tag{3.48}$$

The Green's function solution of this equation is [c.f. (3.14)]

$$p(x,t|x_0,t_0) \quad = \quad \frac{1}{\sqrt{4\pi D(t-t_0)}} \; \exp \left[- \frac{(x-x_0)^2}{4D(t-t_0)} \right] \; . \tag{3.49}$$

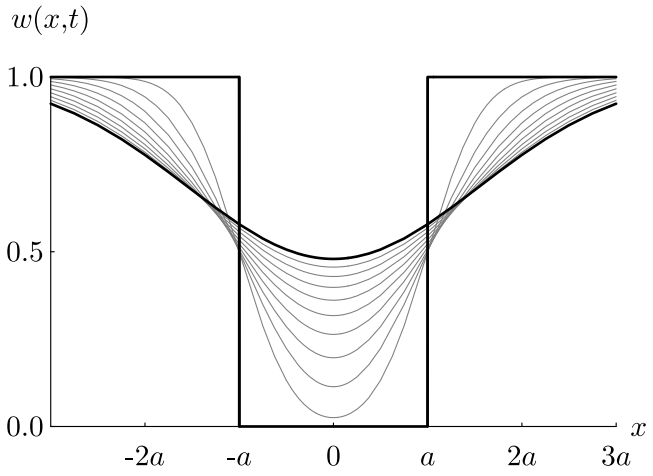

Figure 3.4: Time evolution of the probability distribution $w(x,t)$ for $D = \frac{1}{a^2}$ in time steps $t = 0, 0.1, 0.2, \ldots, 1.0$.

which satisfies the initial condition $p(x,t_0|x_0,t_0) = \delta(x-x_0)$. The solution for the initial probability distribution (3.44), according to (3.16), is then

$$w(x,t) \;=\; \int_{-\infty}^{+\infty} dx_o\; p(x,t|x_o,t_o)\;(\theta(a-x)+\theta(x-a))\;. \tag{3.50}$$

This can be written, using (3.49) and (3.45),

$$\begin{aligned} w(x,t) \;&=\; \int_{-\infty}^{-a} dx_0\;\frac{1}{\sqrt{4\pi D(t-t_0)}}\;\exp\left[-\frac{(x-x_0)^2}{4D(t-t_0)}\right] \\ &\quad + \int_{a}^{\infty} dx_0\;\frac{1}{\sqrt{4\pi D(t-t_0)}}\;\exp\left[-\frac{(x-x_0)^2}{4D(t-t_0)}\right]\;. \end{aligned} \tag{3.51}$$

Identifying the integrals with the error function $\mathrm{erf}(x)$ one obtains

$$\begin{aligned} w(x,t) \;&=\; \frac{1}{2}\,\mathrm{erf}\left[\frac{x-x_0}{2\sqrt{D(t-t_0)}}\right]\Bigg|_{-\infty}^{-a} \;+\; \frac{1}{2}\,\mathrm{erf}\left[\frac{x-x_0}{2\sqrt{D(t-t_0)}}\right]\Bigg|_{a}^{\infty} \\ &=\; \left(\frac{1}{2}\,\mathrm{erf}\left[\frac{x+a}{2\sqrt{D(t-t_0)}}\right] + \frac{1}{2}\right) \;-\; \left(\frac{1}{2}\,\mathrm{erf}\left[\frac{x-a}{2\sqrt{D(t-t_0)}}\right] - \frac{1}{2}\right) \end{aligned}$$

and, finally,

$$w(x,t) \;=\; \frac{1}{2}\left(\mathrm{erf}\left[\frac{x+a}{2\sqrt{D(t-t_0)}}\right] \;-\; \mathrm{erf}\left[\frac{x-a}{2\sqrt{D(t-t_0)}}\right]\right) \;+\; 1\;. \tag{3.52}$$

The time evolution of the probability distribution $w(x,t)$ is displayed in Figure 3.4 for $D = \frac{1}{a^2}$ in time steps $t = 0, 0.1, 0.2, \ldots, 1.0$.
The observable $N(t,|t_o)$, given in (3.43) is presently defined through

$$N(t|t_o) \;=\; c_o \int_{-a}^{+a} dx\; w(x,t) \tag{3.53}$$

Comparision with (3.52) shows that the evaluation requires one to carry out integrals over the error function which we will, hence, determine first. One obtains by means of conventional techniques

$$\begin{aligned}
\int dx\ \mathrm{erf}(x) &= x\ \mathrm{erf}(x) - \int dx\ x \frac{d}{dx}\ \mathrm{erf}(x) \\
&= x\ \mathrm{erf}(x) - \frac{1}{\sqrt{\pi}} \int 2x\, dx\ \exp(-x^2) \\
&= x\ \mathrm{erf}(x) - \frac{1}{\sqrt{\pi}} \int d\xi\ \exp(-\xi) \quad \text{, for } \xi = x^2 \\
&= x\ \mathrm{erf}(x) + \frac{1}{\sqrt{\pi}} \exp(-\xi) \\
&= x\ \mathrm{erf}(x) + \frac{1}{\sqrt{\pi}} \exp(-x^2)\ . \qquad (3.54)
\end{aligned}$$

Equiped with this result one can evaluate (3.53). For this purpose we adopt the normalization factor $c_o = \frac{1}{2a}$ and obtain

$$\begin{aligned}
N(t|t_0) &= \frac{1}{2a} \int_{-a}^{+a} dx\ \frac{1}{2} \left(\mathrm{erf}\left[\frac{x+a}{2\sqrt{D(t-t_0)}} \right] - \mathrm{erf}\left[\frac{x-a}{2\sqrt{D(t-t_0)}} \right] + 2 \right) \\
&= \frac{1}{4a} \left(\frac{2\sqrt{D\,(t-t_0)}}{\pi}\ \exp\left[\frac{(x+a)^2}{4\,D\,(t-t_0)} \right] + (x+a)\ \mathrm{erf}\left[\frac{x+a}{2\sqrt{D\,(t-t_0)}} \right] \right. \\
&- \left. \frac{2\sqrt{D\,(t-t_0)}}{\pi}\ \exp\left[\frac{(x-a)^2}{4\,D\,(t-t_0)} \right] + (x-a)\ \mathrm{erf}\left[\frac{x-a}{2\sqrt{D\,(t-t_0)}} \right] + 2x \right) \Bigg|_{-a}^{a} \\
&= \frac{\sqrt{D(t-t_0)}}{a\sqrt{\pi}} \left(\exp\left[-\frac{a^2}{D\,(t-t_0)} \right] - 1 \right) + \mathrm{erf}\left[\frac{a}{\sqrt{D\,(t-t_0)}} \right] + 1\,. \qquad (3.55)
\end{aligned}$$

The fluorescent recovery signal $N(t|t_o)$ is displayed in Figure 3.5. The result exhibits the increase of fluorescence in illuminated stripe $[-a, a]$: particles with a working fluorescent marker diffuse into segment $[-a, a]$ and replace the bleached fluorophore over time. Hence, $N(t|t_o)$ is an increasing function which approaches asymptotically the value 1, i.e., the signal prior to photolysis at $t = t_0$. One can determine the diffusion constant D by fitting normalized data of fluorescence measurements to $N(t|t_o)$. Values for the diffusion constant D range from 10 μm^2 to 0.001 μm^2. For this purpose we simplify expression (3.55) introducing the dimensionless variable

$$\xi = \frac{a}{\sqrt{D\,(t-t_0)}}\ . \qquad (3.56)$$

One can write then the observable in teh form

$$N(\xi) = \frac{1}{\xi\sqrt{\pi}} \left(\exp\left[-\xi^2\right] - 1 \right) + \mathrm{erf}\left[\xi\right] + 1\ . \qquad (3.57)$$

A characteristic of the fluorescent recovery is the time t_h, equivalently, ξ_h, at which half of the fluorescence is recovered defined through $N(\xi_h) = 0.5$. Numerical calculations, using the *regula falsi* or *secant method* yields ξ_h provide the following equations.

$$\xi_h = 0.961787\ . \qquad (3.58)$$

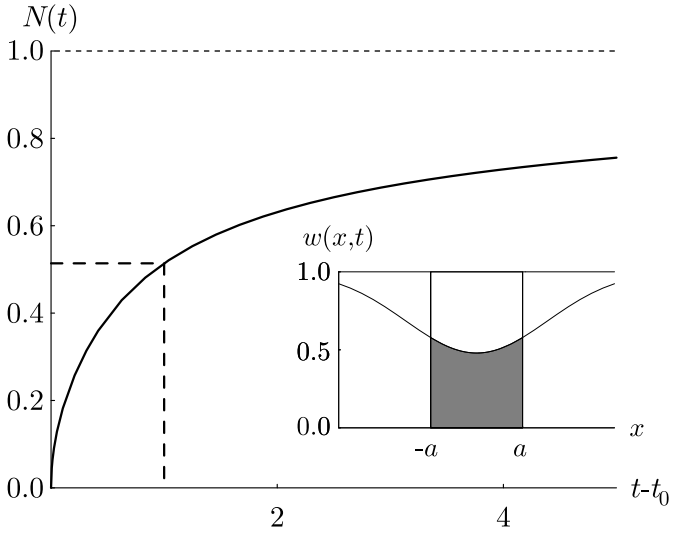

Figure 3.5: Fluorescence recovery after photobleaching as described by $N(t|t_o)$. The inset shows the probability distribution $w(x,t)$ for $t=1$ and the segment $[-a,a]$. ($D=\frac{1}{a^2}$)

the definition (3.56) allows one to determine teh relationship between t_h and D

$$D \;=\; 0.925034\,\frac{a^2}{t_h - t_0}\;. \tag{3.59}$$

Since a is known through the experimental set up, measurement of $t_h - t_o$ provides the value of D.

3.4 Free Diffusion around a Spherical Object

Likely the most useful example of a diffusion process stems from a situation encountered in a chemical reaction when a molecule diffuses around a target and either reacts with it or vanishes out of its vicinity. We consider the idealized situation that the target is stationary (the case that both the molecule and the target diffuse is treated in Chapter **??**. Also we assume that the target is spherical (radius a) and reactions can arise anywwhere on its surface with equal likelyhood. Furthermore, we assume that the diffusing particles are distributed initially at a distance r_0 from the center of the target with all directions being equally likely. In effect we describe an ensemble of reacting molecules and targets which undergo their reaction diffusion processes independently of each other.
The probability of finding the molecule at a distance r at time t is then described by a spherically symmetric distribution $p(r,t|r_0,t_0)$ since neither the initial condition nor the reaction-diffusion condition show any orientational preference. The ensemble of reacting molecules is then described by the diffusion equation

$$\partial_t\, p(r,t|r_0,t_0) \;=\; D\;\nabla^2\; p(r,t|r_0,t_0) \tag{3.60}$$

and the initial condition

$$p(r,t_0|r_0,t_0) \;=\; \frac{1}{4\pi\, r_0^2}\;\delta(r-r_0)\;. \tag{3.61}$$

The prefactor on the r.h.s. normalizes the initial probability to unity since

$$\int_{\Omega_\infty} d^3\boldsymbol{r}\; p(\boldsymbol{r},t_0|\boldsymbol{r}_0,t_0) \;=\; \int_0^\infty 4\pi\, r^2 dr\; p(r,t_0|r_0,t_0)\;. \tag{3.62}$$

We can assume that the distribution vanishes at distances from the target which are much larger than r_0 and, accordingly, impose the boundary condition

$$\lim_{r\to\infty}\; p(r,t|r_0,t_0) \;=\; 0\;. \tag{3.63}$$

The reaction at the target will be described by the boundary condition (3.25), which in the present case of a spherical boundary, can be written

$$D\;\partial_r\, p(r,t|r_0,t_0) \;=\; w\; p(r,t|r_0,t_0)\;, \qquad \text{for } r=a\;. \tag{3.64}$$

As pointed out above, w controls the likelyhood of encounters with the target to be reactive: $w=0$ corresponds to an unreactive surface, $w\to\infty$ to a surface for which every collision leads to reaction and, hence, to a diminishing of $p(r,t|r_0,t_0)$. The boundary condition for arbitrary w values adds significantly to the complexity of the solution, i.e., the following derivation would be simpler if the limits $w=0$ or $w\to\infty$ would be considered. However, a closed expression for the general case can be provided and, in view of the frequent applicability of the example we prefer the general solution.
We first notice that the Laplace operator ∇^2, expressed in spherical coordinates (r,θ,ϕ), reads

$$\nabla^2 \;=\; \frac{1}{r^2}\left[\partial_r\left(r^2\,\partial_r\right) \;+\; \frac{1}{\sin^2\theta}\;\partial_\phi^2 \;+\; \frac{1}{\sin\theta}\;\partial_\theta\left(\sin\theta\,\partial_\theta\right)\right]\;. \tag{3.65}$$

Since the distribution function $p(r,t_0|r_0,t_0)$ is spherically symmetric, i.e., depends solely on r and not on θ and ϕ, one can drop, for all practical purposes, the respective derivatives. Employing furthermore the identity

$$\frac{1}{r^2}\;\partial_r\left(r^2\;\partial_r\;f(r)\right) \;=\; \frac{1}{r}\;\partial_r^2\left(r\;\;f(r)\right)\;. \tag{3.66}$$

one can restate the diffusion equation (3.60)

$$\partial_t\; r\; p(r,t|r_0,t_0) \;=\; D\;\partial_r^2\; r\; p(r,t|r_0,t_0)\;. \tag{3.67}$$

For the solution of (3.61, 3.63, 3.64, 3.67) we partition

$$p(r,t|r_0,t_0) \;=\; u(r,t|r_0,t_0)\;+\;v(r,t|r_0,t_0), \tag{3.68}$$

$$\text{with}\quad u(r,t\to t_0|r_0,t_0) \;=\; \frac{1}{4\pi\, r_0^2}\;\delta(r-r_0) \tag{3.69}$$

$$v(r,t\to t_0|r_0,t_0) \;=\; 0\;. \tag{3.70}$$

The functions $u(r,t|r_0,t_0)$ and $v(r,t|r_0,t_0)$ are chosen to obey individually the radial diffusion equation (3.67) and, together, the boundary conditions (3.63, 3.64). We first construct $u(r,t|r_0,t_0)$ without regard to the boundary condition at $r=a$ and construct then $v(r,t|r_0,t_0)$ such that the proper boundary condition is obeyed.
The function $u(r,t|r_0,t_0)$ has to satisfy

$$\partial_t\left(r\;u(r,t|r_0,t_0)\right) \;=\; D\;\partial_r^2\;\left(r\;u(r,t|r_0,t_0)\right) \tag{3.71}$$

$$r\;u(r,t\to t_0|r_0,t_0) \;=\; \frac{1}{4\pi\, r_0}\;\delta(r-r_0)\;. \tag{3.72}$$

An admissable solution $r\,u(r,t|r_0,t_0)$ can be determined readily through Fourier transformation

$$\tilde{U}(k,t|r_0,t_0) \;=\; \int_{-\infty}^{+\infty} dr\; r\; u(r,t|r_0,t_0)\; e^{-i\,k\,r}\;, \tag{3.73}$$

$$r\; u(r,t|r_0,t_0) \;=\; \frac{1}{2\pi}\; \int_{-\infty}^{+\infty} dk\; \tilde{U}(k,t|r_0,t_0)\; e^{i\,k\,r}\;. \tag{3.74}$$

Inserting (3.74) into (3.67) yields

$$\frac{1}{2\pi}\; \int_{-\infty}^{\infty} dk\; \Big[\, \partial_t\, \tilde{U}(k,t|r_0,t_0) \;+\; D\,k^2\, \tilde{U}(k,t|r_0,t_0) \Big]\; e^{ikr} \;=\; 0\;. \tag{3.75}$$

The uniqueness of the Fourier transform allows one to conclude that the coefficients $[\cdots]$ must vanish. Hence, one can conclude

$$\tilde{U}(k,t|r_0,t_0) \;=\; C_u(k|r_0)\; \exp\big[-D\,(t-t_0)\,k^2\big]\;. \tag{3.76}$$

The time-independent coefficients $C_u(k|r_0)$ can be deduced from the initial condition (3.72). The identity

$$\delta(r-r_0) \;=\; \frac{1}{2\pi} \int_{-\infty}^{+\infty} dk\; e^{i\,k\,(r-r_0)} \tag{3.77}$$

leads to

$$\frac{1}{4\pi\, r_0}\; \delta(r-r_0) \;=\; \frac{1}{8\pi^2\, r_0}\; \int_{-\infty}^{+\infty} dk\; e^{i\,k\,(r-r_0)} \;=\; \frac{1}{2\pi}\; \int_{-\infty}^{+\infty} dk\; C_u(k|r_0)\; e^{i\,k\,r} \tag{3.78}$$

and, hence,

$$C_u(k|r_0) \;=\; \frac{1}{4\pi\, r_0}\; e^{-i\,k\,r_0}\;. \tag{3.79}$$

This results in the expression

$$r\; u(r,t|r_0,t_0) \;=\; \frac{1}{8\,\pi^2\, r_0}\; \int_{-\infty}^{\infty} dk\; \exp\big[-D\,(t-t_0)\,k^2\big]\; e^{i\,(r-r_0)\,k} \tag{3.80}$$

The Fourier integral

$$\int_{-\infty}^{\infty} dk\; e^{-a\,k^2}\; e^{i\,x\,k} \;=\; \sqrt{\frac{\pi}{a}}\; \exp\left[\frac{-x^2}{4\,a}\right] \tag{3.81}$$

yields

$$r\; u(r,t|r_0,t_0) \;=\; \frac{1}{4\,\pi\, r_0}\; \frac{1}{\sqrt{4\pi\, D\,(t-t_0)}}\; \exp\left[-\frac{(r-r_0)^2}{4\,D\,(t-t_0)}\right]\;. \tag{3.82}$$

We want to determine now the solution $v(r,t|r_0,t_0)$ in (3.68, 3.70) which must satisfy

$$\partial_t \left(\, r\; v(r,t|r_0,t_0)\,\right) \;=\; D\; \partial_r^2\; \left(\, r\; v(r,t|r_0,t_0)\,\right) \tag{3.83}$$

$$r\; v(r,t\to t_0|r_0,t_0) \;=\; 0\;. \tag{3.84}$$

Any solution of these homogeneous linear equations can be multiplied by an arbitrary constant C. This freedom allows one to modify $v(r,t|r_0,t_0)$ such that $u(r,t|r_0,t_0) \; + \; C\, v(r,t|r_0,t_0)$ obeys the desired boundary condition (3.64) at $r = a$.
To construct a solution of (3.83, 3.84) we consider the Laplace transformation

$$\check{V}(r,s|r_0,t_0) \;\; = \;\; \int_0^\infty d\tau \; e^{-s\,\tau} \; v(r,t_0+\tau|r_0,t_0) \; . \tag{3.85}$$

Applying the Lapace transform to (3.83) and integrating by parts yields for the left hand side

$$-\, r \; v(r,t_0|r_0,t_0) \; + \; s \; r \; \check{V}(r,s|r_0,t_0) \; . \tag{3.86}$$

The first term vanishes, according to (3.84), and one obtains

$$\frac{s}{D} \; \left(r \; \check{V}(r,s|r_0,t_0) \right) \;\; = \;\; \partial_r^2 \; \left(r \; \check{V}(r,s|r_0,t_0) \right) \; . \tag{3.87}$$

The solution with respect to boundary condition (3.63) is

$$r \; \check{V}(r,s|r_0,t_0) \;\; = \;\; C(s|r_0) \; \exp\!\left[-\sqrt{\frac{s}{D}} \; r \right] \; . \tag{3.88}$$

where $C(s|r_0)$ is an arbitrary constant which will be utilized to satisfy the boundary condition(3.64). Rather than applying the inverse Laplace transform to determine $v(r,t|r_0,t_0)$ we consider the Laplace transform $\check{P}(r,s|r_0,t_0)$ of the complete solution $p(r,t|r_0,t_0)$. The reason is that boundary condition (3.64) applies in an analogue form to $\check{P}(r,s|r_0,t_0)$ as one sees readily applying the Laplace transform to (3.64). In case of the function $r\,\check{P}(r,s|r_0,t_0)$ the extra factor r modifies the boundary condition. One can readily verify, using

$$D \; \partial_r \left(r \; \check{P}(r,s|r_0,t_0) \right) \;\; = \;\; D\, \check{P}(r,s|r_0,t_0) \; + \; r\, D \; \partial_r \, \check{P}(r,s|r_0,t_0) \right) \tag{3.89}$$

and replacing at $r = a$ the last term by the r.h.s. of (3.64),

$$\partial_r \; r\, \check{P}(r,s|r_0,t_0) \Big|_{r=a} \;\; = \;\; \frac{w\,a \; + \; D}{D\,a} \; a \; \check{P}(a,s|r_0,t_0) \; . \tag{3.90}$$

One can derive the Laplace transform of $u(r,t|r_0,t_0)$ using the identity

$$\int_0^\infty dt \; e^{-s\,\tau} \; \frac{1}{4\,\pi\,r_0} \; \frac{1}{\sqrt{4\pi\,D\,\tau}} \; \exp\!\left[-\frac{(r-r_0)^2}{4\,D\,\tau} \right] \;\; = \;\; \frac{1}{4\,\pi\,r_0} \; \frac{1}{\sqrt{4\,D\,s}} \; \exp\!\left[-\sqrt{\frac{s}{D}} \; |r-r_0| \right] \tag{3.91}$$

and obtains for $r\,\check{P}(r,s|r_0,t_0)$

$$r\,\check{P}(r,s|r_0,t_0) \;\; = \;\; \frac{1}{4\,\pi\,r_0} \; \frac{1}{\sqrt{4\,D\,s}} \; \exp\!\left[-\sqrt{\frac{s}{D}} \; |r-r_0| \right] \; + \; C(s|r_0) \; \exp\!\left[-\sqrt{\frac{s}{D}} \; r \right] \; . \tag{3.92}$$

Boundary condition (3.90) for $r = a < r_0$ is

$$\begin{aligned} &\sqrt{\frac{s}{D}} \left(\frac{1}{4\,\pi\,r_0} \; \frac{1}{\sqrt{4\,D\,s}} \; \exp\!\left[-\sqrt{\frac{s}{D}} \; (r_0-a) \right] \; - \; C(s|r_0) \; \exp\!\left[-\sqrt{\frac{s}{D}} \; a \right] \right) \\ &\quad = \;\; \frac{w\,a \; + \; D}{D\,a} \left(\frac{1}{4\,\pi\,r_0} \; \frac{1}{\sqrt{4\,D\,s}} \; \exp\!\left[-\sqrt{\frac{s}{D}} \; (r_0-a) \right] \; + \; C(s|r_0) \; \exp\!\left[-\sqrt{\frac{s}{D}} \; a \right] \right) \end{aligned} \tag{3.93}$$

or

$$\left(\sqrt{\frac{s}{D}} - \frac{w\,a + D}{D\,a}\right) \frac{1}{4\,\pi\,r_0} \frac{1}{\sqrt{4\,D\,s}} \exp\left[-\sqrt{\frac{s}{D}}\,(r_0 - a)\right] \tag{3.94}$$
$$= \left(\frac{w\,a + D}{D\,a} + \sqrt{\frac{s}{D}}\right) C(s|r_0) \exp\left[-\sqrt{\frac{s}{D}}\,a\right] .$$

This condition determines the appropriate factor $C(s|r_0)$, namely,

$$C(s|r_0) = \frac{\sqrt{s/D} - (w\,a + D)/(D\,a)}{\sqrt{s/D} + (w\,a + D)/(D\,a)} \frac{1}{4\,\pi\,r_0} \frac{1}{\sqrt{4\,D\,s}} \exp\left[-\sqrt{\frac{s}{D}}\,(r_0 - 2\,a)\right] . \tag{3.95}$$

Combining (3.88, 3.91, 3.95) results in the expression

$$\begin{aligned} & r\ \check{P}(r, s|r_0, t_0) \\ &= \frac{1}{4\,\pi\,r_0} \frac{1}{\sqrt{4\,D\,s}} \exp\left[-\sqrt{\frac{s}{D}}\,|r - r_0|\right] \\ &\quad + \frac{\sqrt{s/D} - (w\,a + D)/(D\,a)}{\sqrt{s/D} + (w\,a + D)/(D\,a)} \frac{1}{4\,\pi\,r_0} \frac{1}{\sqrt{4\,D\,s}} \exp\left[-\sqrt{\frac{s}{D}}\,(r + r_0 - 2\,a)\right] \\ &= \frac{1}{4\,\pi\,r_0} \frac{1}{\sqrt{4\,D\,s}} \left(\exp\left[-\sqrt{\frac{s}{D}}\,|r - r_0|\right] + \exp\left[-\sqrt{\frac{s}{D}}\,(r + r_0 - 2\,a)\right]\right) \\ &\quad - \frac{(w\,a + D)/(D\,a)}{\sqrt{s/D} + (w\,a + D)/(D\,a)} \frac{1}{4\,\pi\,r_0} \frac{1}{\sqrt{D\,s}} \exp\left[-\sqrt{\frac{s}{D}}\,(r + r_0 - 2\,a)\right] \end{aligned} \tag{3.96}$$

Application of the inverse Laplace transformation leads to the final result

$$\begin{aligned} & r\ p(r, t|r_0, t_0) \\ &= \frac{1}{4\,\pi\,r_0} \frac{1}{\sqrt{4\pi\,D\,(t - t_0)}} \left(\exp\left[-\frac{(r - r_0)^2}{4\,D\,(t - t_0)}\right] + \exp\left[-\frac{(r + r_0 - 2\,a)^2}{4\,D\,(t - t_0)}\right]\right) \\ &\quad - \frac{1}{4\,\pi\,r_0} \frac{w\,a + D}{D\,a} \exp\left[\left(\frac{w\,a + D}{D\,a}\right)^2 D\,(t - t_0) + \frac{w\,a + D}{D\,a}\,(r + r_0 - 2\,a)\right] \\ &\quad \times \operatorname{erfc}\left[\frac{w\,a + D}{D\,a}\sqrt{D\,(t - t_0)} + \frac{r + r_0 - 2\,a}{\sqrt{4\,D\,(t - t_0)}}\right] . \end{aligned} \tag{3.97}$$

The substituion

$$\alpha = \frac{w\,a + D}{D\,a} \tag{3.98}$$

simplifies the solution slightly

$$\begin{aligned} p(r, t|r_0, t_0) &= \frac{1}{4\,\pi\,r\,r_0} \frac{1}{\sqrt{4\pi\,D\,(t - t_0)}} \left(\exp\left[-\frac{(r - r_0)^2}{4\,D\,(t - t_0)}\right] + \exp\left[-\frac{(r + r_0 - 2\,a)^2}{4\,D\,(t - t_0)}\right]\right) \\ &\quad - \frac{1}{4\,\pi\,r\,r_0}\,\alpha\,\exp\left[\,\alpha^2\,D\,(t - t_0) + \alpha\,(r + r_0 - 2\,a)\,\right] \\ &\quad \times \operatorname{erfc}\left[\alpha\sqrt{D\,(t - t_0)} + \frac{r + r_0 - 2\,a}{\sqrt{4\,D\,(t - t_0)}}\right] . \end{aligned} \tag{3.99}$$

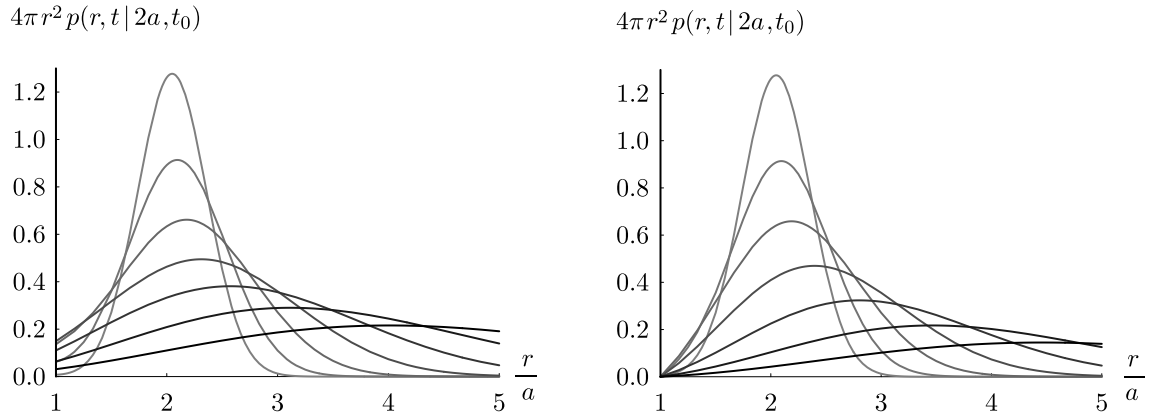

Figure 3.6: Radial probability density distribution of freely diffusing particles around a spherical object according to equation (3.99). The left plot shows the time evolution with $w = 0$ and $(t_1 - t_0) = 0.05, 0.1, 0.2, 0.4, 0.8, 1.6, 3.2$. The right plot depicts the time evolution of equation (eq:fdso27) with $w = \infty$ and $(t_1 - t_0) = 0.05, 0.1, 0.2, 0.4, 0.8, 1.6, 3.2$. The time units are $\frac{a^2}{D}$.

Reflective Boundary at $r = a$ We like to consider now the solution (3.99) in case of a reflective boundary at $r = a$, i.e., for $w = 0$ or $\alpha = 1/a$. The solution is

$$\begin{aligned} p(r,t|r_0,t_0) \;=\; & \frac{1}{4\,\pi\,r\,r_0}\;\frac{1}{\sqrt{4\pi\,D\,(t-t_0)}}\left(\exp\left[-\frac{(r-r_0)^2}{4\,D\;(t-t_0)}\right]\;+\;\exp\left[-\frac{(r+r_0-2\,a)^2}{4\,D\;(t-t_0)}\right]\right) \\ & -\;\frac{1}{4\,\pi\,a\,r\,r_0}\;\exp\left[\frac{D}{a^2}\,(t-t_0)\;+\;\frac{r+r_0-2\,a}{a}\right] \\ & \times\;\mathrm{erfc}\left[\frac{\sqrt{D\,(t-t_0)}}{a}\;+\;\frac{r+r_0-2\,a}{\sqrt{4\,D\,(t-t_0)}}\right]\;. \end{aligned} \tag{3.100}$$

Absorptive Boundary at $r = a$ In case of an absorbing boundary at $r = a$, one has to set $w \to \infty$ and, hence, $\alpha \to \infty$. To supply a solution for this limiting case we note the asymptotic behaviour[1]

$$\sqrt{\pi}\;z\;\exp\left[z^2\right]\;\mathrm{erfc}[z]\;\;\sim\;\;1\;+\;\mathcal{O}\left(\frac{1}{z^2}\right)\;. \tag{3.101}$$

[1]Handbook of Mathematical Functions, Eq. 7.1.14

This implies for the last summand of equation (3.99) the asymptotic behaviour

$$\begin{aligned}
&\alpha\ \exp\big[\,\alpha^2\,D\,(t-t_0)\ +\ \alpha\ (r+r_0-2\,a)\,\big]\ \operatorname{erfc}\left[\alpha\ \sqrt{D\,(t-t_0)}\ +\ \frac{r+r_0-2\,a}{\sqrt{4\,D\,(t-t_0)}}\right] \\
&\quad = \quad \alpha\ \exp\big[z^2\big]\ \exp\big[-z_2^2\big]\ \operatorname{erfc}[z]\,, \qquad \text{with}\quad z\ =\ \alpha\,z_1\ +\ z_2\,, \\
&\qquad\qquad\qquad\qquad\qquad\qquad\qquad\qquad\quad z_1\ =\ \sqrt{D\,(t-t_0)}\,,\ \text{and} \\
&\qquad\qquad\qquad\qquad\qquad\qquad\qquad\qquad\quad z_2\ =\ (r+r_0-2\,a)/\sqrt{4\,D\,(t-t_0)}\,. \\
&\quad \sim \quad \frac{\alpha}{\sqrt{\pi}\,z}\ \exp\big[-z_2^2\big]\ \left(1\ +\ \mathcal{O}\Big(\frac{1}{\alpha^2}\Big)\right) \qquad (3.102) \\
&\quad = \quad \frac{1}{\sqrt{\pi}}\ \frac{\alpha\,\sqrt{4\,D\,(t-t_0)}}{2\,\alpha\,D\,(t-t_0)+r+r_0-2a}\ \exp\left[-\frac{(r+r_0-2\,a)^2}{4\,D\,(t-t_0)}\right]\ \left(1\ +\ \mathcal{O}\Big(\frac{1}{\alpha^2}\Big)\right) \\
&\quad = \quad \left(\frac{1}{\sqrt{\pi\,D\,(t-t_0)}}\ -\ \frac{r+r_0-2\,a}{\sqrt{4\pi}\ \alpha\,\big(D\,(t-t_0)\big)^{3/2}}\ +\ \mathcal{O}\Big(\frac{1}{\alpha^2}\Big)\right)\ \exp\left[-\frac{(r+r_0-2\,a)^2}{4\,D\,(t-t_0)}\right]\,.
\end{aligned}$$

One can conclude to leading order

$$\begin{aligned}
&\alpha\ \exp\big[\,\alpha^2\,D\,(t-t_0)\ +\ \alpha\ (r+r_0-2\,a)\,\big]\ \operatorname{erfc}\left[\alpha\ \sqrt{D\,(t-t_0)}\ +\ \frac{r+r_0-2\,a}{\sqrt{4\,D\,(t-t_0)}}\right] \\
&\qquad \sim \quad \left(\frac{2}{\sqrt{4\pi\,D\,(t-t_0)}}\ +\ \mathcal{O}\left(\frac{1}{\alpha^2}\right)\right)\ \exp\left[-\frac{(r+r_0-2\,a)^2}{4\,D\,(t-t_0)}\right]\,. \qquad (3.103)
\end{aligned}$$

Accordingly, solution (3.99) becomes in the limit $w \to \infty$

$$p(r,t|r_0,t_0)\ =\ \frac{1}{4\,\pi\,r\,r_0}\ \frac{1}{\sqrt{4\pi\,D\,(t-t_0)}}\left(\exp\left[-\frac{(r-r_0)^2}{4\,D\ (t-t_0)}\right]\ -\ \exp\left[-\frac{(r+r_0-2\,a)^2}{4\,D\ (t-t_0)}\right]\right). \qquad (3.104)$$

Reaction Rate for Arbitrary w We return to the general solution (3.99) and seek to determine the rate of reaction at $r=a$. This rate is given by

$$K(t|r_0,t_0)\ \ =\ \ 4\pi\ a^2\ D\ \partial_r\ p(r,t|r_0,t_0)\Big|_{r=a} \qquad (3.105)$$

where the factor $4\pi a^2$ takes the surface area of the spherical boundary into account. According to the boundary condition (3.64) this is

$$K(t|r_0,t_0)\ \ =\ \ 4\pi\ a^2 w\ p(a,t|r_0,t_0)\,. \qquad (3.106)$$

One obtains from (3.99)

$$\begin{aligned}
K(t|r_0,t_0)\ \ &=\ \ \frac{a\,w}{r_0}\ \left(\frac{1}{\sqrt{\pi\,D\,(t-t_0)}}\ \exp\left[-\frac{(r_0-a)^2}{4\,D\,(t-t_0)}\right]\right. \qquad (3.107) \\
&\quad \left.-\ \alpha\ \exp\big[\alpha\,(r_0-a)+\alpha^2\,D\,(t-t_0)\big]\ \operatorname{erfc}\left[\frac{r_0-a}{\sqrt{4\,D\,(t-t_0)}}+\alpha\,\sqrt{D\,(t-t_0)}\right]\right).
\end{aligned}$$

Reaction Rate for $w \to \infty$ In case of an absorptive boundary ($w, \alpha \to \infty$) one can conclude from the asymptotic behaviour (3.102) with $r = a$

$$K(t|r_0,t_0) \;=\; \frac{a\,w}{r_0}\left(\frac{r_0-a}{\sqrt{4\pi}\;\alpha\left(D\,(t-t_0)\right)^{3/2}} + \mathcal{O}\Big(\frac{1}{\alpha^2}\Big)\right)\;\exp\Big[-\frac{(r_0-a)^2}{4\,D\,(t-t_0)}\Big]\;.$$

Employing for the limit $w, \alpha \to \infty$ equation (3.98) as $w/\alpha \sim D$ one obtains the reaction rate for a completely absorptive boundary

$$K(t|r_0,t_0) \;=\; \frac{a}{r_0}\;\frac{1}{\sqrt{4\pi\,D\,(t-t_0)}}\;\frac{r_0-a}{t-t_0}\;\exp\Big[-\frac{(r_0-a)^2}{4\,D\,(t-t_0)}\Big]\;. \tag{3.108}$$

This expression can also be obtained directly from (3.104) using the definition (3.105) of the reaction rate.

Fraction of Particles Reacted for Arbitrary w One can evaluate the fraction of particles which react at the boundary $r = a$ according to

$$N_{\rm react}(t|r_0,t_0) \;=\; \int_{t_0}^{t} dt' K(t'|r_0,t_0)\;. \tag{3.109}$$

For the general case with the rate (3.107) one obtains

$$\begin{aligned} N_{\rm react}(t|r_0,t_0) \;=\; \frac{a\,w}{r_0}\int_{t_0}^{t}dt'\Bigg(&\frac{1}{\sqrt{\pi\,D\,(t'-t_0)}}\;\exp\Big[-\frac{(r_0-a)^2}{4\,D\,(t'-t_0)}\Big] \\ &-\;\alpha\;\exp\big[\,\alpha(r_0-a)+\alpha^2 D\,(t'-t_0)\,\big]\,\mathrm{erfc}\Big[\frac{r_0-a}{\sqrt{4D(t'-t_0)}}+\alpha\sqrt{D\,(t'-t_0)}\Big]\Bigg) \end{aligned} \tag{3.110}$$

To evaluate the integral we expand the first summand of the integrand in (3.110). For the exponent one can write

$$\underbrace{-\frac{(r_0-a)^2}{4\,D\,(t'-t_0)}}_{=x^2(t')} \;=\; \underbrace{(r_0-a)\,\alpha \;+\; D\,(t'-t_0)\,\alpha^2}_{=y(t')} \;-\; \underbrace{\frac{(r_0-a\;+\;2\,D\,(t'-t_0)\,\alpha)^2}{4\,D\,(t'-t_0)}}_{=z^2(t')}\;. \tag{3.111}$$

We introduce the functions $x(t')$, $y(t')$, and $z(t')$ for notational convenience. For the factor in front of the exponential function we consider the expansion

$$\begin{aligned} &\frac{1}{\sqrt{\pi\,D\,(t'-t_0)}} \\ &\quad=\;\frac{2}{\sqrt{\pi}\,D\,\alpha}\left(\frac{D\,(r_0-a)}{4\left(D\,(t'-t_0)\right)^{3/2}} \;-\; \frac{D\,(r_0-a)}{4\left(D\,(t'-t_0)\right)^{3/2}} \;+\; \frac{D^2\,(t'-t_0)\,\alpha}{2\left(D\,(t'-t_0)\right)^{3/2}}\right) \\ &\quad=\;\frac{2}{\sqrt{\pi}\,D\,\alpha}\left(\underbrace{\frac{D\,(r_0-a)}{4\left(D\,(t'-t_0)\right)^{3/2}}}_{=dx(t')/dt'} \;\underbrace{-\;\frac{(r_0-a)}{2\,(t'-t_0)\,\sqrt{4\,D\,(t'-t_0)}} \;+\; \frac{D\,\alpha}{\sqrt{4\,D\,(t'-t_0)}}}_{=dz(t')/dt'}\right)\;. \end{aligned} \tag{3.112}$$

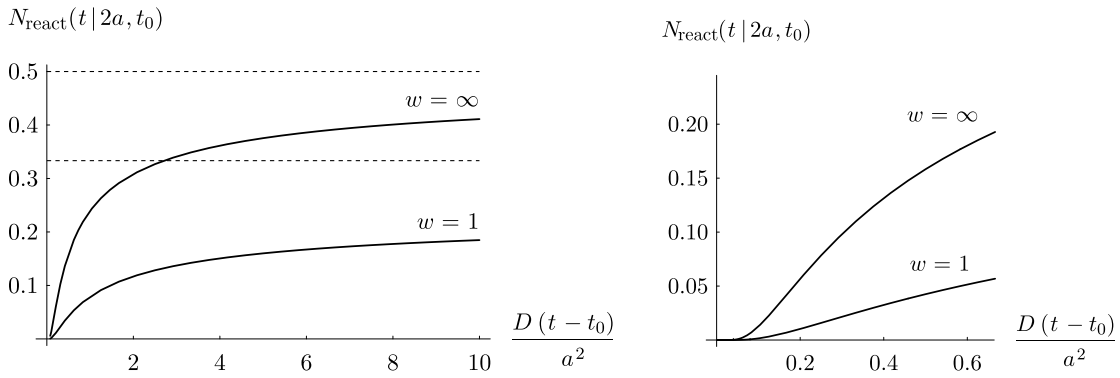

Figure 3.7: The left plot shows the fraction of particles that react at boundary $r = a$. The two cases $w = 1$ and $w = \infty$ of equation (3.114) are displayed. The dotted lines indicate the asymptotic values for $t \to \infty$. The right plot depicts the time evolution of equation (3.114) for small $(t - t_0)$.

Note, that the substitutions in (3.112) define the signs of $x(t')$ and $z(t')$. With the above expansions and substitutions one obtains

$$\begin{aligned} N_{\mathrm{react}}(t|r_0,t_0) &= \frac{a\,w}{D\,\alpha\,r_0}\int_{t_0}^{t}dt'\left(\frac{2}{\sqrt{\pi}}\,\frac{dx(t')}{dt'}\,e^{-x^2(t')}\right. \\ &\qquad \left. +\,\frac{2}{\sqrt{\pi}}\,\frac{dz(t')}{dt'}\,e^{y(t')}\,e^{-z^2(t')} - \frac{dy(t')}{dt'}\,e^{y(t')}\,\mathrm{erfc}[z(t')]\right) \\ &= \frac{a\,w}{D\,\alpha\,r_0}\left(\frac{2}{\sqrt{\pi}}\int_{x(t_0)}^{x(t)}dx\;e^{-x^2} - \int_{t_0}^{t}dt'\,\frac{d}{dt'}\left(e^{y(t')}\,\mathrm{erfc}[z(t')]\right)\right) \\ &= \frac{a\,w}{D\,\alpha\,r_0}\left(\mathrm{erf}[\,x(t')\,] - e^{y(t')}\,\mathrm{erfc}[z(t')]\right)\Big|_{t_0}^{t}. \end{aligned} \tag{3.113}$$

Filling in the integration boundaries and taking $w\,a = D\,(a\,\alpha - 1)$ into account one derives

$$\begin{aligned} N_{\mathrm{react}}(t|r_0,t_0) &= \frac{a\,\alpha-1}{r_0\,\alpha}\left(1 + \mathrm{erf}\left[\frac{a-r_0}{\sqrt{4\,D\,(t-t_0)}}\right]\right. \\ &\qquad \left. -\;e^{(r_0-a)\,\alpha\,+\,D\,(t-t_0)\,\alpha^2}\;\mathrm{erfc}\left[\frac{r_0-a+2\,D\,(t-t_0)\,\alpha}{\sqrt{4\,D\,(t-t_0)}}\right]\right). \end{aligned} \tag{3.114}$$

Fraction of Particles Reacted for $w \to \infty$ One derives the limit $\alpha \to \infty$ for a completely absorptive boundary at $x = a$ with the help of equation (3.102).

$$\begin{aligned} \lim_{\alpha\to\infty} N_{\mathrm{react}}(t|r_0,t_0) &= \frac{a}{r_0}\left(1 + \mathrm{erf}\left[\frac{a-r_0}{\sqrt{4\,D\,(t-t_0)}}\right]\right. \\ &\qquad \left. -\;\frac{1}{\alpha}\left(\frac{2}{\sqrt{4\pi\,D\,(t-t_0)}} + \mathcal{O}\left(\frac{1}{\alpha^2}\right)\right)\exp\left[-\frac{(r_0-a)^2}{4\,D\,(t-t_0)}\right]\right). \end{aligned} \tag{3.115}$$

The second line of equation (3.115) approaches 0 and one is left with

$$\lim_{\alpha\to\infty} N_{\rm react}(t|r_0,t_0) \;=\; \frac{a}{r_0}\;\mathrm{erfc}\left[\frac{r_0-a}{\sqrt{4\,D\,(t-t_0)}}\right]\,. \tag{3.116}$$

Fraction of Particles Reacted for $(t-t_0)\to\infty$ We investigate another limiting case of $N_{\rm react}(t|r_0,t_0)$; the long time behavior for $(t-t_0)\to\infty$. For the second line of equation (3.114) we again refer to (3.102), which renders for $r=a$ and with respect to orders of t instead of α

$$\begin{aligned}\exp\big[\,\alpha^2\,D\,(t-t_0)\,+\,\alpha\,(r_0-a)\,\big]\;\mathrm{erfc}\left[\alpha\,\sqrt{D\,(t-t_0)}\;+\;\frac{r_0-a}{\sqrt{4\,D\,(t-t_0)}}\right]\\ =\;\left(\frac{1}{\sqrt{\pi\,D\,(t-t_0)}}+\mathcal{O}\Big(\frac{1}{t-t_0}\Big)\right)\;\exp\left[-\frac{(r_0-a)^2}{4\,D\,(t-t_0)}\right]\,.\end{aligned} \tag{3.117}$$

Equation (3.117) approaches 0 for $(t-t_0)\to\infty$, and since $\mathrm{erf}[-\infty]=0$, one obtains for $N_{\rm react}(t|r_0,t_0)$ of equation (3.114)

$$\lim_{(t-t_0)\to\infty} N_{\rm react}(t|r_0,t_0) \;=\; \frac{a}{r_0}\;-\;\frac{1}{r_0\,\alpha}\,. \tag{3.118}$$

Even for $w,\alpha\to\infty$ this fraction is less than one in accordance with the ergodic behaviour of particles diffusing in three-dimensional space. In order to overcome the a/r_0 limit on the overall reaction yield one can introduce long range interactions which effectively increase the reaction radius a.
We note that the fraction of particles $N(t|r_0)$ not reacted at time t is $1-N_{\rm react}(t|r_0)$ such that

$$\begin{aligned}N(t|r_0,t_0) \;=\; 1\;-\;\frac{a\,\alpha-1}{r_0\,\alpha}\left(1\;+\;\mathrm{erf}\left[\frac{a-r_0}{\sqrt{4\,D\,(t-t_0)}}\right]\right.\\ \left.-\;e^{(r_0-a)\,\alpha\,+\,D\,(t-t_0)\,\alpha^2}\;\mathrm{erfc}\left[\frac{r_0-a+2\,D\,(t-t_0)\,\alpha}{\sqrt{4\,D\,(t-t_0)}}\right]\right)\,.\end{aligned} \tag{3.119}$$

We will demonstrate in a later chapter that this quantity can be evaluated directly without determining the distribution $p(r,t|r_0,t_0)$ first. Naturally, the cumbersome derivation provided here makes such procedure desirable.

3.5 Free Diffusion in a Finite Domain

We consider now a particle diffusing freely in a finite, one-dimensional interval

$$\Omega \;=\; [0,\,a]\,. \tag{3.120}$$

The boundaries of Ω at $x=0,\,a$ are assumed to be reflective. The diffusion coefficient D is assumed to be constant. The conditional distribution function $p(x,t|x_0,t_0)$ obeys the diffusion equation

$$\partial_t\,p(x,t|x_0,t_0) \;=\; D\;\partial_x^2\,p(x,t|x_0,t_0) \tag{3.121}$$

subject to the initial condition

$$p(x,t_0|x_0,t_0) \;=\; \delta(x\,-\,x_0) \tag{3.122}$$

and to the boundary conditions

$$D\ \partial_x\, p(x,t|x_0,t_0) \;=\; 0\ , \qquad \text{for } x\ =\ 0,\ \text{and } x\ =\ a\ . \tag{3.123}$$

In order to solve (3.121–3.123) we expand $p(x,t|x_0,t_0)$ in terms of eigenfunctions of the diffusion operator

$$\mathcal{L}_0 \;=\; D\ \partial_x^2\ . \tag{3.124}$$

where we restrict the function space to those functions which obey (3.123). The corresponding functions are

$$v_n(x) \;=\; A_n\ \cos\Big[n\,\pi\,\frac{x}{a}\Big]\ , \qquad n\ =\ 0,1,2,\dots\ . \tag{3.125}$$

In fact, for these functions holds for $n\ =\ 0,1,2,\dots$

$$\mathcal{L}_0\ v_n(x) \;=\; \lambda_n\, v_n(x) \tag{3.126}$$

$$\lambda_n \;=\; -\,D\ \Big(\frac{n\,\pi}{a}\Big)^2\ . \tag{3.127}$$

From

$$\partial_x\, v_n(x) \;=\; -\frac{n\,\pi}{a}\,A_n\,\sin\Big[n\,\pi\,\frac{x}{a}\Big]\ , \qquad n\ =\ 0,1\,2,\dots \tag{3.128}$$

follows readily that these functions indeed obey (3.123).
We can define, in the present case, the scalar product for functions $f,\,g$ in the function space considered

$$\langle\, g\,|\,f\,\rangle_\Omega \;=\; \int_0^a dx\ g(x)\,f(x)\ . \tag{3.129}$$

For the eigenfunctions (3.125) we choose the normalization

$$\langle\, v_n\,|\,v_n\,\rangle_\Omega \;=\; 1\ . \tag{3.130}$$

This implies for $n\ =\ 0$

$$\int_0^a dx\ A_0^2 \;=\; A_0^2\,a \;=\; 1 \tag{3.131}$$

and for $n\ \neq\ 0$, using $\cos^2\alpha\ =\ \frac{1}{2}(1\ +\ \cos 2\alpha)$,

$$\int_0^a dx\ v_n^2(x) \;=\; A_n^2\ \frac{a}{2}\ +\ \frac{1}{2}\ A_n^2\ \int_0^a dx\ \cos\Big[2\,n\,\pi\,\frac{x}{a}\Big] \;=\; A_n^2\ \frac{a}{2}\ . \tag{3.132}$$

It follows

$$A_n \;=\; \begin{cases} \sqrt{1/a} & \text{for } n\ =\ 0\ , \\ \sqrt{2/a} & \text{for } n\ =\ 1,2,\dots\ . \end{cases} \tag{3.133}$$

The functions v_n are orthogonal with respect to the scalar product (3.129), i.e.,

$$\langle v_m|v_n\rangle_\Omega \;=\; \delta_{mn}\ . \tag{3.134}$$

To prove this property we note, using

$$\cos\alpha\,\cos\beta \;=\; \frac{1}{2}\left(\cos(\alpha+\beta)\;+\;\cos(\alpha-\beta)\right)\,, \tag{3.135}$$

for $m \neq n$

$$\begin{aligned}
\langle\, v_m \,|\, v_n \,\rangle_\Omega \;&=\; \frac{A_m\,A_n}{2}\left(\int_0^a dx\;\cos\Big[(m+n)\,\pi\,\frac{x}{a}\Big]\;+\;\int_0^a dx\;\cos\Big[(m-n)\,\pi\,\frac{x}{a}\Big]\right)\\
&=\; \frac{A_m\,A_n}{2\,\pi}\left(\frac{a}{(m+n)}\;\sin\Big[(m+n)\,\pi\,\frac{x}{a}\Big]\;+\;\frac{a}{(m-n)}\;\sin\Big[(m-n)\,\pi\,\frac{x}{a}\Big]\right)\Bigg|_0^a\\
&=\; 0\;.
\end{aligned}$$

Without proof we note that the functions v_n, defined in (3.125), form a complete basis for the function space considered. Together with the scalar product (3.129) this basis is orthonormal. We can, hence, readily expand $p(x,t|x_0,t_0)$ in terms of v_n

$$p(x,t|x_0,t_0) \;=\; \sum_{n=0}^{\infty}\,\alpha_n(t|x_0,t_0)\;v_n(x)\;. \tag{3.136}$$

Inserting this expansion into (3.121) and using (3.126) yields

$$\sum_{n=0}^{\infty}\,\partial_t\,\alpha_n(t|x_0,t_0)\;v_n(x) \;=\; \sum_{n=0}^{\infty}\lambda_n\;\alpha_n(t|x_0,t_0)\;v_n(x)\;. \tag{3.137}$$

Taking the scalar product $\langle\, v_m \,|$ leads to

$$\partial_t\,\alpha_m(t|x_0,t_0) \;=\; \lambda_m\,\alpha_m(t|x_0,t_0) \tag{3.138}$$

from which we conclude

$$\alpha_m(t|x_0,t_0) \;=\; e^{\lambda_m\,(t-t_0)}\,\beta_m(x_0,t_0)\;. \tag{3.139}$$

Here, $\beta_m(x_0,t_0)$ are time-independent constants which are determined by the initial condition (3.122)

$$\sum_{n=0}^{\infty}\,\beta_n(x_0,t_0)\,v_n(x) \;=\; \delta(x-x_0)\;. \tag{3.140}$$

Taking again the scalar product $\langle\, v_m \,|$ results in

$$\beta_m(x_0,t_0) \;=\; v_m(x_0)\;. \tag{3.141}$$

Altogether holds then

$$p(x,t|x_0,t_0) \;=\; \sum_{n=0}^{\infty}\,e^{\lambda_n\,(t-t_0)}\,v_n(x_0)\,v_n(x)\;. \tag{3.142}$$

Let us assume now that the system considered is actually distributed initially according to a distribution $f(x)$ for which we assume $\langle\, 1 \,|\, f \,\rangle_\Omega = 1$. The distribution $p(x,t)$, at later times, is then

$$p(x,t) \;=\; \int_0^a dx_0 \; p(x,t|x_0,t_0)\, f(x_0) \;. \tag{3.143}$$

Employing the expansion (3.142) this can be written

$$p(x,t) \;=\; \sum_{n=0}^{\infty} \; e^{\lambda_n\,(t-t_0)}\, v_n(x) \; \int_0^a dx_0 \; v_n(x_0)\, f(x_0) \;. \tag{3.144}$$

We consider now the behaviour of $p(x,t)$ at long times. One expects that the system ultimately assumes a homogeneous distribution in Ω, i.e., that $p(x,t)$ relaxes as follows

$$p(x,t) \;\underset{t\to\infty}{\asymp}\; \frac{1}{a} \;. \tag{3.145}$$

This asymptotic behaviour, indeed, follows from (3.144). We note from (3.127)

$$e^{\lambda_n\,(t-t_0)} \;\underset{t\to\infty}{\asymp}\; \begin{cases} 1 & \text{for } n \,=\, 0 \\ 0 & \text{for } n \,=\, 1,2,\ldots \end{cases} \;. \tag{3.146}$$

From (3.125, 3.133) follows $v_0(x) = 1/\sqrt{a}$ and, hence,

$$p(x,t) \;\underset{t\to\infty}{\asymp}\; \frac{1}{a} \; \int_0^a dx \; v(x_0) \;. \tag{3.147}$$

The property $\langle\, 1 \,|\, f \,\rangle_\Omega = 1$ implies then (3.145).
The solution presented here [cf. (3.120–3.147)] provides in a nutshel the typical properties of solutions of the more general Smoluchowski diffusion equation accounting for the presence of a force field which will be provided in Chapter 4.

3.6 Rotational Diffusion

Dielectric Relaxation

The electric polarization of liquids originates from the dipole moments of the individual liquid molecules. The contribution of an individual molecule to the polarization in the z-direction is

$$P_3 \;=\; P_0\, \cos\theta \tag{3.148}$$

We consider the relaxation of the dipole moment assuming that the rotational diffusion of the dipole moments can be described as diffusion on the unit sphere.
The diffusion on a unit sphere is described by the three-dimensional diffusion equation

$$\partial_t\, p(\boldsymbol{r},t|\boldsymbol{r}_0,t_0) \;=\; D\,\nabla^2\, p(\boldsymbol{r},t|\boldsymbol{r}_0,t_0) \tag{3.149}$$

for the condition $|\boldsymbol{r}| = |\boldsymbol{r}_0| = 1$. In order to obey this condition one employs the Laplace operator ∇^2 in terms of spherical coordinates (r,θ,ϕ) as given in (3.65) and sets $r = 1$, dropping also derivatives with respect to r. This yields the rotational diffusion equation

$$\partial_t\, p(\Omega,t|\Omega_0,t_0) \;=\; \tau_r^{-1} \left[\frac{1}{\sin\theta}\; \partial_\theta \left(\sin\theta\, \partial_\theta \right) \;+\; \frac{1}{\sin^2\theta}\; \partial_\phi^2 \right] \; p(\Omega,t|\Omega_0,t_0) \;. \tag{3.150}$$

We have defined here $\Omega = (\theta, \phi)$. We have also introduced, instead of the diffusion constant, the rate constant τ_r^{-1}since the replacement $r \to 1$ altered the units in the diffusion equation; τ_r has the unit of time. In the present case the diffusion space has no boundary; however, we need to postulate that the distribution and its derivatives are continuous on the sphere.
One way of ascertaining the continuity property is to expand the distribution in terms of spherical harmonics $Y_{\ell m}(\Omega)$ which obey the proper continuity, i.e.,

$$p(\Omega, t|\Omega_0, t_0) \;=\; \sum_{\ell=0}^{\infty} \sum_{m=-\ell}^{+\ell} A_{\ell m}(t|\Omega_0, t_0)\, Y_{\ell m}(\Omega)\ . \tag{3.151}$$

In addition, one can exploit the eigenfunction property

$$\left[\frac{1}{\sin\theta}\, \partial_\theta \left(\sin\theta\, \partial_\theta \right) \;+\; \frac{1}{\sin^2\theta}\, \partial_\phi^2 \right] Y_{\ell m}(\Omega) \;=\; -\ell\,(\ell+1)\, Y_{\ell m}(\Omega)\ . \tag{3.152}$$

Inserting (3.151) into (3.150) and using (3.152) results in

$$\sum_{\ell=0}^{\infty} \sum_{m=-\ell}^{+\ell} \partial_t\, A_{\ell m}(t|\Omega_0, t_0)\; Y_{\ell m}(\Omega) \;=\; -\sum_{\ell=0}^{\infty} \sum_{m=-\ell}^{+\ell} \ell\,(\ell+1)\; \tau_r^{-1}\; A_{\ell m}(t|\Omega_0, t_0)\; Y_{\ell m}(\Omega) \tag{3.153}$$

The orthonormality property

$$\int d\Omega\; Y^*_{\ell' m'}(\Omega)\; Y_{\ell m}(\Omega) \;=\; \delta_{\ell' \ell}\, \delta_{m' m} \tag{3.154}$$

leads one to conclude

$$\partial_t\, A_{\ell m}(t|\Omega_0, t_0) \;=\; -\ell\,(\ell+1)\; \tau_r^{-1}\; A_{\ell m}(t|\Omega_0, t_0) \tag{3.155}$$

and, accordingly,

$$A_{\ell m}(t|\Omega_0, t_0) \;=\; e^{-\ell\,(\ell+1)\,(t-t_0)/\tau_r}\; a_{\ell m}(\Omega_0) \tag{3.156}$$

or

$$p(\Omega, t|\Omega_0, t_0) \;=\; \sum_{\ell=0}^{\infty} \sum_{m=-\ell}^{+\ell} e^{-\ell\,(\ell+1)\,(t-t_0)/\tau_r}\; a_{\ell m}(\Omega_0)\; Y_{\ell m}(\Omega)\ . \tag{3.157}$$

The coefficients $a_{\ell m}(\Omega_0)$ are determined through the condition

$$p(\Omega, t_0|\Omega_0, t_0) \;=\; \delta(\Omega - \Omega_0)\ . \tag{3.158}$$

The completeness relationship of spherical harmonics states

$$\delta(\Omega - \Omega_0) \;=\; \sum_{\ell=0}^{\infty} \sum_{m=-\ell}^{+\ell} Y^*_{\ell m}(\Omega_0)\; Y_{\ell m}(\Omega)\ . \tag{3.159}$$

Equating this with (3.157) for $t = t_0$ yields

$$a_{\ell m}(\Omega_0) \;=\; Y^*_{\ell m}(\Omega_0) \tag{3.160}$$

and, hence,

$$p(\Omega, t|\Omega_0, t_0) \;=\; \sum_{\ell=0}^{\infty} \sum_{m=-\ell}^{+\ell} e^{-\ell\,(\ell+1)\,(t-t_0)/\tau_r}\; Y^*_{\ell m}(\Omega_0)\; Y_{\ell m}(\Omega)\;. \tag{3.161}$$

It is interesting to consider the asymptotic, i.e., the $t \rightarrow \infty$, behaviour of this solution. All exponential terms will vanish, except the term with $\ell = 0$. Hence, the distribution approaches asymptotically the limit

$$\lim_{t\rightarrow\infty} p(\Omega, t|\Omega_0, t_0) \;=\; \frac{1}{4\pi}\;, \tag{3.162}$$

where we used $Y_{00}(\Omega) = 1/\sqrt{4\pi}$. This result corresponds to the homogenous, normalized distribution on the sphere, a result which one may have expected all along. One refers to this distribution as the equilibrium distribution denoted by

$$p_0(\Omega) \;=\; \frac{1}{4\pi}\;. \tag{3.163}$$

The equilibrium average of the polarization expressed in (3.148) is

$$\Big\langle P_3 \Big\rangle \;=\; \int d\Omega P_0\;\cos\theta\; p_0(\Omega)\;. \tag{3.164}$$

One can readily show

$$\Big\langle P_3 \Big\rangle \;=\; 0\;. \tag{3.165}$$

Another quantity of interest is the so-called equilibrium correlation function

$$\Big\langle P_3(t)\, P_3^*(t_0) \Big\rangle \;=\; P_0^2 \int d\Omega \int d\Omega_0\;\cos\theta\;\cos\theta_0\; p(\Omega, t|\Omega_0, t_0)\; p_0(\Omega_0)\;. \tag{3.166}$$

Using

$$Y_{10}(\Omega) \;=\; \sqrt{\frac{3}{4\pi}}\;\cos\theta \tag{3.167}$$

and expansion (3.161) one obtains

$$\Big\langle P_3(t)\, P_3^*(t_0) \Big\rangle \;=\; \frac{4\pi}{3}\; P_0^2 \sum_{m=-\ell}^{+\ell} e^{-\ell\,(\ell+1)\,(t-t_0)/\tau_r}\; |C_{10,\ell m}|^2\;, \tag{3.168}$$

where

$$C_{10,\ell m} \;=\; \int d\Omega\; Y^*_{10}(\Omega)\; Y_{\ell m}(\Omega)\;. \tag{3.169}$$

The orthonormality condition of the spherical harmonics yields immediately

$$C_{10,\ell m} \;=\; \delta_{\ell 1}\;\delta_{m0} \tag{3.170}$$

and, therefore,

$$\Big\langle P_3(t)\, P_3^*(t_0) \Big\rangle \;=\; \frac{4\pi}{3}\; P_0^2\; e^{-2\,(t-t_0)/\tau_r}\;. \tag{3.171}$$

Other examples in which rotational diffusion plays a role are fluorescence depolarization as observed in optical experiments and dipolar relaxation as observed in NMR spectra.

Chapter 4

Smoluchowski Diffusion Equation

Contents

4.1 Derivation of the Smoluchoswki Diffusion Equation for Potential Fields 64

4.2 One-Dimensional Diffuson in a Linear Potential 67

4.2.1 Diffusion in an infinite space $\Omega_\infty =]-\infty, \infty[$ 67

4.2.2 Diffusion in a Half-Space $\Omega_\infty = [0, \infty[$ 70

4.3 Diffusion in a One-Dimensional Harmonic Potential 74

We want to apply now our derivation to the case of a Brownian particle in a force field $\boldsymbol{F}(\boldsymbol{r})$. The corresponding Langevin equation is

$$m\ddot{\boldsymbol{r}} \;=\; -\gamma\,\dot{\boldsymbol{r}} \;+\; \boldsymbol{F}(\boldsymbol{r}) \;+\; \sigma\,\xi(t) \tag{4.1}$$

for scalar friction constant γ and amplitude σ of the fluctuating force. We will assume in this section the *limit of strong friction*. In this limit the magnitude of the frictional force $\gamma\dot{\boldsymbol{r}}$ is much larger than the magnitude of the force of inertia $m\ddot{\boldsymbol{r}}$, i.e.,

$$|\gamma\,\dot{\boldsymbol{r}}| \;\gg\; |m\,\ddot{\boldsymbol{r}}| \tag{4.2}$$

and, therefore, (4.1) becomes

$$\gamma\,\dot{\boldsymbol{r}} \;=\; \boldsymbol{F}(\boldsymbol{r}) \;+\; \sigma\,\xi(t) \tag{4.3}$$

To (4.1) corresponds the Fokker-Planck equation (cf. Eqs. (2.138) and (2.148)

$$\partial_t\, p(\boldsymbol{r}, t|\boldsymbol{r}_0, t_0) \;=\; \left(\boldsymbol{\nabla}^2\,\frac{\sigma^2}{2\gamma^2} \;-\; \boldsymbol{\nabla}\cdot\frac{\boldsymbol{F}(\boldsymbol{r})}{\gamma}\right) p(\boldsymbol{r}, t|\boldsymbol{r}_0, t_0) \tag{4.4}$$

In case that the force field can be related to a scalar potential, i.e., in case $\boldsymbol{F}(\boldsymbol{r}) = -\boldsymbol{\nabla}U(\boldsymbol{r})$, one expects that the Boltzmann distribution $\exp[-U(\boldsymbol{r})/k_BT]$ is a stationary, i.e., time-independent, solution and that, in fact, the system asymptotically approaches this solution. This expectation should be confined to force fields of the stated kind, i.e., to force fields for which holds $\boldsymbol{\nabla}\times\boldsymbol{F} = 0$. Fokker-Planck equations with more general force fields will be considered further below.

4.1 Derivation of the Smoluchoswki Diffusion Equation for Potential Fields

It turns out that the expectation that the Boltzmann distribution is a stationary solution of the Smoluchowski equation has to be introduced as a postulate rather than a consequence of (4.4). Defining the parameters $D = \sigma^2/2\gamma^2$ [cf. (3.12)] and $\beta = 1/k_B T$ the *postulate* of the stationary behaviour of the Boltzmann equation is

$$\left(\boldsymbol{\nabla} \cdot \boldsymbol{\nabla} D(\boldsymbol{r}) \; - \; \boldsymbol{\nabla} \cdot \frac{\boldsymbol{F}(\boldsymbol{r})}{\gamma(\boldsymbol{r})} \right) e^{-\beta U(\boldsymbol{r})} \;\; = \;\; 0 \; . \tag{4.5}$$

We have included here the possibility that the coefficients σ and γ defining the fluctuating and dissipative forces are spatially dependent. In the following we will not explicitly state the dependence on the spatial coordinates $\boldsymbol{r}$ anymore.
Actually, the postulate (4.5) of the stationarity of the Boltzmann distribution is not sufficient to obtain an equation with the appropriate behaviour at thermal equilibrium. Actually, one needs to require the more stringent postulate that at equilibrium there does not exist a net flux of particles (or of probability) in the system. This should hold true when the system asymptotically comes to rest as long as there are no particles generated or destroyed, e.g., through chemical reactions. We need to establish the expression for the flux before we can investigate the ramifications of the indicated postulate.
An expression for the flux can be obtained in a vein similar to that adopted in the case of free diffusion [cf. (3.17–3.21)]. We note that (4.4) can be written

$$\partial_t \, p(\boldsymbol{r}, t|\boldsymbol{r}_0, t_0) \;\; = \;\; \boldsymbol{\nabla} \cdot \left(\boldsymbol{\nabla} \, D \; - \; \frac{\boldsymbol{F}(\boldsymbol{r})}{\gamma} \right) p(\boldsymbol{r}, t|\boldsymbol{r}_0, t_0) \; . \tag{4.6}$$

Integrating this equation over some arbitrary volume Ω, with the definition of the particle number in this volume

$$N_\Omega(t|\boldsymbol{r}_0, t_0) \;\; = \;\; \int_\Omega d\boldsymbol{r} \; p(\boldsymbol{r}, t|\boldsymbol{r}_0, t_0) \tag{4.7}$$

and using (4.6), yields

$$\partial_t \, N_\Omega(t|\boldsymbol{r}_0, t_0) \;\; = \;\; \int_\Omega d\boldsymbol{r} \; \boldsymbol{\nabla} \cdot \left(\boldsymbol{\nabla} \, D \; - \; \frac{\boldsymbol{F}(\boldsymbol{r})}{\gamma} \right) p(\boldsymbol{r}, t|\boldsymbol{r}_0, t_0) \tag{4.8}$$

and, after applying Gauss' theorem (3.19),

$$\partial_t \, N_\Omega(t|\boldsymbol{r}_0, t_0) \;\; = \;\; \int_{\partial\Omega} d\boldsymbol{a} \cdot \left(\boldsymbol{\nabla} \, D \; - \; \frac{\boldsymbol{F}(\boldsymbol{r})}{\gamma} \right) p(\boldsymbol{r}, t|\boldsymbol{r}_0, t_0) \; . \tag{4.9}$$

The l.h.s. of this equation describes the rate of change of the particle number, the r.h.s. contains a surface integral summing up scalar products between the vector quantity

$$\boldsymbol{j}(\boldsymbol{r}, t|\boldsymbol{r}_0, t_0) \;\; = \;\; \left(\boldsymbol{\nabla} \, D \; - \; \frac{\boldsymbol{F}(\boldsymbol{r})}{\gamma} \right) p(\boldsymbol{r}, t|\boldsymbol{r}_0, t_0) \tag{4.10}$$

and the surface elements $d\boldsymbol{a}$ of $\partial\Omega$. Since particles are neither generated nor destroyed inside the volume Ω, we must interpret $\boldsymbol{j}(\boldsymbol{r}, t|\boldsymbol{r}_0, t_0)$ as a particle flux at the boundary $\partial\Omega$. Since the volume

and its boundary are arbitrary, the interpretation of $\boldsymbol{j}(\boldsymbol{r}, t|\boldsymbol{r}_0, t_0)$ as given by (4.10) as a flux should hold everywhere in Ω.
We can now consider the ramifications of the postulate that at equilibrium the flux vanishes. Applying (4.10) to the Boltzmann distribution $p_o(\boldsymbol{r}) = N \exp[-\beta U(\boldsymbol{r})]$, for some appropriate normalization factor N, yields the equilibrium flux

$$\boldsymbol{j}_o(\boldsymbol{r}) = \left(\boldsymbol{\nabla} D - \frac{\boldsymbol{F}(\boldsymbol{r})}{\gamma}\right) N e^{-\beta U(\boldsymbol{r})} . \tag{4.11}$$

With this definition the postulate discussed above is

$$\left(\boldsymbol{\nabla} D - \frac{\boldsymbol{F}(\boldsymbol{r})}{\gamma}\right) N e^{-\beta U(\boldsymbol{r})} \equiv 0 . \tag{4.12}$$

The derivative $\boldsymbol{\nabla} D \exp[-\beta U(\boldsymbol{r})] = \exp[-\beta U(\boldsymbol{r})] \left(\boldsymbol{\nabla} D + \beta \boldsymbol{F}(\boldsymbol{r})\right)$ allows us to write this

$$e^{-\beta U(\boldsymbol{r})} \left(D \beta \boldsymbol{F}(\boldsymbol{r}) + \boldsymbol{\nabla} D - \frac{\boldsymbol{F}(\boldsymbol{r})}{\gamma}\right) \equiv 0 . \tag{4.13}$$

From this follows

$$\boldsymbol{\nabla} D = \boldsymbol{F}(\boldsymbol{r}) \left(\gamma^{-1} - D \beta\right) . \tag{4.14}$$

an identity which is known as the so-called *fluctuation - dissipation theorem*.
The fluctuation - dissipation theorem is better known for the case of spatially independent D in which case follows $D \beta \gamma = 1$, i.e., with the definitions above

$$\sigma^2 = 2 k_B T \gamma . \tag{4.15}$$

This equation implies a relationship between the amplitude σ of the fluctuating forces and the amplitude γ of the dissipative (frictional) forces in the Langevin equation (4.1), hence, the name *fluctuation - dissipation theorem*. The theorem states that the amplitudes of fluctuating and dissipative forces need to obey a temperature-dependent relationship in order for a system to attain thermodynamic equilibrium. There exist more general formulations of this theorem which we will discuss further below in connection with response and correlation functions.
In its form (4.14) the fluctuation - dissipation theorem allows us to reformulate the Fokker-Planck equation above. For any function $f(\boldsymbol{r})$ holds with (4.14)

$$\boldsymbol{\nabla}\cdot\boldsymbol{\nabla}\, D f = \boldsymbol{\nabla} \cdot D\, \boldsymbol{\nabla} f + \boldsymbol{\nabla} \cdot f\, \boldsymbol{\nabla} D = \boldsymbol{\nabla} \cdot D \boldsymbol{\nabla} f + \boldsymbol{\nabla} \cdot \boldsymbol{F} \left(\frac{1}{\gamma} - D\beta\right) f \tag{4.16}$$

From this follows finally for the Fokker-Planck equation (4.4)

$$\partial_t\, p(\boldsymbol{r}, t|\boldsymbol{r}_0, t_0) = \boldsymbol{\nabla} \cdot D \left(\boldsymbol{\nabla} - \beta \boldsymbol{F}(\boldsymbol{r})\right) p(\boldsymbol{r}, t|\boldsymbol{r}_0, t_0) . \tag{4.17}$$

One refers to Eq. (4.17) as the *Smoluchowski equation*.
The Smoluchowski equation (4.17), in the case $\boldsymbol{F}(\boldsymbol{r}) = -\boldsymbol{\nabla} U(\boldsymbol{r})$, can be written in the convenient form

$$\partial_t\, p(\boldsymbol{r}, t|\boldsymbol{r}_0, t_0) = \boldsymbol{\nabla} \cdot D\, e^{-\beta U(\boldsymbol{r})} \boldsymbol{\nabla} e^{\beta U(\boldsymbol{r})}\, p(\boldsymbol{r}, t|\boldsymbol{r}_0, t_0) . \tag{4.18}$$

This form shows immediately that $p \propto \exp[-\beta U(\boldsymbol{r})]$ is a stationary solution. The form also provides a new expression for the flux $\boldsymbol{j}$, namely,

$$\boldsymbol{j}(\boldsymbol{r}, t|\boldsymbol{r}_0, t_0) = D\, e^{-\beta U(\boldsymbol{r})} \boldsymbol{\nabla} e^{\beta U(\boldsymbol{r})}\, p(\boldsymbol{r}, t|\boldsymbol{r}_0, t_0) . \tag{4.19}$$

Boundary Conditions for Smoluchowski Equation

The system described by the Smoluchoswki (4.17) or Einstein (3.13) diffusion equation may either be closed at the surface of the diffusion space Ω or open, i.e., $\partial\Omega$ either may be impenetrable for particles or may allow passage of particles. In the latter case, $\partial\Omega$ describes a reactive surface. These properties of Ω are specified through the boundary conditions for the Smoluchoswki or Einstein equation at $\partial\Omega$. In order to formulate these boundary conditions we consider the flux of particles through consideration of $N_\Omega(t|\boldsymbol{r}_0, t_0)$ as defined in (4.7). Since there are no terms in (4.17) which affect the number of particles the particle number is conserved and any change of $N_\Omega(t|\boldsymbol{r}_0, t_0)$ must be due to particle flux at the surface of Ω, i.e.,

$$\partial_t \, N_\Omega(t|\boldsymbol{r}_0, t_0) \;\; = \;\; \int_{\partial\Omega} d\boldsymbol{a} \cdot \boldsymbol{j}(\boldsymbol{r}, t|\boldsymbol{r}_0, t_0) \tag{4.20}$$

where $\boldsymbol{j}(\boldsymbol{r}, t|\boldsymbol{r}_0, t_0)$ denotes the particle flux defined in (4.10). The fluctuation - dissipation theorem, as stated in (4.14), yields

$$\boldsymbol{\nabla} \, D \, f \;\; = \;\; D \, \boldsymbol{\nabla} \, f \;+\; f \, \boldsymbol{F}(\boldsymbol{r}) \left(\gamma^{-1} \;-\; D \, \beta \right) \tag{4.21}$$

and with (4.10) and (3.12) follows

$$\boldsymbol{j}(\boldsymbol{r}, t|\boldsymbol{r}_0, t_0) \;\; = \;\; D \left(\boldsymbol{\nabla} \;-\; \beta \, \boldsymbol{F}(\boldsymbol{r}) \right) \, p(\boldsymbol{r}, t|\boldsymbol{r}_0, t_0) \tag{4.22}$$

We will refer to

$$\boldsymbol{\mathcal{J}}(\boldsymbol{r}) \;\; = \;\; D \left(\boldsymbol{\nabla} \;-\; \beta \, \boldsymbol{F}(\boldsymbol{r}) \right) \tag{4.23}$$

as the flux operator. This operator, when acting on a solution of the Smoluchowski equation, yields the local flux of particles (probability) in the system.
The flux operator $\boldsymbol{\mathcal{J}}(\boldsymbol{r})$ governs the spatial boundary conditions since it allows to measure particle (probability) exchange at the surface of the diffusion space Ω. There are three types of boundary conditions possible. These types can be enforced simultaneously in disconnected areas of the surface $\partial\Omega$. Let us denote by $\partial\Omega_1, \partial\Omega_2$ two disconnected parts of $\partial\Omega$ such that $\partial\Omega = \partial\Omega_1 \cup \partial\Omega_2$. An example is a volume Ω lying between a sphere of radius R_1 ($\partial\Omega_1$) and of radius R_2 ($\partial\Omega_2$). The separation of the surfaces $\partial\Omega_i$ with different boundary conditions is necessary in order to assure that a continuous solution of the Smoluchowski equation exists. Such solution cannot exist if it has to satisfy in an infinitesimal neighborhood entailing $\partial\Omega$ two different boundary conditions.
The first type of boundary condition is specified by

$$\hat{\boldsymbol{a}}(\boldsymbol{r}) \cdot \boldsymbol{\mathcal{J}}(\boldsymbol{r}) \; p(\boldsymbol{r}, t|\boldsymbol{r}_0, t_0) \;\; = \;\; 0 \; , \quad \boldsymbol{r} \, \in \, \partial\Omega_i \tag{4.24}$$

which, obviously, implies that particles do not cross the boundary, i.e., that particles are reflected there. Here $\hat{\boldsymbol{a}}(\boldsymbol{r})$ denotes a unit vector normal to the surface $\partial\Omega_i$ at $\boldsymbol{r}$. We will refer to (4.24) as the *reflection boundary condition.*
The second type of boundary condition is

$$p(\boldsymbol{r}, t|\boldsymbol{r}_0, t_0) \;\; = \;\; 0 \; , \quad \boldsymbol{r} \, \in \, \partial\Omega_i \; . \tag{4.25}$$

This condition implies that all particles arriving at the surface $\partial\Omega_i$ are taken away such that the probability on $\partial\Omega_i$ vanishes. This boundary condition describes a reactive surface with the highest degree of reactivity possible, i.e., that *every* particle on $\partial\Omega_i$ reacts. We will refer to (4.25) as the *reaction boundary condition.*

The third type of boundary condition,

$$\hat{\boldsymbol{a}}(\boldsymbol{r}) \cdot \boldsymbol{\mathcal{J}}(\boldsymbol{r})\; p(\boldsymbol{r},t|\boldsymbol{r}_0,t_0) \;\; = \;\; w\; p(\boldsymbol{r},t|\boldsymbol{r}_0,t_0)\;, \quad \boldsymbol{r} \text{ on } \partial\Omega_i\;, \tag{4.26}$$

describes the case of intermediate reactivity at the boundary. The reactivity is measured by the parameter w. For $w = 0$ in (4.26) $\partial\Omega_i$ corresponds to a non-reactive, i.e., reflective boundary. For $w \to \infty$ the condition (4.26) can only be satisfied for $p(\boldsymbol{r},t|\boldsymbol{r}_0,t_0) = 0$, i.e., every particle impinging onto $\partial\Omega_i$ is consumed in this case. We will refer to (4.26) as the *radiation boundary condition*.

4.2 One-Dimensional Diffuson in a Linear Potential

We consider now diffusion in a linear potential

$$U(x) \;\; = \;\; c\,x \tag{4.27}$$

with a position-independent diffusion coefficient D. This system is described by the Smoluchowski equation

$$\partial_t\, p(x,t|x_0,t_0) \;\; = \;\; \left(D\,\partial_x^2 \;+\; D\,\beta\,c\,\partial_x \right)\, p(x,t|x_0,t_0)\;. \tag{4.28}$$

This will be the first instance of a system in which diffusing particles are acted on by a non-vanishing force. The techniques to solve the Smoluchowski equation in the present case will be particular for the simple force field, i.e., the solution techniques adopted cannot be generalized to other potentials.

4.2.1 Diffusion in an infinite space $\Omega_\infty = \,]-\infty,\infty[$

We consider first the situation that the particles diffusing under the influence of the potential (4.27) have available the infinite space

$$\Omega_\infty \;\; = \;\;]-\infty,\infty[\;. \tag{4.29}$$

In this case hold the boundary conditions

$$\lim_{x\to\pm\infty}\; p(x,t|x_0,t_0) \;\; = \;\; 0\;. \tag{4.30}$$

The initial condition is as usual

$$p(x,t_0|x_0,t_0) \;\; = \;\; \delta(x-x_0)\;. \tag{4.31}$$

In order to solve (4.28, 4.30, 4.31) we introduce

$$\tau \;=\; D\,t \quad , \qquad b \;=\; \beta\,c\;. \tag{4.32}$$

The Smoluchowski equation (4.28) can be written

$$\partial_\tau\, p(x,\tau|x_0,\tau_0) \;\; = \;\; \left(\partial_x^2 \;+\; b\,\partial_x \right)\, p(x,\tau|x_0,\tau_0)\;. \tag{4.33}$$

We introduce the time-dependent spatial coordinates

$$y \;=\; x \;+\; b\,\tau \quad , \qquad y_0 \;=\; x_0 \;+\; b\,\tau_0 \tag{4.34}$$

and express the solution

$$p(x,\tau|x_0,\tau_0) \;=\; q(y,\tau|y_0,\tau_0)\;. \tag{4.35}$$

Introducing this into (4.33) yields

$$\partial_\tau\, q(y,\tau|y_0,\tau_0) \;+\; b\;\partial_y\, q(y,\tau|y_0,\tau_0) \;=\; \left(\,\partial_y^2 \;+\; b\,\partial_y\,\right)\, q(y,\tau|y_0,\tau_0) \tag{4.36}$$

or

$$\partial_\tau\, q(y,\tau|y_0,\tau_0) \;=\; \partial_y^2\, q(y,\tau|y_0,\tau_0)\;. \tag{4.37}$$

This equation has the same form as the Einstein equation for freely diffusing particles for which the solution in case of the diffusion space Ω_∞ is

$$q(y,\tau|y_0,\tau_0) \;=\; \frac{1}{\sqrt{4\pi\,(\tau-\tau_0)}}\,\exp\!\left[-\frac{(y-y_0)^2}{4\,(\tau-\tau_0)}\right]\;. \tag{4.38}$$

Expressing the solution in terms of the original coordinates and constants yields

$$p(x,t|x_0,t_0) \;=\; \frac{1}{\sqrt{4\pi\,D\,(t-t_0)}}\,\exp\!\left[-\frac{\big(x-x_0+D\,\beta\,c\,(t-t_0)\big)^2}{4\,D\,(t-t_0)}\right]\;. \tag{4.39}$$

This solution is identical to the distribution of freely diffusing particles, except that the center of the distribution drifts down the potential gradient with a velocity $-D\,\beta\,c$.

Exercise 4.1:
Apply this to the case (i) of an ion moving between two electrodes at a distance of 1cm in water with a potential of 1 Volt. Estimate how long the ion needs to drift from one electrode to the other. (ii) an ion moving through a channel in a biological membrane of 40Å at which is applied a typical potential of 0.1eV. Assume the ion experiences a diffusion coefficient of $D = 10^{-5} cm^2/s$. Estimate how long the ion needs to cross the membrane.
Answer i) Let's assume that at the moment $t_0 = 0$ the ion is at $x_0 = 0$ with

$$p(x_0,t_0) \;=\; \delta(x_0)\;. \tag{4.40}$$

Then, according to (4.39) we have

$$p(x,t) \;=\; p(x,t|0,0) \;=\; \frac{1}{\sqrt{4\pi\,D\,t}}\,\exp\!\left[-\frac{\big(x+D\,\beta\,c\,t\big)^2}{4\,D\,t}\right]\;. \tag{4.41}$$

Calculate now the mean value of x:

$$\Big\langle x(t)\Big\rangle \;=\; \int_{-\infty}^{\infty} dx\; x\,p(x,t) \;=\; \frac{1}{\sqrt{4\pi\,D\,t}}\int_{-\infty}^{\infty} dx\; x\,\exp\!\big[-(x+\beta\,c\,D\,t)^2/4\,D\,t\big]\;. \tag{4.42}$$

In order to solve this integral add and substract a $\beta\,c\,D\,t$ term to x and make the change of variable $z = x + \beta\,D\,c\,t$. This yields

$$\Big\langle x(t)\Big\rangle \;=\; -D\,\beta\,c\,t \;=\; v_d\,t \tag{4.43}$$

where $v_d = -D\,\beta\,c$ is the drift velocity of the ion. Taking into consideration that the electrical force that acts on the ion is $c = q\,E$, $E = U/d$, $\beta = 1/k_bT$ and $\langle x(\tau)\rangle = d$ we obtain for the time τ needed by the ion to drift from one electrod to another

$$\tau \;=\; \frac{k_b\,T\,d^2}{D\,q\,U}\;. \tag{4.44}$$

For $d = 1\,\mathrm{cm}$, $k_B = 1.31 \times 10^{-23}\,\mathrm{J/K}$, $T = 300\,\mathrm{K}$, $D = 1.545 \times 10^{-5}\,\mathrm{cm^2/sec}$, $q = 1.6 \times 10^{-19}\,\mathrm{C}$, $U = 1\,\mathrm{V}$ we obtain $\tau = 1674\,\mathrm{sec}$.
ii) Applying the same reasoning to the ion moving through a membrane one gets $\tau = 4.14 \times 10^{-9}\,\mathrm{sec}$.

Diffusion and exponential growth

The above result (4.39) can be used for a stochastic processes with exponential growth by performing a simple substitution.
Comparing the Fokker-Planck equation (2.148) with the Smoluchowski equation (4.28) of the previous example one can easily derive within Ito calculus the corresponding stochastic differential equation

$$\partial_t\,x(t) \;=\; -D\,\beta\,c \;+\; \sqrt{D}\,\xi(t)\;, \tag{4.45}$$

or equivalently

$$dx \;=\; -D\,\beta\,c\;dt \;+\; \sqrt{D}\;d\omega\;. \tag{4.46}$$

Equation (4.46) displays the mechanism that generates the stochastic trajectories within a linear potential (4.27) . The increment dx of a trajectory $x(t)$ is given by the drift term $-D\,\beta\,c\;dt$, which is determined by the force c of the lineare potential and the friction $\gamma = D\,\beta$. Furthermore the increment dx is subject to Gaussian noise $d\omega$ scaled by $\sqrt{D}$.
We now consider a transformation of the spatial variable x. Let $x \mapsto y = \exp x$. This substitution and the resulting differential $dy/y = dx$ render the stochastic differential equation

$$dy \;=\; -D\,\beta\,c\;y\;dt \;+\; \sqrt{D}\;y\;d\omega\;. \tag{4.47}$$

Equation (4.47) describes a different stochastic process $y(t)$. Just considering the first term on the r.h.s. of (4.47), one sees that $y(t)$ is subject to exponential growth or decay depending on the sign of c. Neglecting the second term on the r.h.s of (**??**) one obtains the deterministic trajectory

$$y(t) \;=\; y(0)\;\exp\left[-\,D\,\beta\,c\;t\right]\;. \tag{4.48}$$

This dynamic is typical for growth or decay processes in physics, biology or economics. Furthermore, $y(t)$ is subject to Gaussian noise $d\omega$ scaled by $y\sqrt{D}$. The random fluctuation are consequently proportional to y, which is the case when the growth rate and not just the increment are subject to stochastic fluctuations.
Since (4.46) and (4.47) are connected via the simple mapping $y = \exp x$ we can readily state the solution of equation (4.47) by substituting $\log y$ for x in (4.39) .

$$p(y,t|y_0,t_0) = p(x(y),t|x(y_0),t_0)\,\frac{dx}{dy}$$
$$= \frac{1}{\sqrt{4\pi\,D\,(t-t_0)}\,y}\,\exp\left[-\frac{\left(\log\left(\frac{y}{y_0}\right)+D\,\beta\,c\,(t-t_0)\right)^2}{4\,D\,(t-t_0)}\right]\,. \tag{4.49}$$

4.2.2 Diffusion in a Half-Space $\Omega_\infty = [0,\infty[$

We consider now diffusion in a half-space $\Omega_\infty = [0,\infty[$ under the influence of a linear potential with a reflective boundary at $x = 0$. To describe this system by a distribution function $p(x,t|x_0,t_0)$ we need to solve the Smoluchowski equation (4.28) subject to the boundary conditions

$$D\,(\partial_x + \beta\,c)\,p(x,t|x_0,t_0) = 0\,, \quad \text{at } x = 0 \tag{4.50}$$
$$p(x,t|x_0,t_0) \underset{x\to\infty}{\asymp} 0\,. \tag{4.51}$$

The solution has been determined by Smoluchowski ([47], see also [22]) and can be stated in the form

$$p(x,t|x_0,0) = \sum_{j=1}^{3} p_j(x,t|x_0,0) \tag{4.52}$$
$$p_1(x,t|x_0,0) = \frac{1}{\sqrt{4\pi\,D\,t}}\,\exp\left[-(x-x_0+\beta\,c\,D\,t)^2/4\,D\,t\right] \tag{4.53}$$
$$p_2(x,t|x_0,0) = \frac{1}{\sqrt{4\pi\,D\,t}}\,\exp\left[\beta\,c\,x_0-(x+x_0+\beta\,c\,D\,t)^2/4\,D\,t\right] \tag{4.54}$$
$$p_3(x,t|x_0,0) = \frac{\beta\,c}{2}\,\exp[-\beta\,c\,x]\;\mathrm{erfc}\left[(x+x_0-\beta\,c\,D\,t)/\sqrt{4\,D\,t}\right]\,. \tag{4.55}$$

In this expression $\mathrm{erfc}(z)$ is the complementary error function

$$\mathrm{erfc}(z) = \frac{2}{\sqrt{\pi}}\int_z^\infty dx\; e^{-x^2} \tag{4.56}$$

for which holds

$$\mathrm{erfc}(0) = 1 \tag{4.57}$$
$$\mathrm{erfc}(z) \underset{z\to\infty}{\asymp} \frac{1}{\sqrt{\pi}\,z}\;e^{-z^2} \tag{4.58}$$
$$\partial_z\,\mathrm{erfc}(z) = -\frac{2}{\sqrt{\pi}}\;e^{-z^2}\,. \tag{4.59}$$

Plots of the distributions p_1, p_2 and p_3 as functions of x for different t's are shown in Figure 4.1. In Figure 4.2 the total distribution function $p(x,t) = p_1(x,t)+p_2(x,t)+p_3(x,t)$ is ploted as a function of x for three consecutive instants of time, namely for $t = 0.0, 0.025, 0.05, 0.1, 0.2, 0.4, 0.8, \infty$. The contribution (4.53) to the solution is identical to the solution derived above for diffusion in $]-\infty,\infty[$, i.e., in the absence of a boundary at a finite distance. The contribution (4.54) is analogous to the second term of the distribution (3.31) describing free diffusion in a half-space with reflective boundary; the term describes particles which have impinged on the boundary and have been carried away from the boundary back into the half-space Ω. However, some particles which impinged on

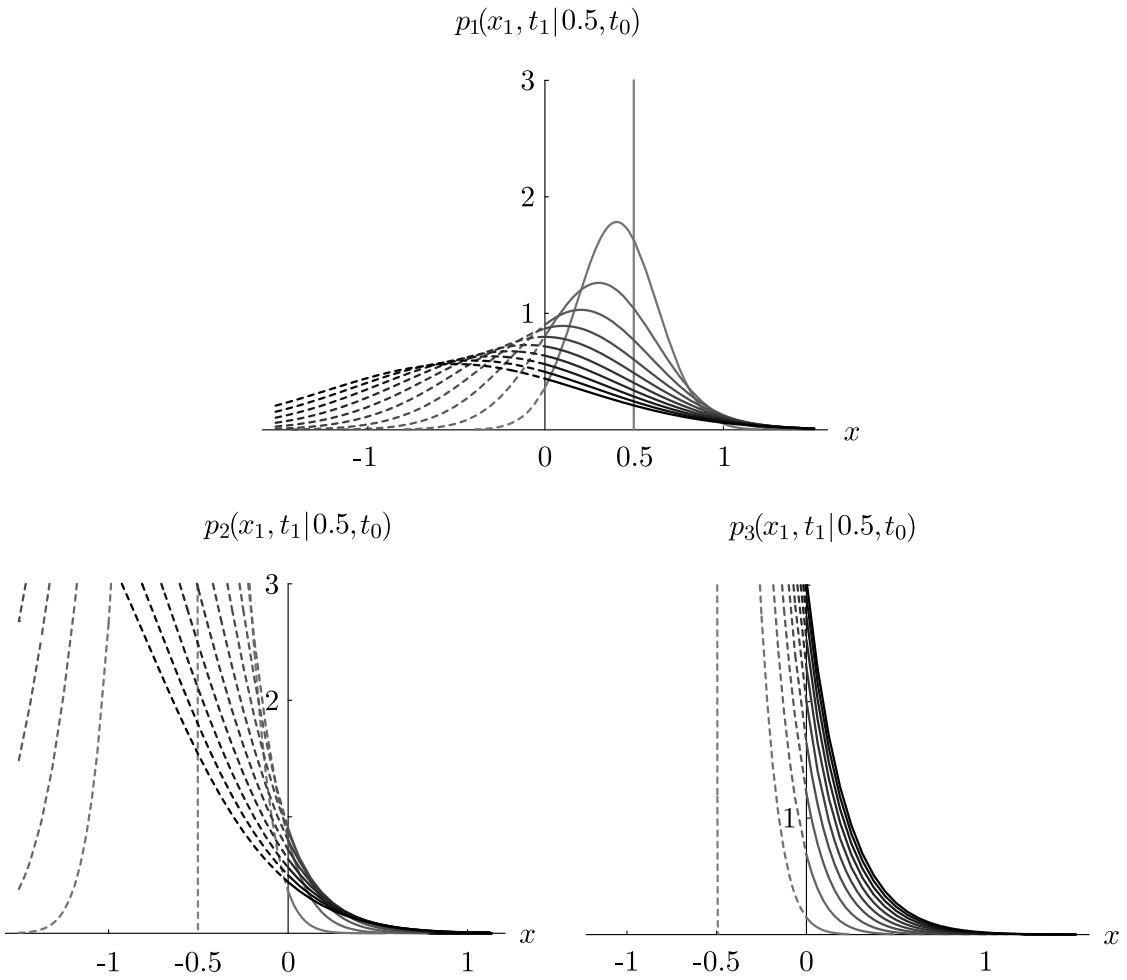

Figure 4.1: These three plots show p_1, p_2 and p_3 as a function of x for consecutive times $t = 0.0, 0.1, \ldots, 1.0$ and $x_0 = 0.5$; the length unit is $L = \frac{4}{\beta c}$, the time unit is $T = \frac{4}{D\beta^2 c^2}$ while p_i $(i = 1, 2, 3)$ is measured in $\frac{1}{L}$.

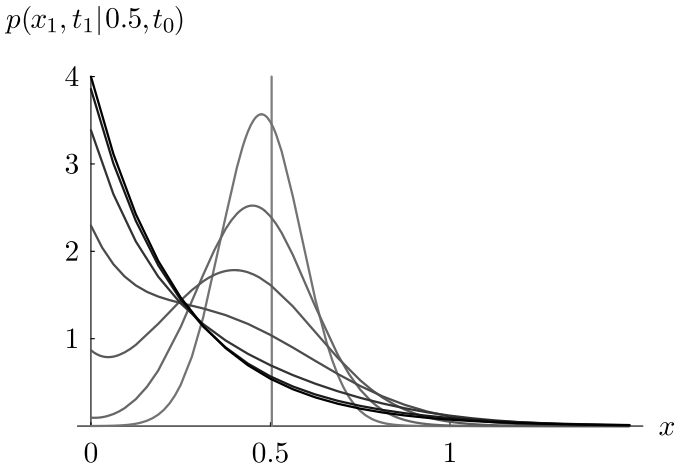

Figure 4.2: Plot of $p(x,t|0.5,0) = p_1(x,t|0.5,0) + p_2(x,t|0.5,0) + p_3(x,t|0.5,0)$ vs. x for $t = 0.0, 0.025, 0.05, 0.1, 0.2, 0.4, 0.8, \infty$. Same units as in Figure 4.1.

the boundary equilibrate into a Boltzmann distribution $\exp(-\beta\, c\, x)$. These particles are collected in the term (4.55). One can intuitively think of the latter term as accounting for particles which impinged onto the surface at $x = 0$ more than once.
In order to prove that (4.52–4.55) provides a solution of (4.28, 4.31, 4.50, 4.51) we note

$$\lim_{t\to 0} p_1(x,t|x_0,0) = \delta(x - x_0) \tag{4.60}$$

$$\lim_{t\to 0} p_2(x,t|x_0,0) = e^{\beta\, c\, x_0}\ \delta(x + x_0) \tag{4.61}$$

$$\lim_{t\to 0} p_3(x,t|x_0,0) = 0 \tag{4.62}$$

where (4.60, 4.61) follow from the analogy with the solution of the free diffusion equation, and where (4.62) follows from (4.59). Since $\delta(x + x_0)$ vanishes in $[0, \infty[$ for $x_0 > 0$ we conclude that (4.31) holds.
The analogy of $p_1(x,t|x_0,0)$ and $p_2(x,t|x_0,0)$ with the solution (4.39) reveals that these two distributions obey the Smoluchowski equation and the boundary condition (4.51), but individually not the boundary condition (4.50). To demonstrate that p_3 also obeys the Smoluchowski equation we introduce again $\tau = D\, t$, $b = \beta\, c$ and the function

$$f = \frac{1}{\sqrt{4\pi\tau}}\ \exp\left[-b\, x\ -\ \frac{(x + x_0 - b\,\tau)^2}{4\,\tau}\right]\ . \tag{4.63}$$

For $p_3(x, \tau/D|x_0, 0)$, as given in (4.55), holds then

$$\partial_\tau\, p_3(x,\tau|x_0,0) = f\, b\, \frac{x + x_0 + b\,\tau}{2\,\tau} \tag{4.64}$$

$$\partial_x\, p_3(x,\tau|x_0,0) = -\frac{1}{2}\, b^2\, e^{-b\, x}\ \mathrm{erfc}\left[\frac{x + x_0 - b\,\tau}{\sqrt{4\,\tau}}\right]\ -\ f\, b \tag{4.65}$$

$$\partial_x^2\, p_3(x,\tau|x_0,0) = \frac{1}{2}\, b^3\, e^{-b\, x}\ \mathrm{erfc}\left[\frac{x + x_0 - b\,\tau}{\sqrt{4\,\tau}}\right]\ +\ f\, b\ \frac{x + x_0 - b\,\tau}{2\,\tau}\ +\ f\, b^2\ . \tag{4.66}$$

It follows for the r.h.s. of the Smoluchowski equation

$$\left(\partial_x^2\ +\ b\,\partial_x\right)\ p_3(x,\tau|x_0,0) = f\, b\ \frac{x + x_0 + b\,\tau}{2\,\tau}\ . \tag{4.67}$$

Since this is identical to (4.64), i.e., to the l.h.s. of the Smoluchowski equation, $p_3(x,t|,x_0,0)$ is a solution of this equation.
We want to demonstrate now that $p(x,t|,x_0,0)$ defined through (4.52–4.55) obey the boundary condition at $x = 0$, namely, (4.50). We define for this purpose the function

$$g \;=\; \frac{1}{\sqrt{4\pi\,\tau}}\,\exp\!\left[-\frac{(x_0-b\,\tau)^2}{4\,\tau}\right]\,. \tag{4.68}$$

It holds then at $x = 0$

$$b\,p_1(0,\tau|,x_0,0) \;=\; g\,b \tag{4.69}$$
$$b\,p_2(0,\tau|,x_0,0) \;=\; g\,b \tag{4.70}$$
$$b\,p_3(0,\tau|,x_0,0) \;=\; \frac{1}{2}\,b^2\;\mathrm{erfc}\!\left[\frac{x_0-b\,\tau}{\sqrt{4\,\tau}}\right] \tag{4.71}$$
$$\partial_x\,p_1(x,\tau|,x_0,0)\Big|_{x=0} \;=\; g\,b\;\frac{x_0-b\,\tau}{2\,\tau} \tag{4.72}$$
$$\partial_x\,p_2(x,\tau|,x_0,0)\Big|_{x=0} \;=\; g\,b\;\frac{-x_0-b\,\tau}{2\,\tau} \tag{4.73}$$
$$\partial_x\,p_3(x,\tau|,x_0,0)\Big|_{x=0} \;=\; -\,g\,b\;-\;\frac{1}{2}\,b^3\;\mathrm{erfc}\!\left[\frac{x_0-b\,\tau}{\sqrt{4\,\tau}}\right] \tag{4.74}$$

where we used for (4.70, 4.73) the identity

$$b\,x_0\;-\;\frac{(x_0+b\,\tau)^2}{4\,\tau} \;=\; -\frac{(x_0-b\,\tau)^2}{4\,\tau}\,. \tag{4.75}$$

From (4.69–4.74) one can readily derive the boundary condition (4.50).
We have demonstrated that (4.52–4.55) is a proper solution of the Smoluchowski equation in a half-space and in a linear potential. It is of interest to evaluate the fraction of particles which are accounted for by the three terms in (4.52). For this purpose we define

$$N_j(t|x_0) \;=\; \int_0^\infty dx\;p_j(x,t|x_0,0)\,. \tag{4.76}$$

One obtains then

$$\begin{aligned} N_1(t|x_0) \;&=\; \frac{1}{\sqrt{4\pi\,\tau}}\;\int_0^\infty dx\;\exp\!\left[-\frac{(x-x_0+b\,\tau)^2}{4\,\tau}\right] \\ &=\; \frac{1}{\sqrt{4\pi\,\tau}}\;\int_{-x_0+b\tau}^\infty dx\;\exp\!\left[-\frac{x^2}{4\,\tau}\right] \\ &=\; \frac{1}{2}\,\frac{2}{\sqrt{\pi}}\;\int_{\frac{-x_0+b\tau}{\sqrt{4\tau}}}^\infty dx\;\exp\!\left[-x^2\right] \;=\; \frac{1}{2}\,\mathrm{erfc}\!\left[\frac{-x_0+b\,\tau}{\sqrt{4\,\tau}}\right] \end{aligned} \tag{4.77}$$

Similarly one obtains

$$N_2(t|x_0) \;=\; \frac{1}{2}\,\exp[b\,x_0]\;\mathrm{erfc}\!\left[\frac{x_0+b\,\tau}{\sqrt{4\,\tau}}\right]\,. \tag{4.78}$$

For $N_3(t|x_0)$ one derives, employing (4.56),

$$N_3(t|x_0) \;=\; \frac{1}{2}\,b\;\int_0^\infty dx\;\exp[-b\,x]\;\frac{2}{\sqrt{\pi}}\;\int_{\frac{x+x_0-b\tau}{\sqrt{4\tau}}}^\infty dy\;\exp\!\left[-y^2\right] \tag{4.79}$$

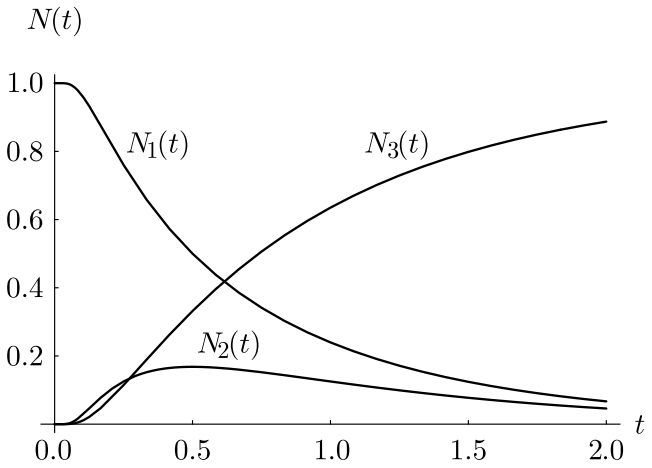

Figure 4.3: Plots of N_1, N_2 and N_3 vs. t, for $x_0 = 0$. The length and time units are the same as in Figure 4.1. For all $t > 0$ holds $N_1 + N_2 + N_3 = 1$.

Changing the order of integration yields

$$\begin{aligned} N_3(t|x_0) &= \frac{b}{\sqrt{\pi}} \int_{\frac{x_0-b\tau}{\sqrt{4\tau}}}^{\infty} dy \ \exp\bigl[-y^2\bigr] \int_0^{\sqrt{4\tau}y-x_0+b\tau} dx \ \exp[-b\,x] \\ &= \frac{1}{\sqrt{\pi}} \int_{\frac{x_0-b\tau}{\sqrt{4\tau}}}^{\infty} dy \ \exp\bigl[-y^2\bigr] \ - \ \frac{1}{\sqrt{\pi}} \int_{\frac{x_0-b\tau}{\sqrt{4\tau}}}^{\infty} dy \ \exp\bigl[-(y+b\sqrt{\tau})^2 \ + \ b\,x_0\bigr] \\ &= \frac{1}{2} \ \mathrm{erfc}\left[\frac{x_0 - b\,\tau}{\sqrt{4\tau}}\right] \ - \ \frac{1}{2} \ \exp[b\,x_0] \ \mathrm{erfc}\left[\frac{x_0 + b\,\tau}{\sqrt{4\,\tau}}\right] \ . \end{aligned}$$

Employing the identity

$$\frac{1}{2} \ \mathrm{erfc}(z) \ = \ 1 \ - \ \frac{1}{2} \ \mathrm{erfc}(-z) \tag{4.80}$$

one can write finally

$$\begin{aligned} N_3(t|x_0) &= 1 \ - \ \frac{1}{2} \ \mathrm{erfc}\left[\frac{-x_0 + b\,\tau}{\sqrt{4\,\tau}}\right] \ - \ \frac{1}{2} \ \exp[b\,x_0] \ \mathrm{erfc}\left[\frac{x_0 + b\tau}{\sqrt{4\tau}}\right] \\ &= 1 \ - \ N_1(t|x_0) \ - \ N_2(t|x_0) \ . \end{aligned} \tag{4.81}$$

This result demonstrates that the solution (4.52–4.55) is properly normalized. The time dependence of N_1, N_2 and N_3 are shown in Figure 4.3.

4.3 Diffusion in a One-Dimensional Harmonic Potential

We consider now diffusion in a harmonic potential

$$U(x) = \frac{1}{2}\, f\, x^2 \tag{4.82}$$

which is simple enough to yield an analytical solution of the corresponding Smoluchowski equation

$$\partial_t p(x,t|x_0,t_0) = D(\partial_x^2 + \beta f \ \partial_x x)\, p(x,t|x_0,t_0) \ . \tag{4.83}$$

We assume presently a constant diffusion coefficient D. The particle can diffuse in the infinite space Ω_∞. However, the potential confines the motion to a finite area such that the probability distribution vanishes exponentially for $x \to \pm\infty$ as expressed through the boundary condition

$$\lim_{x\to\pm\infty} x^n\, p(x,t|x_0,t_0) = 0, \quad \forall n \in I\!N\,. \tag{4.84}$$

We seek the solution of (4.83, 4.84) for the initial condition

$$p(x,t_0|x_0,t_0) = \delta(x-x_0)\,. \tag{4.85}$$

In thermal equilibrium, particles will be distributed according to the Boltzmann distribution

$$p_0(x) = \sqrt{f/2\pi k_B T}\,\exp\bigl(-fx^2/2k_BT\bigr) \tag{4.86}$$

which is, in fact, a stationary solution of (4.83, 4.84). We expect that the solution for the initial condition (4.85) will asymptotically decay towards (4.86).
The mean square deviation from the average position of the particle at equilibrium, i.e., from $\langle x\rangle = 0$, is

$$\begin{aligned}\delta^2 &= \int_{-\infty}^{+\infty} dx\,(x-\langle x\rangle)^2\,p_0(x)\\ &= \sqrt{f/2\pi k_BT}\int_{-\infty}^{+\infty} dx\,x^2\,\exp\bigl(-fx^2/2k_BT\bigr)\,.\end{aligned} \tag{4.87}$$

This quantity can be evaluated considering first the integral

$$I_n(\alpha) \;=\; (-1)^n \int_{-\infty}^{+\infty} dx\,x^{2n}\,e^{-\alpha x^2}\,.$$

One can easily verify

$$I_1(\alpha) \;=\; -\,\partial_\alpha I_0(\alpha) \;=\; \frac{\sqrt{\pi}}{2\alpha^{3/2}}\,. \tag{4.88}$$

and, through recursion,

$$I_n(\alpha) \;=\; \frac{\Gamma\bigl(n+\frac{1}{2}\bigr)}{\alpha^{n+\frac{1}{2}}}\,, \qquad n \;=\; 0,1,\ldots \tag{4.89}$$

One can express δ^2 in terms of the integral I_1. Defining

$$\kappa = \sqrt{\frac{f}{2k_BT}} \tag{4.90}$$

and changing the integration variable $x \to y = \kappa x$ yields

$$\delta^2 \;=\; \frac{1}{\kappa^2}\frac{1}{\sqrt{\pi}}\int_{-\infty}^{+\infty} dy\,y^2\,e^{-y^2} \;=\; \frac{1}{\kappa^2}\frac{1}{\sqrt{\pi}}\,I_1(1)\,. \tag{4.91}$$

According to (4.88) holds $I_1(1) = \sqrt{\pi}/2$ and, hence,

$$\delta^2 = \frac{1}{2\kappa^2}\,, \tag{4.92}$$

or

$$\delta \;=\; \sqrt{k_B T/f}\;. \tag{4.93}$$

For a solution of (4.83, 4.84, 4.85) we introduce dimensionless variables. We replace x by

$$\xi \;=\; x/\sqrt{2}\delta \tag{4.94}$$

We can also employ δ to define a natural time constant

$$\tilde{\tau} \;=\; 2\delta^2/D \tag{4.95}$$

and, hence, replace t by

$$\tau \;=\; t/\tilde{\tau}\;. \tag{4.96}$$

The Smoluchowski equation for

$$q(\xi,\tau|\xi_0,\tau_0) \;=\; \sqrt{2}\,\delta\; p(x,t|x_0,t_0) \tag{4.97}$$

reads then

$$\partial_\tau q(\xi,\tau|\xi_0,\tau_0) = (\partial_\xi^2 + 2\,\partial_\xi\;\xi)\,q(\xi,\tau|\xi_0,\tau_0)\;, \tag{4.98}$$

The corresponding initial condition is

$$q(\xi,\tau_0|\xi_0,\tau_0) = \delta(\xi-\xi_0)\,, \tag{4.99}$$

and the boundary condition

$$\lim_{\xi\to\pm\infty}\;\xi^n\,q(\xi,\tau|\xi_0,\tau_0) = 0, \quad \forall n\in I\!N\;. \tag{4.100}$$

The prefactor of $p(x,t|x_0,t_0)$ in the definition (4.97) is dictated by the condition that $q(\xi,\tau|\xi_0,\tau_0)$ should be normalized, i.e.,

$$\int_{-\infty}^{+\infty} dx\, p(x,t|x_0,t_0) \;=\; \int_{-\infty}^{+\infty} d\xi\, q(\xi,\tau|\xi_0,\tau_0) \;=\; 1 \tag{4.101}$$

In the following we choose

$$\tau_0 \;=\; 0\;. \tag{4.102}$$

In order to solve (4.98, 4.99, 4.100) we seek to transform the Smoluchowski equation to the free diffusion equation through the choice of the time-dependent position variable

$$y \;=\; \xi\, e^{2\tau}\;, \qquad y_0 \;=\; \xi_0\;, \tag{4.103}$$

replacing

$$q(\xi,\tau|\xi_0,0) \;=\; v(y,\tau|y_0,0)\;. \tag{4.104}$$

We note that this definition results in a time-dependent normalization of $v(y,\tau|y_0,0)$, namely,

$$1 \;=\; \int_{-\infty}^{+\infty} d\xi\, q(\xi,\tau|\xi_0,0) \;=\; e^{-2\tau}\int_{-\infty}^{+\infty} dy\, v(y,\tau|y_0,0)\;. \tag{4.105}$$

The spatial derivative ∂_y, according to the chain rule, is determined by

$$\partial_\xi \;=\; \frac{\partial y}{\partial \xi}\,\partial_y \;=\; e^{2\tau}\,\partial_y \tag{4.106}$$

and, hence,

$$\partial_\xi^2 \;=\; e^{4\tau}\,\partial_y^2 \tag{4.107}$$

The l.h.s. of (4.98) reads

$$\partial_\tau q(\xi,\tau|\xi_0,0) \;=\; \partial_\tau v(y,\tau|y_0,0) \;+\; \underbrace{\frac{\partial y}{\partial \tau}}_{2y}\,\partial_y v(y,\tau|y_0,0)\;. \tag{4.108}$$

The r.h.s. of (4.98) becomes

$$e^{4\tau}\,\partial_y^2 v(y,\tau|y_0,0) \;+\; 2\,v(y,\tau|y_0,0) \;+\; 2\,\underbrace{\xi e^{2\tau}}_{y}\,\partial_y v(y,\tau|y_0,0)\,, \tag{4.109}$$

such that the Smoluchowski equation for $v(y,\tau|y_0,0)$ is

$$\partial_\tau v(y,\tau|y_0,0) \;=\; e^{4\tau}\,\partial_y^2 v(y,\tau|y_0,0) \;+\; 2\,v(y,\tau|y_0,0)\;. \tag{4.110}$$

To deal with a properly normalized distribution we define

$$v(y,\tau|y_0,0) \;=\; e^{2\tau}\,w(y,\tau|y_0,0) \tag{4.111}$$

which yields, in fact,

$$\int_{-\infty}^{\infty} d\xi\, q(\xi,\tau|\xi_0,0) \;=\; e^{-2\tau}\int_{-\infty}^{\infty} dy\, v(y,\tau|y_0,0) \;=\; \int_{-\infty}^{\infty} dy\, w(y,\tau|y_0,0) \;=\; 1\;. \tag{4.112}$$

The Smoluchowski equation for $w(y,\tau|y_0,0)$ is

$$\partial_\tau w(y,\tau|y_0,0) \;=\; e^{4\tau}\,\partial_y^2\, w(y,\tau|y_0,0) \tag{4.113}$$

which, indeed, has the form of a free diffusion equation, albeit with a time-dependent diffusion coefficient. The initial condition which corresponds to (4.99) is

$$w(y,0|y_0,0) \;=\; \delta(y-y_0)\;. \tag{4.114}$$

It turns out that the solution of a diffusion equation with time-dependent diffusion coefficient $\tilde{D}(\tau)$

$$\partial_\tau w(y,\tau|y_0,\tau_0) \;=\; \tilde{D}(\tau)\,\partial_y^2\, w(y,\tau|y_0,\tau_0) \tag{4.115}$$

in Ω_∞ with

$$w(y,\tau_0|y_0,\tau_0) \;=\; \delta(y\,-\,y_0) \tag{4.116}$$

is a straightforward generalization of the corresponding solution of the free diffusion equation (3.30), namely,

$$w(y,\tau|y_0,\tau_0) \;=\; \left(4\pi\int_0^\tau d\tau'\,\tilde{D}(\tau')\right)^{-\frac{1}{2}} \exp\left[-\frac{(y-\xi_0)^2}{4\int_0^\tau d\tau'\,\tilde{D}(\tau')}\right]\;. \tag{4.117}$$

This can be readily verified. Accordingly, the solution of (4.113, 4.114) is

$$w(y,\tau|y_0,0) \;=\; \left(4\pi \int_0^\tau d\tau'\, e^{4\tau'}\right)^{-\frac{1}{2}} \exp\left[-\frac{(y-y_0)^2}{4\int_0^\tau d\tau'\, e^{4\tau'}}\right] . \tag{4.118}$$

The corresponding distribution $q(\xi,\tau|\xi_0,0)$ is, using (4.103, 4.104, 4.111),

$$q(\xi,\tau|\xi_0,0) \;=\; \frac{1}{\sqrt{\pi(1-e^{-4\tau})}} \exp\left[-\frac{(\xi-\xi_0 e^{-2\tau})^2}{1-e^{-4\tau}}\right] . \tag{4.119}$$

and, hence, using (4.94, 4.95, 4.96, 4.97), we arrive at

$$p(x,t|x_0,t_0) \;=\; \frac{1}{\sqrt{2\pi k_B T\, S(t,t_0)/f}} \exp\left[-\frac{\left(x \,-\, x_0\, e^{-2(t-t_0)/\tilde\tau}\right)^2}{2k_BTS(t,t_0)/f}\right] \tag{4.120}$$

$$S(t,t_0) \;=\; 1 \,-\, e^{-4(t-t_0)/\tilde\tau} \tag{4.121}$$

$$\tilde\tau \;=\; 2k_BT \,/\, fD\ . \tag{4.122}$$

One notices that this distribution asymptotically, i.e., for $t \to \infty$, approaches the Boltzmann distribution (4.86). We also note that (4.120, 4.121, 4.122) is identical to the conditional probability of the Ornstein-Uhlenbeck process (2.81, 2.82) for $\gamma = 2/\tilde\tau$ and $\sigma^2 = 2k_BT$.

Chapter 5

Random Numbers

Contents

5.1 Randomness 80
5.2 Random Number Generators 83
5.2.1 Homogeneous Distribution 83
5.2.2 Gaussian Distribution 86
5.3 Monte Carlo integration 88

In this chapter we introduce numerical methods suited to model stochastic systems. Starting point is the Fokker-Planck equation (2.148) within the frame-work of Ito calculus

$$\partial_t\, p(\boldsymbol{x},t|\boldsymbol{x}_0,t_0) \;=\; -\sum_i\, \partial_i\, A_i\; p(\boldsymbol{x},t|\boldsymbol{x}_0,t_0) \;+\; \frac{1}{2}\,\sum_{i,j}\,\partial_i\partial_j\,[\mathbf{B}\cdot\mathbf{B}^{\mathsf{T}}]_{\mathbf{ij}}\;\mathbf{p}(\boldsymbol{x},\mathbf{t}|\boldsymbol{x_0},\mathbf{t_0})\;. \tag{5.1}$$

which proved useful in analytical descriptions of Brownian dynamics. There exist two approaches to solve this equation by numerical means.
On the one hand one can treat the Fokker-Planck equation as an ordinary parabolic partial differential equation and apply numerical tools like finite differencing, spectral or variational methods that are applicable to partial differential equations in general. These methods will be described in a yet unwritten chapter of these notes.
On the other hand one can resort to the stochastic processes that underlie the Fokker-Planck equation. We have shown in chapter 2.5 that the Fokker-Planck equation (2.148, 5.1) corresponds to a stochastic differential equation [c.f., (2.135)]

$$\begin{aligned} d\boldsymbol{x}(t) \;&=\; \Big(\boldsymbol{A}[\boldsymbol{x}(t),t] \;+\; \mathbf{B}[\boldsymbol{x}(\mathbf{t}),\mathbf{t}]\cdot\boldsymbol{\xi}(\mathbf{t})\Big)\;\mathbf{dt} \\ &=\; \boldsymbol{A}[\boldsymbol{x}(t),t]\;dt \;+\; \mathbf{B}[\boldsymbol{x}(\mathbf{t}),\mathbf{t}]\cdot\mathbf{d}\boldsymbol{\omega}(\mathbf{t})\;. \end{aligned} \tag{5.2}$$

Instead of solving (5.1) one may simulate, therefore, stochastic processes that obey the stochastic differential equation (5.2). The probability distribution $p(\boldsymbol{x},t|\boldsymbol{x}_0,t_0)$ resulting from an ensemble of simulated stochastic processes starting at $\boldsymbol{x}(t_0)=\boldsymbol{x}_0$ can then be taken as a solution of the Fokker-Planck equation (5.1). This approach is called the *Brownian dynamics* method.
We will address the Brownian dynamics method first. Two ingredients are needed to generate sample trajectories $\boldsymbol{x}(t)$ of stochastic processes as displayed in Figure 5.4.First, one has to generate random numbers to simulate the random variables $\boldsymbol{\xi}(t)$ and $d\boldsymbol{\omega}(t)$. Second, one needs rules to

Figure 5.1: Two dimensional random walk generated by adding up 1000 random number tuples with a standard Gaussion distribution.

translate the stochastic differential equation (5.2) into a dicretized numerical form with which one can generate discretized stochastic trajectories. The generation of random numbers is the subject of the current chapter. In chapter 6 we derive rules for generating numerically stochastic trajectories. In chapter 7 we consider typical applications.
We begin the current chapter about random numbers with a definition of randomness in mathematical terms. We then address the problem of generating random numbers on a digital computer. The chapter closes with a short introduction to the *Monte Carlo* integration method, one of the most prominent random number applications and part in the derivation of the Brownian dynamics method introduced in chapter 6.

5.1 Randomness

Microscopic systems down to the level of small molecules exhibit strong random characteristics when one views selected degrees of freedom or non-conserved physical properties. The laws of statistical mechanics, even though strictly applicable only to very large systems, are realized at the molecular level, exceptions being rare. Underlying this behaviour are seemingly random events connected with transfer of momentum and energy between degress of freedom of strongly coupled classical and quantum mechanical systems. One can describe these events through random processes. We have stated above that solutions to the Fokker-Planck equations which govern the approach to statistical mechanical equilibrium can also be cast in terms of random processes. This leaves one to consider the problem how random events themselves can be mathematically modelled. This is achieved through so-called random numbers.
The concept of randomness and random numbers is intuitive and easily explained. The best known example of randomness is the throw of a dice. With each throw, a dice reveals a random number r between 1 and 6. A dice is thus a random number generator with a random number domain equal to the set $\{1, 2, 3, 4, 5, 6\}$. Other random number generators and domains are of course possible; take a dime, a roulet game, and so on.
Once a random number is obtained it is no longer random. The randomness refers to the process generating the numbers, not to a single number as such. Nevertheless a sequence of random numbers exhibits properties that reflect the generating process. In this section we will introduce

and investigate these properties. In the section thereafter we will address the problem of generating random numbers on a digital computer.
What makes a sequence of numbers $\{r_i\}$ random? Certainly, it is not just the overall probability distribution $p(r)$. A sorted and, hence, non-random list of numbers could easily satisfy this criterium. Instead, we approach randomness via the related notion of *unpredictability*. A sequence $\{r_i\}$ is unpredictable if it is impossible to foretell the value of a subsequent element r_{m+1} based on the occurence of preceding elements $r_l, \ldots, r_m$. This criterium translates into

$$p(r_{m+1}|r_l, \ldots, r_m) \;=\; p(r_{m+1}) \qquad \forall\; 0 \le l \le m < n. \tag{5.3}$$

The elements $r_l, \ldots, r_m$ must not condition r_{m+1} and, hence, conditional probabilities $p(r_{m+1}|r_l, \ldots, r_m)$ must equal the unconditional probabilities $p(r_{m+1})$. Furthermore, $p(r_{m+1})$ should be the same as the probability distribution $p(r)$ which applies to all elements of $\{r_i\}$.
Since unconditional probabilities can be factorized by conditional probabilties one obtains

$$\begin{aligned} p(r_l, \ldots, r_m, r_{m+1}) &= p(r_{m+1}|r_l, \ldots, r_m)\; p(r_l, \ldots, r_m) \\ &= p(r_{m+1})\; p(r_l, \ldots, r_m)\;, \end{aligned} \tag{5.4}$$

and, since (5.4) holds true for any $l \le m$, one can write

$$p(r_l, \ldots, r_m) \;=\; \prod_{j=\ell}^{m} p(r_j)\;. \tag{5.5}$$

Equation (5.5) provides a criterium for randomness. However, to verify criterium (5.5) for a given number sequence one has to derive a measurable quantity. Note, that the probability distributions $p(r_l, \ldots, r_m)$ are unkown. We begin this endeavor by considering the generating functions $G_{r_l \ldots r_m}(s_l \ldots s_m)$ of the unconditional probabilties $p(r_l, \ldots, r_m)$ and by applying these to equation (5.5).

$$\begin{aligned} G_{r_l \ldots r_m}(s_l \ldots s_m) &= \int \cdots \int \left(\prod_{k=l}^{m} dr_k \right)\; p(r_l, \ldots, r_m)\; \exp\left[i \sum_{k=l}^{m} s_k r_k \right] \\ &= \prod_{k=l}^{m} \int dr_k\; p(r_k)\; e^{i s_k r_k} \\ &= \big(G_r(s) \big)^{m-l+1}\;. \end{aligned} \tag{5.6}$$

Taking the logarithm of equation (5.6) and comparing the coefficients of the Taylor expansion

$$\log[G_{r_l \ldots r_m}(s_l \ldots s_m)] \;=\; \sum_{n_l, \ldots, n_m = 0}^{n} \left\langle\!\!\left\langle r_l^{n_l} \ldots r_k^{n_m} \right\rangle\!\!\right\rangle \frac{(i\, s_l)^{n_l}}{n_l!} \ldots \frac{(i\, s_m)^{n_m}}{n_m!} \tag{5.7}$$

one finds for the cumulants [c.f. Eq. (2.18) and Eq.(2.30)]

$$\left\langle\!\!\left\langle r_l^{n_l} \ldots r_m^{n_m} \right\rangle\!\!\right\rangle \;=\; 0\;, \qquad \text{if } 1 \le n_{(l \le i \le m)} \text{ and } l < m\;. \tag{5.8}$$

One can verify the criteria (5.8) of unpredictability and thus randomness by utilizing the relation

between cumulants and moments

$$\begin{aligned}
\Big\langle\!\Big\langle r_k\, r_l \Big\rangle\!\Big\rangle &= \Big\langle r_k\, r_l \Big\rangle - \Big\langle r_k \Big\rangle \Big\langle r_l \Big\rangle \,, && (5.9)\\
\Big\langle\!\Big\langle r_k\, r_l^2 \Big\rangle\!\Big\rangle &= \Big\langle r_k\, r_l^2 \Big\rangle - \Big\langle r_k \Big\rangle \Big\langle r_l^2 \Big\rangle - 2\Big\langle r_l \Big\rangle \Big\langle r_k r_l \Big\rangle + 2 \Big\langle r_k \Big\rangle \Big\langle r_l \Big\rangle^2 \,, && (5.10)\\
\Big\langle\!\Big\langle r_k\, r_l\, r_m \Big\rangle\!\Big\rangle &= \Big\langle r_k\, r_l\, r_m \Big\rangle - \Big\langle r_k \Big\rangle \Big\langle r_l r_m \Big\rangle - \Big\langle r_l \Big\rangle \Big\langle r_k r_m \Big\rangle - \Big\langle r_m \Big\rangle \Big\langle r_k r_l \Big\rangle \\
&\quad + 2 \Big\langle r_k \Big\rangle \Big\langle r_l \Big\rangle \Big\langle r_m \Big\rangle \,, && (5.11)\\
&\;\;\vdots
\end{aligned}$$

Each moment on the r.h.s. of (5.12) can be determined by taking the arithmetic average of the expression within the brackets $\langle \ldots \rangle$.
However, to take the arithmetic average one needs an ensemble of values. What, if only a single random number sequence is given? In such a case it is often permissable to create an ensemble by shifting the elements of the number sequence in a cyclic fashion. We denote a shift $\mathcal{S}_k$ of a sequence $\{r_i\}$ by k numbers by

$$\mathcal{S}_k\big(\{r_0, r_1, \ldots, r_n\}\big) \;=\; \{r_k, r_{k+1}, \ldots, r_n, r_0, \ldots, r_{k-1}\} \,. \tag{5.12}$$

The notation for a corresponding shift of a single numbers r_i is

$$\mathcal{S}_k\big(r_i\big) \;=\; r_{i+k} \,. \tag{5.13}$$

It is permissable to create an ensembles of random number sequences through operation $\mathcal{S}_k$ if one investigates a sequence that stems from an iterative generating process. This is usually the case when working with random number generators on digital computers. Such routines start with an initial number, a seed, and then generate a list of numbers by iteratively applying a mapping over and over again. The resulting number sequence starts to repeat as soon as the routine returns to the initial seed, thus forming a number cylce. This is inevitable for mappings that operate in a discrete and finite number domain. To avoid short repetitious number cycles, good number generators exhibit just one long number cycle that completely covers the available number domain. No matter which seed one chooses, the routine produces the same cycle of numbers simply shifted by a certain number of elements. Hence, applying the shift operation $\mathcal{S}_k$ j times with j different k's is equivalent to generating an ensemble of j sequences with j different seeds. One can thus write for a statisitcal moment in (5.12)

$$\Big\langle r_l^{n_l} \ldots r_m^{n_m} \Big\rangle \;=\; \frac{1}{j} \sum_{k=0}^{j-1} \big(\mathcal{S}_k\,(r_l)\big)^{n_l} \ldots \big(\mathcal{S}_k\,(r_m)\big)^{n_m} \,. \tag{5.14}$$

To verify if a number sequence is truely random, one has to check all cumulants $\big\langle\!\big\langle r_l^{n_l} \ldots r_m^{n_m} \big\rangle\!\big\rangle$ of all orders $(n_l, \ldots, n_k)$ in (5.8). These correlations should be approximately zero. Of course, due to statistical error, a variance around zero of the order of $(1/\sqrt{n}) \big\langle\!\big\langle r_l^2 \big\rangle\!\big\rangle \ldots \big\langle\!\big\langle r_m^2 \big\rangle\!\big\rangle$ is to be expected.
In practice cumulants of higher order are laborious to caluculate. One therefore performs the verification of randomness (5.8) for low orders only. We will see that a correlation check of low order is sometimes insufficient. We will give an example by applying criteria (5.8) to a linear congruential random generator, the kind of generator that we are going to introduce next.

5.2 Random Number Generators

At the begining of this chapter we already encountered a random number generator; the dice. Obviously it is not feasible to role a dice to generate a large sequence of random numbers. To automate the generation process one uses digital computers instead. A computer, however, is a deterministic machine and, thus, cannot provide truely random numbers. Nevertheless, deterministic programs, so-called random number generators, provide a good substitute.
Any program that creates a sequence of numbers $\{r_i\}$, $i = 0, 1, 2, \ldots, n$ which appear to be random with respect to the test (5.8) derived in the previous section can serve as a random number generator. In this section we introduce some of the standard random number generating programs. We begin with a mechanism that creates random number sequences with a uniform distribution in a given interval. In the paragraph thereafter we outline techniques to generate sequences with different probability distributions, in particular the Gaussian distribution. For further reading in this matter we refer the reader to chapter 3.5 of [20] and to [37].

5.2.1 Homogeneous Distribution

The best known random number generators are so-called *linear congruential generators*. They produce random numbers with a homogeneous probability distribution. Random number generators which emulate other probability distributions are, in general, based on the method introduced here. Linear congruential generators produce integer number sequences $\{r_j\}$ with a homogeneous probability distribution between 0 and some maximum number m using the recurrence relation

$$r_{i+1} \;=\; (a\, r_i \;+\; c) \mod m\,. \tag{5.15}$$

a and c are positive integers called *multiplier* and *increment*. A sequence $\{r_i\}$ starts with an arbitrarily chosen seed r_0. The linear congruential generators exhibit features common to most random number generators:

1. The sequence of random numbers is deterministic and depends on an intial value (or list of values), the seed r_0. Hence, the random number sequence is reproducible.

2. The random number generator is a mapping within a finite number range (or finite region of number tuples). Such a generator can only produce a finite sequence of random numbers and will eventually repeat that sequence all over again, thus, forming a number cycle.

3. The random number sequence tends to exhibit some sequential correlations.

Hence, before employing a random number generator one should check the following criteria.
To avoid a repitition of random numbers one should make sure that the random number cycle produced by the generator contains more elements than the random number sequence that one intends to use. A large value for m and carefully chosen parameters a and c can produce a nonrepetitious sequence of up to m random numbers. A feasible set of constants is for example $m = 2^{31} - 1$, $a = 7^5$ and $c = 0$ [44].
One should verify, if sequential correlations in a random number sequence influence the result of the calculation. One can do so by monitoring the cumulants $\langle\!\langle r_l^{n_l} \ldots r_m^{n_m} \rangle\!\rangle$ of (5.8) or by applying different random number generators and comparing the results. If needed, one can suppress sequential correlations by reshuffling a random number sequence, by merging two sequences or by similar techniques [37].
So far we can generate homogeneously distributed positive random integers on an interval $[0, m]$. One can transform these integers r into fractions or floating point numbers with a homogenous

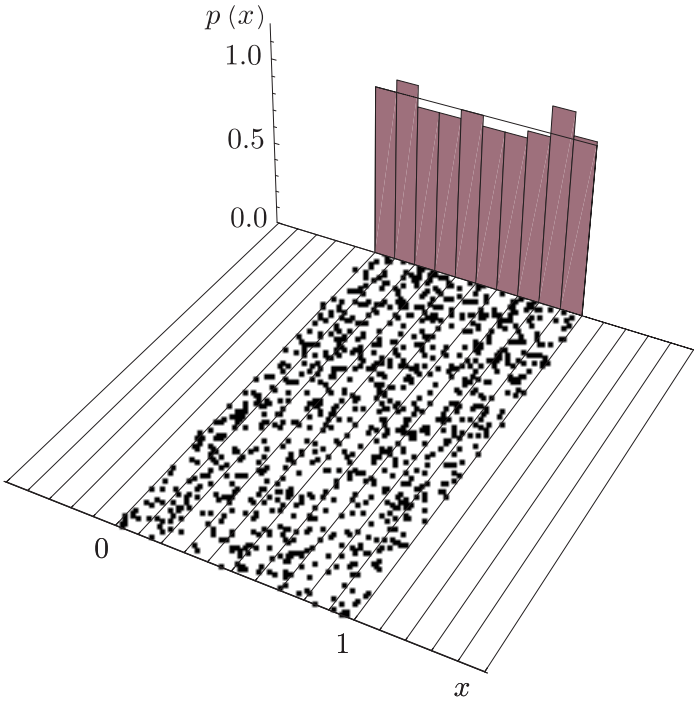

Figure 5.2: Random number sequence with a homogenous distribution in $[0,1]$ generated using (5.15) with $m = 2^{31}$, $a = 65539$, $c = 0$, and $r_0 = 1$.

distribution on an arbitrary interval $[l,u]$ by applying the linear mapping $f(r) = \frac{u-l}{m}\, r + l$. Thus, we can assume from now on to have available a basic random number generator with real-valued (or rather floating point) numbers homogeneously distributed in the interval $[0,1]$.
Before one employs any random number generator needs to be concerned about its quality. Are the numbers generated truely random? To demonstrate typical problems we will consider a pathological example which arises if one chooses in (5.15) $m = 2^{31}$, $a = 65539$ and $c = 0$. Figure 5.2 demonstrates that the linear congruential generator (5.15) produces actually for the present parameters a homogeneous distribution in the interval $[0,1]$. This figure displays a random number sequence of 1000 elements starting in the front and proceeding in 1000 steps to the rear. To verify the probability distribution a bin count with a bin width of 0.1 is displayed in the background. The bar hights represent the normalized probability density in each bin. The line superimposed on the bar chart depicts the ideal theoretical distribution.
The scattered plot in Fig. 5.3 showing the distribution of adjacent random number pairs in $\mathbb{R} \times \mathbb{R}$ allows one to detect statistical correlations $\langle\!\langle r_i\, r_{i+1} \rangle\!\rangle$ of second order. The homogeneous distribution of points in the square $[0,1] \times [0,1]$ indicates that such correlations do not exist in the present case. We can support the graphical correlation check in Fig. 5.3 numerically by calculating the correlation coefficients of order k.

$$C^{(k)}_{(n_1,n_2,\ldots,n_k)}\big(\{r_i\}\big) \;=\; \frac{\langle\!\langle r_{n_1} \ldots r_{n_k} \rangle\!\rangle}{\sqrt{\langle\!\langle r^2_{n_1} \rangle\!\rangle \cdots \langle\!\langle r^2_{n_k} \rangle\!\rangle}}\,. \tag{5.16}$$

The correlation coefficients may be viewed as normalized correlations. We have seen in (5.8) that one can detect correlations or rather the lack thereof by verifying if the cumulants $\langle\!\langle r_{n_1} \ldots r_{n_k} \rangle\!\rangle$ are zero. However, these verifications are subject to statistical errors that not only depend on the size

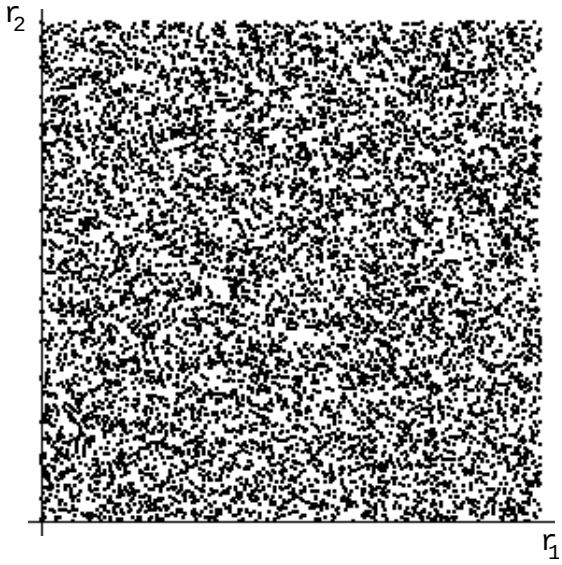

Figure 5.3: Scattered plot of 10000 adjacent random number pairs generated as in Fig. 5.2.

$C^{(2)}_{(0,0)}(\{r_i\})$	=	1.00000	=	1 ,	$C^{(4)}_{(0,0,0,0)}(\{r_i\})$	=	-1.19844	$\sim -\frac{6}{5}$,
$C^{(2)}_{(0,1)}(\{r_i\})$	=	0.01352	$\sim$	0 ,	$C^{(4)}_{(0,0,0,1)}(\{r_i\})$	=	-0.02488	$\sim$ 0 ,
$C^{(3)}_{(0,0,0,)}(\{r_i\})$	=	-0.00099	$\sim$	0 ,	$C^{(4)}_{(0,0,1,1)}(\{r_i\})$	=	0.00658	$\sim$ 0 ,
$C^{(3)}_{(0,0,1)}(\{r_i\})$	=	-0.01335	$\sim$	0 ,	$C^{(4)}_{(0,0,1,2)}(\{r_i\})$	=	0.00695	$\sim$ 0 ,
$C^{(3)}_{(0,1,2)}(\{r_i\})$	=	-0.00670	$\sim$	0 ,	$C^{(4)}_{(0,1,2,3)}(\{r_i\})$	=	-0.00674	$\sim$ 0 .

Table 5.1: The table lists the correlation coefficients of adjacent random numbers in a sequence $\{r_i\}$ of 10000 elements generated by a linear congruential generator of equation (5.15) with $m = 2^{31}$, $a = 65539$, $c = 0$, and $r_0 = 1$.

of the ensemble of random number sequences, but are also influenced by the range of the random number domain. A scaling of the random numbers by a factor s would result in a scaling of the above cumulant by a factor s^k. Hence, to achieve comparable results one divides the cumulant by the square root of the variance of each random number. One normalizes the random number domain according to the definition (5.16).

Table 5.2.1 lists all correlation coefficients up to fourth order for adjacent random numbers of a sequence of 10000 elements. The results are compared with the ideal values of an ideal random number sequence.

All simulated correlations coefficients of two or more different sequences are roughly zero, thus satisfying the criterium in equation (5.8). To prove true randomness one would have to proceed this way and determine all correlation coefficients of all orders. Since this is an impossible endeavor one truncates the test at some low order. This, however, can be dangerous.

Figure 5.4 presents random number triplets as Figure 5.3 presented pairs of random numbers. At first sight the left scatter plot displays a perfectly homogeneous distribution indicating perfect randomness. However, rotating the coordinate system slightly reveals a different picture as shown on the right side of Fig. 5.4. We can discern that the random number triplets gather on 15 planes.

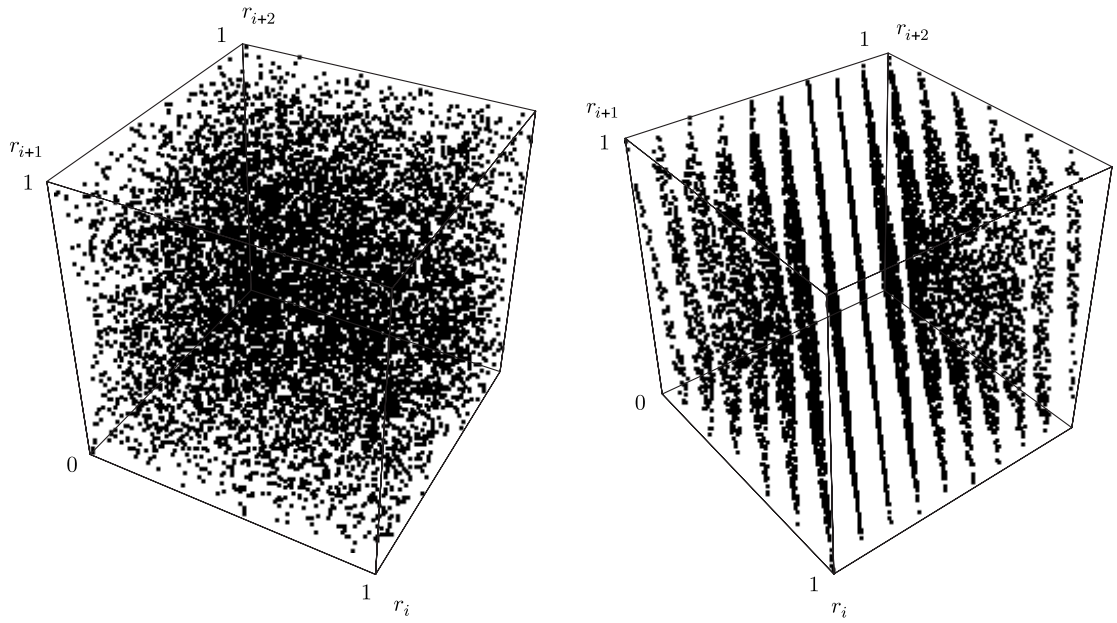

Figure 5.4: The left and right scatter plots display the same three-dimensional distribution of 10000 adjacent random number triplets as generated by the linear congruential generator used in Fig. 5.2. The right results from the left plot through rotation around the r_{i+2}-axis.

Hence, the numbers in these triplets are not completely independent of each other and, therefore, not truely random.
The lack of randomness may or may not have influenced the result of a calculation. Imagine sampling a three-dimenional density function using the pseudo random sampling points as displayed in Figure 5.4. All features of the density function that lie inbetween those 15 planes would go undetected. However, sampling a two-dimensional function with the same random numbers as displayed in Figure 5.3 would be sufficient.
Unfortunately, it is impossible to give general guidelines for the quality and feasibility of random number generators.

5.2.2 Gaussian Distribution

Random numbers with a homogeneous distribution are fairly easy to create, but for our purposes, the simulation of random processes, random numbers with a Gaussian distribution are more important. Remember that the source of randomness in the stochastic equation (5.2) is the random variable $d\omega$ which exhibits a Gaussian and not a homogeneous distribution. Hence, we have to introduce techniques to convert a random number sequence with homogeneous distribution into a sequence with a different probability distribution, e.g., a Gaussian distribution.
Given a real valued random number sequence $\{r_i\}$ with a normalized, uniform probability distribution in the interval $[0, 1]$

$$p(r)\,dr \quad = \quad \begin{cases} dr & \text{for } 0 \le r \le 1 \\ 0 & \text{otherwise} \end{cases} \tag{5.17}$$

one can create a new random number sequence $\{s_i\}$ by mapping a strictly monotonous function $f(r)$ onto the sequence $\{r_i\}$. The probability distribution of the new sequence $\{s_i\} = \{f(r_i)\}$ is

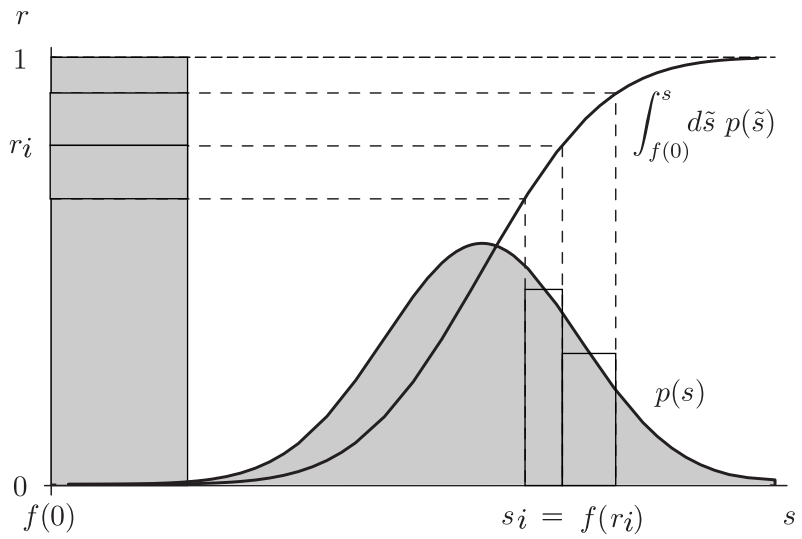

Figure 5.5: The transformation f of homogeneous random numbers r_i into random numbers s_i with a probability distribution $p(s)$.

then given by

$$p(s)\,ds \;=\; p(r)\left|\frac{\partial r}{\partial s}\right| ds\ . \tag{5.18}$$

To find the function $f(r)$ for a desired probability distribution $p(s)$ one integrates both sides of equation (5.18) over the interval $s \in [f(0), f(1)]$ or $s \in [f(1), f(0)]$ depending on $f(r)$ being a montonously increasing (i.e., $\frac{\partial f(r)}{\partial r} > 0$) or decreasing (i.e., $\frac{\partial f(r)}{\partial r} < 0$) function. We assume here for simplicity $\frac{\partial f(r)}{\partial r} > 0$. One obtains

$$\begin{aligned}\int_{f(0)}^{s} d\tilde{s}\ p(\tilde{s}) &= \int_{f(0)}^{s} d\tilde{s}\ p(r)\ \frac{\partial r}{\partial \tilde{s}} \\ &= \int_{f(0)}^{s} d\tilde{s}\ \frac{\partial f^{(-1)}(\tilde{s})}{\partial \tilde{s}} \\ &= f^{(-1)}(\tilde{s})\ \Big|_{f(0)}^{s}\end{aligned}$$

and, consequently,

$$f^{(-1)}(s) \;=\; \int_{f(0)}^{s} d\tilde{s}\ p(\tilde{s})\ . \tag{5.19}$$

The inverse of equation (5.19) renders $f(r)$. The above calculation is depicted in Fig. 5.5. The homogeneous distribution of r on the interval $[0, 1]$ is placed on the vertial axes on the left. Each (infinitesimal) bin dr is mapped by the function $f(r)$ defined in (5.19) onto the horizontal s-axes. Depending on the slope of $f(r)$ the width of the bins on the s-axes increases or decreases. However, the probability for each bin depicted by the area of the rectangles is conserved resulting in a new probability density distribution $p(s)$.
The method described here fails if one cannot find a closed or at least numerically feasable form for $f(r)$. Unfortunately, this is the case for the Gaussian distribution. Fortunately one can resort to a similar, two-dimensional approach.

Equation (5.18) reads in a multi-dimensional case

$$p(s_1, s_2, \dots)\, ds_1\, ds_2\, \dots \;=\; p(r_1, r_2, \dots) \left| \frac{\partial(r_1, r_2, \dots)}{\partial(s_1, s_2, \dots)} \right| ds_1\, ds_2\, \dots \;, \tag{5.20}$$

where $|\partial(\ )/\partial(\ )|$ is the Jacobian determinant. One obtains Gaussian-distributed random numbers through the following algorithm. One first generates two random numbers r_1 and r_2 uniformly distributed in the interval $[0, 1]$. The functions

$$\begin{aligned} s_1 &= \sqrt{-2\, \ln r_1}\; \sin[2\pi\, r_2] \\ s_2 &= \sqrt{-2\, \ln r_1}\; \cos[2\pi\, r_2] \end{aligned} \tag{5.21}$$

render then two Gaussian-distributed numbers s_1 and s_2. To verify this claim, one notes that the inverse of (5.21) is

$$\begin{aligned} r_1 &= \exp\left[-\frac{1}{2}\, \left(s_1^2 + s_2^2 \right) \right] \;, \\ r_2 &= \frac{1}{2\pi}\, \arctan \frac{s_1}{s_2} \;. \end{aligned} \tag{5.22}$$

Applying (6.57) one obtains

$$\begin{aligned} p(s_1, s_2)\, ds_1\, ds_2 &= p(r_1, r_2) \begin{vmatrix} \partial r_1/\partial s_1 & \partial r_1/\partial s_2 \\ \partial r_2/\partial s_1 & \partial r_2/\partial s_2 \end{vmatrix} ds_1\, ds_2 \\ &= p(r_1, r_2) \begin{vmatrix} -s_1\, e^{-\frac{1}{2}(s_1^2+s_2^2)} & -s_2\, e^{-\frac{1}{2}(s_1^2+s_2^2)} \\ \frac{1}{2\pi} \frac{s_2}{s_1^2+s_2^2} & -\frac{1}{2\pi} \frac{s_1}{s_1^2+s_2^2} \end{vmatrix} ds_1\, ds_2 \\ &= \frac{1}{2\pi} \left(\frac{s_1^2}{s_1^2 + s_2^2} + \frac{s_2^2}{s_1^2 + s_2^2} \right) e^{-\frac{1}{2}(s_1^2+s_2^2)}\; ds_1\, ds_2 \\ &= \left(\frac{1}{\sqrt{2\pi}}\; e^{-s_1^2/2}\, ds_1 \right) \left(\frac{1}{\sqrt{2\pi}}\; e^{-s_2^2/2}\, ds_2 \right) \;. \end{aligned} \tag{5.23}$$

This shows that s_1 and s_2 are independent Gaussian distributed numbers. Hence, one can employ (5.21) to produce Gaussian random numbers, actually, two at a time.
Figure 5.6 displays a sequence of 1000 Gaussian random numbers generated with the algorithm outlined above. The Gaussian random numbers around 0 with a standard deviation of 1 are displayed by points starting in the front and proceeding to the rear. To verify the distribution, a bin count with a bin width of 0.3 is displayed in the background. The bar hights represent the normalized probability density in each bin. The line depicts the ideal theoretical distribution as in (5.23).

5.3 Monte Carlo integration

The most prominent application of random numbers is the Monto Carlo integration method. The concept is very simple. To evaluate an integral

$$\int_\Omega d\boldsymbol{x}\; f(\boldsymbol{x}) \tag{5.24}$$

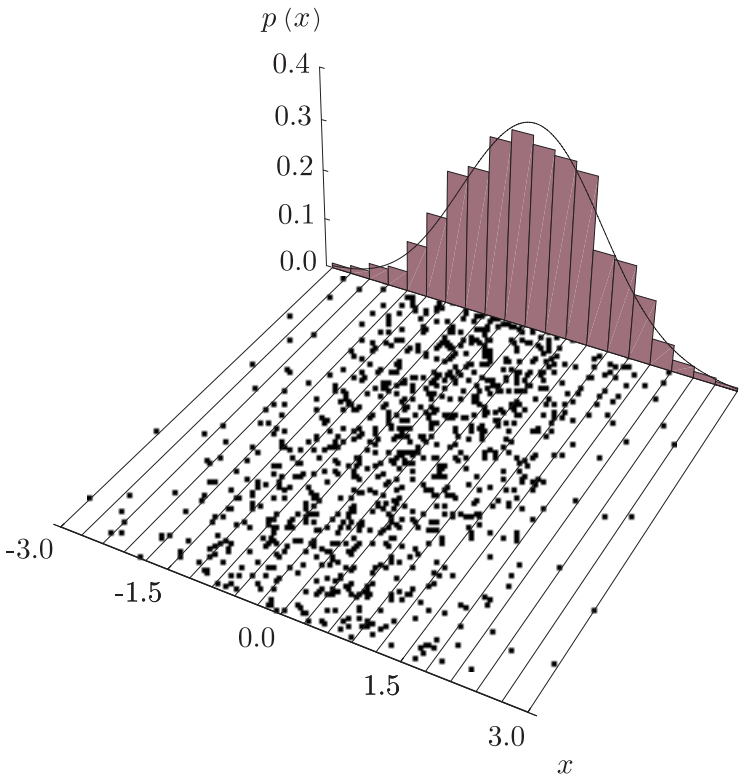

Figure 5.6: Gaussian random number sequence around 0 with a standard deviation of 1.

with the Monto Carlo method one samples the function $f(\boldsymbol{x})$ at M homogeneously distributed random points $\boldsymbol{r}_k$ in the integration domain Ω. The average of the function values at these random points times the volume $|\Omega|$ of the integration domain Ω can be taken as an estimate for the integral (5.24), as shown in Figure 5.7

$$\int_\Omega d\boldsymbol{x}\ f(\boldsymbol{x}) \quad = \quad \frac{|\Omega|}{M} \sum_{k=1}^{M} f(\boldsymbol{r}_k) \quad + \quad \mathcal{O}\left(\frac{1}{\sqrt{M}}\right) . \tag{5.25}$$

The more function values $f(\boldsymbol{r}_k)$ are taken into account the more accurate the Monte Carlo method becomes. The average $\langle f(x)\rangle$ exhibits a statistical errors proportional to $1/\sqrt{M}$. Thus the error of the numerical integration result is of the order of $\mathcal{O}(1/\sqrt{M})$.
The integration by random sampling seems rather inaccurate at first. Systematic integration methods like the trapezoidal rule (see right Figure 5.7) appear more precise and faster. This is true in many, but not all cases.
The trapezoidal rule approximates a function $f(x)$ linearly. An approximation over intervals of length h between sampling points is thus correct up to the order of $f''(x)\,h^2$. In one dimension the length of the integration step h is given by the number of sampling points M and the length of the integration domain Ω according to $h = |\Omega|/(M+1)$. Hence, the trapezoidal rule is an approximation up to the order of $\mathcal{O}(1/M^2)$. Other systematic integration methods exhibit errors of similar polynomial order. Obviously, systematic numerical integration techniques are superior to the Monte Carlo method introduced above. However, the rating is different for integrals on higher dimensional domains.
Consider an integration domain of n-dimensions. A systematic sampling would be done over an

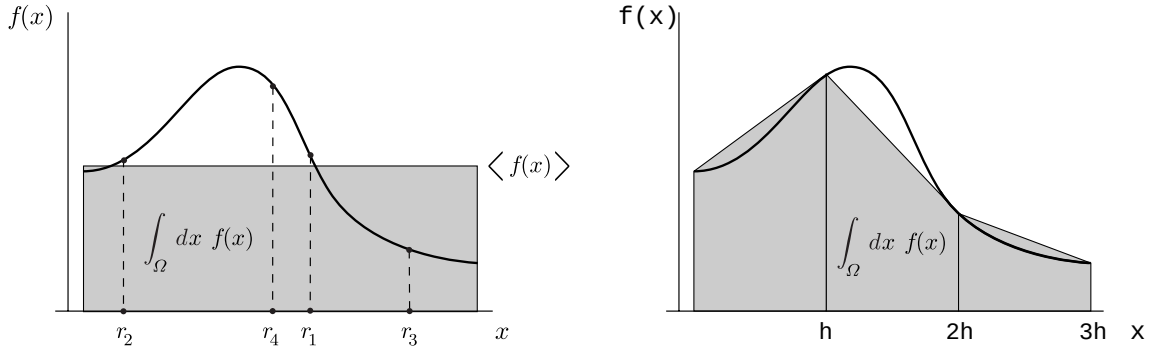

Figure 5.7: Examples for the numerical integration of $f(x)$ according to the Monte Carlo method (left) and the trapezoidal rule (right).

n-dimensional grid. A total of M sampling points would result in $\sqrt[n]{M}$ sampling points in each grid dimension. The trapezoidal rule would, thus, be correct up to the order of $\mathcal{O}(M^{-2/n})$. A random sampling, however, is not affected by dimensional properties of the sampling domain. The Monte Carlo precision remains in the order of $\mathcal{O}(M^{-1/2})$. Hence, we see that the Monte Carlo method becomes feasible for $(n = 4)$-dimensions and that it is superior for high-dimensional integration domains Ω.
One can modify the straight forward Monte Carlo integration method (5.25). Suppose one uses random points $\tilde{\boldsymbol{r}}_k$ with a normalized probability distribution $p(\boldsymbol{x})$ in Ω. Instead of evaluating integral (5.25) with a homogeneous distribution of $1/|\Omega|$ one would approximate

$$\int_\Omega d\boldsymbol{x}\ f(\boldsymbol{x})\, p(\boldsymbol{x}) \quad \sim \quad \frac{1}{M} \sum_{k=1}^{M} f(\tilde{\boldsymbol{r}}_k)\ . \tag{5.26}$$

Modification (5.26) is appropriate if a factor of the integrand happens to be a probability density distribution, for which one can generate random numbers $\tilde{\boldsymbol{r}}_k$. This will be the case in the next chapter where we will show how the Monte Carlo integration method (5.26) is incorporated in the simulation of stochastic processes.

Chapter 6

Brownian Dynamics

Contents

6.1 Discretization of Time 91
6.2 Monte Carlo Integration of Stochastic Processes 93
6.3 Ito Calculus and Brownian Dynamics 95
6.4 Free Diffusion 96
6.5 Reflective Boundary Conditions 100

In 1827 the botanist Robert Brown examined under his microspcope pollen of plants suspended in water. He observed that the pollen, about 10^{-6}m in diameter, performed stochastic motions of the order of 10^{-5}m. Even though Brown could not explain the cause of this motion any continuous stochastic process like that of a pollen is now referred to as *Brownian dynamics*.
In this chapter we introduce a numerical technique that generates a solution of the Fokker-Planck equation (5.1) by simulating an ensemble of stochastic processes. Due to these stochastic processes one calls this numerical method *Brownian dynamics* as well.
We provide two derivations of the numerical method of Brownian dynamics. In the first section we transform the Fokker-Planck equation (5.1) into a multi-dimensional integral. We then explain in the second section how to evaluate this multi-dimensional integral using the Monte Carlo integration method introduced in the previous chapter. We show in the third section that this Monte Carlo integration is equivalent to simulating an ensemble of stochastic processes. The equivalence is shown by deriving the Brownian dynamics method a second time starting with the stochastic differential equation (5.2). We examplify the idea of Brownian dynamics by applying it to a free diffusion model in the fourth section and conclude this chapter in the fifth section by showing how to incorporate boundary conditions in Brownian dynamics.

6.1 Discretization of Time

Discretization is the basis of many numerical procedures. This also holds true for Brownian dynamics. The object of discretization is the continuous time axis. A computer can not represent a continuous line or function. The infinitely many points would simply not fit into a finite digital computer nor could they be processed in a finite amount of time. Hence, one needs to approximate a continuous dimension with a finite set of points. This approximation is called discretization.

We solve the Fokker-Planck equation numerically by breaking the time axes paramerized by t into discrete points labeled by $t_0, t_1, t_2, \ldots$. These time points do not need to be equally spaced, but they usually are to simplfy the calculations.
One now has to adapt the Fokker-Planck equation (2.148) to the discretized time axis. For the sake of simplicity we consider the one-dimensional version

$$\partial_t\, p(x,t|x_0,t_0) \;=\; -\partial_x\, A(x,t)\, p(x,t|x_0,t_0) \,+\, \frac{1}{2}\,\partial_x^2\, B^2(x,t)\, p(x,t|x_0,t_0)\;. \tag{6.1}$$

Let $p(x,t|x_0,t_0)$ be the, yet unknown, solution of (6.1) for the initial condition $x(t_0) = x_0$. One finds a solution $p(x,t|x_0,t_0)$ on a discrete sequence of times $\{t_0, t_1, t_2, \ldots\}$ by constructiong transition probabilities $p(x_{i+1}, t_{i+1}|x_i, t_i)$ from one discrete time point t_i to the next. With these transition probabilities one can reassemble the complete solution $p(x,t|x_0,t_0)$.
We need to first disassemble the time evolution of $p(x,t|x_0,t_0)$ into many small time increments. For this purpose we proceed as follows. To obtain a solution $p(x_2,t_2|x_0,t_0)$ with an initial starting position at $x(t_0) = x_0$ one can first solve for $p(x_1,t_1|x_0,t_0)$ which describes the solution for an intermediate state at some time t_1 prior to t_2 and after t_0. The probability distribution at time t_1 may then be taken as the initial condition for a second solution of (6.1) reaching from time t_1 to time t_2. This second solution can be assembled due to the linearity of (6.1) using $p(x_2,t_2|x_1,t_1)$ for the initial condition $x(t_1) = x_1$. Summing $p(x_2,t_2|x_1,t_1)$ over all possible initial positions x_1 in the domain Ω weighted with the initial probability determined through $p(x_1,t_1|x_0,t_0)$ one obtains $p(x_2,t_2|x_0,t_0)$ and the Chapman Kolmogorow equation

$$p(x_2,t_2|x_0,t_0) \;=\; \int_\Omega dx_1\; p(x_2,t_2|x_1,t_1)\, p(x_1,t_1|x_0,t_0)\;. \tag{6.2}$$

This is the Chapman-Kolmogorov equation encountered already above [c.f. (9.17)]. The process of dividing the evolution in the interval $[t_0,t_2]$ into consecutive evolution in the intervals $[t_0,t_1]$ and $[t_1,t_2]$ can be repeated. For this purpose one starts from (6.2), replaces variables x_2 and t_2 with x_3 and t_3, and applies (6.2) to $p(x_3,t_3|x_1,t_1)$ while naming the intermediate state x_2 and t_2. One derives

$$\begin{aligned} p(x_3,t_3|x_0,t_0) \;&=\; \int_\Omega dx_1\; p(x_3,t_3|x_1,t_1)\, p(x_1,t_1|x_0,t_0) \\ &=\; \iint_\Omega dx_2\, dx_1\; p(x_3,t_3|x_2,t_2)\, p(x_2,t_2|x_1,t_1)\, p(x_1,t_1|x_0,t_0)\;. \end{aligned} \tag{6.3}$$

These steps may be repeated again. Doing so $(N-1)$-times one obtains

$$p(x_N,t_N|x_0,t_0) \;=\; \underbrace{\int\cdots\int_\Omega}_{(N-1)\,\text{times}} \left(\prod_{i=1}^{N-1} dx_i\; p(x_{i+1},t_{i+1}|x_i,t_i)\right) p(x_1,t_1|x_0,t_0)\;. \tag{6.4}$$

The procedure above has divided now the time evolution of $p(x_N,t_N|x_0,t_0)$ into N steps over time intervals $[t_{i+1},t_i]$ where t_i, $i = 1,2,\ldots,N-1$ denotes the intermediate times. We will identify below t and t_N. In order to evaluate $p(x_N,t_N|x_0,t_0)$ we need to determine the transition probabilities $p(x_{i+1},t_{i+1}|x_i,t_i)$. The respective algorithm can exploit the possibility that one can choose the time intervals $[t_{i+1},t_i]$ very short such that certain approximations can be envoked without undue errors. In fact, for equally spaced time points t_i the length of each time segment is $\Delta t = (t_i - t_{i-1}) = (t-t_0)/N$. One can choose N always large enough that the time period Δt is short enough to justify the approximations introduced below.

Let Δx be the typical distance that a particle governed by the probability distribution $p(x, t_0 + \Delta t|x_0, t_0)$ may cover due to drift and diffusion within a time period Δt, i.e.

$$\begin{aligned} \Delta x &= \Big|\langle\!\langle x \rangle\!\rangle\Big| + \sqrt{\langle\!\langle x^2 \rangle\!\rangle} \\ &\sim \big|A(x_0, t_0)\big|\,\Delta t + B(x_0, t_0)\,\sqrt{\Delta t}\ . \end{aligned} \tag{6.5}$$

The approximation introduced assumes that $A(x, t)$ and $B(x, t)$ are constant for each time period $[t_i, t_{i+1}]$ and spatially independent in each range $[x_i - \Delta x, x_i + \Delta x]$,

$$A\big(t \in [t_i, t_{i+1}], x \in [x_i - \Delta x, x_i + \Delta x]\big) \sim A(t_i, x_i) \tag{6.6}$$

$$B\big(t \in [t_i, t_{i+1}], x \in [x_i - \Delta x, x_i + \Delta x]\big) \sim B(t_i, x_i)\ , \tag{6.7}$$

One replaces than the functions $p(x_{i+1}, t_{i+1}|x_i, t_i)$ in (6.4) by solutions of the Fokker-Planck equation (6.1) with constant coefficients $A(x, t)$ and $B(x, t)$. In case of boundary conditions at $x \to \pm\infty$ the resulting expression is, according to (4.28, 4.39)

$$\begin{aligned} p(x_{i+1},&t_{i+1}|x_i, t_i) = \\ &\frac{1}{\sqrt{2\pi\, B^2(x_i, t_i)\,(t_{i+1} - t_i)}}\ \exp\left(-\frac{\big(x_{i+1} - x_i - A(x_i, t_i)\,(t_{i+1} - t_i)\big)^2}{2\, B^2(x_i, t_i)\,(t_{i+1} - t_i)}\right)\ . \end{aligned} \tag{6.8}$$

We will consider solutions for other boundary conditions on page 100 further below.
Employing (6.8) in the iterated form of the Chapman-Kolmogorow equation (6.4), one derives

$$\begin{aligned} p(x,&t|x_0, t_0) = \\ &\underbrace{\int\cdots\int_{\Omega}}_{(N-1)\,\text{times}} \left(\prod_{i=1}^{N-1} dx_i\right) \prod_{i=0}^{N-1} \frac{1}{\sqrt{2\pi\, B^2(x_i, t_i)\,\Delta t}}\ \exp\left(-\frac{\big(x_{i+1} - x_i - A(x_i, t_i)\,\Delta t\big)^2}{2\, B^2(x_i, t_i)\,\Delta t}\right)\ . \end{aligned} \tag{6.9}$$

Thus, we have solved the Fokker-Planck equation (6.1) up to an N-dimensional integral. This integral needs to be evaluated numerically for which purpose one applies the Monte Carlo integration method.

6.2 Monte Carlo Integration of Stochastic Processes

The integral on the r.h.s. of (6.4) and (6.9) is a truely high-dimensional integral. The Monte Carlo method is therefore the appropriate integration method.
Before we apply the Monte Carlo method we modify equation (6.4) slightly. The probability distribution $p(x, t|x_0, t_0)$ is not always what one wants to determine. A more feasible construct is the average $\bar{q}(t|x_0, t_0)$ of an arbitrary observable Q with a sensitivity function $q(x)$ in state space Ω given by the integral

$$\bar{q}(t|x_0, t_0) = \int_{\Omega} dx\ q(x)\ p(x, t|x_0, t_0)\ . \tag{6.10}$$

Equation (6.10) is very comprehensive. Even the probability distribution $p(\tilde{x}, t|x_0, t_0)$ can be viewed as an observable Q, namely, for the sensitivity function $q_{\tilde{x}}(x) = \delta(x - \tilde{x})$.

We now apply the Monte Carlo integration method as stated in equation (5.26) to the expanded form of (6.10)

$$\bar{q}(t|x_0,t_0) = \int_\Omega dx\ q(x)\ \times \underbrace{\int\cdots\int_\Omega}_{(N-1)\,\text{times}} \left(\prod_{i=1}^{N-1} dx_i\ p(x_{i+1},t_{i+1}|x_i,t_i)\right) p(x_1,t_1|x_0,t_0)\ . \tag{6.11}$$

One can associate $q(x)$ with $f(\boldsymbol{x})$ and the product of $p(x_{i+1},t_{i+1}|x_i,t_i)$ with $p(\boldsymbol{x})$. The only problem now is finding a random number generator that produces random numbers $\tilde{r}$ with a distribution equivalent to the product of all $p(x_{i+1},t_{i+1}|x_i,t_i)$. This seems to be an impossible endeavor unless one recalls how the product of all the $p(x_{i+1},t_{i+1}|x_i,t_i)$ came about.
Let us start with the case $N = 0$. Given a random number generator that produces numbers $\tilde{r}(x_0,t_0)$ with a distribution $p(x,t|x_0,t_0)$ the solution is

$$\begin{aligned}\bar{q}(t|x_0,t_0) &= \int_\Omega dx\ q(x)\ p(x,t|x_0,t_0)\\ &\sim \frac{1}{M}\sum_{k=1}^{M} q(\tilde{r}_k(x_0,t_0))\ .\end{aligned} \tag{6.12}$$

We denote the x_0 and t_0-dependence of the random numbers $\tilde{r}_k(x_0,t_0)$ explicitly for later use. The reader should note that $\tilde{r}_k(x_0,t_0)$ exhibits a distribution $p(x,t|x_0,t_0)$ around x_0.
Implementing the Chapman-Kolmogorov equation (6.2) for $p(x,t|x_0,t_0)$ once we obtain the case $N = 1$ and two nested integrals.

$$\bar{q}(t|x_0,t_0) = \int_\Omega dx\ q(x)\ \int_\Omega dx_1\ p(x,t|x_1,t_1)\,p(x_1,t_1|x_0,t_0)\ . \tag{6.13}$$

To approximate (6.13) numerically one determines first the inner integral with the integration variable x_1. The Monte Carlo method yields

$$\bar{q}(t|x_0,t_0) \sim \int_\Omega dx\ q(x)\ \frac{1}{M}\sum_{k_0=1}^{M} p(x,t|r_{k_0}(x_0,t_0),t_1)\ . \tag{6.14}$$

In a second step one applies applies the Monte Carlo method to the outer integral, now however with a probability distribution $p(x,t|\tilde{r}_{k_0}(x_0,t_0),t_1)$ exhibiting the inital starting point $\tilde{r}_{k_1}(x_0,t_0)$. We therefore use the random numbers $\tilde{r}_{k_1}(\tilde{r}_{k_0}(x_0,t_0),t_1)$.

$$\bar{q}(t|x_0,t_0) \sim \frac{1}{M^2}\sum_{k_1=1}^{M}\sum_{k_0=1}^{M} q(\tilde{r}_{k_1}(\tilde{r}_{k_0}(x_0,t_0),t_1))\ . \tag{6.15}$$

Note the nesting of random numbers $\tilde{r}_{k_1}(\tilde{r}_{k_0}(x_0,t_0),t_1)$. The Gaussian random number $\tilde{r}_{k_1}(\dots)$ is distributed around the previous random number $\tilde{r}_{k_0}(\dots)$ which itself is distributed around x_0.
Performing the above steps N times, thus iterating the Chapman-Kolmogorov equation (6.9), one

obtains

$$\bar{q}(t|x_0,t_0) = \int_\Omega dx\ q(x) \underbrace{\int\cdots\int_\Omega}_{(N-1)\,\text{times}} \left(\prod_{i=1}^{N-1} dx_i\ p(x_{i+1},t_{i+1}|x_i,t_i)\right) p(x_1,t_1|x_0,t_0)$$
$$\sim \frac{1}{M^N}\sum_{k_0=1}^{M}\sum_{k_1=1}^{M}\cdots\sum_{k_N=1}^{M} q(\tilde{r}_{k_N}(\ldots\tilde{r}_{k_1}(\tilde{r}_{k_0}(x_0,t_0),t_1)\ldots,t_N))\ , \tag{6.16}$$

where the random numbers $\tilde{r}_{k_j}(x_j,t_j)$ should exhibit the probability distributions

$$p\big(\tilde{r}_{k_j}(x_j,t_j)\big) = p(x_{j+1}t_{j+1}|x_j,t_j)\ . \tag{6.17}$$

The iteration above simplifies the problem of finding an appropriate random number generator. We now need random numbers that simply obey (6.17). In the specific case (6.8) one can generate the appropriate random numbers $\tilde{r}_k(x_0,t_0)$ utilizing a Gaussian number generator as described in the previous chapter. If r_k is a random number with the normalized Gaussian probability distribution $\exp(-r^2/2)/\sqrt{2\pi}\,dr$ one obtains $\tilde{r}_k(x_0,t_0)$ with the mapping

$$\tilde{r}_k(x_0,t_0) = B(x_0,t_0)\sqrt{t-t_0}\ r_k\ +\ A(x_0,t_0)\,(t-t_0)\ +\ x_0\ . \tag{6.18}$$

With the help of (5.18) one can verify

$$p(\tilde{r}(x_0,t_0)) = \frac{1}{\sqrt{2\pi\,B^2(x_0,t_0)\,(t-t_0)}}\ \exp\left(-\frac{\big(\tilde{r}(x_0,t_0)-x_0-A(x_0,t_0)\,(t-t_0)\big)^2}{2\,B^2(x_0,t_0)\,(t-t_0)}\right)\ . \tag{6.19}$$

Thus, we finally have all the ingredients to perform the Monte Carlo integration (6.16). However, before putting (6.16) to use we can simplify the summations. The nesting of random numbers $\tilde{r}_{k_N}(\ldots\tilde{r}_{k_1}(\tilde{r}_{k_0}(x_0,t_0),t_1)\ldots,t_N)$ is in effect a random walk starting at x_0 and proceeding with Gaussian random steps $\tilde{r}_{k_i}$. With the summations in (6.16) one takes the average over all random walks that can be formed with a given set of M random steps $\tilde{r}_{k_i}$ for $i=1,\ldots,N$. One can simplify this equation by summing over M^N independent random pathes $\tilde{r}_{l_N}(\ldots\tilde{r}_{l_1}(\tilde{r}_{l_0}(x_0,t_0),t_1)\ldots,t_N)$ instead. Equation (6.16) becomes

$$\bar{q}(t|x_0,t_0) \sim \frac{1}{M^N}\sum_{l=1}^{M^N} q(\tilde{r}_{l_N}(\ldots\tilde{r}_{l_1}(\tilde{r}_{l_0}(x_0,t_0),t_1)\ldots,t_N))\ . \tag{6.20}$$

6.3 Ito Calculus and Brownian Dynamics

Before applying Brownian dynamics in the form of equation (6.20) we want to shed light on the close relation between the Monte Carlo integration introduced above and the concept of stochastic processes as described in chapter 2.
Equation (6.20) describes the algorithm of Brownian dynamics. In essence one simulates the random walk of a given number of Brownian particles and samples their final position in state space Ω. To demonstrate this we return to chapter 2. Within the framework of Ito calculus we consider the stochastic differential equation (2.138) that corresponds to the Fokker-Planck equation (6.1)

$$\partial_t\, x(t) = A(x(t),t)\ +\ B(x(t),t)\ \eta(t)\ . \tag{6.21}$$

The corresponding Ito-formula (2.137) is

$$df[x(t)] = A(x(t),t)\Big(\partial_x f[x(t)]\Big)\, dt + B(x(t),t)\Big(\partial_x f[x(t)]\Big)\, d\omega(t) + \frac{1}{2}\, B^2(x(t),t)\, \Big(\partial_x^2 f[x(t)]\Big)\, dt\ . \tag{6.22}$$

Assume $f[x(t)] = x(t)$. We thus derive for $x(t)$

$$dx(t) = A(x(t),t)\, dt + B(x(t),t)\, d\omega(t)\ . \tag{6.23}$$

Integrating (6.23) over small time periods Δt for which we can assume $A(x(t),t)$ and $B(x(t),t)$ to be constant we obtain the finite difference equation

$$x(t+\Delta t) - x(t) = A(x(t),t)\ \Delta t + B(x(t),t)\ \Delta\omega\ , \tag{6.24}$$

with $\Delta\omega$ being a random variable with the Gaussian probability distribution (2.48) for $D = 1/2$. Such a random variable can be generated with a normalized Gaussian random number r and the mapping $\Delta\omega = \sqrt{\Delta t}\ r$

$$x(t+\Delta t) - x(t) = A(x(t),t)\ \Delta t + B(x(t),t)\ \sqrt{\Delta t}\ r\ . \tag{6.25}$$

Note, that $x(t+\Delta t) - x(t)$ in (6.25) is the same as $\tilde{r}(x_0,t) - x_0$ defined in (6.18). Iterating equation (6.25) and thus numerically integrating the stochastic differential equation (6.21) according to Ito calculus, we generate a sample path $x(t)$ starting at any given $x(t_0) = x_0$. Such a sample path can then be used in the Monte Carlo procedure (6.20).

6.4 Free Diffusion

We now test the numerical Brownian dynamics procedure outlined above. For this purpose we resort to examples that can be solved analytically.
We begin with free diffusion in an infinite domain. The Fokker Planck equation, i.e., the respectively Einstein diffusion equation, is

$$\partial_t\, p(x,t|x_0,t_0) = D\, \partial_x^2\, p(x,t|x_0,t_0)\ . \tag{6.26}$$

Comparing (6.26) and (6.1) one finds the drift coefficient $A(x,t)$ to be zero and the noise coupling coefficient $B(x,t) = \sqrt{2\,D}$ to be constant in time and space. Thus, assumptions (6.6) and (6.7) are met for any time step size $\Delta t = t_{i+1} - t_i$. Due to this fact one could choose $\Delta t = t - t_0$ and obtain with (6.8) the final result right away, thereby, rendering the following numerical simulation, employing a division into many short time intervals, unneccessary. Since we intend to verify the numerical approach we choose a division into N intermediate time steps nevertheless. These intermediate steps will become necessary when considering a potential and consequently a spatially dependent $A(x,t)$ further below.
One can proceed in a straight forward manner. Starting with Gaussian random numbers r_k as generated in (5.23) one derives the required random numbers $\tilde{r}_k(x,t)$ according to (6.18).

$$\tilde{r}_k(x,t) = \sqrt{2\,D\,\Delta t}\ r_k\ + x. \tag{6.27}$$

These random numbers $\tilde{r}_k(x,t)$ exhibit the probability distribution

$$p(\tilde{r}(x,t)) = \frac{1}{\sqrt{4\pi\, D\, \Delta t}}\ \exp\left(-\frac{\big(\tilde{r}(x,t) - x\big)^2}{4\, D\, \Delta t}\right)\ . \tag{6.28}$$

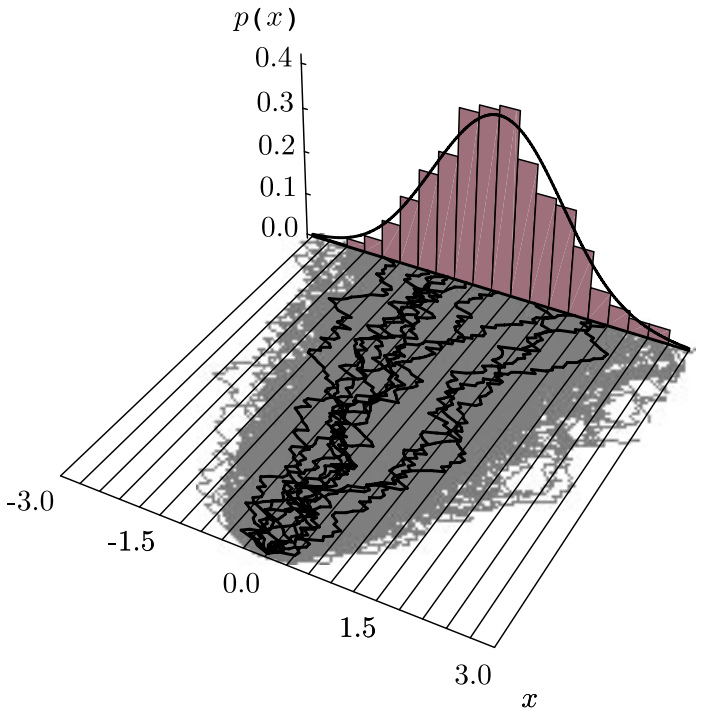

Figure 6.1: 1000 random trajectories generated by a Brownian dynamics simulation defined by (6.29).

as shown in (6.19). To determine the endpoint $x(t)$ of a sample path of free diffusion one creates a chain of random numbers, i.e., a random walk,

$$\begin{aligned} x(t = t_N) &= \tilde{r}_N(\ldots \tilde{r}_1(\tilde{r}_0(x_0, t_0), t_1) \ldots, t_N) \\ &= \sqrt{2\,D\,\Delta t}\,\sum_{k=1}^{N} r_k\ . \end{aligned} \tag{6.29}$$

Figure 6.1 displays an ensemble of 1000 such paths, each path being $N = 100$ steps long. The trajectories start at $x = 0$ and proceed towards the rear, as indicated by the time axis. $D = 1$ defines the relation between temporal and spatial units. Ten paths are displayed in black to examplify the behavior of single random walks. The other 990 paths are shown as a grey background. Note the parabolic shape of the trajectory distribution in time. This property, the broadening of the standard deviation of the trajectory distribution proportional to $\sqrt{t}$ was derived in (2.51). In the rear of the figure is a bin count of all trajectory locations at $t = 1$. The solid line imposed on the bar chart represents the theoretical solution according to equation (6.28) with $\Delta t = t - t_0$.
The paths of (6.29) can be used to determine the expectation value $\bar{q}(t|x_0, t_0)$ of an observable Q at time $t = t_N$ as described in (6.10) and (6.20). Obviously such a sampling of an observable value can only be done with a finite ensemble of trajectories. A statistical error in the result is inevitable. Hence the question: how large is the statistical error?
Assume we know the probability $p(x, t|x_0, t_0)$. The exact expectation value $\langle q(t|x_0, t_0)\rangle$ is then given by

$$\Big\langle q(t|x_0, t_0)\Big\rangle = \int_\Omega dx\ q(x)\ p(x, t|x_0, t_0)\ . \tag{6.30}$$

One can rewrite (6.30) in terms of a probabilty distribution $\tilde{p}(q,t|x_0,t_0)$ that does not depend on x but on the observable value q.

$$\left\langle q(t|x_0,t_0)\right\rangle \;=\; \int_\Omega dq\; q\; \underbrace{\frac{\partial x(q)}{\partial q}\; p(x(q),t|x_0,t_0)}_{\tilde{p}(q,t|x_0,t_0)}\;. \tag{6.31}$$

With respect to $\tilde{p}(q,t|x_0,t_0)$ we can then express the exact average (6.31) and the variance of the observable value $q(t|x_0,t_0)$ in terms of cumulants.

$$\left\langle q(t|x_0,t_0)\right\rangle \;=\; \left\langle\!\left\langle q(t|x_0,t_0)\right\rangle\!\right\rangle\,, \tag{6.32}$$

$$\left\langle \Big(q(t|x_0,t_0)\;-\;\left\langle q(t|x_0,t_0)\right\rangle\Big)^2\right\rangle \;=\; \left\langle\!\left\langle q^2(t|x_0,t_0)\right\rangle\!\right\rangle\,. \tag{6.33}$$

The variance (6.33) is the variance of single sample readings of an observable Q. Equation (6.33) does not apply to an expectation value $\bar{q}(t|x_0,t_0)$, which is the average of an ensemble of samples. Nevertheless, denoting the outcome of an i-th reading by $q^{(i)}(t|x_0,t_0)$ one can express the expectation value according to (6.20)

$$\bar{q}(t|x_0,t_0) \;=\; \frac{1}{M}\;\sum_{i=1}^{M}\; q^{(i)}(t|x_0,t_0)\;. \tag{6.34}$$

The second order cumulant of (6.34) renders

$$\begin{aligned}\left\langle\!\left\langle \bar{q}^2(t|x_0,t_0)\right\rangle\!\right\rangle \;&=\; \left\langle\!\left\langle \left(\frac{1}{M}\;\sum_{i=1}^{M}\; q^{(i)}(t|x_0,t_0)\right)^2\right\rangle\!\right\rangle \\ &=\; \frac{1}{M^2}\left\langle\!\left\langle \left(\sum_{i=1}^{M}\; q^{(i)}(t|x_0,t_0)\right)^2\right\rangle\!\right\rangle\,. \end{aligned}\tag{6.35}$$

Since every $q^{(i)}(t|x_0,t_0)$ stems from an independent trajectory sample one can apply (2.44) and we can write

$$\left\langle\!\left\langle \bar{q}^2(t|x_0,t_0)\right\rangle\!\right\rangle \;=\; \frac{1}{M^2}\;\sum_{i=1}^{M}\left\langle\!\left\langle \Big(q^{(i)}(t|x_0,t_0)\Big)^2\right\rangle\!\right\rangle\,. \tag{6.36}$$

Every sample $q^{(i)}(t|x_0,t_0)$ should also exhibit the same variance (6.33) so that we finally obtain

$$\begin{aligned}\left\langle\!\left\langle \bar{q}^2(t|x_0,t_0)\right\rangle\!\right\rangle \;&=\; \frac{1}{M^2}\;\sum_{i=1}^{M}\left\langle\!\left\langle q^2(t|x_0,t_0)\right\rangle\!\right\rangle \\ &=\; \frac{1}{M}\left\langle\!\left\langle q^2(t|x_0,t_0)\right\rangle\!\right\rangle\,. \end{aligned}\tag{6.37}$$

Hence, the variance of the average of M samples is about $1/M$ times smaller than the variance of a single sample. Consequently the standard deviation of the expectation value decreases with $1/\sqrt{M}$.

To finally determine the statistical error of an expectation value $\bar{q}(t|x_0,t_0)$ given by the standard deviation $\sqrt{\left\langle\!\left\langle \bar{q}^2(t|x_0,t_0)\right\rangle\!\right\rangle}$ one has to provide a value for the cumulant $\left\langle\!\left\langle q^2(t|x_0,t_0)\right\rangle\!\right\rangle$ in (6.37). An

estimate for the upper limit of this variance is sufficient in most cases. One can provide an estimate either with the help of some analytical approximation or by simply determining the variance of an ensemble of $\tilde{M}$ samples $q^{(i)}(t|x_0,t_0)$ according to

$$\left\langle\!\left\langle q^2(t|x_0,t_0)\right\rangle\!\right\rangle \approx \frac{1}{\tilde{M}-1}\sum_{i=1}^{\tilde{M}}\left(q^{(i)}(t|x_0,t_0) - \bar{q}(t|x_0,t_0)\right)^2 . \tag{6.38}$$

To examplify the tools just introduced we will consider a bin count. For a bin count one measures the probability $q_{[a,b]}$ to find a trajectory end point within a given interval $[a,b]$, called bin. The sensitivity function $q(x)$ for a single bin reaching from a to b is $q_{[a,b]}(x) = \Theta(x-a) - \Theta(x-b)$[1]. One can determine the expectation value $\bar{q}_{[a,b]}(t|x_0,t_0)$ with the help of (6.15), (6.20) and (6.29)

$$\begin{aligned}\bar{q}_{[a,b]}(t|x_0,t_0) &= \int_\Omega dx\; q_{[a,b]}(x)\; p(x,t|x_0,t_0) \\ &\approx \frac{1}{M}\sum_{l=1}^{M} q_{[a,b]}\left(\sqrt{2\,D\,\Delta t}\sum_{k_l=1}^{N} r_{k_l}\right) .\end{aligned} \tag{6.39}$$

Performing calculation (6.39) for an array of adjacent bins one can approximate a probability density distribution $p(\boldsymbol{x},t|\boldsymbol{x}_0,t_0)$ as shown in the rear of Figure 6.1. For that purpose one takes the expectation value $\bar{q}_{[a,b]}(t|x_0,t_0)$ of each bin and divides it by the base length $|b-a|$. One thereby obtains an estimate for the probability density between a and b

$$\begin{aligned}p(x\in[a,b],t|x_0,t_0) &\approx \bar{p}_{[a,b]}(t|x_0,t_0) \\ &= \frac{\bar{q}_{[a,b]}(t|x_0,t_0)}{|b-a|} .\end{aligned} \tag{6.40}$$

How much confidence can we have in a probability density distribution determined through (6.40)? There are two precision objectives to consider. First, one would like to have a sufficient spatial resolution. The bin size should be smaller than the spatial features of the probability distribution $p(x,t|x_0,t_0)$. This can be achieved by implementing a grid with many tiny bins; the smaller the bin, the better. This however is counteracting the second objective. The statistical error of a probability density within a bin increases as the bin size decreases. Thus, one has to balance these two objectives as we will do in the following calculation.
We will focus our attention on a bin $[a,b]$. The spatial resolution res_s of a bin count based on bins like $[a,b]$ is given by the bin size in relation to the relevant diffusion domain Ω

$$res_s = \frac{|a-b|}{|\Omega|} . \tag{6.41}$$

One can define a resolution of the probability density res_p in a similar fashion. Let $\Delta\bar{p}_{[a,b]}(t|x_0,t_0)$ be the standard deviation of the probability density in bin $[a,b]$. One can view this standard deviation $\Delta\bar{p}_{[a,b]}(t|x_0,t_0)$ as the analog to the bin size $|a-b|$. The relation between the standard deviation $\Delta\bar{p}_{[a,b]}(t|x_0,t_0)$ and the size $|p(\Omega)|$ of the overall range of probabilty density values in a distribution would then define the resolution res_p. Hence

$$res_p = \frac{\Delta\bar{p}_{[a,b]}(t|x_0,t_0)}{|p(\Omega)|} . \tag{6.42}$$

[1] $\Theta(x)$ represents Heaviside's step function: $\Theta(x)=0$ for $x<0$, and $\Theta(x)=1$ for $x>0$.

To optimize a bin count one has to balance the resolutions res_s and res_p. We thus assume

$$res_s \approx res_p \, . \tag{6.43}$$

Out of this equation we can derive the sample number M needed to achieve the desired precision goal.
The sample number M enters equation (6.43) via (6.42) and $\Delta\bar{p}_{[a,b]}(t|x_0,t_0)$. Starting with (6.40) one can derive

$$\begin{aligned} \Delta\bar{p}_{[a,b]}(t|x_0,t_0) &= \sqrt{\left\langle\!\left\langle \bar{p}^2_{[a,b]}(t|x_0,t_0) \right\rangle\!\right\rangle} \\ &= \sqrt{\frac{\left\langle\!\left\langle p^2_{[a,b]}(t|x_0,t_0) \right\rangle\!\right\rangle}{M}} \\ &= \sqrt{\frac{\left\langle\!\left\langle q^2_{[a,b]}(t|x_0,t_0) \right\rangle\!\right\rangle}{M\ |a-b|^2}} \, . \end{aligned} \tag{6.44}$$

$\left\langle\!\left\langle q^2_{[a,b]}(t|x_0,t_0) \right\rangle\!\right\rangle$ can be approximated assuming $\left\langle q_{[a,b]}(t|x_0,t_0) \right\rangle$ to be equal $\bar{q}_{[a,b]}(t|x_0,t_0)$.

$$\left\langle\!\left\langle q^2_{[a,b]}(t|x_0,t_0) \right\rangle\!\right\rangle = \left\langle \left(q_{[a,b]}(t|x_0,t_0) - \left\langle q_{[a,b]}(t|x_0,t_0) \right\rangle \right)^2 \right\rangle \tag{6.45}$$

$$\approx \left\langle \left(q_{[a,b]}(t|x_0,t_0) - \bar{q}_{[a,b]}(t|x_0,t_0) \right)^2 \right\rangle \tag{6.46}$$

$$= \left(1 - \bar{q}_{[a,b]}(t|x_0,t_0)\right)^2 \bar{q}_{[a,b]}(t|x_0,t_0) + \left(0 - \bar{q}_{[a,b]}(t|x_0,t_0)\right)^2 \left(1 - \bar{q}_{[a,b]}(t|x_0,t_0)\right) \tag{6.47}$$

$$= \bar{q}_{[a,b]}(t|x_0,t_0) \left(1 - \bar{q}_{[a,b]}(t|x_0,t_0)\right) \tag{6.48}$$

Inserting (6.48) back into (6.44) one obtains

$$\Delta\bar{p}_{[a,b]}(t|x_0,t_0) = \sqrt{\frac{\bar{q}_{[a,b]}(t|x_0,t_0) \left(1 - \bar{q}_{[a,b]}(t|x_0,t_0)\right)}{M\ |a-b|^2}} \tag{6.49}$$

Implementing (6.49) in (6.42) and (6.43) and solving for M we derive

$$M = \bar{q}_{[a,b]}(t|x_0,t_0) \left(1 - \bar{q}_{[a,b]}(t|x_0,t_0)\right) \left(\frac{|\Omega|}{|a-b|^2\ |p(\Omega)|} \right)^2 \, . \tag{6.50}$$

One can use equation (6.50) to estimate the number of particles needed in a Brownian dynamics simulation when creating probability distributions via a bin count. In Figure 6.1 we had to consider the parameters $|\Omega| = 6$, $\Delta x = 0.3$, $|p(\Omega)| = 0.4$ and $\bar{q}_{[a,b]} = \Delta x\, \bar{p}_{[a,b]} \approx 0.04$. With these numbers equation (6.50) renders $M = 1067$ which is roughly the number of trajectories used in our example. Unfortunately many interesting simulations require much larger M and thus tremendous computational resources.

6.5 Reflective Boundary Conditions

So far in this chapter we have considered solely Brownian dynamics with boundaries at $x \to \pm\infty$. We now seek to account for the existence of refelctive boundaries at finite positions in the diffusion domain. For the purspose of a numerical Brownian dynamics description we divide

again teh evolution of teh probability function into many small time intervals, assuming that the corresponding Δx and Δt values are small such that conditions (6.6) and(6.7) are satisfied. Furthermore we now assume, that the average spatial increment Δx of a simulated trajectory is minute compared to the spatial geometry of the diffusion domain and its reflective boundary. In this case a stochastic trajectory will most likely encounter not more than a single boundary segment in each time interval. It will be permissible, therefore, to consider only one boundary segment at a time. Furthermore, we approximate these boundary segments by planes, which is appropriate as long as the curvature of the boundary is small in comparison to Δx.
Under all these conditions one can again provide an approximate analytical solution $p(\boldsymbol{x}, t_0 + \Delta t|\boldsymbol{x}_0, t_0)$ for a single simulation step. One can then use this solution to construct an adequate numerical simulation over longer time intervals.
As stated, we assume refelective boundaries governed by the boundary condition (4.24)

$$\hat{\boldsymbol{a}}(\boldsymbol{x}) \cdot \boldsymbol{\mathcal{J}}\ p(\boldsymbol{x}, t|\boldsymbol{x}_0, t_0) \quad = \quad 0\ , \quad \boldsymbol{x}\ \text{on}\ \partial\Omega_i\ , \tag{6.51}$$

where $\hat{\boldsymbol{a}}(\boldsymbol{x})$ denotes the normalized surface vector of the planar boundary segment. One derives an analytical solution for $p(\boldsymbol{x}, t|\boldsymbol{x}_0, t_0)$ in the present case by emulating a mirror image of a diffusing particle behind the planar boundary segment so that the flow of particles and the flow of mirror particles through the boundary segment cancel each other to satisfy (6.51). This is established through the probability

$$\begin{aligned} p(\boldsymbol{x}, t_0 + \Delta t|\boldsymbol{x}_0, t_0) \quad = \quad & \left(\frac{1}{\sqrt{2\pi\ [\mathbf{B}\cdot\mathbf{B}^{\mathbf{T}}]\,(\boldsymbol{x}_0, t_0)\,\Delta t}} \right)^n \exp\left[-\frac{(\boldsymbol{x} - \boldsymbol{x}_0 - \boldsymbol{A}(\boldsymbol{x}_0, t_0)\,\Delta t)^2}{2\ [\mathbf{B}\cdot\mathbf{B}^{\mathbf{T}}]\,(\boldsymbol{x}_0, t_0)\,\Delta t} \right] \\ & + \left(\frac{1}{\sqrt{2\pi\ [\mathbf{B}\cdot\mathbf{B}^{\mathbf{T}}]\,(\boldsymbol{x}_0, t_0)\,\Delta t}} \right)^n \exp\left[-\frac{(\boldsymbol{x} - \mathcal{R}_{\partial\Omega}[\boldsymbol{x}_0 + \boldsymbol{A}(\boldsymbol{x}_0, t_0)\,\Delta t])^2}{2\ [\mathbf{B}\cdot\mathbf{B}^{\mathbf{T}}]\,(\boldsymbol{x}_0, t_0)\,\Delta t} \right] . \end{aligned} \tag{6.52}$$

$\mathcal{R}_{\partial\Omega}$ denotes the operation of reflection at the boundary plane $\partial\Omega$. To perform the reflection operation $\mathcal{R}_{\partial\Omega}$ explicitly one splits every position vector $\boldsymbol{x}$ into two components, one parallel $x_\parallel$ and one orthogonal $x_\perp$ to the planar boundary $\partial\Omega$. If $\boldsymbol{b} \in \partial\Omega$ one can express the operation of reflection as

$$x_\parallel \quad \overset{\mathcal{R}_{\partial\Omega}}{\longmapsto} \quad x_\parallel \tag{6.53}$$

$$x_\perp \quad \overset{\mathcal{R}_{\partial\Omega}}{\longmapsto} \quad 2\,b_\perp \ - \ x_\perp\ . \tag{6.54}$$

With this notation one can write boundary condition (6.51) as

$$\left(\frac{\left[\mathbf{B}\cdot\mathbf{B}^{\mathbf{T}}\right](\boldsymbol{x}, t)}{2}\,\partial_{x_\perp} \ - \ \boldsymbol{A}(\boldsymbol{x}, t) \right)\ p(\boldsymbol{x}, t_0 + \Delta t|\boldsymbol{x}_0, t_0) \Bigg|_{\boldsymbol{x}\in\partial\Omega} \quad = \quad 0\ . \tag{6.55}$$

and one can easily verify that equation (6.52)

$$\begin{aligned} p(\boldsymbol{x}, t|\boldsymbol{x}_0, t_0) \quad = \quad & \left(\frac{1}{\sqrt{2\pi\ [\mathbf{B}\cdot\mathbf{B}^{\mathbf{T}}]\,(\boldsymbol{x}_0, t_0)\,\Delta t}} \right)^n \left(\exp\left[-\frac{(\boldsymbol{x} - \boldsymbol{x}_0)^2}{4\,D\,\Delta t} \right] \right. \\ & \left. + \ \exp\left[-\frac{\left(\boldsymbol{x}_\parallel - \boldsymbol{x}_{0\parallel}\right)^2 + \left(\boldsymbol{x}_\perp + \boldsymbol{x}_{0\perp} - 2\,b_\perp\right)^2}{2\ [\mathbf{B}\cdot\mathbf{B}^{\mathbf{T}}]\,(\boldsymbol{x}_0, t_0)\,\Delta t} \right] \right) \end{aligned} \tag{6.56}$$

is a solution of the diffusion equation which obeys (6.55).

The function on the r.h.s. of (6.56) describes a Wiener process which is modified, in that the endpoint of the Gaussian distribution which reaches across the boundary $\partial\Omega$ is 'reflected' back into the domain Ω. The modified Wiener process is therefore defined as follows

$$\boldsymbol{x}(t+\Delta t) \;=\; \begin{cases} \boldsymbol{x}(t) \;+\; \sqrt{2\,D\,\Delta t}\;\boldsymbol{r}(t) & \text{, if } \boldsymbol{x}(t) \;+\; \sqrt{2\,D\,\Delta t}\;\boldsymbol{r}(t) \;\in\; \Omega \\ \mathcal{R}_{\partial\Omega}\left[\boldsymbol{x}(t) \;+\; \sqrt{2\,D\,\Delta t}\;\boldsymbol{r}(t)\right] & \text{, if } \boldsymbol{x}(t) \;+\; \sqrt{2\,D\,\Delta t}\;\boldsymbol{r}(t) \;\notin\; \Omega \end{cases} \tag{6.57}$$

Whenever $\boldsymbol{x}(t+\Delta t)$ reaches outside the domain Ω the actual value of the coordinate $\boldsymbol{x}(t+\Delta t)$ is readjusted according to the rules set by Eq. (6.57).

Chapter 7

The Brownian Dynamics Method Applied

Contents

7.1 Diffusion in a Linear Potential 103
7.2 Diffusion in a Harmonic Potential 104
7.3 Harmonic Potential with a Reactive Center 107
7.4 Free Diffusion in a Finite Domain 107
7.5 Hysteresis in a Harmonic Potential 108
7.6 Hysteresis in a Bistable Potential 112

In this chapter we apply the Brownian dynamics method to motion in prototypical force fields. We consider first the cases of constant and linear forrce fields for which analytical solutions exist which allow one to test the accuracy of teh Brownian dynamics method. We consider, in particular, statistical uncertainties inherent in Brownian dynamic simulations. Estimates for the statistical error of observables are derived. We consider also examples with reflecting and absorbing boundaries. Finally we describe hysteresis in a harmonic and in a bistable potential. The later case is not amenable to analytical solutions and, thus, the aproach described constitutes a truely useful application of the Brownian dynamics method.

7.1 Diffusion in a Linear Potential

As a first example we consider the simple scenario of diffusion in a linear potential $V(x) = a\,x$ with boundaries at infinity. In this model the diffusive particles are subject to a constant force $F(x) = -a$. One obatins with (4.17) the Fokker Planck respectively Smoluchowski diffusion equation

$$\partial_t\, p(x,t|x_0,t_0) \;\; = \;\; D\,\left(\partial_x^2 \; + \beta\; a\,\partial_x\right)\; p(x,t|x_0,t_0)\;. \tag{7.1}$$

By comparing (7.1) with (6.1) one identifies the drift coefficient $A(x,t) = -D\,\beta\,a$ and the noise coupling coefficient $B(x,t) = \sqrt{2\,D}$. Both coefficients are constant and again as in the free diffusion model assumptions (6.6) and (6.7) are met for any step size $\Delta t = t_{i+1} - t_i$.
The random numbers needed in the Brownian dynamics procedure (6.20) are generated according to (6.18) with the mapping

$$\tilde{r}_k(x,t) \;\; = \;\; \sqrt{2\,D\,\Delta t}\; r_k \;\; - \;\; D\,\beta\,a\,\Delta t \;\; + \;\; x \tag{7.2}$$

The random number probability density distribution is

$$p(\tilde{r}(x,t)) \;=\; \frac{1}{\sqrt{4\pi\, D\, \Delta t}}\; \exp\left(-\frac{\left(\tilde{r}(x,t) + D\,\beta\, a\, \Delta t - x\right)^2}{4\, D\, \Delta t}\right)\;. \tag{7.3}$$

The end points $x(t)$ of a sample path in (6.20) result from chains of random numbers given in (7.2). This chain of random numbers $\tilde{r}_k(x_k, t_k)$ can be rewritten as a sum

$$\begin{aligned} x(t = t_N) &= \tilde{r}_N(\ldots \tilde{r}_1(\tilde{r}_0(x_0, t_0), t_1) \ldots, t_N) \\ &= -D\,\beta\, a\; (t - t_0) \;+\; \sqrt{2\, D\, \Delta t}\; \sum_{k=1}^{N}\; r_k\;. \end{aligned} \tag{7.4}$$

The only difference between equation (7.4) and equation (6.29) of the free diffusion model is the term $-D\,\beta\, a\, t$. One apparently generates the same sample trajectories as in the case of free diffusion except for a displacement. The endpoints $x(t)$ of a trajectory are shifted by $-D\,\beta\, a\, t$.
Due to this similarity we are not going to repeat a bin count as done in section 6.4. Instead we investigate a new observable. We consider a measurement Q_{x_m} that renders the probability of finding a particle beyond a certain point x_m on the x-axes. The sensitifity function of such an observable is $q_{x_m}(x) = \Theta(x - x_m)$. We will now estimate the number M of sample trajectories needed to determine

$$q_{x_m}(t|x_0, t_0) \;=\; \int_\Omega dx\; \Theta(x - x_m)\; p(x, t|x_0, t_0)\;. \tag{7.5}$$

The value range of observable Q_{x_m} is the interval $[0, 1]$. Hence, the variance $\left\langle\!\left\langle q^2_{x_m}(t|x_0, t_0)\right\rangle\!\right\rangle$ can not exceed 1. One can therefore assume, according to (6.37), that the standard deviation of $\bar{q}_{x_m}(t|x_0, t_0)$ is less than $1/\sqrt{M}$. To push the statistical error of $\bar{q}_{x_m}(t|x_0, t_0)$ below a margin of $\pm 2\%$ one has to simulate and sample ($M = 2500$) trajectries. The result of such a simulation is displayed in Figure 7.1. The plot describes the time dependent increase in probability for finding a particle beyond x_m. The units are chosen so that $D = 1$. The force constant a is set equal $-2/\beta$ and x_m is located at $+1$.

7.2 Diffusion in a Harmonic Potential

We alter the previous Brownian dynamics simulation by implementing a harmonic potential $V(x) = \frac{k}{2}\, x^2$. This harmonic potential introduces a decisive difference to the previously used examples. It requires the introduction of intermediate times t_i in the simulation of stochastic trajectories (6.20) since in this case $A(x, t)$ is not constant. The more intermediate times t_i and the smaller the time steps Δt the better the simluation. We will examine the impact of the time step length Δt on the numerical results and derive guidelines for the right choice of Δt.
Inserting the harmonic force $F(x) = -k\, x$ into the Smoluchowski diffusion equation (4.17) one derives

$$\partial_t\, p(x, t|x_0, t_0) \;=\; D\; \left(\partial_x^2 \;+\; \beta\, k\, \partial_x\; x\right)\; p(x, t|x_0, t_0)\;. \tag{7.6}$$

Again comparing (7.1) with (6.1) one identifies the drift coefficient $A(x, t) = -\,D\,\beta\, k\, x$ and the noise coupling coefficient $B(x, t) = \sqrt{2\, D}$. Note that $A(x, t)$ is no longer a spatial constant. One, thus, has to pay special attention to assumptions (6.6) and (6.7).

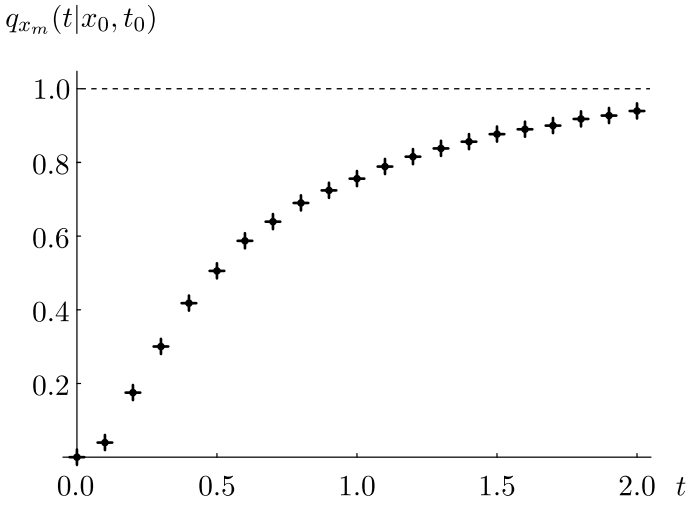

Figure 7.1: The plot displays the readings of observable Q_{x_m} according to (7.5) in a Brownian dynamics calulation (7.4) with 2500 trajectories.

Each trajectory step in a Brownian Dynamics simulation is exact for a linear potential $V(x) = a\,x$. During a time step Δt a simulated particle diffuses as if the potential $V(x)$ extrapolates linearly. One has to asure that this linear extrapolation is a good approximation for the average spatial simulation step Δx given in (6.5). The difference $\Delta V(x)$ between the exact and the linearly extrapolated potential is given by

$$\Delta V(x+\Delta x) \;=\; V(x+\Delta x) \;-\; \big[V(x) \,+\, V'(x)\,\Delta x\big]\;. \tag{7.7}$$

Conversely one can determine the approximation radius $\pm\Delta x$ for a given potential deviation $\Delta V(x+\Delta x)$.

$$\Delta x \;=\; \frac{V(x+\Delta x) \;-\; V(x) \;-\; \Delta V(x+\Delta x)}{V'(x)}\;. \tag{7.8}$$

Hence, if we intend to keep the approximation of $V(x)$ within the interval $[V(x)-\Delta V(x), V(x)+\Delta V(x)]$ we can derive the necessary upper limit for the spatial step size Δx according to (7.8) and determine the corresponding upper limit for the temporal step size

$$\Delta t \;=\; \frac{B(x,t) \;+\; 2\,|A(x,t)|\,\Delta x \;-\; \sqrt{B^2(x,t) \;+\; 4\,|A(x,t)|\,B(x,t)\,\Delta x}}{2\,A^2(x,t)}\;. \tag{7.9}$$

We consider a specific example. We set D and β equal 1, thus measuring the potential in units of the average thermal energy $1/\beta$ and relating the units of space and time via D. Within these units we simulate trajectories with the initial position $x_0 = 1$ in a potential with $k = 6$. If one intends to keep the approximation of $V(x)$ within 10% of the thermal energy $1/\beta$, one can determine the upper limit for the spatial step size with (7.8) and derive $\Delta x \approx 0.2$.
To obtain the corresponding upper limit for the temporal step size Δt with (7.9), one has to estimate maximum values for $|A(x,t)|$ and $B(x,t)$. Assuming an effective diffusion domain of $[-2,2]$ one finds $|A(x,t)| \le 2\,k\,D\,\beta$ and $B(x,t) = \sqrt{2D}$ and consequently $\Delta t \approx 0.01$. Simulation results with these parameters are shown in Figures 7.2. The three bar charts display the time evolution of a bin count at times $t = 0.02, 0.08$, and 0.40 The bin count, based on 1000 trajectories, exhibits 20 bins with a width of 0.2 each. The bin count approximates probability distribution $p(x,t|1,0)$ with the analytical solution (3.142), which is superimposed for comparison.

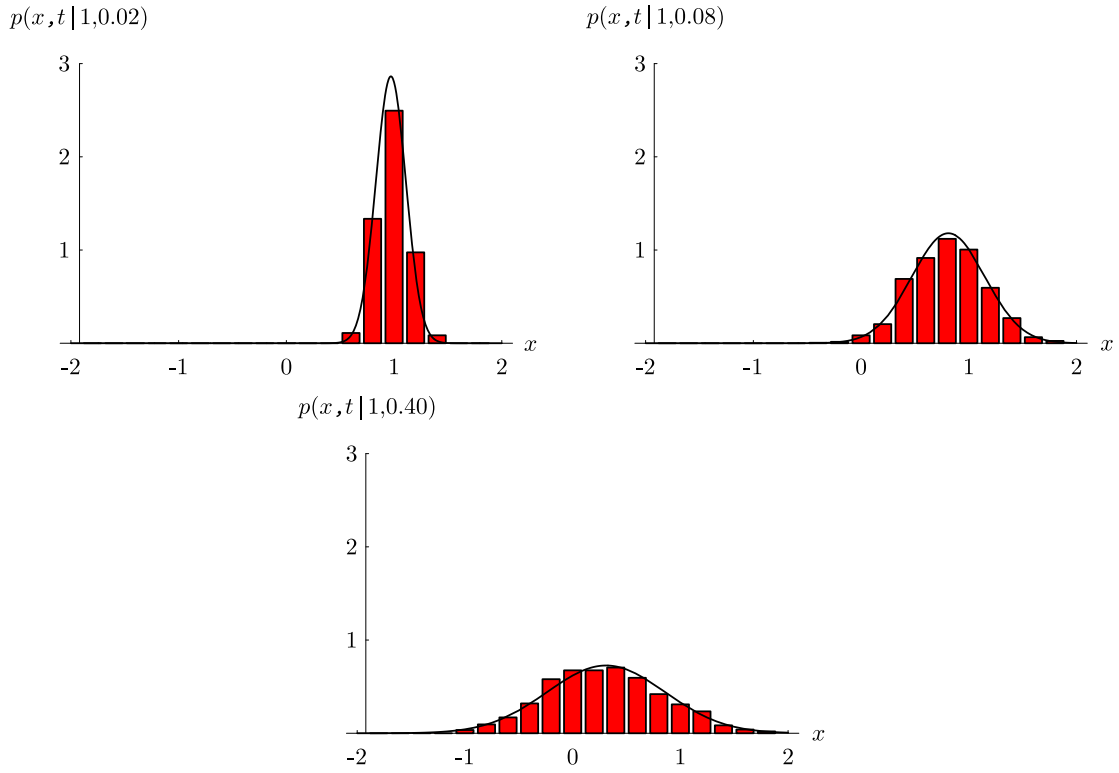

Figure 7.2: The bar charts depict bin counts of a Brownian Dynamics simulation with the harmonic potential $V(x) = \frac{k}{2}\,x^2$. The three figures display the probability distribution $p(x,t|1,0)$ of the simulated trajetories at times $t = 0.02, 0.08$, and 0.40. The analytical results (3.142) are superimposed for comparison.

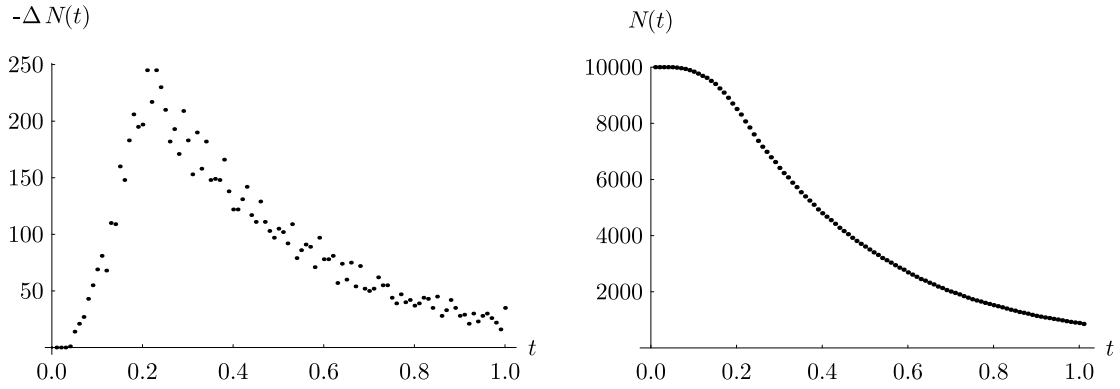

Figure 7.3: The number of particles absorbed by boundary $x = 0$ per time step Δt (left). The number $N(t)$ of particles remaining in the system (right).

7.3 Harmonic Potential with a Reactive Center

We refine the harmonic potential example by introducing a reactive center at $x = 0$. We thereby address the issue of reactive boundary conditions in Brownian dynamics.
In a one-dimensional model a reactive site within a potential is equivalent to a reactive boundary. The particles cannot cross the reactive site without being absorbed or reflected. Thus, for particles, never being able to reach the other side, a reactive site appears as wall or boundary.
There is a simple and intuative way to incorporate reactive boundaries in a Brownian dynamic calculation. At each time step Δt one determines the number of trajectories crossing the reactive wall. One then removes a certain percentage of trajectories from the ensemble depending on reaction rate of the boundary. The remaining percentage is reflected according to the rules developed in section 6.5.
To verify the drain of particles one can calculate the particle number $N(t)$ and determine the time-dependence by counting the remaining particles at different times t.
We quickly consider a particular example. Assume a sink at the center of the harmonic potential. This sink is in effect a completely absorbing wall. Thus, in a simulation we simply remove all particles crossing this boundary. With the same paramters as in the calcualtion of the previous section we compute the particle flux $-\Delta N(t)/\Delta t$ absorbed by the sink at $x = 0$ and we determine the number $N(t)$ of particles still present in the system. The results of a simulation with $N(0) = 10000$ initial particles are plotted with respect to time t in Figure 7.3.

7.4 Free Diffusion in a Finite Domain

We revisit the model of free diffusion in a finite domain $\Omega = [0, a]$ with reflective boundaries. We solved this model analytically in section 3.5.
Under the condition $D\,dt \ll a^2$ one can use the solutions (6.56) for the conditional probability distribution $p(x, t_0 + dt|x_0, t_0)$ at the left and right boundary. These solutions in the half-spaces $[0, \infty[$ and $]-\infty, a]$ can be patched together at $x = a/2$.

$$p(x, t_0 + dt|x_0, t_0) \approx \frac{1}{\sqrt{4\pi\, D\, dt}} \begin{cases} \exp\left[-\frac{(x-x_0)^2}{4\,D\,dt}\right] + \exp\left[-\frac{(x+x_0)^2}{4\,D\,dt}\right] & x \le \frac{a}{2} \\ \exp\left[-\frac{(x-x_0-a)^2}{4\,D\,dt}\right] + \exp\left[-\frac{(x+x_0-a)^2}{4\,D\,dt}\right] & x > \frac{a}{2} \end{cases} . \quad (7.10)$$

A distribution of this form results from a Wiener process which is modified, in that the pathes with $x < 0$ and $x > a$ are 'reflected' back into the domain $\Omega = [0, a]$. Hence, the Wiener process in the interval $[0, a]$ is defined as in (6.57) and one can write

$$x(t+\Delta t) \;=\; \begin{cases} x(t) \;+\; \sqrt{2\,D\,\Delta t}\; r(t) & \text{, if } x(t)+\sqrt{2\,D\,\Delta t}\; r(t) \;\in\; \Omega \\ -x(t) \;-\; \sqrt{2\,D\,\Delta t}\; r(t) & \text{, if } x(t)+\sqrt{2\,D\,\Delta t}\; r(t) \;<\; 0 \\ 2\,a \;-\; x(t) \;-\; \sqrt{2\,D\,\Delta t}\; r(t) & \text{, if } x(t)+\sqrt{2\,D\,\Delta t}\; r(t) \;>\; a \end{cases} . \qquad (7.11)$$

The function $p(x, t|x_0, t_0)$ is the probability density of the stochastic trajectories $x(t)$, subject to the initial condition $x(t_0) = x_0$. By simulating on a computer a fairly large number of random walks according to (7.11), one can determine, within the limits of statistical and numerical errors, the probability distribution $p(x, t|x_0, t_0)$. For this purpose one performs a bin count as in section 6.4.
To perform a simulation of an ensemble of stochastic trajectories $x(t)$ we choose specific parameters. We set the unit of length to be a and the unit of time to be D/a^2; hence $a = 1$ and $D = 1$. We choose an arbitrary value for x_0 and deterimine a Δt satisfying $D\,\Delta t \ll a^2$.
According to the scheme described above, one starts the actual Brownian Dynamics simulation of $(N = 1000)$ trajectories at $x_0 = a/4$. To approximate $p(x, t|x_0, t_0)$ one can perform a bin count after $(t - t_0)/\Delta t$ number of time steps Δt by counting and recording the numbers of trajectories in each bin. One can then estimate $p(x, t|x_0, t_0)$ in each bin with equation (6.40). Results of an actual simulation at $t = 0.01$, 0.03, 0.1, 0.3 are presented in Figures 7.4. The bin counts exhibit 20 bins with a base length of $0.05a$ each. The analytical solution (3.142) for $p(x, t|x_0, 0)$ are superimposed for comparison.

7.5 Hysteresis in a Harmonic Potential

For an application of the Brownian Dynamics method we consider now particles moving in a one-dimensional potential $V(x)$ subject to a driving force $F_d(t)$ with a sinusodial time-dependence $\sin(\omega\, t)$. This example allows us to investigate the properties of hysteresis, which arises, for example, when proteins are subjected to time-dpendent electric fields.
Before providing numerical answers we have to identify the right questions and the important aspects of hysteresis. Since we consider systems governed by the Smoluchowski equation (4.17) which arises from a Langevin equation with frictional forces the external forces lead to teh dissipation of energy leading to a net energy consumption of the system in the case of periodic forces. The energy dE delivered through an external force field to a single particle during an infinitesimal time step dt is given by the scalar product of the particles path segment dx and the excerted force F_d. The average energy $\langle dE \rangle$ delivered to the particle ensembel is therefore

$$\begin{aligned} \langle dE \rangle &= \Big\langle F_d \cdot dx \Big\rangle \\ &= F_d \cdot \langle dx \rangle \;. \end{aligned} \qquad (7.12)$$

The system compensates the energy uptake with an energy loss via the stochastic interactions. The aim of our numerical calculations will be to quantify and to investigate this energy consumption.
We will base the subsequent calculations on the following premises. For times t much larger then the relaxation times of the system the particle ensemble will assume a so-called *asymptotic state* in which it will exhibit the same temporal cyclic variation as the driving force $F_d(t)$. In such an

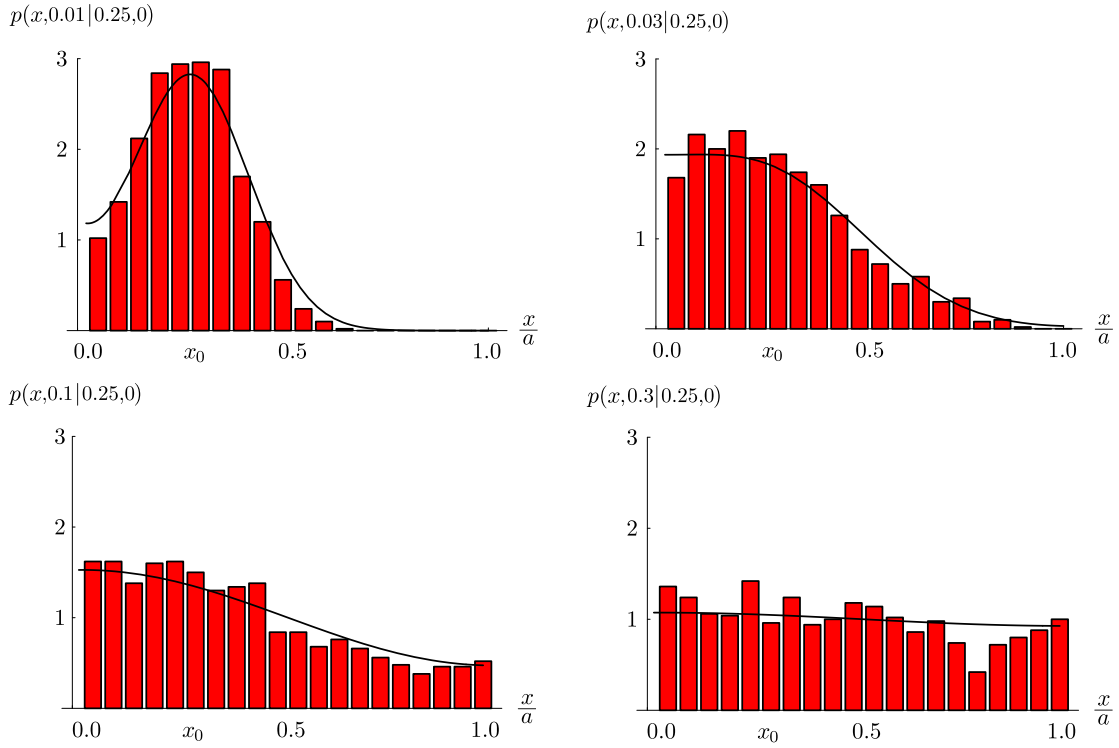

Figure 7.4: These bin counts present a Brownian dynamics simulation with 1000 particles diffusing according to (7.11) in an interval $[0, a]$ with reflective boundaries.

asymptotic state the energy gain and loss will compensate each other over each cycle and one can, thus, measure the energy dissipation by observing the energy uptake dE.
For a periodic asymptotic state it is sufficient to consider the time evolution during just one variation cylce. We therefore focus on the energy uptake E_c during a single cycle. We parameterize the cylce by $\phi = \omega\, t$ ranging from 0 to 2π and obtain with (7.12) for the energy E_c provided by linear force field $F_d(t) = a\, \sin(\omega\, t)$

$$\langle E_c \rangle \;=\; a \oint d \sin(\phi)\; \langle x(\phi) \rangle \;. \tag{7.13}$$

It is customary to express equation (7.13) in terms of hysteresis $\mathcal{H}$ which is defined as

$$\mathcal{H} \;=\; -\oint d \sin(\phi)\; x(\phi) \;. \tag{7.14}$$

To proceed we have to choose a particular potential $V(x)$. In this section we first consider the simplest form of a potential, the harmonic potential in conjunction with a linear force field

$$V(x) \;=\; \frac{k}{2} x^2 \;+\; F_d(t)\, x \;, \tag{7.15}$$

$$F_d(t) \;=\; a\, \sin(\omega t) \;. \tag{7.16}$$

The Fokker-Planck equation determining the time evolution of the probability distribution $p(x, t|x_0, t_0)$ can then be written as

$$\partial_t\, p(x, t|x_0, t_0) \;=\; D\, \left(\partial_x^2 \;+\; \beta\, (a\, \sin(\omega\, t) \;+\; k\, \partial_x\, x)\right)\; p(x, t|x_0, t_0) \;. \tag{7.17}$$

To determine the hysteresis $\mathcal{H}$ as in (7.17) it is beneficial to substitute t by ϕ. We derive

$$\partial_\phi\, p(x,\phi|x_0,\phi_0) \;=\; \frac{D}{\omega}\left(\partial_x^2 \;+\; \beta\;(a\,\sin(\phi)\;+\;k\,\partial_x\;x)\right)\;p(x,\phi|x_0,\phi_0)\;. \tag{7.18}$$

Before solving equation (7.18) numerically we will quickly outline the analytical solution. For the solution of the Smoluchowski equation for the harmonic potential without a driving force one assumes the functional form

$$p(x,\phi) \;=\; \sqrt{\frac{\beta\,k}{2\pi}}\;\exp\left[-\frac{1}{2}\,\beta\,k\,\left(x-\langle x(\phi)\rangle\right)^2\right]\;. \tag{7.19}$$

Substituting (7.19) into (7.18) one obtains an ordinary differential equation for the mean path $\langle x(\phi)\rangle$.

$$\partial_\phi\;\langle x(\phi)\rangle \;=\; -\beta\,\frac{D}{\omega}\;\left(k\;\langle x(\phi)\rangle\;+\;a\,\sin\phi\right)\;. \tag{7.20}$$

The solution of (7.20) is

$$\langle x(\phi)\rangle \;=\; -\frac{a\,\beta D/\omega}{k^2\,(\beta D/\omega)^2\;+\;1}\;e^{-k\,(\beta D/\omega)\,\phi}\;+\;a\;\frac{(\beta D/\omega)\;\cos\phi\;-\;k\,(\beta D/\omega)^2\,\sin\phi}{k^2\,(\beta D/\omega)^2\;+\;1}\;. \tag{7.21}$$

In determining the hysteresis we consider only the asymptotic state with $\omega t = \phi \to \infty$. In this limit the first term of (7.21) vanishes and one obtains

$$\langle x(\phi)\rangle \;=\; a\;\frac{(\beta D/\omega)\;\cos\phi\;-\;k\,(\beta D/\omega)^2\,\sin\phi}{k^2\,(\beta D/\omega)^2\;+\;1}\;. \tag{7.22}$$

This expression is all one needs to evaluate (7.14) and to determine the mean hysteresis

$$\begin{aligned}
\langle\mathcal{H}\rangle \;&=\; -\oint d\sin\phi\;\;\langle x(\phi)\rangle \\
&=\; \oint d\sin\phi\;a\;\frac{(\beta D/\omega)\;\cos\phi\;-\;k\,(\beta D/\omega)^2\,\sin\phi}{k^2\,(\beta D/\omega)^2\;+\;1} \\
&=\; \frac{\pi\,a\,\beta D/\omega}{k^2\,(\beta D/\omega)^2\;+\;1}\;.
\end{aligned} \tag{7.23}$$

Having derived an analytical description we turn now to the application of the Brownian Dynamics method which should reproduce the result (7.23). We determine first the mean path $\langle x(\phi)\rangle$ numerically and evaluate then (7.14). For the evaluation of the mean path we proceed in the same way as in the previous sections. Comparing (7.18) and (6.1) we identify the drift coefficient $A(x,\phi) = -D\,\beta(k\,x + a\,\sin(\phi))/\omega$ and the noise coupling coefficient $B(x,\phi) = \sqrt{2\,D/\omega}$ The resulting equation for the numerical integration of a particle trajectory is

$$x(\phi+\Delta\phi) \;=\; x(\phi)\;-\;\frac{D\,\beta}{\omega}\;\left(a\,\sin(\phi)\;+\;k\,x\right)\;\Delta\phi\;+\;\sqrt{\frac{2\,D}{\omega}\;\Delta\phi}\;. \tag{7.24}$$

We start the Brownian Dynamics simulation with reasonably small phase steps $\Delta\phi$ and hope that assumptions (6.6) and (6.7) are met. We, thus, obtain rough results which we will refine later. The results of a simulation with 10000 particles initially distributed according to the thermal equilibrium distribution of the harmonic potential (see (4.86) or (7.19))

$$p_0(x,\phi=0) \;=\; \sqrt{\frac{k\,\beta}{2\pi}}\;\exp\left(-\frac{k\,\beta\,x^2}{2}\right) \tag{7.25}$$

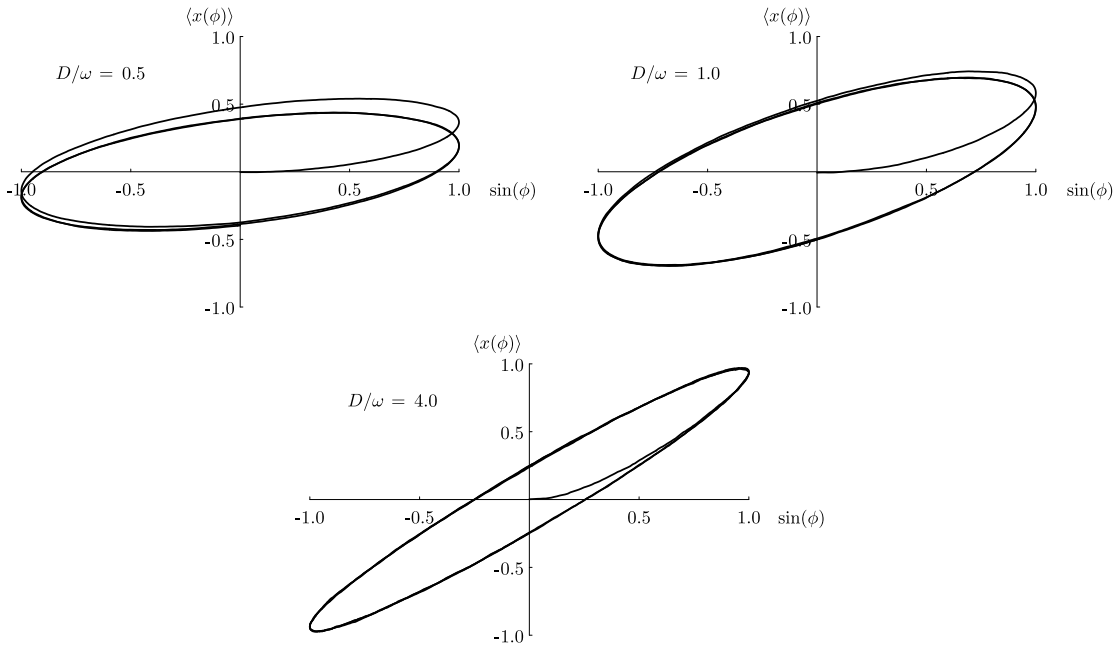

Figure 7.5: Mean trajectories of 10000 Brownian particles simulated according to (7.24) with $\Delta\phi = 0.002\pi$, $a = 6/\beta$, $k = 6/\beta$ and $2\pi\, D/\omega = 0.5, 1.0, 4.0$ (arbitrary spatial unit).

are presented in Figure 7.5. These graphs display the mean trajectory $\langle x(\phi)\rangle$ with respect to $\sin(\phi)$ varying ϕ from 0 to 6π for different values of D/ω.
The mean trajectory $\langle x(\phi)\rangle$ starts at the origin of the coordinate system of $\langle x\rangle$ and ϕ and converges after the first one or two cylces on an ellipse. The area encircled by the ellipse is the integral (7.14) and, hence represents the hysteresis $\mathcal{H}$ and energy consumption E_c. One can determine the encircled area numerically by applying standard numerical integration methods like the *closed Newton-Cotes Formula* [37] to (7.14).
Before we proceed we have to investigate the influence of the step size $\Delta\phi$ on our numerical results. For this purpose we calculate $\langle\mathcal{H}\rangle$ for different step size values $\Delta\phi$. The results of $\langle\mathcal{H}\rangle$ with $2\pi\, D/\omega = 1$ for $\Delta\phi = 0.002\pi, 0.004\pi, 0.01\pi, 0.02\pi$, and 0.04π are shown in Figure 7.6. One can observe a linear dependence between $\langle\mathcal{H}\rangle$ and $\Delta\phi$. Hence, we can extrapolate to the limit $\Delta\phi \to 0$ by performing a lineare regression. The value of the linear regression at $\Delta\phi = 0$ can be taken as the *true* value of $\mathcal{H}$, which in this case lies within one per mille of the analytical result $3/((3/\pi)^2+1) = 1.56913$ of (7.23).
One can observe in equation (7.23) and in Figures 7.7 that the mean hysteresis $\langle\mathcal{H}\rangle$ varies with respect to D/ω. To elucidate this D/ω-dependence we determine $\langle\mathcal{H}\rangle$ for a sequence of different D/ω values ranging from 0.1 to 5.0. The resulting plot is displayed in Figure 7.7. The numerical and analytical solutions are identical with respect to the resolution in Figure 7.7. The hysteresis $\langle\mathcal{H}\rangle$ reaches a maximum for

$$\frac{D}{\omega} \;=\; \frac{1}{\beta\, k}\;. \tag{7.26}$$

For higher $\frac{D}{\omega}$-values or equivalently for lower frequencies ω the ensemble has sufficient time to follow the external force $F_d(t)$ almost instantly. The time delayed response is shorter and the hysteresis $\langle\mathcal{H}\rangle$ is reduced. For lower $\frac{D}{\omega}$-values or equivalently for higher frequencies ω the system cannot

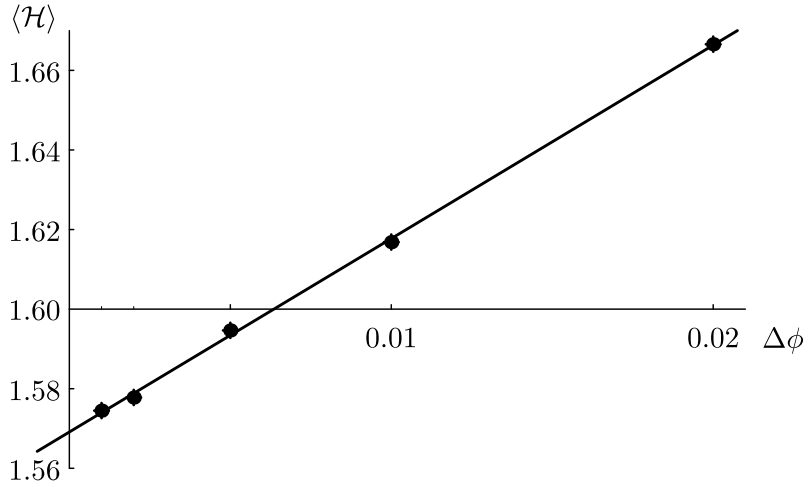

Figure 7.6: $\Delta\phi$-dependence of the numerical results of the mean hysteresis $\langle\mathcal{H}\rangle$ based on 100000 trajectories. The points mark the results for $\Delta\phi = 0.002\pi, 0.004\pi, 0.01\pi, 0.02\pi$, and 0.04π. The other parameters are $a = 6/\beta$, $k = 6/\beta$ and $2\pi\, D/\omega = 1$ with respect to some arbitrary spatial unit. The line represents the linear regression of the five numerical results. It allows one to extrapolate the linear dependence between $\langle\mathcal{H}\rangle$ and $\Delta\phi$, and to approximate the hysteresis for the limit $\Delta\phi \to 0$.

follow the driving force in time. The effect of the driving force thereby cancels itself with each cylce and the amplitude of the mean path $\langle x(\phi)\rangle$ approaches zero. The smaller the amplited the smaller the hysteresis $\langle\mathcal{H}\rangle$.

7.6 Hysteresis in a Bistable Potential

In our last application of the Brownian Dynamics method we leave the domain of analytically solvable problems and simulate a system accessible only by numerical means. We consider again a system exhibiting hysteresis, but in cases that the observed hysteresis cannot be reconciled with a harmonic potential model. For example, the deflection $x(t)$ of a system does usually not increase linearly with the strenght of the external force field $F_d(t)$. A non-linear saturation effect can only be modeled with a potential of fourth or higher order in x. Furthmore one usually observes a remaining deflection in x after switching off the external force $F_d(t)$. The remaining magnitization of an iron core in a transformer is a typical example. Such an effect cannot be modeled with a one-minimum-potential. With no external force the systems would always decay to the thermal equilibrium of its one minimum without sustaining a remaining deflection in time. Hence, to create a model with a remaining deflection one needs to consider a bistable potential.
To investigate the above effects we employ the bistable potential

$$\begin{aligned} V(x) &= \frac{k_1}{4}\,x^4 \;-\; \frac{k_2}{2}\,x^2 \;+\; x\;F_d(t)\;, \\ F_d(t) &= a\,\sin(\omega t)\;. \end{aligned} \tag{7.27}$$

For the following simulations we assume the parameters $k_1 = 1/\beta$, $k_2 = 1/\beta$ and $a = 1/2\beta$. We, thus, obtain with (7.27) a potential $V(x)$ that has two minima, one at $x = -1$ and one at $x = 1$ with a barrier of height $1/(4\beta)$ inbetween. During a cycle of the external driving force $F_d(t)$ the minima of the potential vary. The locations of the minima are depicted in Figure 7.8.

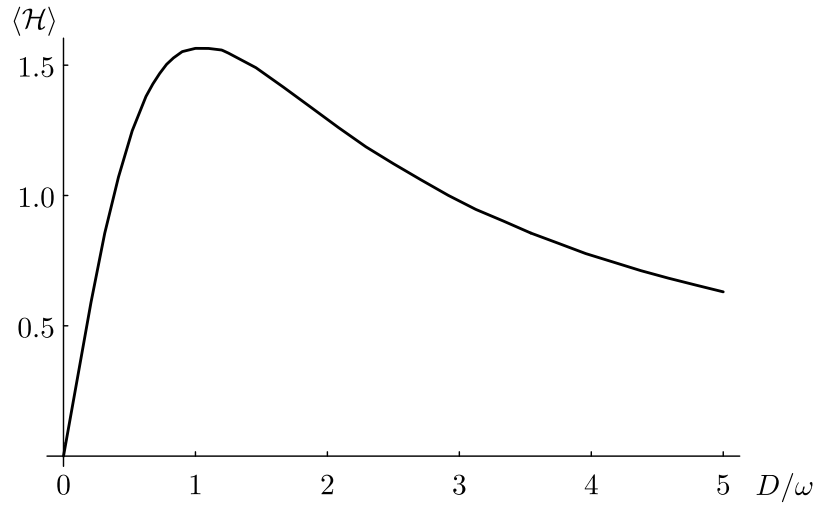

Figure 7.7: D/ω-dependence of the mean hysteresis $\langle \mathcal{H} \rangle$. The calculations were performed with 10000 trajectories simulated according to (7.24). The mean hystersis $\langle \mathcal{H} \rangle$ was determine after 3 cycles, with $a = 6/\beta$, $k = 6/\beta$ and $2\pi\, D/\omega = 0.0, 0.1, \ldots, 5.0$ with respect to some arbitrary spatial unit. The limit for $\Delta\phi \to 0$ was performed as outlined in Figure 7.6

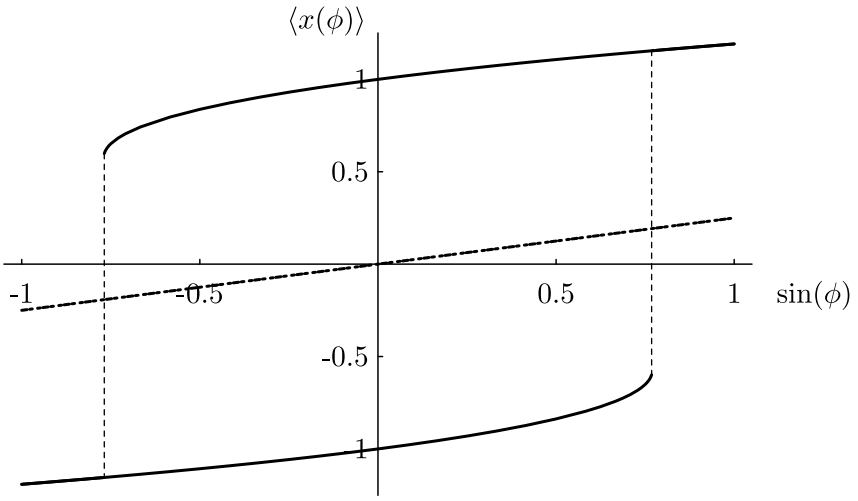

Figure 7.8: The two minima of the potential (7.27) for $k_1 = 1/\beta$, $k_2 = 1/\beta$ and $a = 1/2\beta$ are inidicated by the solid lines. If one takes the harmonic approximations of both minima and neglects any transfer rate between them, one obtains the dashed curve through the origin of the coordinate system describing the average of the two potential minima.

The trace of the potential minima, as shown in Figure 7.8, indicate the special features of this hysteresis model. For example, for a phase $\phi = \pi/2$ of the external driving force $F_d(t)$ and for a very low temperature $1/\beta$, i.e., negligible thermal diffusion, a particle in the potential $V(x)$ would be located only in the minimum on the right side. This location corresponds to the right corner of the top solid line in Figure 7.8. Increasing the phase ϕ adiabatically the particle would follow the local minimum. The particle, hence, follows the top solid line from right to left. For ϕ defined through $\sin\phi = -4/\sqrt{27}$ the right minimum disappears. The particle would consequently fall into the minimum on the left depicted by the bottom solid line in Figure 7.8. The particle would follow then the left minimum until this minimum disappears for a ϕ defined through $\sin\phi = 4/\sqrt{27}$ returning to the initial position in the right minimum.
In a simulation with a thermal energy $1/\beta$ comparable to the characteristics of the potential $V(x)$ and with a frequency ω of the driving force $F_d(t)$ comparable to the rate of diffusional crossing of the barrier between minima, the above behaviour gets siginificantly modified. Due to diffusion we will observe a transition from one local minimum to the other previous to the moment that ϕ assumes teh value specified through $\sin\phi = \pm 4/\sqrt{27}$.
In the case of high frequencies ω the transition from left to right and back might not occur all together. For high frequencies particles would not have the time to propagate from one minimum to the other and the hysteresis model would seem to consist of simply two disjunct harmonic potentials at $x = \pm 1$. In this case the adiabatic approximation of a particle ensemble is given by the dashed trajectory in Figure 7.8.
We will now verify these predictions numerically. The equation analog to (7.24), needed for the calculation of Brownian Dynamic trajectories, is

$$x(\phi + \Delta\phi) \;=\; x(\phi) \;-\; \frac{D\,\beta}{\omega}\left(a\,\sin(\phi) \;+\; k_1\,x^3 - k_2\,x\right)\,\Delta\phi \;+\; \sqrt{\frac{2\,D}{\omega}\,\Delta\phi}\,. \tag{7.28}$$

A simulation of 10000 trajectories in the potential given by (7.27) with different driving frequencies ω and for a temperature of $\beta = 0.1$ is displayed in Figure 7.12.
In the first case, $D/\omega = 1$, the frequency ω is so high that a substantial transition of the ensemble from the left to the right minimum and vice versa does not occur. This can be discerned in Figure 7.10 which displays the distribution of the ensemble for different phases ϕ in the first column. Consequently the first case resembles the hysteresis of a harmonic potential.
In the second case, $D/\omega = 10$, the frequency ω is low enough for an almost complete shift of the ensemble from the right to teh left side and back. The hysteresis, therefore, resembles the adiabatic hysteresis in Figure 7.8. A complete cycle of this case is shown in Figure 7.11.
In the third case, $D/\omega = 100$, the frequency ω is so low that the system has sufficient time for a diffusive transition across the barrier from one local minimum to the other, thus, reducing the hysteresis substantially.
With the trajectories $\langle x(t)\rangle$ as displayed in Figure 7.12 and equation (7.14) one can finally determine the mean hysteresis $\langle\mathcal{H}\rangle$. In contrast to the hysteresis in a harmonic potential, the bistable potential exhibits a strong temperature dependence. To illustrate this one can determine the hysteresis $\mathcal{H}$ for different frequencies ω and temperatures $1/\beta$. The results are displayed in Figure 7.12. One notes that higher temperatures reduce the hysteresis $\langle\mathcal{H}\rangle$. At high temperatures the hysteresis enforcing barrier inbetween the two local minima becomes less significant since the crossing rate over the barrier increases relative to the driving frequency of teh external force.

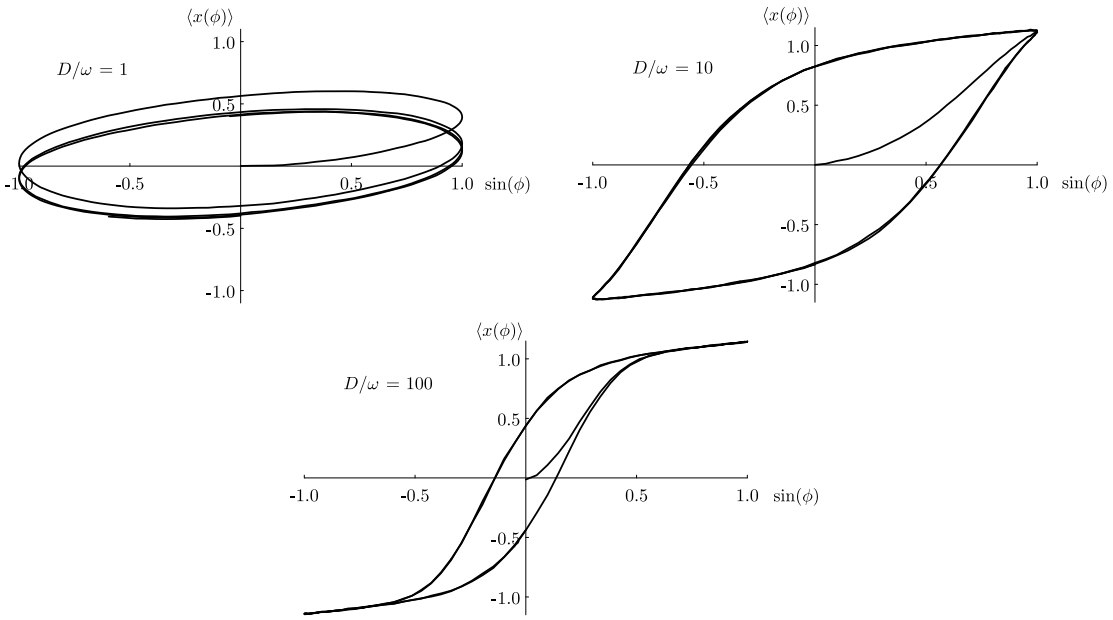

Figure 7.9: Mean trajectory of 10000 particles simulated according to (7.28) with $\Delta\phi = 0.002\,\pi$, $a = 1/2\beta$, $k_1 = 1/\beta$, $k_2 = 1/\beta$and $D/\omega = 1, 10, 100$ (arbitrary spatial unit).

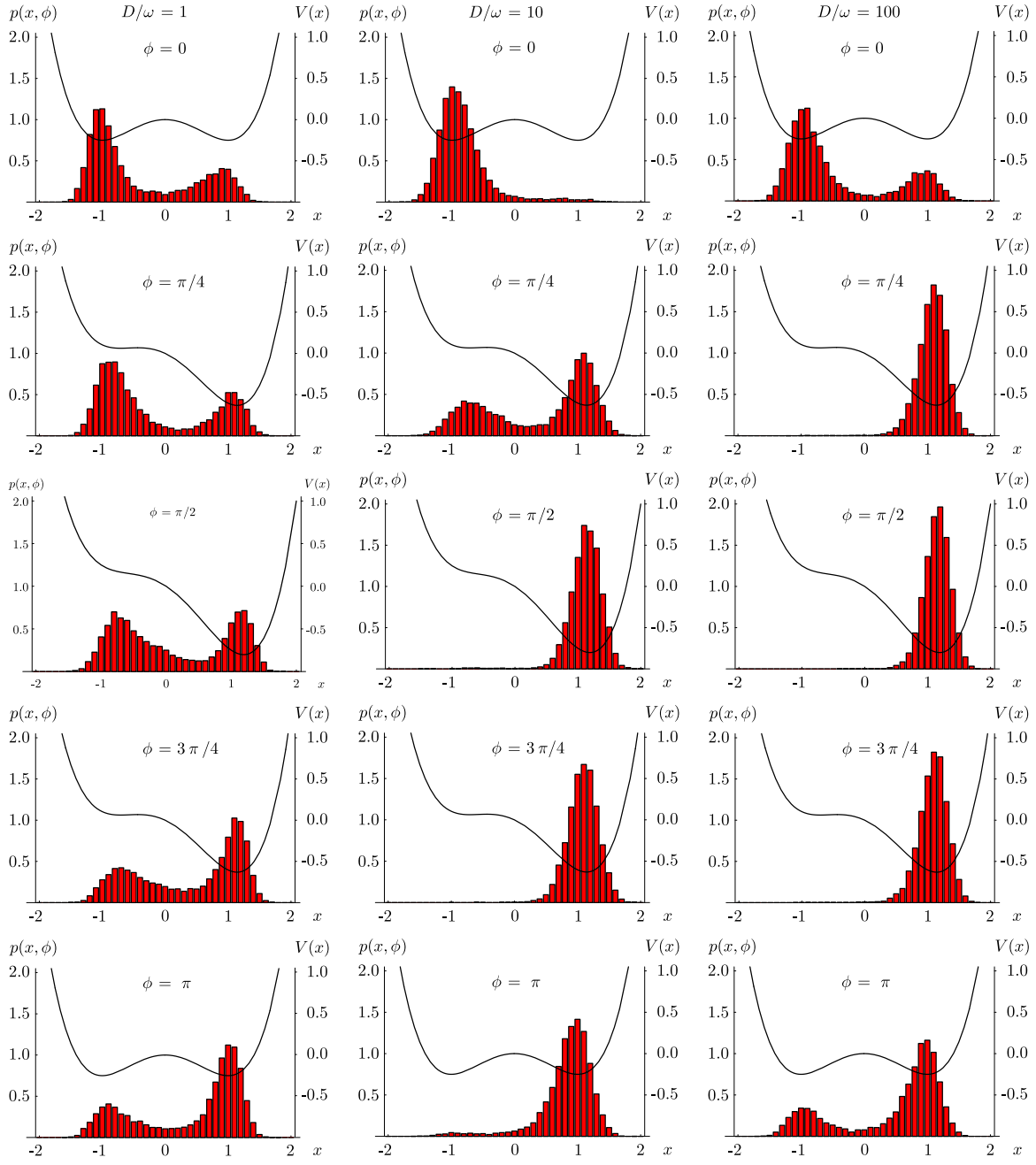

Figure 7.10: These plots display bin counts that approximate the probability distributions of an ensembel in a double potential (7.27) for different driving frequencies ω. The first column depicts the distribution for $\frac{D}{\omega} = 1$ at $\phi = 0, \pi/4, \pi/2, 3\pi/4$, and π. The second column displays the same dynamics for $\frac{D}{\omega} = 10$ and the third column represents the time evolution for $\frac{D}{\omega} = 100$.

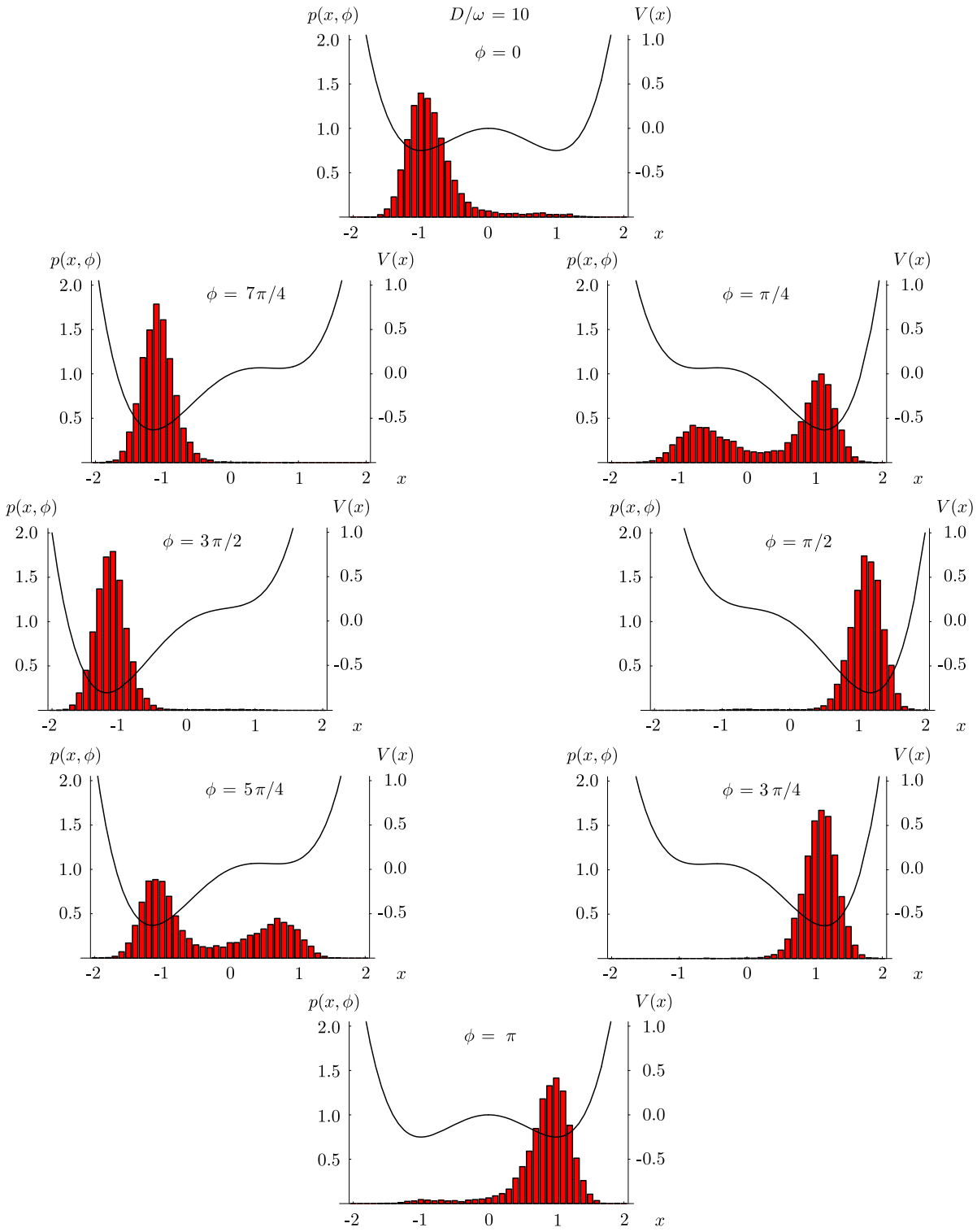

Figure 7.11: These plots display bin counts that approximate the probability distributions of an ensembel in a double potential (7.27) for $D/\omega = 1$. The cirlce of plots follows the cylce for ϕ from 0 to 2π.

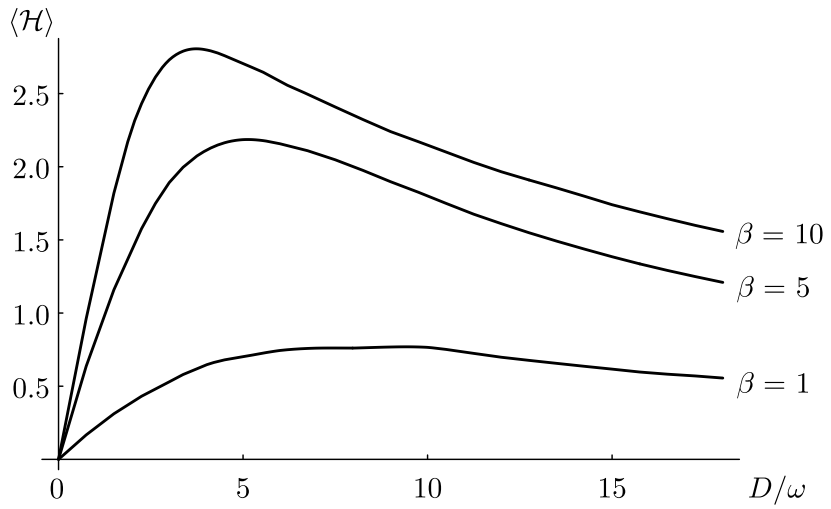

Figure 7.12: D/ω-dependence of the mean hysteresis $\langle \mathcal{H} \rangle$ at different temperatures $1/\beta = 0.1, 0.2,$ and 1.

Chapter 8

Noise-Induced Limit Cycles

Contents

8.1 The Bonhoeffer–van der Pol Equations 119
8.2 Analysis 121
8.2.1 Derivation of Canonical Model 121
8.2.2 Linear Analysis of Canonical Model 122
8.2.3 Hopf Bifurcation Analysis 124
8.2.4 Systems of Coupled Bonhoeffer–van der Pol Neurons 126
8.3 Alternative Neuron Models 128
8.3.1 Standard Oscillators 128
8.3.2 Active Rotators 129
8.3.3 Integrate-and-Fire Neurons 129
8.3.4 Conclusions 130

In this chapter, we discuss models describing the nonlinear dynamics of neuronal systems. First, we analyze the Bonhoeffer–van der Pol (BvP) equations, a system of coupled nonlinear differential equations which describe the dynamics of a single neuron cell in terms of physiological quantities. Then we discuss other neuronal models which are based on a description of the state of a neuron in terms of a "phase" variable and investigate, in how far they are useful in approximating the dynamics of the BvP system.

8.1 The Bonhoeffer–van der Pol Equations

The initial breakthrough in describing the dynamics of neuronal systems in terms of physiological quantities like ionic concentrations and trans-membrane voltage was achieved by Hodgkin and Huxley[16]. They provided a quantitative description of the changes of concentrations and trans-membrane voltages as a function of the current state for the case of the squid axon.
Fitzhugh [**?**] wanted to study more qualitative features of the neuronal dynamics and, therefore, proposed a simplified model for neuronal dynamics which he called the Bonhoeffer–van der Pol equations. He derived them in actually two different ways: first, by reducing the number of coupled nonlinear differential equations of the Hodgkin–Huxley model from four to two by what essentially amounts to a projection onto the center manifold of the system. Although the BvP system is quite

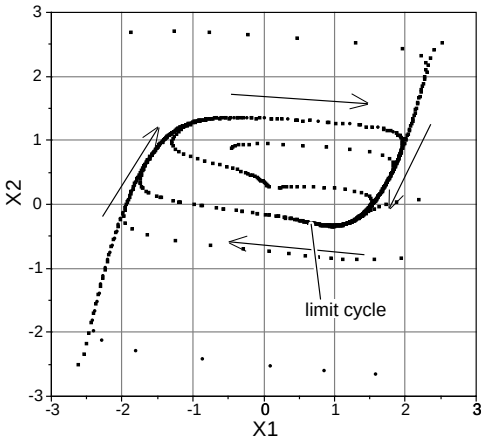

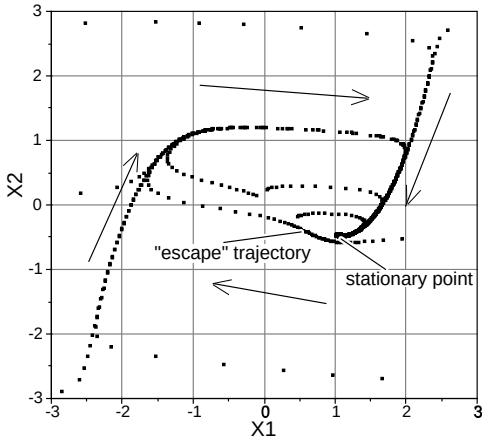

Figure 8.1: (left side) Some typical phase space trajectories for $z = -0.4$: All trajectories eventually lead into a stable limit cycle. Represented is a stroboscopic view of trajectories for 9 different initial states.

Figure 8.2: (right side) Some typical phase space trajectories for $z = 0$: All trajectories lead to the stable stationary point at about (1.1,-0.5). Note that a trajectory which passes very near by the stationary point may lead the phase point back to its stationary state only after a long path through phase space.

abstract, its variables can still be interpreted in terms of physiological variables, since they have been derived from the physiological variables of the Hodgkin–Huxley model.
The other way in which Fitzhugh derived these equations was by introducing one additional parameter in the original van der Pol oscillator equations which modifies them so that they have the qualitative features which Bonhoeffer had postulated, namely showing excitable and oscillatory behavior. The original van der Pol oscillator equations are symmetric in the sense that they are unaffected by a reversal of the sign of the variables. Since this symmetry is broken in the BvP model by the introduction of an additional parameter, the BvP model represents an important generalization of the van der Pol oscillator for the description of oscillatory phenomena.
By studying the BvP system, we can thus learn something about physiological neuronal systems, and study a very important modification and generalization of the van der Pol oscillator dynamics.
In the Bonhoeffer–van der Pol model, the dynamics of a single neuron is described by a system of two coupled differential equations

$$\begin{aligned} \dot{x}_1 &= F_1(x_1, x_2) &&= c \cdot (x_1 - x_1^3/3 + x_2 + z) \\ \dot{x}_2 &= F_2(x_1, x_2) &&= -\tfrac{1}{c} \cdot (x_1 + b x_2 - a). \end{aligned} \tag{8.1}$$

According to Fitzhugh's derivation of the BvP equations [**?**], x_1 represents the negative transmembrane voltage and x_2 is closely related to the potassium conductivity. The dynamical character of the solutions of this system of equations is determined by the parameter z, which represents the excitation of a neuron. In the absence of noise, z determines whether the system is an oscillator which periodically changes its voltage, or an excitable element which rests at a fixed voltage. The phase portrait for these two dynamical modes is shown in Figs. 8.1 and 8.2.
For an analysis of the BvP system, we first want to determine the stationary point of the system. It can be obtained as the intersection point of the nullclines. The nullclines for the dynamical system

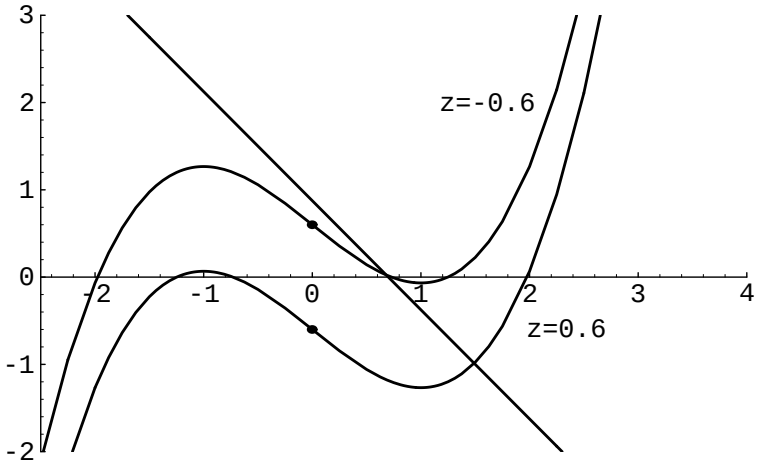

Figure 8.3: Nullclines for the BvP model for two different z–values. The parameter z indicates the x_2 coordinate of the symmetry point (indicated by a dot) of the first nullcline. The second nullcline, a straight line, is not affected by changes of z.

Eq. (8.1) are obtained by setting $\dot{x}_1 = 0$ and $\dot{x}_2 = 0$ as

$$x_2 = \frac{1}{3}x_1^3 - x_1 - z \tag{8.2}$$

$$x_2 = \frac{1}{b}(a - x_1) \tag{8.3}$$

They are shown for two different z values in Figure 8.3. Previous analysis of the BvP model [51] has shown that the system undergoes a Hopf bifurcation around $z = -0.34$, when the linear nullcline intersects the other nullcline near its local minimum.
When we analyze the properties of the BvP system, we have to concern ourselves mainly with the vicinity of the stationary point. The location of the stationary point depends in a quite complicated way on the parameter z. Before we analyze the dynamics of the BvP system in more depth, we therefore first want to derive a simpler *canonical* description of the BvP system in which the nullclines always intersect in the origin.

8.2 Analysis

8.2.1 Derivation of Canonical Model

We can obtain a canonical version of the BvP system by linearly transforming the coordinates (x_1, x_2) into new coordinates (y_1, y_2). In the new coordinates, both nullclines will have to go through the point $(0, 0)$. Using

$$\begin{aligned} x_1 &= y_1 + p \\ x_2 &= y_2 - z + (\tfrac{1}{3}p^3 - p), \end{aligned} \tag{8.4}$$

we transform Eq. (8.2) and (8.3) into

$$y_2 = \frac{1}{3}(y_1 + p)^3 - (y_1 + p) - \frac{1}{3}p^3 + p \tag{8.5}$$

and

$$y_2 = -y_1/b - p/b + a/b + z - (\frac{1}{3}p^3 - p) \tag{8.6}$$

which will both go through the point $(0, 0)$ if

$$z = (\frac{1}{3}p^3 - p) + (p - a)/b \tag{8.7}$$

As long as $0 < b < 1$, this equation indicates a unique relation between z and p. If $b > 1$, the nullclines can intersect three times. Accordingly, there will then also be three different values of p which fulfill Eq. (8.7). Which of the three p's one should choose will then depend on which of the three stationary points one wants to shift into the origin. In this paper, we will however mainly be concerned with the case $0 < b < 1$ and only occasionally comment on $b > 1$. As long as $b > 0$, there will always be either a stable stationary point or a stable limit cycle to which all solutions converge. The case $b < 0$ is physiologically uninteresting since it yields solutions with only diverging trajectories, which is not the concern of this thesis.
We thus obtain the canonical BvP model

$$\begin{array}{rcl} \dot{y}_1 & = & c(y_1 + y_2 - \frac{1}{3}(y_1 + p)^3 + \frac{1}{3}p^3) \\ \dot{y}_2 & = & -\frac{1}{c} \cdot (y_1 + by_2). \end{array} \tag{8.8}$$

This set of equation is connected with the original BvP Eqs. (8.1) via Eq. (8.4) and Eq. (8.7). In the original BvP model (8.1) the parameter z indicated the x_2 coordinate of the symmetry point of the first nullcline; in the canonical BvP model (8.8), the parameter p indicates the y_1 distance between the symmetry point of the first nullcline and the stationary point. In the original BvP model (8.1), the properties of the stationary point depend *indirectly* on the parameter z, while in the canonical BvP model (8.8), properties of the stationary point depend directly on the parameter p. Using the canonical BvP model will thus often lead to a simpler analytical description of the properties of the system.
The nullclines for the canonical BvP model are shown in Figure 8.4. Figure 8.5 shows how the parameters p and z in the two versions of the BvP model are related.
Due to the symmetry of the nullclines, the qualitative behavior of the solutions of Eq. (8.8) does not depend on the sign of p. We will therefore restrict our analysis to the case $p > 0$. The first nullcline can be divided into three parts with positive slope on the left branch, negative slope an the central branch and positive slope again on the right branch. For $p > 1$ the nullclines intersect on the right branch, otherwise on the central branch.

8.2.2 Linear Analysis of Canonical Model

First we want to determine the properties of the stationary point, i.e., whether the stationary point is a stable or unstable node or focus, or whether it is a saddle point. These questions can be answered by considering the Jacobian at the stationary point $(0, 0)$

$$J = \begin{pmatrix} \partial F_1/\partial y_1 & \partial F_1/\partial y_2 \\ \partial F_2/\partial y_1 & \partial F_2/\partial y_2 \end{pmatrix} = \begin{pmatrix} c(1 - p^2) & c \\ -\frac{1}{c} & -\frac{b}{c} \end{pmatrix}. \tag{8.9}$$

The qualitative properties of the fix point actually depend only on two combinations of the elements of this matrix, namely on the trace β and the determinant γ:

$$\beta = J_{11} + J_{22} = c(1 - p^2) - \frac{b}{c} \tag{8.10}$$

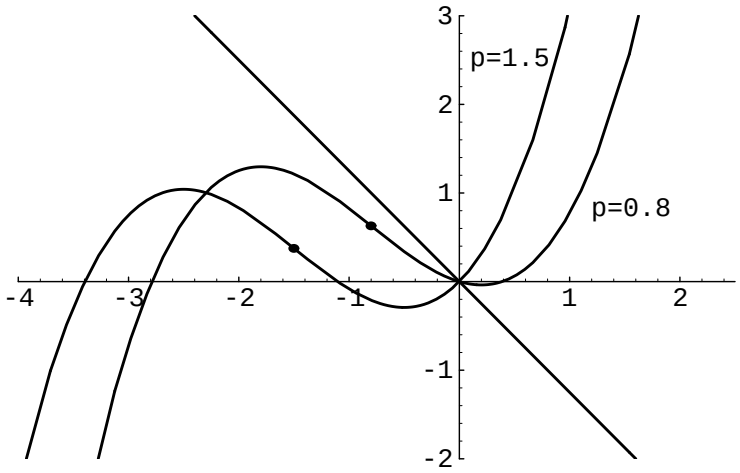

Figure 8.4: Nullclines for the canonical BvP model for two different p–values. The parameter p indicates the x_1 coordinate of the symmetry point (indicated by a dot) of the first nullcline. The second nullcline, a straight line, is not affected by changes of p.

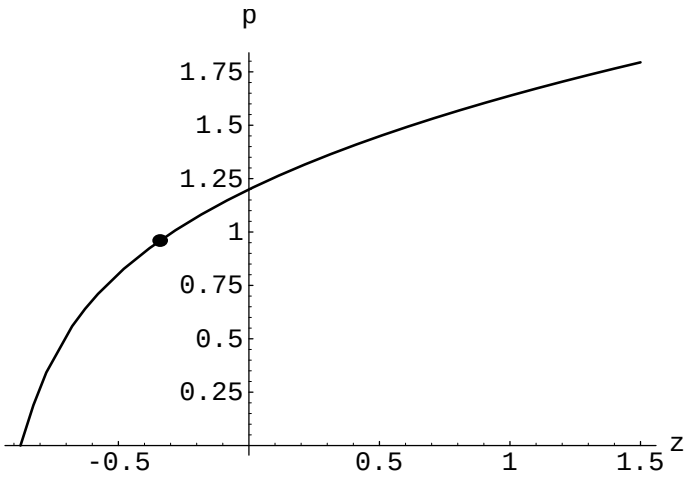

Figure 8.5: This plot shows what parameter p in the canonical BvP model has to be chosen in order to reproduce the dynamics given by z in the original BvP model, using the standard values $a = 0.7, b = 0.8, c = 3$. The dot indicates the values $(z, p) = (-0.346478, 0.954521)$ at which a Hopf bifurcation occurs.

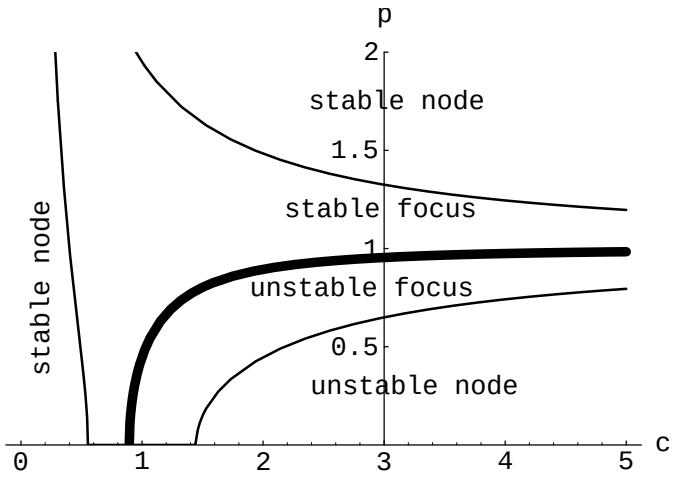

=

Figure 8.6: Diagram showing the properties of the fix point as function of p and c for $0 < b < 1$ ($b = 0.8$). The thick line indicates the values of p and c for which a Hopf bifurcation occurs.

$$\gamma = J_{11}J_{22} - J_{12}J_{21} = 1 - b(1 - p^2) \tag{8.11}$$

The eigenvalues which reveal the quality of the stationary point can be obtained from Eq. (**??**). Since $0 < b < 1$, γ will always be positive, i.e., the stationary point will be either a node or a focus. It will be a focus if $4\gamma > \beta^2$, or

$$\sqrt{1 + \frac{b}{c^2} - \frac{2}{c}} < p < \sqrt{1 + \frac{b}{c^2} + \frac{2}{c}}. \tag{8.12}$$

A focus or node will be unstable if $\beta < 0$, i.e.,

$$p < \sqrt{1 - \frac{b}{c^2}}, \tag{8.13}$$

otherwise it will be stable. Finally, we obtain a saddle point when $\gamma < 0$, i.e.,

$$p < \sqrt{1 - \frac{1}{b}}. \tag{8.14}$$

From the last formula it is clear that we can only obtain a saddle point if $b > 1$, and even then the saddle point can only be found at $|p| < 1$. Thus, if the slope of the second nullcline is so small that it intersects the first nullcline in three points, then the middle intersection point will be a saddle point. The above phase boundaries are visualized in the Figures 8.6 and 8.7, which indicate the nature of the fix point as a function of p and c for the two cases $0 < b < 1$ and $b > 1$.

8.2.3 Hopf Bifurcation Analysis

We now want to examine whether the transition is a subcritical or supercritical Hopf bifurcation. Here, we follow the recipe outlined in Segel [**?**]:

First, we start with the BvP equations for $p = \sqrt{1 - \frac{b}{c^2}}$ (the value of p at which the transition occurs). Then we transform the coordinates into a rotated system of coordinates in which the

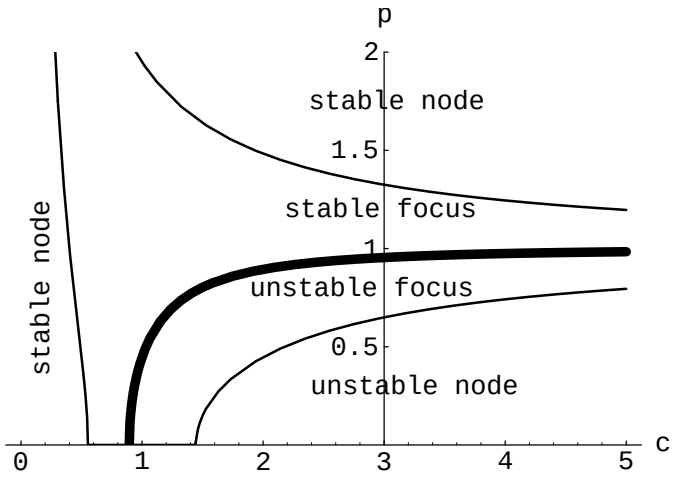

Figure 8.7: Diagram showing the properties of the fix point as function of p and c for $b > 1$ ($b = 1.2$). The thick line indicates the values of p and c for which a Hopf bifurcation occurs.

Jacobi matrix has only non-diagonal elements

$$J = \begin{pmatrix} 0 & |\omega| \\ -|\omega| & 0 \end{pmatrix} \tag{8.15}$$

which are given by its imaginary eigenvalues. Third we determine certain derivatives of the rotated BvP equations (derivatives up to third order) and combine them into an expression D. The sign of D will then tell whether we have a subcritical ($D > 0$) or supercritical ($D < 0$) Hopf bifurcation. Calculations to determine D are notoriously involved; rather than overwhelming the reader with a derivation that will be nearly impossible to check, we present in the appendix the Mathematica [58] code which can be used to derive D as a function of the parameters b and c. We obtain

$$\begin{aligned} \mathtt{D} \;=\; & -\frac{2\,c^2\,\left(b^4+b^2\,c^2+b^2\,c^4+c^6\right)}{\left(b^2-c^2\right)^4} \\ & +\frac{4\,b\,c^2\,\left(-1+c^2\right)\,\left(-b^5-b^3\,c^2+b^4\,c^2+b^2\,c^4-b^3\,c^4-b\,c^6+b^2\,c^6+c^8\right)}{\left(-b^2+c^2\right)^6} \end{aligned} \tag{8.16}$$

We now want to determine for which values of the parameters b and c we obtain a sub- or supercritical Hopf bifurcation. We obtained eight roots of the equation $D(b, c) = 0$, giving values of b which solve the equation for a given c. For $0 < c < 1$ all roots are imaginary. For $c > 1$ two of the roots are real; while the analytical expressions for these roots are very involved, they can be approximated within one percent accuracy by the functions

$$b_1(c) = \frac{1.25}{1 + 0.25c^{-3/2}}c^{4/3} \qquad c \overset{\sim}{\to} \infty \quad 1.25\,c^{4/3} \tag{8.17}$$

$$b_2(c) = \frac{1}{2}\frac{2 - 1.25c + 1.25c^2}{1 - 1.25c + 1.25c^2} \quad c \overset{\sim}{\to} \infty \quad 0.5 \tag{8.18}$$

Actually, for the range of parameters b and c where a Hopf bifurcation occurs, only the second relation needs to be considered (the first relation relates values of b and c for which no Hopf bifurcation occurs). Figure 8.8 shows the combinations of b and c for which a subcritical, supercritical,

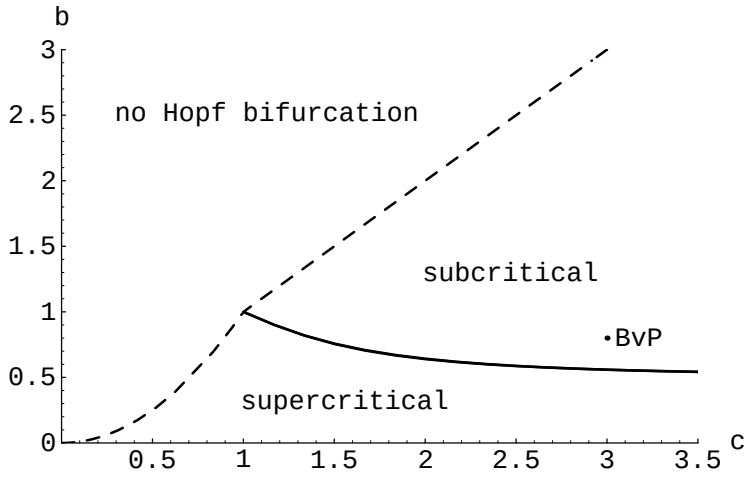

Figure 8.8: Phase diagram denoting the kind of bifurcation to expect for a certain combination of b and c. For pairs (b, c) to the left of the broken curve, no Hopf transition occurs. On the right of the broken curve, the Hopf bifurcation will subcritical if (b, c) lies above the continuous curve, otherwise supercritical. The single dot shows the values of b and c usually chosen for the BvP model.

or no Hopf bifurcation at all occurs. Specifically, it shows that a Hopf bifurcation will always be supercritical for $b < 0.5$, always subcritical for $b > 1$, and sub- or supercritical for $0.5 < b < 1$ depending on the value of c.

8.2.4 Systems of Coupled Bonhoeffer–van der Pol Neurons

We now want to consider systems of coupled BvP neurons. In this section we first investigate systems of two coupled BvP neurons in order to determine how coupling can lead to synchronization of neuronal firing.

We therefore integrated numerically the equations of motion for two interacting neurons. The interaction was assumed to be mediated by the voltage difference of the neurons, represented by the x_1-values of the model neurons. It was assumed that the interaction is only effective when one neuron is "firing" a pulse of negative x–values:

$$\begin{array}{rcl} \dot{x}_{1,i} & = & c(x_1 - x_1^3/3 + x_2 + z) \quad + \quad \sum_{j \neq i} w_{ij}(x_{1,j} - x_{1,i})\,\theta(-x_{1,j}) \\ \dot{x}_{2,i} & = & \frac{1}{c}(a - x_1 - bx_2) \end{array} \tag{8.19}$$

Initially, two neurons were placed with a phase difference of π on the limit cycle. During the numerical integration, we calculated the relative phase shift of the neurons as a function of the momentary phase difference, thus obtaining *phase response curves*. The phase shifts were averaged over one limit cycle revolution. Figure 8.9 shows the phase response curve for $z = -0.875, -0.4, \text{and} -0.36$.

As z is shifted further in the direction of the critical value $z_{cr} = -0.34$, the height of the phase response curves changes considerably, which leads to an increase of the synchronization speed. It is important to note that the phase response curves are approximately sinusoidal.

In Figure 8.10, we plotted the time needed to shift the two neurons from a phase difference of $0.45 * 2\pi$ to a phase difference of $0.01 * 2\pi$. We see that the same interaction strength leads to different synchronization speeds as the parameter z is varied. Actually, the synchronization speed, defined as the inverse of the synchronization time, diverges at $z = z_{cr}$.

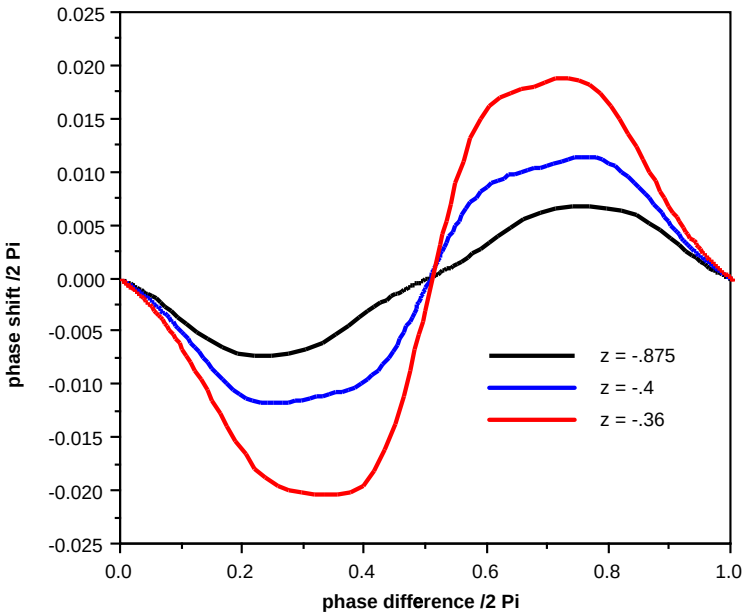

Figure 8.9: Phase response curves of a system of two coupled BvP oscillators (see Eq. 8.1) with different values of the input parameter z. The horizontal axis denotes the phase difference between the two oscillators and the vertical axis displays the amount by which these phase differences have changed due to the interaction during one limit cycle revolution. $w_{ij} = 0.005$.

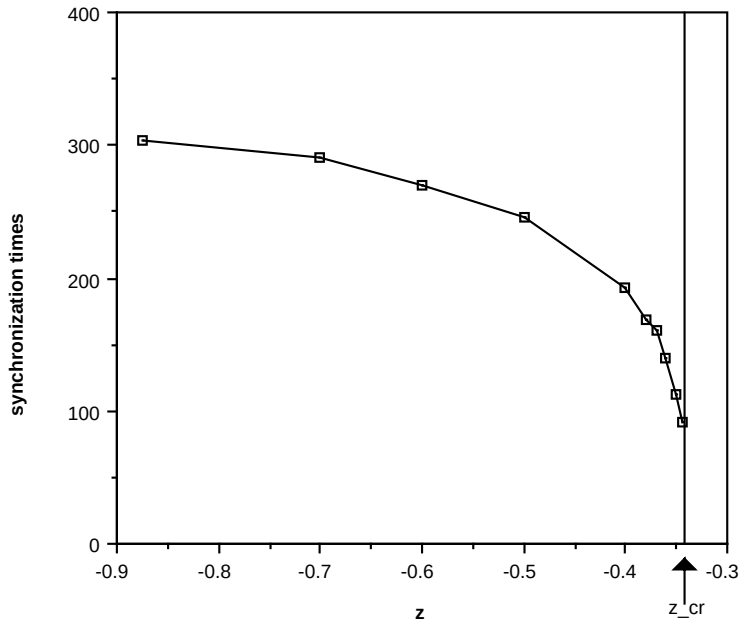

Figure 8.10: Time required for synchronization of two coupled BvP neurons (see Eq. 8.19) as a function of the input parameter z.

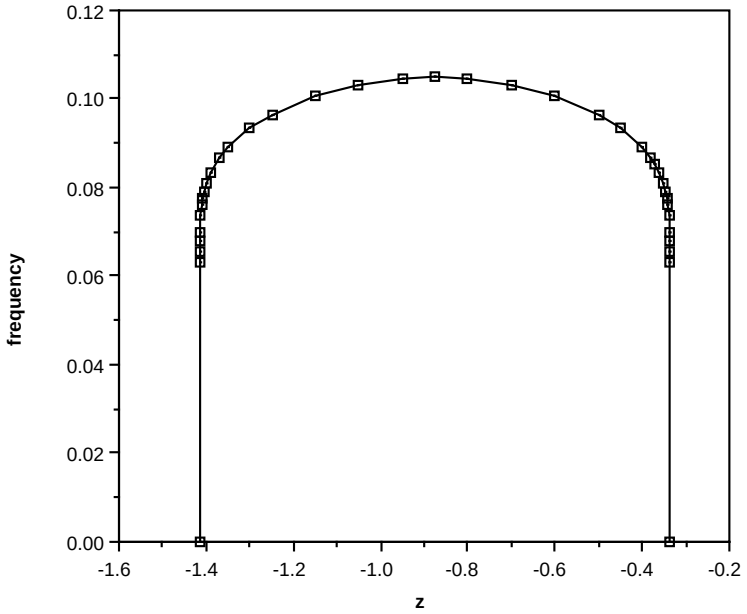

Figure 8.11: Oscillation frequency ω of a BvP oscillator as a function of the parameter z.

Variations of the parameter z actually also change the oscillation frequency of the BvP oscillator, as shown in Figure 8.11. The oscillation frequency drops discontinuously to zero at $z = z_{cr}$.

8.3 Alternative Neuron Models

We have so far discussed the nonlinear dynamics of BvP neurons. We next want to discuss possibilities of describing the essential dynamical features by a simpler model.

8.3.1 Standard Oscillators

If the parameter z or p is chosen such that the BvP neuron behaves as a limit cycle oscillator, we can parametrize the position of the system along the limit cycle by a phase variable ϕ and describe the dynamical system by a standard oscillator [**?**]

$$\dot{\phi} = \omega. \tag{8.20}$$

From the fact that the phase response curves in Figure 8.9 are approximately sinusoidal, one sees that the synchronization behaviour of BvP neurons is very similar to that of standard oscillators i and j coupled via their phase differences

$$\dot{\phi_i} = \omega + w_{ji} \sin(\phi_j - \phi_i) \tag{8.21}$$

$$\dot{\phi_j} = \omega + w_{ij} \sin(\phi_i - \phi_j). \tag{8.22}$$

This is all fine as long as one deals with oscillators with fixed z. However, if we allow the excitation z of the neurons to vary, one sees that both the effective coupling strength (Figure 8.9) and the frequency of the oscillator (Figure 8.11) vary considerably.
All these effects could in principle be incorporated into a model described by

$$\dot{\phi_i} = \omega(z) + w_{ji}(z) \sin(\phi_j - \phi_i). \tag{8.23}$$

However, such parametrization of ω and w_{ji} would result in a system that is as complex as the original BvP neuron. Furthermore, the standard oscillator model largely fails to describe the dynamical properties for $z > -0.34$, if we just set $\omega(z) = 0$ for $z > -0.34$. In this range of parameters, the neuron behaves as an excitable system, a fact which can not be described in terms of Eq. (8.23).

8.3.2 Active Rotators

If an oscillator system is subjected to small noise, the state will not be confined to the limit cycle, but will still be found in the immediate vicinity of the limit cycle. Without further perturbations the system would ultimately return to the limit cycle. Therefore, one can assign the systems in the vicinity of the limit cycle the same phase as another system *on* the limit cycle if the trajectories of the systems in the vicinity of the limit cycle converge towards the trajectory of the system on the limit cycle [**?**].
If the system does not have a limit cycle but rather a stationary point, as depicted in Figure 8.2, and if this system is subjected to noise, then the system can occasionally leave the immediate vicinity of the stationary point and follow one trajectory through the phase space that very much resembles the limit cycle in Figure 8.1. In that case, we can speak of a stochastic limit cycle [51] and parametrize it by starting from the stationary point along the most likely escape trajectory [**?**] and connecting back to the stationary point along the most likely return path.
In the case of small noise, it can thus be useful to approximate the BvP dynamics by parametrizing the phase velocity

$$\dot{\phi} = F(\phi) \tag{8.24}$$

along the real or stochastic limit cycle. As long as $F(\phi)$ is always positive, we obtain oscillator behaviour. If $F(\phi)$ is negative at some point, we obtain excitable element behaviour. If $F(\phi)$ is positive but close to zero for some phases, then the oscillator will spend a lot of time in that phase range. Small variations of the phase velocity in that region will cause a significant change in the oscillation period, while changes of $F(\phi)$ in phase regions were $F(\phi)$ is large will not change the oscillation period significantly. Like every other periodic function, $F(\phi)$ can be expanded in a Fourier series

$$F(\phi) = a_0 + \sum_n a_n \sin(n\phi - n\phi_0) + \sum_n b_n \cos(n\phi - n\phi_0). \tag{8.25}$$

In the active rotator model [**?**], the phase velocity is approximated by

$$F(\phi) = 1 - a\sin(\phi) \tag{8.26}$$

where the time scale has been chosen such that $a_0 = 1$. This simple caricature of the BvP system actually provides a good description of the BvP dynamics both for the oscillator ($|a| < 1$) and for the excitable system case ($|a| > 1$). In particular, it reproduces the frequency dependence on the excitation parameter and approximates well the properties of the excitable system.

8.3.3 Integrate-and-Fire Neurons

If we concentrate mainly on excitable neurons, there is yet another way to parameterize the BvP dynamics, namely in terms of so-called integrate-and-fire neurons [**?**]. There, the phase dynamics near the stationary point ϕ_s is described by

$$F(\phi) = -k(\phi - \phi_s). \tag{8.27}$$

When the phase reaches a certain threshold value $\phi_t > \phi_s$, a firing event is recorded and the phase is reset to zero, sometimes with a time lag corresponding to the refractory time of the neuron, i.e., the time needed by the neuron to return along the limit cycle back to the stationary point.
This integrate and fire neuron is obtained from the active rotator model by setting

$$\phi_s = \arcsin\left(\frac{1}{a}\right) \tag{8.28}$$

and

$$k = a\,\cos(\phi_s) = a\sqrt{1-\left(\frac{1}{a}\right)^2} = \sqrt{a^2-1}. \tag{8.29}$$

These formulas indicate how the parameters k and ϕ_s have to be adjusted to reflect changes in the parameter a of the active rotator model. However, this parametrization is only possible for $a > 1$ and fails for $a < 1$ where the system behaves as a limit cycle oscillator.

8.3.4 Conclusions

While oscillator models and integrate-and-fire models both describe some aspect of the BvP dynamics fairly well, namely, the oscillator and excitable systems mode, respectively, the active rotator model allows a unified description of both modes without added complexity. If we want to study only the properties of limit cycle oscillators, or only the properties of excitable neurons, then the oscillator or integrate and fire description may be appropriate. However, if we want to investigate transitions between these two dynamical modes, it becomes imperative to use a description which describes both modes. In chapter **??**, we will discuss on the example of the stochastic BvP system why the stochastic active rotator is an appropriate parametrization of the stochastic dynamics of the neuron along its real or stochastic limit cycle.

Chapter 9

Adjoint Smoluchowski Equation

Contents

9.1 The Adjoint Smoluchowski Equation 131
9.2 Correlation Functions 135

9.1 The Adjoint Smoluchowski Equation

The *adjoint* or *backward Smoluchowski equation* governs the $\boldsymbol{r}_0$-dependence of the solution $p(\boldsymbol{r}, t|\boldsymbol{r}_0, t_0)$ of the Smoluchowski equation also referred to as the *forward equation*. The backward equation complements the forward equation and it often useful to determine observables connected with the solution of the Smoluchowski equation.

Forward and Backward Smoluchowski Equation

The Smoluchowski equation in a diffusion domain Ω can be written

$$\partial_t\, p(\boldsymbol{r}, t|\boldsymbol{r}_0, t_0) \;=\; \mathcal{L}(\boldsymbol{r})\; p(\boldsymbol{r}, t|\boldsymbol{r}_0, t_0) \tag{9.1}$$

where

$$\mathcal{L}(\boldsymbol{r}) \;=\; \boldsymbol{\nabla}\cdot D\left(\boldsymbol{\nabla} \;-\; \beta\, \boldsymbol{F}(\boldsymbol{r})\right) . \tag{9.2}$$

For $\boldsymbol{F}(\boldsymbol{r}) = -\boldsymbol{\nabla} U(\boldsymbol{r})$ one can express

$$\mathcal{L}(\boldsymbol{r}) \;=\; \boldsymbol{\nabla}\cdot D\; e^{-\beta U(\boldsymbol{r})}\, \boldsymbol{\nabla}\; e^{\beta U(\boldsymbol{r})} . \tag{9.3}$$

With the Smoluchowski equation (9.1) are associated three possible spatial boundary conditions for $h(\boldsymbol{r}) = p(\boldsymbol{r}, t|\boldsymbol{r}_0, t_0)$ on the surface $\partial\Omega$ of the diffusion domain Ω with local normal $\hat{\boldsymbol{a}}(\boldsymbol{r})$:

$$\text{(i)}\quad \hat{\boldsymbol{a}}(\boldsymbol{r})\cdot D\left(\boldsymbol{\nabla} \;-\; \beta\, \boldsymbol{F}(\boldsymbol{r})\right) h(\boldsymbol{r}) \;=\; 0\,, \qquad \boldsymbol{r}\;\in\;\partial\Omega \tag{9.4}$$

$$\text{(ii)}\quad h(\boldsymbol{r}) \;=\; 0\,, \qquad \boldsymbol{r}\;\in\;\partial\Omega \tag{9.5}$$

$$\text{(iii)}\quad \hat{\boldsymbol{a}}(\boldsymbol{r})\cdot D\left(\boldsymbol{\nabla} \;-\; \beta\, \boldsymbol{F}(\boldsymbol{r})\right) h(\boldsymbol{r}) \;=\; w(\boldsymbol{r})\; h(\boldsymbol{r})\,, \qquad \boldsymbol{r}\;\in\;\partial\Omega \tag{9.6}$$

where, in the latter equation, $w(\boldsymbol{r})$ is a continuous function which describes the effectivity of the surface $\partial\Omega$ to react locally. In case of $\boldsymbol{F}(\boldsymbol{r}) = -\boldsymbol{\nabla}U(\boldsymbol{r})$ one can express (9.4)

$$\text{(i)} \quad \hat{\boldsymbol{a}}(\boldsymbol{r}) \cdot D\, e^{-\beta U(\boldsymbol{r})} \boldsymbol{\nabla}\, e^{\beta U(\boldsymbol{r})}\; h(\boldsymbol{r}) \;=\; 0\;, \qquad\qquad \boldsymbol{r} \in \partial\Omega\;. \tag{9.7}$$

Similarly, one can write (9.6) in the form

$$\text{(iii)} \quad \hat{\boldsymbol{a}}(\boldsymbol{r}) \cdot D\, e^{-\beta U(\boldsymbol{r})} \boldsymbol{\nabla}\, e^{\beta U(\boldsymbol{r})}\; h(\boldsymbol{r}) \;=\; w(\boldsymbol{r})\; h(\boldsymbol{r})\;, \quad \boldsymbol{r} \in \partial\Omega\;. \tag{9.8}$$

The equations (9.1–9.6) allow one to determine the probability $p(\boldsymbol{r}, t|\boldsymbol{r}_0, t_0)$ to find a particle at position $\boldsymbol{r}$ at time t, given that the particle started diffusion at position $\boldsymbol{r}_0$ at time t_0. It holds

$$p(\boldsymbol{r}, t_0|\boldsymbol{r}_0, t_0) \;=\; \delta(\boldsymbol{r} - \boldsymbol{r}_0)\;. \tag{9.9}$$

For the Smoluchowski equation (9.1) exists an alternative form

$$\partial_t p(\boldsymbol{r}, t|\boldsymbol{r}_0, t_0) \;=\; \mathcal{L}^\dagger(\boldsymbol{r}_0)\; p(\boldsymbol{r}, t|\boldsymbol{r}_0, t_0)\;, \tag{9.10}$$

the so-called *adjoint* or *backward* equation, which involves a differential operator that acts on the $\boldsymbol{r}_0$-dependence of $p(\boldsymbol{r}, t|\boldsymbol{r}_0, t_0)$. The latter operator $\mathcal{L}^\dagger(\boldsymbol{r}_0)$ is the adjoint of the operator $\mathcal{L}(\boldsymbol{r})$ defined in (9.2) above.
Below we will determine the operator $\mathcal{L}^\dagger(\boldsymbol{r}_0)$ as well as the boundary conditions which the solution $p(\boldsymbol{r}, t|\boldsymbol{r}_0, t_0)$ of (9.10) must obey when $p(\boldsymbol{r}, t|\boldsymbol{r}_0, t_0)$ obeys the boundary conditions (9.4–9.6) in the original, so-called *forward* Smoluchowski equation (9.1).
Before proceeding with the derivation of the *backward* Smoluchowski equation we need to provide two key properties of the solution $p(\boldsymbol{r}, t|\boldsymbol{r}_0, t_0)$ of the *forward* Smoluchowski equation (9.1) connected with the time translation invariance of the equation and with the Markov property of the underlying stochastic process.

Homogeneous Time

In case that the Smoluchowski operator $\mathcal{L}(\boldsymbol{r})$ governing (9.1) and given by (9.3) is time-independent, one can make the substitution $t \to \tau = t - t_0$ in (9.1). This corresponds to the substitution $t_0 \to \tau_0 = 0$. The Smoluchowski equation (9.1) reads then

$$\partial_\tau\, p(\boldsymbol{r}, \tau|\boldsymbol{r}_0, 0) \;=\; \mathcal{L}(\boldsymbol{r})\, p(\boldsymbol{r}, \tau|\boldsymbol{r}_0, 0) \tag{9.11}$$

the solution of which is $p(\boldsymbol{r}, t - t_0|\boldsymbol{r}_0, 0)$, i.e., the solution of (9.1) for $p(\boldsymbol{r}, 0|\boldsymbol{r}_0, 0) = \delta(\boldsymbol{r} - \boldsymbol{r}_0)$. It follows

$$p(\boldsymbol{r}, t|\boldsymbol{r}_0, t_0) \;=\; p(\boldsymbol{r}, t - t_0|\boldsymbol{r}_0, 0)\;. \tag{9.12}$$

Chapman-Kolmogorov Equation

The solution $p(\boldsymbol{r}, t|\boldsymbol{r}_0, t_0)$ of the Smoluchowski equation corresponds to the initial condition (9.9). The solution $p(\boldsymbol{r}, t)$ for an initial condition

$$p(\boldsymbol{r}, t_0) \;=\; f(\boldsymbol{r}) \tag{9.13}$$

can be expressed

$$p(\boldsymbol{r}, t) \;=\; \int_\Omega d\boldsymbol{r}_0\; p(\boldsymbol{r}, t|\boldsymbol{r}_0, t_0)\; f(\boldsymbol{r}_0) \tag{9.14}$$

as can be readily verified. In fact, taking the time derivative yields

$$\begin{aligned} \partial_t\, p(\boldsymbol{r},t) &= \int_\Omega d\boldsymbol{r}_0\ \partial_t\, p(\boldsymbol{r},t|\boldsymbol{r}_0,t_0)\ f(\boldsymbol{r}_0) \\ &= \mathcal{L}(\boldsymbol{r}) \int_\Omega d\boldsymbol{r}_0\ p(\boldsymbol{r},t|\boldsymbol{r}_0,t_0)\ f(\boldsymbol{r}_0) \;=\; \mathcal{L}(\boldsymbol{r})\ p(\boldsymbol{r},t)\ . \end{aligned} \tag{9.15}$$

Furthermore, we note using (9.9)

$$p(\boldsymbol{r},t_0) \;=\; \int_\Omega d\boldsymbol{r}_0\ \delta(\boldsymbol{r}-\boldsymbol{r}_0)\ f(\boldsymbol{r}_0) \;=\; f(\boldsymbol{r})\ . \tag{9.16}$$

One can apply identity (9.14) to express $p(\boldsymbol{r},t|\boldsymbol{r}_0,t_0)$ in terms of the probalities $p(\boldsymbol{r},t|\boldsymbol{r}_1,t_1)$ and $p(\boldsymbol{r}_1,t_1|\boldsymbol{r}_0,t_0)$

$$p(\boldsymbol{r},t|\boldsymbol{r}_0,t_0) \;=\; \int_\Omega d\boldsymbol{r}_1\ p(\boldsymbol{r},t|\boldsymbol{r}_1,t_1)\ p(\boldsymbol{r}_1,t_1|\boldsymbol{r}_0,t_0)\ . \tag{9.17}$$

This latter identity is referred to as the *Chapman-Kolmogorov equation*. Both (9.14) and (9.17) state that knowledge of the distribution at a single instance t, i.e., $t=t_0$ or $t=t_1$, allows one to predict the distributions at all later times. The *Chapman-Kolmogorov equation* reflects the Markov property of the stochastic process assumed in the derivation of the Smoluchowski equation.
We like to state finally the *Chapman-Kolmogorov equation* (9.17) for the special case $t_1 = t-\tau$. Employing identity (9.12) one obtains

$$p(\boldsymbol{r},t|\boldsymbol{r}_0,t_0) \;=\; \int_\Omega d\boldsymbol{r}_1\ p(\boldsymbol{r},\tau|\boldsymbol{r}_1,0)\ p(\boldsymbol{r}_1,t-\tau|\boldsymbol{r}_0,t_0)\ . \tag{9.18}$$

Taking the time derivative yields, using (9.1),

$$\partial_t\, p(\boldsymbol{r},t|\boldsymbol{r}_0,t_0) \;=\; \int_\Omega d\boldsymbol{r}_1\ p(\boldsymbol{r},\tau|\boldsymbol{r}_1,0)\ \mathcal{L}(\boldsymbol{r}_1)\ p(\boldsymbol{r}_1,t-\tau|\boldsymbol{r}_0,t_0)\ . \tag{9.19}$$

The Adjoint Smoluchowski Operator

We want to determine now the operator $\mathcal{L}^\dagger$ in (9.10). For this purpose we prove the following identity [48]:

$$\int_\Omega d\boldsymbol{r}\ g(\boldsymbol{r})\ \mathcal{L}(\boldsymbol{r})\ h(\boldsymbol{r}) \;=\; \int_\Omega d\boldsymbol{r}\ h(\boldsymbol{r})\ \mathcal{L}^\dagger(\boldsymbol{r})\ g(\boldsymbol{r}) \;+\; \int_{\partial\Omega} d\boldsymbol{a}\cdot\boldsymbol{P}(g,h) \tag{9.20}$$

$$\mathcal{L}(\boldsymbol{r}) \;=\; \boldsymbol{\nabla}\cdot D\,\boldsymbol{\nabla} \;-\; \beta\,\boldsymbol{\nabla}\cdot D\,\boldsymbol{F}(\boldsymbol{r}) \tag{9.21}$$

$$\mathcal{L}^\dagger(\boldsymbol{r}) \;=\; \boldsymbol{\nabla}\cdot D\,\boldsymbol{\nabla} \;+\; \beta\, D\,\boldsymbol{F}(\boldsymbol{r})\cdot\boldsymbol{\nabla} \tag{9.22}$$

$$\begin{aligned} \boldsymbol{P}(g,h) &= g(\boldsymbol{r})\ D\,\boldsymbol{\nabla}\,h(\boldsymbol{r}) \;-\; h(\boldsymbol{r})\ D\,\boldsymbol{\nabla}\,g(\boldsymbol{r}) \\ &\qquad -\ \beta\, D\,\boldsymbol{F}(\boldsymbol{r})\ g(\boldsymbol{r})\ h(\boldsymbol{r})\ . \end{aligned} \tag{9.23}$$

The operator $\mathcal{L}^\dagger(\boldsymbol{r})$ is called the *adjoint* to the operator $\mathcal{L}(\boldsymbol{r})$, and $\boldsymbol{P}(g,h)$ is called the *concomitant* of $\mathcal{L}(\boldsymbol{r})$.
To prove (9.20–9.23) we note, using $\boldsymbol{\nabla}\cdot w(\boldsymbol{r})\,\boldsymbol{q}(\boldsymbol{r}) = \boldsymbol{q}(\boldsymbol{r})\cdot\boldsymbol{\nabla}\,w(\boldsymbol{r}) + w(\boldsymbol{r})\,\boldsymbol{\nabla}\cdot\boldsymbol{q}(\boldsymbol{r})$

$$\begin{aligned} \boldsymbol{\nabla}\cdot\big(\,g\,D\,\boldsymbol{\nabla}\,h \;-\; h\,D\,\boldsymbol{\nabla}\,g\,\big) &= (\!(\boldsymbol{\nabla}g)\!)\,D\,(\!(\boldsymbol{\nabla}h)\!) \;+\; g\,\boldsymbol{\nabla}\cdot D\,\boldsymbol{\nabla}\,h \\ &\qquad -\ (\!(\boldsymbol{\nabla}h)\!)\,D\,(\!(\boldsymbol{\nabla}g)\!) \;-\; h\,\boldsymbol{\nabla}\cdot D\,\boldsymbol{\nabla}\,g \\ &= g\,\boldsymbol{\nabla}\cdot D\,\boldsymbol{\nabla}\,h \;-\; h\,\boldsymbol{\nabla}\cdot D\,\boldsymbol{\nabla}\,g \end{aligned} \tag{9.24}$$

or

$$g\,\boldsymbol{\nabla}\cdot D\,\boldsymbol{\nabla}h \;=\; h\,\boldsymbol{\nabla}\cdot D\,\boldsymbol{\nabla}g \;+\; \boldsymbol{\nabla}\cdot(\,g\,D\,\boldsymbol{\nabla}h \;-\; h\,D\,\boldsymbol{\nabla}g\,)\;. \tag{9.25}$$

The double brackets $(\!(\ldots)\!)$ limit the scope of the differential operators.
Furthermore, one can show

$$\boldsymbol{\nabla}\cdot D\,\boldsymbol{F}\,g\,h \;\;=\;\; g\,\boldsymbol{\nabla}\cdot D\,\boldsymbol{F}\,h \;+\; h\,D\,\boldsymbol{F}\cdot\boldsymbol{\nabla}\,g \tag{9.26}$$

or

$$-g\,\boldsymbol{\nabla}\cdot\beta D\,\boldsymbol{F}\,h \;\;=\;\; h\,\beta\,D\,\boldsymbol{F}\cdot\boldsymbol{\nabla}\,g \;-\; \boldsymbol{\nabla}\cdot\beta\,D\,\boldsymbol{F}\,g\,h\;. \tag{9.27}$$

Equations (9.26, 9.27) can be combined, using (9.21–9.23),

$$g\;\mathcal{L}\;h \;\;=\;\; h\;\mathcal{L}^{\dagger}\;g \;+\; \boldsymbol{\nabla}\cdot\boldsymbol{P}(g,h) \tag{9.28}$$

from which follows (9.20).
In case

$$\boldsymbol{P}(g,h) \;\;=\;\; 0\;,\;\text{for}\;\boldsymbol{r}\;\in\;\partial\Omega\;, \tag{9.29}$$

which implies a condition on the functions $g(\boldsymbol{r})$ and $h(\boldsymbol{r})$, (9.20) corresponds to the identity

$$\langle g|\mathcal{L}(\boldsymbol{r})\,h\rangle_{\Omega} \;\;=\;\; \langle\mathcal{L}^{\dagger}(\boldsymbol{r})\,g|h\rangle_{\Omega}\;, \tag{9.30}$$

a property which is the conventional definition of a pair of adjoint operators. We like to determine now which conditions $g(\boldsymbol{r})$ and $h(\boldsymbol{r})$ must obey for (9.30) to be true.
We assume that $h(\boldsymbol{r})$ obeys one of the three conditions (9.4–9.6) and try to determine if conditions for $g(\boldsymbol{r})$ on $\partial\Omega$ can be found such that (9.29) and, hence, (9.30) hold. For this purpose we write (9.29) using (9.23)

$$g(\boldsymbol{r})\,D\left[\,\boldsymbol{\nabla}\,f(\boldsymbol{r}) \;-\; \beta\,\boldsymbol{F}(\boldsymbol{r})\,f(\boldsymbol{r})\,\right] \;-\; h(\boldsymbol{r})\,D\,\boldsymbol{\nabla}\,g(\boldsymbol{r}) \;\;=\;\; 0\;,\quad \boldsymbol{r}\;\in\;\partial\Omega\;. \tag{9.31}$$

In case that $h(\boldsymbol{r})$ obeys (9.4) follows

$$\text{(i')}\qquad\qquad \hat{\boldsymbol{a}}(\boldsymbol{r})\cdot D\,\boldsymbol{\nabla}\,g(\boldsymbol{r}) \;\;=\;\; 0\;,\qquad \boldsymbol{r}\;\in\partial\Omega\;. \tag{9.32}$$

In case that $h(\boldsymbol{r})$ obeys (9.5), follows

$$\text{(ii')}\qquad\qquad g(\boldsymbol{r}) \;\;=\;\; 0\;,\qquad \boldsymbol{r}\;\in\partial\Omega \tag{9.33}$$

and, in case that $h(\boldsymbol{r})$ obeys (9.6), follows

$$\text{(iii')}\qquad w\,g(\boldsymbol{r}) \;-\; \hat{\boldsymbol{a}}(\boldsymbol{r})\cdot D\,\boldsymbol{\nabla}\,g(\boldsymbol{r}) \;\;=\;\; 0\;,\qquad \boldsymbol{r}\;\in\partial\Omega\;. \tag{9.34}$$

From this we can conclude:

1. $\langle g|\mathcal{L}(\boldsymbol{r})\,h\rangle_{\Omega} \;=\; \langle\mathcal{L}^{\dagger}(\boldsymbol{r})\,g|h\rangle_{\Omega}$ holds if h obeys (i), i.e., (9.4), and g obeys (i′), i.e., (9.32);
2. $\langle g|\mathcal{L}(\boldsymbol{r})\,h\rangle_{\Omega} \;=\; \langle\mathcal{L}^{\dagger}(\boldsymbol{r})\,g|h\rangle_{\Omega}$ holds if h obeys (ii), i.e., (9.5), and g obeys (ii′), i.e., (9.33);
3. $\langle g|\mathcal{L}(\boldsymbol{r})\,h\rangle_{\Omega} \;=\; \langle\mathcal{L}^{\dagger}(\boldsymbol{r})\,g|h\rangle_{\Omega}$ holds if h obeys (iii), i.e., (9.6), and g obeys (iii′), i.e., (9.34).

Derivation of the Adjoint Smoluchowski Equation

The Chapman-Kolmogorov equation in the form (9.19) allows one to derive the adjoint Smoluchowski equation (9.10). For this purpose we replace $\mathcal{L}(\boldsymbol{r}_0)$ in (9.19) by the adjoint operator using (9.30)

$$\partial_\tau p(\boldsymbol{r},t|\boldsymbol{r}_0,t_0) = \int_\Omega d\boldsymbol{r}_1\; p(\boldsymbol{r},\tau|\boldsymbol{r}_1,0)\;\mathcal{L}(\boldsymbol{r}_1)\;p(\boldsymbol{r}_1,t-\tau|\boldsymbol{r}_0,t_0) \tag{9.35}$$

$$= \int_\Omega d\boldsymbol{r}_1\; p(\boldsymbol{r}_1,t-\tau|\boldsymbol{r}_0,t_0)\;\mathcal{L}^\dagger(\boldsymbol{r}_1)\;p(\boldsymbol{r},\tau|\boldsymbol{r}_1,0)\;. \tag{9.36}$$

Note that $\mathcal{L}(\boldsymbol{r}_1)$ in (9.35) acts on the *first* spatial variable of $p(\boldsymbol{r}_1,t-\tau|\boldsymbol{r}_0,t_0)$ whereas $\mathcal{L}^\dagger(\boldsymbol{r}_1)$ in (9.36) acts on the *second* spatial variable of $p(\boldsymbol{r},\tau|\boldsymbol{r}_1,0)$. Taking the limit $\tau\to(t-t_0)$ yields, with $p(\boldsymbol{r}_1,t-\tau|\boldsymbol{r}_0,t_0)\to\delta(r_1-r_0)$,

$$\partial_t\, p(\boldsymbol{r},t|\boldsymbol{r}_0,t_0) = \mathcal{L}^\dagger(\boldsymbol{r}_0)\;p(\boldsymbol{r},t-t_0|\boldsymbol{r}_0,0)\;, \tag{9.37}$$

i.e., the *backward* Smoluchowski equation (9.10).
We need to specify now the boundary conditions which the solution of the adjoint Smoluchowski equation (9.37) must obey. It should be noted here that the adjoint Smoluchowski equation (9.37) considers $p(\boldsymbol{r},t|\boldsymbol{r}_0,t_0)$ a function of $\boldsymbol{r}_0$, i.e., we need to specify boundary conditions for $\boldsymbol{r}_0\in\Omega$. The boundary conditions arise in the step (9.35) $\to$ (9.36) above. This step requires:

1. In case that $p(\boldsymbol{r},t|\boldsymbol{r}_0,t_0)$ obeys (i) for its $\boldsymbol{r}$-dependence, i.e., (9.4) for $\boldsymbol{r}\in\partial\Omega$, then $p(\boldsymbol{r},t|\boldsymbol{r}_0,t_0)$ must obey (i′) for its $\boldsymbol{r}_0$-dependence, i.e., (9.32) for $\boldsymbol{r}_0\in\partial\Omega$;
2. In case that $p(\boldsymbol{r},t|\boldsymbol{r}_0,t_0)$ obeys (ii) for its $\boldsymbol{r}$-dependence, i.e., (9.5) for $\boldsymbol{r}\in\partial\Omega$, then $p(\boldsymbol{r},t|\boldsymbol{r}_0,t_0)$ must obey (ii′) for its $\boldsymbol{r}_0$-dependence, i.e., (9.33) for $\boldsymbol{r}_0\in\partial\Omega$;
3. In case that $p(\boldsymbol{r},t|\boldsymbol{r}_0,t_0)$ obeys (iii) for its $\boldsymbol{r}$-dependence, i.e., (9.6) for $\boldsymbol{r}\in\partial\Omega$, then $p(\boldsymbol{r},t|\boldsymbol{r}_0,t_0)$ must obey (iii′) for its $\boldsymbol{r}_0$-dependence, i.e., (9.34) for $\boldsymbol{r}_0\in\partial\Omega$.

We note finally that $\mathcal{L}^\dagger(\boldsymbol{r})$, given by (9.22), in case that the force $\boldsymbol{F}(\boldsymbol{r})$ is related to a potential, i.e., $\boldsymbol{F}(\boldsymbol{r})=-\boldsymbol{\nabla}U(\boldsymbol{r})$, can be written

$$\mathcal{L}^\dagger(\boldsymbol{r}) = e^{\beta U(\boldsymbol{r})}\,\boldsymbol{\nabla}\cdot D\;e^{-\beta U(\boldsymbol{r})}\,\boldsymbol{\nabla}\;. \tag{9.38}$$

This corresponds to expression (9.3) for $\mathcal{L}$.

9.2 Correlation Functions

Often an experimentalist prepares a system in an initial distribution $B(\boldsymbol{r})\,p_o(\boldsymbol{r})$ at a time t_0 and probes the spatial distribution of the system with sensitivity $A(\boldsymbol{r})$ at any time $t > t_0$. The observable is then the socalled **correlation function**

$$C_{A(\boldsymbol{r})\,B(\boldsymbol{r})}(t) = \int_\Omega d\boldsymbol{r}\int_\Omega d\boldsymbol{r}_{\mathbf{o}}\;A(\boldsymbol{r})\;p(\boldsymbol{r},t|\boldsymbol{r}_{\mathbf{o}},t_0)\;B(\boldsymbol{r}_{\mathbf{o}})\;, \tag{9.39}$$

where $p(\boldsymbol{r},t|\boldsymbol{r}_{\mathbf{o}},t_0)$ obeys the backward Smoluchowski equation (9.37) with the initial condition

$$p(\boldsymbol{r},t_0|\boldsymbol{r}_0,t_0) = \delta(\boldsymbol{r}-\boldsymbol{r}_0)\;. \tag{9.40}$$

and the adjoint boundary conditions (9.32, 9.33, 9.34).
We like to provide a three examples of correlation functions. A trivial example arises in the case of $A(\boldsymbol{r}) = \delta(\boldsymbol{r} - \boldsymbol{r}\,')$ and $B(\boldsymbol{r}) = \delta(\boldsymbol{r} - \boldsymbol{r}\,'')/p_o(\boldsymbol{r})\,')$ which yields

$$C_{A\,B}\,(t) \;=\; p(\boldsymbol{r}\,', t|\boldsymbol{r}\,'', t_0)\;. \tag{9.41}$$

In the case one can only observe the total number of particles, i.e. $A(\boldsymbol{r}) = 1$, and for the special case $B(\boldsymbol{r}) = \delta(\boldsymbol{r} - \boldsymbol{r}\,')/p_o(\boldsymbol{r})\,')$, the correlation function is equal to the total particle number , customarily written

$$N(t, \boldsymbol{r}\,') \;=\; C_{1\,\delta(\boldsymbol{r}-\boldsymbol{r}')/p_o(\boldsymbol{r})\,')}\,(t) \;=\; \int_\Omega d\boldsymbol{r}\; p(\boldsymbol{r}, t|\boldsymbol{r}\,', t_0)\;. \tag{9.42}$$

The third correlation function, the so-called Mößbauer Lineshape Function, describes the absorption and re-emissions of γ-quants by ^{57}Fe. This isotope of iron can be enriched in the heme group of myoglobin. The excited state of ^{57}Fe has a lifetime $\Gamma^{-1} \approx 100\,ns$ before te isotope reemits the γ-quant. The re-emitted γ-quants interfere with the incident, affecting the lineshape of the spectrum. In the limit of small motion of the iron the following function holds for the spectral intensity

$$I(\omega) \;=\; \frac{\sigma_0\Gamma}{4}\int_{-\infty}^{\infty} dt\; e^{-i\omega t-\frac{1}{2}\Gamma|t|}\; G(\boldsymbol{k}, t)\;, \tag{9.43}$$

where

$$G(\boldsymbol{k}, t) \;=\; \int d\boldsymbol{r} \int d\boldsymbol{r}_{\mathbf{o}}\; e^{i\boldsymbol{k}\cdot(\boldsymbol{r}\,-\,\boldsymbol{r}_0)}\; p(\boldsymbol{r}, t|\boldsymbol{r}_{\mathbf{o}}, 0)\; p_0(\boldsymbol{r}_0) \;=\; C_{e^{i\boldsymbol{k}\cdot\boldsymbol{r}}\;e^{-i\boldsymbol{k}\cdot\boldsymbol{r}_o}}\;. \tag{9.44}$$

The term $-\frac{1}{2}\Gamma|t|$ in the exponent of (9.43) reflects the Lorentzian broadening of the spectral line due to the limited lifetime of the quants.
In order to evaluate a correlation function $C_{A(\boldsymbol{r})\,B(\boldsymbol{r})}\,(t)$ one can determine first the quantity

$$C_{A(\boldsymbol{r})}(t|\boldsymbol{r}_o) \;=\; \int_\Omega d\boldsymbol{r}\; A(\boldsymbol{r})\, p(\boldsymbol{r}, t|\boldsymbol{r}_o, t_o) \tag{9.45}$$

and evaluate then

$$C_{A(\boldsymbol{r})B(\boldsymbol{r})}(t|\boldsymbol{r}_o) \;=\; \int d\boldsymbol{r}_o\, B(\boldsymbol{r}_o) p(\boldsymbol{r}, t|\boldsymbol{r}_o, t_o)\;. \tag{9.46}$$

$C_{A(\boldsymbol{r})}(t|\boldsymbol{r}_o)$ can be obtained by carrying out the integral in (9.45) over the backward Smoluchowski equation (**??**9.37)). One obtains

$$\partial_t C_{A(\boldsymbol{r})}(t|\boldsymbol{r}_o) \;=\; \mathcal{L}^\dagger(\boldsymbol{r})\, C_{A(\boldsymbol{r})}(t|\boldsymbol{r}_o) \tag{9.47}$$

with the initial condition

$$C_{A(\boldsymbol{r})}(t_0|\boldsymbol{r}_o) \;= A(\boldsymbol{r}_0) \tag{9.48}$$

and the appropriate boundary condition selected from (9.32, 9.33, 9.34).

Chapter 10

Rates of Diffusion-Controlled Reactions

Contents

10.1 Relative Diffusion of two Free Particles 137
10.2 Diffusion-Controlled Reactions under Stationary Conditions 139
10.2.1 Examples 141

The metabolism of the biological cell, the control of its development and its communication with other cells in the organism or with its environment involves a complex web of biochemical reactions. The efficient functioning of this web relies on the availability of suitable reaction rates. Biological functions are often controlled through inhibition of these reaction rates, so the base rates must be as fast as possible to allow for a wide range of control. The maximal rates have been increased throughout the long evolution of life, often surpassing by a wide margin rates of comparable test tube reactions. In this respect it is important to realize that the rates of biochemical reactions involving two molecular partners, e.g., an enzyme and its substrate, at their optimal values are actually determined by the diffusive process which leads to the necessary encounter of the reactants. Since many biochemical reactions are proceeding close to their optimal speed, i.e., each encounter of the two reactants leads to a chemical transformation, it is essential for an understanding of biochemical reactions to characterize the diffusive encounters of biomolecules.
In this section we want to describe first the relative motion of two diffusing biomolecules subject to an interaction between the partners. We then determine the rates of reactions as determined by the diffusion process. We finally discuss examples of reactions for various interactions.

10.1 Relative Diffusion of two Free Particles

We consider first the relative motion in the case that two particles are diffusing freely. One can assume that the motion of one particle is independent of that of the other particle. In this case the diffusion is described by a distribution function $p(\boldsymbol{r}_1, \boldsymbol{r}_2, t|\boldsymbol{r}_{10}, \boldsymbol{r}_{20}, t_0)$ which is governed by the diffusion equation

$$\partial_t\, p(\boldsymbol{r}_1, \boldsymbol{r}_2, t|\boldsymbol{r}_{10}, \boldsymbol{r}_{20}, t_0) \;=\; \left(D_1\nabla_1^2 \;+\; D_2\nabla_2^2 \right)\; p(\boldsymbol{r}_1, \boldsymbol{r}_2, t|\boldsymbol{r}_{10}, \boldsymbol{r}_{20}, t_0) \tag{10.1}$$

where $\nabla_j \;=\; \partial/\partial\boldsymbol{r}_j$, $j = 1, 2$. The additive diffusion operators $D_j\nabla_j^2$ in (10.1) are a signature of the statistical independence of the Brownian motions of each of the particles.

Our goal is to obtain from (10.1) an equation which governs the distribution $p(\boldsymbol{r}, t|r_0, t_0)$ for the relative position

$$\boldsymbol{r} \;=\; \boldsymbol{r}_2 \;-\; \boldsymbol{r}_1 \tag{10.2}$$

of the particles. For this purpose we express (10.1) in terms of the coordinates $\boldsymbol{r}$ and

$$\boldsymbol{R} \;=\; a\,\boldsymbol{r}_1 \;+\; b\,\boldsymbol{r}_2 \tag{10.3}$$

which, for suitable constants a, b, are linearly independent. One can express

$$\nabla_1 \;=\; a\nabla_{\boldsymbol{R}} \;-\; \nabla\,, \quad \nabla_2 \;=\; b\,\nabla_{\boldsymbol{R}} \;+\; \nabla \tag{10.4}$$

where $\nabla \;=\; \partial/\partial\boldsymbol{r}$. One obtains, furthermore,

$$\nabla_1^2 \;=\; a^2\nabla_{\boldsymbol{R}}^2 \;+\; \nabla^2 \;-\; 2a\,\nabla_{\boldsymbol{R}}\nabla \tag{10.5}$$
$$\nabla_2^2 \;=\; b^2\nabla_{\boldsymbol{R}}^2 \;+\; \nabla^2 \;+\; 2b\,\nabla_{\boldsymbol{R}}\nabla \tag{10.6}$$

The diffusion operator

$$\widehat{\mathcal{D}} \;=\; D_1\nabla_1^2 \;+\; D_2\nabla_2^2 \tag{10.7}$$

can then be written

$$\widehat{\mathcal{D}} \;=\; (D_1a^2 \;+\; D_2b^2)\,\nabla_{\boldsymbol{R}}^2 \;+\; (D_1 \;+\; D_2)\,\nabla^2 \;+\; 2\,(D_2b \;-\; D_1a)\,\nabla_{\boldsymbol{R}}\nabla \tag{10.8}$$

If one defines

$$a \;=\; \sqrt{D_2/D_1}\,, \quad b \;=\; \sqrt{D_1/D_2} \tag{10.9}$$

one obtains

$$\widehat{\mathcal{D}} \;=\; (D_1 \;+\; D_2)\,\nabla_{\boldsymbol{R}}^2 \;+\; (D_1 \;+\; D_2)\,\nabla^2\,. \tag{10.10}$$

The operator (10.10) can be considered as describing two independent diffusion processes, one in the coordinate $\boldsymbol{R}$ and one in the coordinate $\boldsymbol{r}$. Thus, the distribution function may be written $p(\boldsymbol{R}, t|\boldsymbol{R}_0, t_0)p(\boldsymbol{r}, t|\boldsymbol{r}_0, t_0)$. If one disregards the diffusion along the coordinate $\boldsymbol{R}$ the relevant remaining relative motion is governed by

$$\partial_t p(\boldsymbol{r}, t|\boldsymbol{r}_0, t_0) \;=\; (D_1 \;+\; D_2)\,\nabla^2 p(\boldsymbol{r}, t|\boldsymbol{r}_0, t_0)\,. \tag{10.11}$$

This equation implies that the relative motion of the two particles is also governed by a diffusion equation, albeit for a diffusion coefficient

$$D \;=\; D_1 \;+\; D_2\,. \tag{10.12}$$

Relative Motion of two Diffusing Particles with Interaction

We seek to describe now the relative motion of two molecules which diffuse while interacting according to a potential $U(\boldsymbol{r})$ where $\boldsymbol{r} = \boldsymbol{r}_2 - \boldsymbol{r}_1$. The force acting on particle 2 is $-\nabla_2 U(\boldsymbol{r}) = \boldsymbol{F}$; the force acting on particle 1 is $-\boldsymbol{F}$. The distribution function $p(\boldsymbol{r}_1, \boldsymbol{r}_2, t|\boldsymbol{r}_{10}, \boldsymbol{r}_{20}, t_0)$ obeys the Smoluchowski equation

$$\begin{aligned} \partial_t p &= \left[\left(D_1 \nabla_1^2 + D_2 \nabla_2^2 \right) \right. \\ &- \left. D_2 \beta \nabla_2 \cdot \boldsymbol{F}(\boldsymbol{r}) + D_1 \beta \nabla_1 \cdot \boldsymbol{F} \right] p \, . \end{aligned} \tag{10.13}$$

The first two terms on the r.h.s. can be expressed in terms of the coordinates $\boldsymbol{R}$ and $\boldsymbol{r}$ according to (10.10). For the remaining terms holds, using (10.4, 10.9),

$$D_2 \nabla_2 - D_1 \nabla_1 = (D_1 + D_2) \nabla \tag{10.14}$$

Hence, one can write the Smoluchowski equation (10.13)

$$\partial_t p = \left[(D_1 + D_2) \nabla_{\boldsymbol{R}}^2 + (D_1 + D_2) \nabla \cdot (\nabla - \beta \boldsymbol{F}) \right] p \, . \tag{10.15}$$

This equation describes two independent random processes, free diffusion in the $\boldsymbol{R}$ coordinate and a diffusion with drift in the $\boldsymbol{r}$ coordinate. Since we are only interested in the relative motion of the two molecules, i.e., the motion which governs their reactive encounters, we describe the relative motion by the Smoluchowski equation

$$\partial_t p(\boldsymbol{r}, t|\boldsymbol{r}_0, t_0) = D \nabla \cdot (\nabla - \beta \boldsymbol{F}) p(\boldsymbol{r}, t|\boldsymbol{r}_0, t_0) \, . \tag{10.16}$$

10.2 Diffusion-Controlled Reactions under Stationary Conditions

We want to consider now a reaction vessel which contains a solvent with two types of particles , particle 1 and particle 2, which engage in a reaction

$$\text{particle 1} + \text{particle 2} \rightarrow \text{products} \, . \tag{10.17}$$

We assume that particle 1 and particle 2 are maintained at concentrations c_1 and c_2, respectively, i.e., the particles are replenished as soon as they are consumed by reaction (10.17). We also consider that the reaction products are removed from the system as soon as they are formed.
One can view the reaction vessel as containing pairs of particles 1 and 2 at various stages of the relative diffusion and reaction. This view maintains that the concentration of particles is so small that only rarely triple encounters, e.g., of two particles 1 and one particle 2, occur, so that these occurences can be neglected. The system considered contains then many particle 1 and particle 2 pairs described by the Smoluchowski equation (10.16). Since the concentration of the particles is maintained at a steady level one can expect that the system adopts a stationary distribution of inter-pair distances $p(\boldsymbol{r})$ which obeys (10.16), i.e.,

$$\nabla D(\boldsymbol{r}) \cdot (\nabla - \beta \boldsymbol{F}) p(\boldsymbol{r}) = 0 \, , \tag{10.18}$$

subject to the condition

$$p(\boldsymbol{r}) \asymp |\boldsymbol{r}| \rightarrow \infty \, c_1 \, c_2 \, . \tag{10.19}$$

Reaction (10.17) is described by the boundary condition

$$\hat{n} \cdot D(\boldsymbol{r}) \, (\nabla \, - \, \beta \boldsymbol{F}) \, p(\boldsymbol{r}) \; = \; w \, p(\boldsymbol{r}) \qquad \text{at } |\boldsymbol{r}| \; = \; R_o. \tag{10.20}$$

for some constant w.
The occurence of reaction (10.17) implies that a stationary current develops which describes the continuous diffusive approach and reaction of the particles. We consider in the following the case that the particles are governed by an interaction potential which depends solely on the distance $|\boldsymbol{r}|$ of the particles and that the diffusion coefficient D also depends solely on $|\boldsymbol{r}|$. The stationary Smoluchowski equation (10.18) reads then

$$(\, \partial_r D(r) \,)(\, (\, \partial_r \, - \, \beta \, F(r) \,) \, p(\boldsymbol{r})) \; = \; 0 \tag{10.21}$$

to which is associated the radial current

$$J_{\rm tot}(r) \; = \; 4\pi r^2 D(r) (\, \partial_r \, - \, \beta \, F(r) \,) \, p(\boldsymbol{r})) \tag{10.22}$$

where we have summed over all angles θ, ϕ obtaining the total current at radius r. For $F(r) = - \, \partial_r U(r)$ one can express this

$$J_{\rm tot}(r) \; = \; 4\pi r^2 D(r) \, \exp[-\beta U(r)] \, (\, \partial_r \, \exp[\beta U(r)] \, p \,) \; . \tag{10.23}$$

However, $J_{\rm tot}(r)$ must be the same at all r since otherwise $p(r)$ would change in time, in contrast to the assumption that the distribution is stationary. It must hold, in particular,

$$J_{\rm tot}(R_o) \; = \; J_{\rm tot}(r) \; . \tag{10.24}$$

The boundary condition (10.20), together with (10.23), yields

$$4\pi R_o^2 \, w \, p(R_o) \; = \; 4\pi r^2 \, D(r) \, \exp[-\beta U(r)] \, (\, \partial_r \, \exp[\beta U(r)] \, p(r) \,) \; . \tag{10.25}$$

This relationship, a first order differential equation, allows one to determine $p(r)$.
For the evaluation of $p(r)$ we write (10.25)

$$\partial_r \left(e^{\beta U(r)} \, p(r) \right) \; = \; \frac{R_o^2 w}{r^2 D(r)} \, p(R_o) \, e^{\beta U(r)} \; . \tag{10.26}$$

Integration $\int_r^\infty dr \, \cdots$ yields

$$p(\infty) \, e^{\beta U(\infty)} \; - \; p(r) \, e^{\beta U(r)} \; = \; R_o^2 w \, p(R_o) \int_r^\infty dr' \frac{e^{\beta U(r')}}{r'^2 \, D(r')} \tag{10.27}$$

or, using (10.19) and $U(\infty) \, = \, 0$

$$p(r) \, e^{\beta U(r)} \; = c_1 c_2 \; - \; R_o^2 w \, p(R_o) \int_r^\infty dr' \frac{e^{\beta U(r')}}{r'^2 \, D(r')} \tag{10.28}$$

Evaluating this at $r \, = \, R_o$ and solving for $p(R_o)$ yields

$$p(R_o) \; = \; \frac{c_1 c_2 \, e^{-\beta U(R_o)}}{1 \; + \; R_o^2 w \, e^{-\beta U(R_o)} \int_{R_o}^\infty dr \, e^{\beta U(r)} / r^2 D(r)} \; . \tag{10.29}$$

Using this in (10.28) leads to an expression of $p(r)$.

We are presently interested in the rate at which reaction (10.17) proceeds. This rate is given by $J_{\rm tot}(R_o) = 4\pi R_o^2 w\, p(R_o)$. Hence, we can state

$$\text{Rate} \;=\; \frac{4\pi R_o^2 w\, c_1 c_2\, e^{-\beta U(R_o)}}{1 \;+\; R_o^2 w\, e^{-\beta U(R_o)} \int_{R_o}^{\infty} dr\, e^{\beta U(r)}/r^2 D(r)} \;. \tag{10.30}$$

This expression is proportional to $c_1 c_2$, a dependence expected for a bimolecular reaction of the type (10.17). Conventionally, one defines a bimolecular rate constant k as follows

$$\text{Rate} \;=\; k\, c_1 c_2 \;. \tag{10.31}$$

This constant is then, in the present case,

$$k \;=\; \frac{4\pi}{e^{\beta U(R_o)}/R_o^2 w \;+\; \int_{R_o}^{\infty} dr\, \mathcal{R}(r)} \;. \tag{10.32}$$

Here, we defined

$$\mathcal{R}(r) \;=\; e^{\beta U(r)}/r^2 D(r) \tag{10.33}$$

a property which is called the resistance of the diffusing particle, a name suggested by the fact that $\mathcal{R}(r)$ describes the Ohmic resistance of the system as shown further below.

10.2.1 Examples

We consider first the case of very ineffective reactions described by small w values. In this case the time required for the diffusive encounter of the reaction partners can become significantly shorter than the time for the local reaction to proceed, if it proceeds at all. In this case it may hold

$$\frac{e^{\beta U(R_o)}}{R_o^2 w} \;>>\; \int_{R_o}^{\infty} dr\, \mathcal{R}(r) \tag{10.34}$$

and the reaction rate (10.32) becomes

$$k \;=\; 4\pi R_o^2\, w\, e^{-\beta U(R_o)} \;. \tag{10.35}$$

This expression conforms to the well-known Arrhenius law.
We want to apply (10.32, 10.33) to two cases, free diffusion ($U(r) \equiv 0$) and diffusion in a Coulomb potential ($U(r) = q_1 q_2/\epsilon r$, ϵ = dielectric constant). We assume in both cases a distance-independent diffusion constant. In case of free diffusion holds $\mathcal{R}(r) = D^{-1} r^{-2}$ and, hence,

$$\int_{R_o}^{\infty} dr\, \mathcal{R}(r) \;=\; 1/DR_o \;. \tag{10.36}$$

From this results

$$k \;=\; \frac{4\pi D R_o}{1 \;+\; D/R_o w} \;. \tag{10.37}$$

In case of very effective reactions, i.e., for very large w, this becomes

$$k \;=\; 4\pi D R_o \tag{10.38}$$

which is the well-known rate for diffusion-controlled reaction processes. No bi-molecular rate constant involving a diffusive encounter in a three-dimensional space without attracting forces between the reactants can exceed (10.38). For instance, in a diffusion-controlled reaction in a solvent with relative diffusion constant $D = 10^{-5}\,cm^2\,s^{-1}$ and with reactants such that $R_o = 1\,nm$, the maximum possible reaction rate is $7.56 \times 10^9\,L\,mol^{-1}\,s{-}1$.
In case of a Coulomb interaction between the reactants one obtains

$$\begin{aligned}\int_{R_o}^{\infty} dr\,\mathcal{R}(r) &= \frac{1}{D}\int_{R_o}^{\infty} dr\,\frac{1}{r^2}\,\exp\left[\frac{\beta q_1 q_2}{\epsilon r}\right] \\ &= \frac{1}{D}\int_0^{1/R_o} dy\,\exp\left[\frac{\beta q_1 q_2 y}{\epsilon}\right] \\ &= \frac{1}{R_L D}\left(e^{R_L/R_o} - 1\right) \end{aligned} \tag{10.39}$$

where

$$R_L = \beta q_1 q_2 \,/\, \epsilon \tag{10.40}$$

defines the so-called Onsager radius. Note that R_L can be positive or negative, depending on the sign of $q_1 q_2$, but that the integral over the resistance (10.39) is always positive. The rate constant (10.32) can then be written

$$k = \frac{4\pi D R_L}{\frac{R_L D}{R_o^2 w}\,e^{R_L/R_o} + e^{R_L/R_o} - 1}\,. \tag{10.41}$$

For instance, suppose we wish to find the maximum reaction rate for a reaction between pyrene-N and N-dimethylaniline in acetoneitrile. The reaction consists of an electron exchange from pyrene to dimethylaniline, and the reactants have charges of $\pm e$. The relative diffusion constant of both reactants in acetonitrile at $25^\circ\,C$ is $4.53 \times 10^{-5}\,cm^2\,s^{-1}$, the dielectric constant of acetonitrile at that temperature is 37.5, and the effective reaction radius R_o of the reactants is $0.7\,nm$. Using these values, and assuming $w \to \infty$ in (10.41) we obtain an Onsager radius of $-10.8\,nm$, and a maximum reaction rate of $k = 6.44 \times 10^{11}\,L\,mol^{-1}\,s^{-1}$.
In a different solvent, C_3H_7OH, with relative diffusion constant $D = 0.77 \times 10^{-5}\,cm^2\,s^{-1}$ at $25^\circ\,C$ and a dielectric constant of 19.7, the Onsager radius is $-35.7\,nm$ and the maximum reaction rate is $k = 2.08 \times 10^{11}\,L\,mol^{-1}\,s^{-1}$.

Chapter 11

Ohmic Resistance and Irreversible Work

Contents

Chapter 12

Smoluchowski Equation for Potentials: Extremum Principle and Spectral Expansion

Contents

12.1 Minimum Principle for the Smoluchowski Equation 146
12.2 Similarity to Self-Adjoint Operator 149
12.3 Eigenfunctions and Eigenvalues of the Smoluchowski Operator 151
12.4 Brownian Oscillator 155

In this section we will consider the general properties of the solution $p(\boldsymbol{r},t)$ of the Smoluchowski equation in the case that the force field is derived from a potential, i.e., $\boldsymbol{F}(\boldsymbol{r}) = -\nabla U(\boldsymbol{r})$ and that the potential is finite everywhere in the diffusion doamain Ω. We will demonstrate first that the solutions, in case of reaction-free boundary conditions, obey an extremum principle, namely, that during the time evolution of $p(\boldsymbol{r},t)$ the total free energy decreases until it reaches a minimum value corresponding to the Boltzmann distribution.
We will then characterize the time-evolution through a so-called spectral expansion, i.e., an expansion in terms of eigenfunctions of the Smoluchowski operator $\mathcal{L}(\boldsymbol{r})$. Since this operator is not self-adjoint, expressed through the fact that, except for free diffusion, the adjoint operator $\mathcal{L}^\dagger(\boldsymbol{r})$ as given by (9.22) or (9.38) is not equal to $\mathcal{L}(\boldsymbol{r})$, the existence of appropriate eigenvalues and eigenfunctions is not evident. However, in the present case $[\boldsymbol{F}(\boldsymbol{r}) = -\nabla U(\boldsymbol{r})]$ the operators $\mathcal{L}(\boldsymbol{r})$ and $\mathcal{L}^\dagger(\boldsymbol{r})$ are similar to a self-adjoint operator for which a complete set of orthonormal eigenfunctions exist. These functions and their associated eigenvalues can be transferred to $\mathcal{L}(\boldsymbol{r})$ and $\mathcal{L}^\dagger(\boldsymbol{r})$ and a spectral expansion can be constructed. The expansion will be formulated in terms of projection operators and the so-called propagator, which corresponds to the solutions $p(\boldsymbol{r},t|\boldsymbol{r}_0,t0)$, will be stated in a general form.
A pointed out, we consider in this chapter specifically solutions of the Smoluchowski equation

$$\partial_t p(\boldsymbol{r},t) \;=\; \mathcal{L}(\boldsymbol{r})\, p(\boldsymbol{r},t) \tag{12.1}$$

in case of diffusion in a potential $U(\boldsymbol{r})$, i.e., for a Smoluchowski operator of the form (9.3)

$$\mathcal{L}(\boldsymbol{r}) \;=\; \nabla \cdot D(\boldsymbol{r})\, e^{-\beta U(\boldsymbol{r})}\, \nabla\, e^{\beta U(\boldsymbol{r})}\;. \tag{12.2}$$

We assume the general initial condition

$$p(\boldsymbol{r}, t_o) \;=\; f(\boldsymbol{r}) \tag{12.3}$$

and appropriate boundary conditions as specified by equations (9.4–9.6). It is understood that the initial distribution is properly normalized

$$\int_\Omega d\boldsymbol{r}\; f(\boldsymbol{r}) \;=\; 1\;. \tag{12.4}$$

The results of the present section are fundamental for many direct applications as well as for a formal approach to the evaluation of observables, e.g., correlation functions, which serves to formulate useful approximations. We have employed already, in Chapter 2, spectral expansions for free diffusion, a casew in which the Smoluchowski operator $\mathcal{L}(\boldsymbol{r}) \;=\; D\nabla^2$ is self-adjoint ($\mathcal{L}(\boldsymbol{r}) \;=\; \mathcal{L}^\dagger(\boldsymbol{r})$). In the present chapter we consider spectral expansion for diffusion in arbitrary potentials $U(x)$ and demonstrate the expansion for a harmonic potential.

12.1 Minimum Principle for the Smoluchowski Equation

In case of diffusion in a domain Ω with a 'non-reactive' boundary $\partial\Omega$ the total free energy of the system develops toward a minimum value characterized through the Boltzmann distribution. This property will be demonstrated now. The stated boundary condition is according to (9.4)

$$\hat{n}(\boldsymbol{r}) \cdot \boldsymbol{\jmath}(\boldsymbol{r}, t) \;=\; 0 \tag{12.5}$$

where the flux $\boldsymbol{\jmath}(\boldsymbol{r}, t)$ is [c.f. (4.19)]

$$\boldsymbol{\jmath}(\boldsymbol{r}, t) \;=\; D(\boldsymbol{r})\, e^{-\beta U(\boldsymbol{r})}\, \nabla\, e^{\beta U(\boldsymbol{r})}\; p(\boldsymbol{r}, t)\;. \tag{12.6}$$

The total free energy for a given distribution $p(\boldsymbol{r}, t)$, i.e., the quantity which develops towards a minimum during the diffusion process, is a functional defined through

$$G[p(\boldsymbol{r}, t)] \;=\; \int_\Omega d\boldsymbol{r}\; g(\boldsymbol{r}, t) \tag{12.7}$$

where $g(\boldsymbol{r}, t)$ is the free energy density connected with $p(\boldsymbol{r}, t)$

$$g(\boldsymbol{r}, t) \;=\; U(\boldsymbol{r})\, p(\boldsymbol{r}, t) \;+\; k_B T\, p(\boldsymbol{r}, t) \ln \frac{p(\boldsymbol{r}, t)}{\rho_o}\;. \tag{12.8}$$

Here ρ_o is a constant which serves to make the argument of $\ln(\cdots)$ unitless. ρ_o adds effectively only a constant to $G[p(\boldsymbol{r}, t)]$ since, for the present boundary condition (12.5) [use (12.1, 12.2)],

$$\begin{aligned} \partial_t \int_\Omega d\boldsymbol{r}\, p(\boldsymbol{r}, t) \quad &= \quad \int_\Omega d\boldsymbol{r}\, \partial_t p(\boldsymbol{r}, t) \;=\; \int_\Omega d\boldsymbol{r}\, \nabla \cdot D(\boldsymbol{r})\, e^{-\beta U(\boldsymbol{r})} \nabla\, e^{\beta U(\boldsymbol{r})}\, p(\boldsymbol{r}, t) \\ &= \quad \int_{\partial\Omega} d\boldsymbol{a}\, \cdot D(\boldsymbol{r})\, e^{-\beta U(\boldsymbol{r})} \nabla\, e^{\beta U(\boldsymbol{r})}\, p(\boldsymbol{r}, t) \;=\; 0\;. \end{aligned} \tag{12.9}$$

From this follows that $\int_\Omega d\boldsymbol{r}\, p(\boldsymbol{r}, t)$ is constant and, hence, the contribution stemming from ρ_o, i.e., $-k_B T\, p(\boldsymbol{r}, t) \ln \rho_o$ contributes only a constant to $G[p(\boldsymbol{r}, t)]$ in (12.7). The first term on the r.h.s. of (12.7) describes the local energy density

$$u(\boldsymbol{r}, t) \;=\; U(\boldsymbol{r})\, p(\boldsymbol{r}, t) \tag{12.10}$$

and the second term, written as $-T\,s(\boldsymbol{r},t)$, the local entropy density[1]

$$s(\boldsymbol{r},t) \;=\; -k\,p(\boldsymbol{r},t)\ln\frac{p(\boldsymbol{r},t)}{\rho_o}\;. \tag{12.11}$$

We want to assume for some t

$$p(\boldsymbol{r},t) \;>\; 0 \qquad \forall \boldsymbol{r},\, \boldsymbol{r} \,\in\, \Omega\;. \tag{12.12}$$

This assumption can be made for the initial condition, i.e., at $t \;=\; t_o$, since a negative initial distribution could not be reconciled with the interpretation of $p(\boldsymbol{r},t)$ as a probability. We will see below that if, at any moment, (12.12) does apply, $p(\boldsymbol{r},t)$ cannot vanish anywhere in Ω at later times.
For the time derivative of $G[p(\boldsymbol{r},t)]$ can be stated

$$\partial_t G[p(\boldsymbol{r},t)] \;=\; \int_\Omega d\boldsymbol{r}\;\partial_t g(\boldsymbol{r},t) \tag{12.13}$$

where, according to the definition (12.8),

$$\partial_t g(\boldsymbol{r},t) \;=\; \left[U(\boldsymbol{r}) \;+\; k_B T\ln\frac{p(\boldsymbol{r},t)}{\rho_o} \;+\; k_B T\right]\partial_t p(\boldsymbol{r},t)\;. \tag{12.14}$$

Using the definition of the local flux density one can write (12.14)

$$\partial_t g(\boldsymbol{r},t) \;=\; \left[U(\boldsymbol{r}) \;+\; k_B T\ln\frac{p(\boldsymbol{r},t)}{\rho_o} \;+\; kT\right]\nabla\cdot\boldsymbol{\jmath}(\boldsymbol{r},t) \tag{12.15}$$

or, employing $\nabla\cdot w(\boldsymbol{r})\boldsymbol{v}(\boldsymbol{r}) \;=\; w(\boldsymbol{r})\nabla\cdot\boldsymbol{v}(\boldsymbol{r}) \;+\; \boldsymbol{v}(\boldsymbol{r})\cdot\nabla w(\boldsymbol{r})$,

$$\begin{aligned}\partial_t g(\boldsymbol{r},t) \quad &=\quad \nabla\cdot\left\{\left[U(\boldsymbol{r}) \;+\; k_B T\ln\frac{p(\boldsymbol{r},t)}{\rho_o} \;+\; k_B T\right]\boldsymbol{\jmath}(\boldsymbol{r},t)\right\}\\ &\qquad - \boldsymbol{\jmath}(\boldsymbol{r},t)\;\cdot\;\nabla\left[U(\boldsymbol{r}) \;+\; k_B T\ln\frac{p(\boldsymbol{r},t)}{\rho_o} \;+\; k_B T\right].\end{aligned} \tag{12.16}$$

Using

$$\begin{aligned}\nabla\left[U(\boldsymbol{r}) \;+\; k_B T\ln\frac{p(\boldsymbol{r},t)}{\rho_o} \;+\; k_B T\right] \quad &=\quad -\boldsymbol{F}(\boldsymbol{r}) \;+\; \frac{k_B T}{\boldsymbol{p}(\boldsymbol{r},t)}\,\nabla p(\boldsymbol{r},t)\\ &=\quad +\frac{k_B T}{\boldsymbol{p}(\boldsymbol{r},t)}\,[\,\nabla p(\boldsymbol{r},t) \;-\; \beta\,\boldsymbol{F}(\boldsymbol{r})\,p(\boldsymbol{r},t)\,]\\ &=\quad \frac{k_B T}{\boldsymbol{p}(\boldsymbol{r},t)}\,\boldsymbol{\jmath}(\boldsymbol{r},t)\end{aligned} \tag{12.17}$$

one can write (12.16)

$$\partial_t g(\boldsymbol{r},t) \;=\; -\frac{k_B T}{\boldsymbol{p}(\boldsymbol{r},t)}\,\boldsymbol{\jmath}^2(\boldsymbol{r},t) \;+\; \nabla\cdot\left\{\left[U(\boldsymbol{r}) \;+\; k_B T\ln\frac{p(\boldsymbol{r},t)}{\rho_o} \;+\; k_B T\right]\boldsymbol{\jmath}(\boldsymbol{r},t)\right\}\;. \tag{12.18}$$

[1]For a definition and explanation of the entropy term, often referred to as mixing entropy, see a textbook on Statistical Mechanics, e.g., "Course in Theoretical Physics, Vol. 5, Statistical Physics, Part 1, 3rd Edition", L.D. Landau and E.M. Lifshitz, Pergamon Press, Oxford)

For the total free energy holds then, according to (12.13),

$$\begin{aligned}\partial_t G[p(\boldsymbol{r},t)] \;\; &= \;\; -\int_\Omega d\boldsymbol{r}\;\frac{k_BT}{p(\boldsymbol{r},t)}\,\boldsymbol{\jmath}^2(\boldsymbol{r},t) \\ &\quad + \int_{\partial\Omega} d\boldsymbol{a}\cdot\left\{\left[U(\boldsymbol{r}) \;+\; k_BT\ln\frac{p(\boldsymbol{r},t)}{\rho_o} \;+\; k_BT\right]\boldsymbol{\jmath}(\boldsymbol{r},t)\right\}\,.\end{aligned} \tag{12.19}$$

Due to the boundary condition (12.5) the second term on the r.h.s. vanishes and one can conclude

$$\partial_t G[p(\boldsymbol{r},t)] \;=\; -\int_\Omega d\boldsymbol{r}\;\frac{k_BT}{p(\boldsymbol{r},t)}\,\boldsymbol{\jmath}^2(\boldsymbol{r},t) \;\le\; 0\,. \tag{12.20}$$

According to (12.20) the free energy, during the time course of Smoluchowski dynamics, develops towards a state $p_o(\boldsymbol{r})$ which minimizes the total free energy G. This state is characterized through the condition $\partial_t G = 0$, i.e., through

$$\boldsymbol{\jmath}_o(\boldsymbol{r}) \;=\; D(\boldsymbol{r})\,e^{-\beta U(\boldsymbol{r})}\,\nabla\,e^{\beta U(\boldsymbol{r})}\,p_o(\boldsymbol{r}) \;=\; 0\,. \tag{12.21}$$

The Boltzmann distribution

$$p_o(\boldsymbol{r}) \;=\; N\,e^{-\beta U(\boldsymbol{r})}\,, \qquad N^{-1} \;=\; \int_\Omega d\boldsymbol{r}\,p_o(\boldsymbol{r}) \tag{12.22}$$

obeys this condition which we, in fact, enforced onto the Smoluchowski equation as outlined in Chapter 3 [cf. (4.5–4.19)]. Hence, the solution of (12.1–12.3, 12.5) will develop asymptotically , i.e., for $t \to \infty$, towards the Boltzmann distribution.
We want to determine now the difference between the free energy density $g(\boldsymbol{r},t)$ and the equilibrium free energy density. For this purpose we note

$$U(\boldsymbol{r})\,p(\boldsymbol{r},t) \;=\; -k_BT\,p(\boldsymbol{r},t)\ln\left[e^{-\beta U(\boldsymbol{r})}\right] \tag{12.23}$$

and, hence, according to (12.8)

$$g(\boldsymbol{r},t) \;=\; k_BT\,p(\boldsymbol{r},t)\ln\frac{p(\boldsymbol{r},t)}{\rho_o e^{-\beta U(\boldsymbol{r})}}\,. \tag{12.24}$$

Choosing $\rho_o^{-1} = \int_\Omega d\boldsymbol{r}\,\exp[-\beta U(\boldsymbol{r})]$ one obtains, from (12.22)

$$g(\boldsymbol{r},t) \;=\; k_BT\,p(\boldsymbol{r},t)\ln\frac{p(\boldsymbol{r},t)}{p_o(\boldsymbol{r})}\,. \tag{12.25}$$

For $p(\boldsymbol{r},t) \to p_o(\boldsymbol{r})$ this expression vanishes, i.e., $g(\boldsymbol{r},t)$ is the difference between the free energy density $g(\boldsymbol{r},t)$ and the equilibrium free energy density.
We can demonstrate now that the solution $p(\boldsymbol{r},t)$ of (12.1–12.3, 12.5) remains positive, as long as the initial distribution (12.3) is positive. This follows from the observation that for positive distributions the expression (12.25) is properly defined. In case that $p(\boldsymbol{r},t)$ would then become very small in some region of Ω, the free energy would become $-\infty$, except if balanced by a large positive potential energy $U(\boldsymbol{r})$. However, since we assumed that $U(\boldsymbol{r})$ is finite everywhere in Ω, the distribution cannot vanish anywhere, lest the total free energy would fall below the zero equilibrium value of (12.25). We conclude that $p(\boldsymbol{r},t)$ cannot vanish anywhere, hence, once positive everywhere the distribution $p(\boldsymbol{r},t)$ can nowhere vanish or, as a result, become negative.

12.2 Similarity to Self-Adjoint Operator

In case of diffusion in a potential $U(\boldsymbol{r})$ the respective Smoluchowski operator (12.2) is related, through a similarity transformation, to a self-adjoint or Hermitean operator $\mathcal{L}_h$. This has important ramifications for its eigenvalues and its eigenfunctions as we will demonstrate now.
The Smoluchowski operator $\mathcal{L}$ acts in a function space with elements $f, g, \ldots$. We consider the following transformation in this space

$$f(\boldsymbol{r}),\ g(\boldsymbol{r}) \quad \rightarrow \quad \tilde{f}(\boldsymbol{r}) \ = \ e^{\frac{1}{2}\beta U(\boldsymbol{r})}\, f(\boldsymbol{r}),\ \tilde{g}(\boldsymbol{r}) \ = \ e^{\frac{1}{2}\beta U(\boldsymbol{r})}\, g(\boldsymbol{r})\ .$$

Note that such transformation is accompanied by a change of boundary conditions.
A relationship

$$g \ = \ \mathcal{L}(\boldsymbol{r})\, f(\boldsymbol{r}) \tag{12.26}$$

implies

$$\tilde{g} \ = \ \mathcal{L}_h(\boldsymbol{r})\, \tilde{f}(\boldsymbol{r}) \tag{12.27}$$

where $\mathcal{L}_h$,

$$\mathcal{L}_h(\boldsymbol{r}) \ = \ e^{\frac{1}{2}\beta U(\boldsymbol{r})}\, \mathcal{L}(\boldsymbol{r})\, e^{-\frac{1}{2}\beta U(\boldsymbol{r})} \tag{12.28}$$

is connected with $\mathcal{L}$ through a similarity transformation. Using (12.2) one can write

$$\mathcal{L}_h(\boldsymbol{r}) \ = \ e^{\frac{1}{2}\beta U(\boldsymbol{r})}\, \nabla \cdot D(\boldsymbol{r})\, e^{-\beta U(\boldsymbol{r})}\, \nabla\, e^{\frac{1}{2}\beta U(\boldsymbol{r})}\ . \tag{12.29}$$

We want to prove now that $\mathcal{L}_h(\boldsymbol{r})$, as given by (12.29), is a self-adjoint operator for suitable boundary conditions restricting the elements of the function space considered. Using, for some scalar test function f, the property $\nabla \exp[\frac{1}{2}\beta U(\boldsymbol{r})]\, f \ = \ \exp[\frac{1}{2}\beta U(\boldsymbol{r})] \nabla f \ - \ \frac{1}{2}\beta \boldsymbol{F}\, f$ yields

$$\mathcal{L}_h(\boldsymbol{r}) \ = \ e^{\frac{1}{2}\beta U(\boldsymbol{r})}\, \nabla \cdot D(\boldsymbol{r})\, e^{-\frac{1}{2}\beta U(\boldsymbol{r})} \left[\nabla \ - \ \frac{1}{2}\boldsymbol{F} \right]\ . \tag{12.30}$$

Employing the property $\nabla \cdot \exp[-\frac{1}{2}\beta U(\boldsymbol{r})]\, \boldsymbol{v} \ = \ \exp[-\frac{1}{2}\beta U(\boldsymbol{r})]\, (\nabla \cdot \boldsymbol{v} \ + \ \frac{1}{2}\beta \boldsymbol{F} \cdot \boldsymbol{v})$, which holds for some vector-valued function $\boldsymbol{v}$, leads to

$$\mathcal{L}_h(\boldsymbol{r}) \ = \ \nabla \cdot D\, \nabla \ - \ \frac{1}{2}\beta \nabla \cdot D\, \boldsymbol{F} \ + \ \frac{1}{2}\beta \boldsymbol{F} \cdot (\, D \nabla \ - \ \frac{1}{2}\beta \boldsymbol{F}\,)\ . \tag{12.31}$$

The identity $\nabla D \boldsymbol{F} f \ = \ D\boldsymbol{F} \cdot \nabla f \ + \ f\, \nabla \cdot D\boldsymbol{F}$ allows one to express finally

$$\mathcal{L}_h(\boldsymbol{r}) \ = \ \nabla \cdot D\, \nabla \ + \ \frac{1}{2}\beta((\nabla \cdot \boldsymbol{F})) \ - \ \frac{1}{4}\beta^2 \boldsymbol{F}^{\,2} \tag{12.32}$$

where $((\cdots))$ indicates a multiplicative operator, i.e., indicates that the operator inside the double brackets acts solely on functions within the bracket. One can write the operator (12.32) also in the form

$$\mathcal{L}_h(\boldsymbol{r}) \ = \ \mathcal{L}_{oh}(\boldsymbol{r}) \ + \ U(\boldsymbol{r}) \tag{12.33}$$

$$\mathcal{L}_{oh}(\boldsymbol{r}) \ = \ \nabla \cdot D\, \nabla \tag{12.34}$$

$$U(\boldsymbol{r}) \ = \ \frac{1}{2}\beta((\nabla \cdot \boldsymbol{F})) \ - \ \frac{1}{4}\beta^2 \boldsymbol{F}^{\,2} \tag{12.35}$$

where it should be noted that $U(\boldsymbol{r})$ is a multiplicative operator.
One can show now, using (9.20–9.23), that Eqs. (12.33–12.35) define a self-adjoint operator. For this purpose we note that the term (12.35) of $\mathcal{L}_h$ is self-adjoint for any pair of functions $\tilde{f}, \tilde{g}$, i.e.,

$$\int_\Omega d\boldsymbol{r}\, \tilde{g}(\boldsymbol{r})\, U(\boldsymbol{r})\, \tilde{f}(\boldsymbol{r}) \;=\; \int_\Omega d\boldsymbol{r}\, \tilde{f}(\boldsymbol{r})\, U(\boldsymbol{r})\, \tilde{g}(\boldsymbol{r})\;. \tag{12.36}$$

Applying (9.20–9.23) for the operator $\mathcal{L}_{oh}(\boldsymbol{r})$, i.e., using (9.20–9.23) in the case $\boldsymbol{F} \equiv 0$, implies

$$\int_\Omega d\boldsymbol{r}\, \tilde{g}(\boldsymbol{r})\, \mathcal{L}_{oh}(\boldsymbol{r})\, \tilde{f}(\boldsymbol{r}) \;=\; \int_\Omega d\boldsymbol{r}\, \tilde{f}(\boldsymbol{r})\, \mathcal{L}^\dagger_{oh}(\boldsymbol{r})\, \tilde{g}(\boldsymbol{r}) \;+\; \int_{\partial\Omega} d\boldsymbol{a}\cdot \boldsymbol{P}(\tilde{g},\tilde{f}) \tag{12.37}$$

$$\mathcal{L}^\dagger_{oh}(\boldsymbol{r}) \;=\; \nabla\cdot D(\boldsymbol{r})\,\nabla \tag{12.38}$$

$$\boldsymbol{P}(\tilde{g},\tilde{f}) \;=\; \tilde{g}(\boldsymbol{r})D(\boldsymbol{r})\nabla\tilde{f}(\boldsymbol{r}) \;-\; \tilde{f}(\boldsymbol{r})D(\boldsymbol{r})\nabla\tilde{g}(\boldsymbol{r})\;. \tag{12.39}$$

In the present case holds $\mathcal{L}_{oh}(\boldsymbol{r}) = \mathcal{L}^\dagger_{oh}(\boldsymbol{r})$, i.e., in the space of functions which obey

$$\hat{n}(\boldsymbol{r})\cdot\boldsymbol{P}(\tilde{g},\tilde{f}) \;=\; 0 \qquad \text{for } \boldsymbol{r}\in\partial\Omega \tag{12.40}$$

the operator $\mathcal{L}_{oh}$ is self-adjoint. The boundary condition (12.40) implies

$$(\tilde{\imath}) \qquad \hat{\mathrm{n}}(\boldsymbol{r})\cdot \mathrm{D}(\boldsymbol{r})\nabla\,\tilde{\mathrm{f}}(\boldsymbol{r}) \;=\; 0, \qquad \boldsymbol{r}\in\partial\Omega \tag{12.41}$$

$$(\tilde{\imath\imath}) \qquad \tilde{\mathrm{f}}(\boldsymbol{r}) \;=\; 0, \qquad \boldsymbol{r}\in\partial\Omega \tag{12.42}$$

$$(\tilde{\imath\imath\imath}) \qquad \hat{\mathrm{n}}(\boldsymbol{r})\cdot \mathrm{D}(\boldsymbol{r})\nabla\,\tilde{\mathrm{f}}(\boldsymbol{r}) \;=\; w(\boldsymbol{r})\,\tilde{f}(\boldsymbol{r}), \quad \boldsymbol{r}\in\partial\Omega \tag{12.43}$$

and the same for $\tilde{g}(\boldsymbol{r})$, i.e., $(\tilde{\imath})$ must hold for both $\tilde{f}$ and $\tilde{g}$, or $(\tilde{\imath\imath})$ must hold for both $\tilde{f}$ and $\tilde{g}$, or $(\tilde{\imath\imath\imath})$ must hold for both $\tilde{f}$ and $\tilde{g}$.
In the function space characterized through the boundary conditions (12.41–12.43) the operator $\mathcal{L}_h$ is then also self-adjoint. This property implies that eigenfunctions $\tilde{u}_n(\boldsymbol{r})$ with real eigenvalues exists, i.e.,

$$\mathcal{L}_h(\boldsymbol{r})\,\tilde{u}_n(\boldsymbol{r}) \;=\; \lambda_n\tilde{u}_n(\boldsymbol{r})\,, n \;=\; 0,1,2,\ldots\,, \qquad \lambda_n\in\mathbb{R} \tag{12.44}$$

a property, which is discussed at length in textbooks of quantum mechanics regrading the eigenfunctions and eigenvalues of the Hamiltonian operator[2]. The eigenfunctions and eigenvalues in (12.44) can form a discrete set, as indicated here, but may also form a continuous set or a mixture of both; continuous eigenvalues arise for diffusion in a space Ω, an infinite subspace of which is accessible. We want to assume in the following a discrete set of eigenfunctions.
The volume integral defines a scalar product in the function space

$$\langle f|g\rangle_\Omega \;=\; \int_\Omega d\boldsymbol{r}\, f(\boldsymbol{r})\, g(\boldsymbol{r})\;. \tag{12.45}$$

With respect to this scalar product the eigenfunctions for different eigenvalues are orthogonal, i.e.,

$$\langle\tilde{u}_n|\tilde{u}_m\rangle_\Omega \;=\; 0 \qquad \text{for } \lambda_n \neq \lambda_m. \tag{12.46}$$

This property follows from the identity

$$\langle\tilde{u}_n|\mathcal{L}_h\,\tilde{u}_m\rangle_\Omega \;=\; \langle\mathcal{L}_h\,\tilde{u}_n|\tilde{u}_m\rangle_\Omega \tag{12.47}$$

[2]See also textbooks on Linear Alegebra, e.g., "Introduction to Linear Algebra", G. Strang (Wellesley-Cambridge Press, Wellesley, MA, 1993)

which can be written, using (12.44),

$$(\lambda_n - \lambda_m)\,\langle\tilde{u}_n|\tilde{u}_m\rangle_\Omega = 0\,. \tag{12.48}$$

For $\lambda_n \neq \lambda_m$ follows $\langle\tilde{u}_n|\tilde{u}_m\rangle_\Omega = 0$. A normalization condition $\langle\tilde{u}_n|\tilde{u}_n\rangle_\Omega = 1$ can be satisfied for the present case of a finite diffusion domain Ω or a confining potential in which case discrete spectra arise. The eigenfunctions for identical eigenvalues can also be chosen orthogonal, possibly requiring a linear transformation[3], and the functions can be normalized such that the following orthonormality property holds

$$\langle\tilde{u}_n|\tilde{u}_m\rangle_\Omega = \delta_{nm}\,. \tag{12.49}$$

Finally, the eigenfunctions form a complete basis, i.e., any function f in the respective function space, observing boundary conditions (12.41–12.43), can be expanded in terms of the eigenfunctions

$$\tilde{f}(\boldsymbol{r}) = \sum_{n=0}^{\infty} \alpha_n \tilde{u}_n(\boldsymbol{r}) \tag{12.50}$$

$$\alpha_n = \langle\tilde{u}_n|\tilde{f}\rangle_\Omega\,. \tag{12.51}$$

The mathematical theory of such eigenfunctions is not trivial and has been carried out in connection with quantum mechanics for which the operator of the type $\mathcal{L}_h$, in case of constant D, plays the role of the extensively studied Hamiltonian operator. We will assume, without further comments, that the operator $\mathcal{L}_h$ gives rise to a set of eigenfunctions with properties (12.44, 12.49–12.51)[4].

12.3 Eigenfunctions and Eigenvalues of the Smoluchowski Operator

The eigenfunctions $\tilde{u}_n(\boldsymbol{r})$ allow one to obtain the eigenfunctions $v_n(\boldsymbol{r})$ of the Smoluchowski operator $\mathcal{L}$. It holds, inverting the transformation (12.2),

$$v_n(\boldsymbol{r}) = e^{-\beta U/2}\,\tilde{u}_n(\boldsymbol{r}) \tag{12.52}$$

For this function follows from (12.2, 12.28, 12.44)

$$\begin{aligned} \mathcal{L}\,v_n &= e^{-\beta U/2}\,e^{\beta U/2}\nabla\cdot D(\boldsymbol{r})\,e^{-\beta U(\boldsymbol{r})}\,\nabla\,e^{\beta U(\boldsymbol{r})/2}\,\tilde{u}_n \\ &= e^{-\beta U/2}\,\mathcal{L}_h\tilde{u}_n = e^{-\beta U/2}\,\lambda_n\,\tilde{u}_n\,, \end{aligned} \tag{12.53}$$

i.e.,

$$\mathcal{L}(\boldsymbol{r})\,v_n(\boldsymbol{r}) = \lambda_n v_n(\boldsymbol{r})\,. \tag{12.54}$$

The eigenfunctions w_n of the adjoint Smoluchowski operator $\mathcal{L}^\dagger$ (9.38) are given by

$$w_n(\boldsymbol{r}) = e^{\beta U(\boldsymbol{r})/2}\,\tilde{u}_n(\boldsymbol{r}) \tag{12.55}$$

and can be expressed equivalently, comparing (12.55) and (12.52),

$$w_n(\boldsymbol{r}) = e^{\beta U(\boldsymbol{r})}\,v_n(\boldsymbol{r})\,. \tag{12.56}$$

[3] A method to obtain orthogonal eigenfunctions is the Schmitt orthogonalization.

[4] see also "Advanced Calculus for Applications, 2nd Ed." F.B.. Hildebrand, Prentice Hall 1976, ISBN 0-13-011189-9, which contains e.g., the proof of the orthogonality of eigenfunctions of the Smoluchowski operator.

In fact, using (9.38, 12.2, 12.54), one obtains

$$\mathcal{L}^\dagger w_n \;=\; e^{\beta U}\nabla\cdot D\, e^{-\beta U}\,\nabla\, e^{\beta U}\, v_n \;=\; e^{\beta U}\,\mathcal{L}\, v_n = \; e^{\beta U}\,\lambda_n\, v_n \tag{12.57}$$

or

$$\mathcal{L}^\dagger(\boldsymbol{r})\, w_n(\boldsymbol{r}) \;=\; \lambda_n\, w_n(\boldsymbol{r}) \tag{12.58}$$

which proves the eigenfunction property.
The orthonormality conditions (12.49) can be written

$$\begin{aligned}\delta_{nm} \;&=\; \langle\tilde{u}_n|\tilde{u}_m\rangle_\Omega \;=\; \int_\Omega d\boldsymbol{r}\;\tilde{u}_n(\boldsymbol{r})\,\tilde{u}_m(\boldsymbol{r}) \\ &=\; \int_\Omega d\boldsymbol{r}\, e^{-\beta U(\boldsymbol{r})/2}\,\tilde{u}_n(\boldsymbol{r})\; e^{\beta U(\boldsymbol{r})/2}\,\tilde{u}_m(\boldsymbol{r})\;.\end{aligned} \tag{12.59}$$

or, using (12.52, 12.55),

$$\langle w_n|v_m\rangle_\Omega \;=\; \delta_{nm}\;. \tag{12.60}$$

Accordingly, the set of eigenfunctions $\{w_n, n=0,1,\dots\}$ and $\{v_n, n=0,1,\dots\}$, defined in (12.55) and (12.52), form a so-called *bi-orthonormal system*, i.e., the elements of the sets $\{w_n, n=0,1,\dots\}$ and $\{v_n, n=0,1,\dots\}$ are mutually orthonormal.
We want to investigate now the boundary conditions obeyed by the functions $e^{\beta U/2}\,\tilde{f}$ and $e^{-\beta U/2}\,\tilde{g}$ when $\tilde{f},\tilde{g}$ obey conditions (12.41–12.43). According to (12.2) holds, in case of $e^{\beta U/2}\,\tilde{f}$,

$$e^{\beta U/2}\,\tilde{f} \;=\; e^{\beta U}\, f\;. \tag{12.61}$$

According to (12.41–12.43), the function f obeys then

$$\text{(i)}\qquad \widehat{n}(\boldsymbol{r})\cdot D(\boldsymbol{r})\nabla\, e^{\beta U}\, f(\boldsymbol{r}) \;=\; 0, \qquad \boldsymbol{r}\;\in\;\partial\Omega \tag{12.62}$$

$$\text{(ii)}\qquad e^{\beta U}\, f(\boldsymbol{r}) \;=\; 0, \qquad \boldsymbol{r}\;\in\;\partial\Omega \tag{12.63}$$

$$\text{(iii)}\qquad \widehat{n}(\boldsymbol{r})\cdot D(\boldsymbol{r})\nabla\, e^{\beta U}\, f(\boldsymbol{r}) \;=\; w(\boldsymbol{r})\, e^{\beta U}\, f(\boldsymbol{r}),\; \boldsymbol{r}\;\in\;\partial\Omega \tag{12.64}$$

which is equivalent to the conditions (9.7, 9.5, 9.8) for the solutions of the Smoluchowski equation. We have established, therefore, that the boundary conditions assumed for the function space connected with the self-adjoint Smoluchowski operator $\mathcal{L}_h$ are consistent with the boundary conditions assumed previously for the Smoluchowski equation. One can veryfy similarly that the functions $e^{-\beta U/2}\,\tilde{g}$ imply the boundary conditions (9.7, 9.5, 9.8) for the adjoint Smoluchowski equation.

Projection Operators

We consider now the following operators defined through the pairs of eigenfunctions v_n, w_n of the Smoluchowski operators $\mathcal{L}, \mathcal{L}^\dagger$

$$\hat{J}_n\, f \;=\; v_n\,\langle w_n|f\rangle_\Omega \tag{12.65}$$

where f is some test function. For these operators holds

$$\hat{J}_n\hat{J}_m\, f \;=\; \hat{J}_n v_m\,\langle w_m|f\rangle_\Omega \;=\; v_n\,\langle w_n|v_m\rangle_\Omega\,\langle w_m|f\rangle_\Omega\;. \tag{12.66}$$

Using (12.60) one can write this

$$\hat{J}_n \hat{J}_m f \;=\; v_n \, \delta_{nm} \langle w_m | f \rangle_\Omega \tag{12.67}$$

and, hence, using the definition (12.65)

$$\hat{J}_n \hat{J}_m \;=\; \delta_{nm} \hat{J}_m \; . \tag{12.68}$$

This property identifies the operators $\hat{J}_n$, $n = 0, 1, 2, \ldots$ as mutually complementary projection operators, i.e., each $\hat{J}_n$ is a projection operator ($\hat{J}_n^2 = \hat{J}_n$) and two different $\hat{J}_n$ and $\hat{J}_m$ project onto orthogonal subspaces of the function space.
The completeness property (12.50, 12.51) of the set of eigenfunctions $\tilde{u}_n$ can be expressed in terms of the operators $\hat{J}_n$. For this purpose we consider

$$\alpha_n \;=\; \langle \tilde{u}_n | \tilde{f} \rangle_\Omega \;=\; \int_\Omega d\boldsymbol{r} \; \tilde{u}_n \; \tilde{f} \tag{12.69}$$

Using $\tilde{u}_n = \exp(\beta U/2) \, v_n$ and $\tilde{f} = \exp(\beta U/2) \, f$ [see (12.52, 12.2)] as well as (12.56) one can express this

$$\alpha_n \;=\; \int_\Omega d\boldsymbol{r} \, \exp(\beta U/2) \, v_n \, \exp(\beta U/2) \, f \;=\; \int_\Omega d\boldsymbol{r} \, \exp(\beta U) \, v_n \, f \;=\; \langle w_n | f \rangle_\Omega$$

Equations (12.50, 12.51) read then for $\tilde{f} = \exp(\beta U/2) \, f$

$$f \;=\; \sum_{n=0}^{\infty} e^{\beta U/2} \; u_n \, \langle w_n | f \rangle_\Omega \tag{12.70}$$

and, using again (12.52) and (12.65)

$$f \;=\; \sum_{n=0}^{\infty} \hat{J}_n \, f \tag{12.71}$$

Since this holds for any f in the function space with proper boundary conditions we can conclude that within the function space considered holds

$$\sum_{n=0}^{\infty} \hat{J}_n \;=\; \mathbb{1} \; . \tag{12.72}$$

The projection operators $\hat{J}_n$ obey, furthermore, the property

$$\mathcal{L}(\boldsymbol{r}) \, \hat{J}_n \;=\; \lambda_m \, \hat{J}_n \; . \tag{12.73}$$

This follows from the definition (12.65) together with (12.54).

The Propagator

The solution of (12.1–12.3) can be written formally

$$p(\boldsymbol{r}, t) \;=\; \left[e^{\mathcal{L}(\boldsymbol{r})(t - t_o)} \right]_{\mathrm{bc}} f(\boldsymbol{r}) \; . \tag{12.74}$$

The brackets $[\cdots]_{\rm bc}$ indicate that the operator is defined in the space of functons which obey the chosen spatial boundary conditions. The exponential operator $\exp[\mathcal{L}(\boldsymbol{r})(t-t_o)]$ in (12.74) is defined through the Taylor expansion

$$\left[e^A\right]_{\rm bc} \;=\; \sum_{\nu=0}^{\infty} \frac{1}{\nu!}\,[A]^{\nu}_{\rm bc}\;. \tag{12.75}$$

The operator $[\exp[\mathcal{L}(\boldsymbol{r})(t-t_o)]\,]_{\rm bc}$ plays a central role for the Smoluchowski equation; it is referred to as the *propagator*. One can write, dropping the argument $\boldsymbol{r}$,

$$\left[\,e^{\mathcal{L}(t-t_o)}\,\right]_{\rm bc} \;=\; e^{\mathcal{L}(t-t_o)}\,\sum_{n=0}^{\infty}\hat{J}_n \tag{12.76}$$

since the projection operators project out the functions with proper boundary conditions. For any function $Q(z)$, which has a convergent Taylor series for all $z = \lambda_n$, $n = 0, 1, \ldots$, holds

$$Q(\mathcal{L})\,v_n \;=\; Q(\lambda_n)\,v_n \tag{12.77}$$

and, hence, according to (12.73)

$$Q(\mathcal{L})\,\hat{J}_n \;=\; Q(\lambda_n)\,\hat{J}_n \tag{12.78}$$

This property, which can be proven by Taylor expansion of $Q(\mathcal{L})$, states that if a function of $\mathcal{L}$ "sees" an eigenfunction v_n, the operator $\mathcal{L}$ turns itself into the scalar λ_n. Since the Taylor expansion of the exponential operator converges everywhere on the real axis, it holds

$$e^{\mathcal{L}(t-t_o)}\,v_n \;=\; e^{\lambda_n(t-t_o)}\,v_n\;. \tag{12.79}$$

The expansion can then be written

$$\left[\,e^{\mathcal{L}(t-t_o)}\,\right]_{\rm bc} \;=\; \sum_{n=0}^{\infty} e^{\lambda_n(t-t_o)}\,\hat{J}_n\;. \tag{12.80}$$

We assume here and in the following the ordering of eigenvalues

$$\lambda_0 \;\geq\; \lambda_1 \;\geq\; \lambda_2 \;\cdots \tag{12.81}$$

which can be achieved by choosing the labels n, $n = 0, 1, \ldots$ in the appropriate manner.

The Spectrum of the Smoluchowski Operator

We want to comment finally on the eigenvalues λ_n appearing in series (12.81). The minimum principle for the free energy $G[p(\boldsymbol{r},t)]$ derived in the beginning of this section requires that for reflective boundary conditions (9.4, 9.32) any solution $p(\boldsymbol{r},t)$ of the Smoluchowski equation (12.1–12.3), at long times, decays towards the equilibrium distribution (12.22) for which holds [cf. (12.21)]

$$\mathcal{L}\,p_o(\boldsymbol{r}) \;=\; \nabla\cdot D(\boldsymbol{r})\,e^{-\beta U(\boldsymbol{r})}\,\nabla\,e^{\beta U(\boldsymbol{r})}\,p_o(\boldsymbol{r}) \;=\; 0\;. \tag{12.82}$$

This identifies the equilibrium (Botzmann) distribution as the eigenfunction of $\mathcal{L}$ with vanishing eigenvalue. One can argue that this eigenvalue is, in fact, the largest eigenvalue of $\mathcal{L}$, i.e., for the "reflective" boundary condition (9.4)

$$\lambda_0 \;=\; 0 \;>\; \lambda_1 \;\geq\; \lambda_2 \;\cdots \tag{12.83}$$

The reason is that the minimum principle (12.20) for the free energy $G[p(\boldsymbol{r},t)]$ implies that any solution of the Smoluchowski equation with reflective boundary condition must asymptotically, i.e., for $t \to \infty$, decay towards $p_o(\boldsymbol{r})$ [cf. (12.21, 12.22)].
One can identify $p_o(\boldsymbol{r})$ with an eigenfunction $v_{n_o}(\boldsymbol{r})$ of $\mathcal{L}$ since $\mathcal{L}v_o = 0$ implies that $p_o(\boldsymbol{r})$ is an eigenfunction with vanishing eigenvalue. According to (12.22) and (12.57) holds that $w_{n_o}(\boldsymbol{r})$, the respective eigenfunction of $\mathcal{L}^\dagger$, is a constant which one may choose

$$w_{n_o} \equiv 1 \,. \tag{12.84}$$

Adopting the normalization $\langle w_{n_o}|v_{n_o}\rangle_\Omega = 1$ implies

$$v_{n_o}(\boldsymbol{r}) = p_o(\boldsymbol{r}) \,. \tag{12.85}$$

One can expand then any solution of the Smoluchowski equation, using (12.74, 12.80) and $\lambda_{n_o} = 0$,

$$\begin{aligned} p(\boldsymbol{r},t) &= \sum_{n=0}^{\infty} e^{\lambda_n (t-t_o)} \hat{J}_n \, f(\boldsymbol{r}) \\ &= \hat{J}_{n_o} \, f(\boldsymbol{r}) + \sum_{n \neq n_o} e^{\lambda_n (t-t_o)} \hat{J}_n \, f(\boldsymbol{r}) \,. \end{aligned} \tag{12.86}$$

The definition of $\hat{J}_{n_o}$ yields with (12.84, 12.85) and (12.4),

$$p(\boldsymbol{r},t) = p_o(\boldsymbol{r}) + \sum_{n \neq n_o} e^{\lambda_n (t-t_o)} v_n(\boldsymbol{r}) \langle w)n|f\rangle_\Omega \,. \tag{12.87}$$

The decay of $p(\boldsymbol{r},t)$ towards $p_o(\boldsymbol{r})$ for $t \to \infty$ implies then

$$\lim_{t\to\infty} e^{\lambda_n (t-t_o)} = 0 \tag{12.88}$$

from which follows $\lambda_n < 0$ for $n \neq n_o$. One can conclude for the spectrum of the Smuluchowski operator

$$\lambda_0 = 0 > \lambda_1 \geq \lambda_2 \geq \cdots \tag{12.89}$$

12.4 Brownian Oscillator

We want to demonstrate the spectral expansion method, introduced in this chapter, to the case of a Brownian oscillator governed by the Smoluchowski equation for a harmonic potential

$$U(x) = \frac{1}{2} f \, x^2 \,, \tag{12.90}$$

$$namely, by \partial_t p(x,t|x_0,t_0) = D(\partial_x^2 + \beta f \; \partial_x x) \, p(x,t|x_0,t_0) \tag{12.91}$$

with the boundary condition

$$\lim_{x\to\pm\infty} x^n \, p(x,t|x_0,t_0) = 0, \quad \forall n \in I\!N \tag{12.92}$$

and the initial condition

$$p(x,t_0|x_0,t_0) = \delta(x - x_0) \,. \tag{12.93}$$

In order to simplify the analysis we follow the treatment of the Brownian oscillator in Chapter 3 and introduce dimensionless variables

$$\xi \;=\; x/\sqrt{2}\delta\,, \qquad \tau \;=\; t/\tilde{\tau}\,, \tag{12.94}$$

where

$$\delta = \sqrt{k_B T/f}\,, \qquad \tilde{\tau} \;=\; 2\delta^2/D\,. \tag{12.95}$$

The Smoluchowski equation for the normalized distribution in ξ, given by

$$q(\xi,\tau|\xi_0,\tau_0) \;=\; \sqrt{2}\,\delta\; p(x,t|x_0,t_0)\,, \tag{12.96}$$

is then again [c.f. (4.98)]

$$\partial_\tau q(\xi,\tau|\xi_0,\tau_0) = (\partial_\xi^2 + 2\,\partial_\xi\;\xi)\, q(\xi,\tau|\xi_0,\tau_0) \tag{12.97}$$

with the initial condition

$$q(\xi,\tau_0|\xi_0,\tau_0) \;=\; \delta(\xi-\xi_0) \tag{12.98}$$

and the boundary condition

$$\lim_{\xi\to\pm\infty} \xi^n\, q(\xi,\tau|\xi_0,\tau_0) = 0, \quad \forall n \in I\!N\,. \tag{12.99}$$

This equation describes diffusion in thepotential $\tilde{U}(\xi) \;=\; \xi^2$. Using (13.9, 13.9, 12.90) one can show $\tilde{U}(\xi) \;=\; \beta U(x)$.
We seek to expand $q(\xi,\tau_0|\xi_0,\tau_0)$ in terms of the eigenfunctions of the operator

$$\mathcal{L}(\xi) \;=\; \partial_\xi^2 + 2\partial_\xi\xi\,, \tag{12.100}$$

restricting the functions to the space

$$\{h(\xi)\,|\,\lim_{\xi\to\pm\infty}\, \xi^n\, h(\xi) = 0\}\,. \tag{12.101}$$

The eigenfunctions $f_n(\xi)$ of $\mathcal{L}(\xi)$ are defined through

$$\mathcal{L}(\xi) f_n(\xi) \;=\; \lambda_n f_n(\xi) \tag{12.102}$$

Corresponding functions, which also obey (13.14), are

$$f_n(\xi) = c_n\, e^{-\xi^2}\, H_n(\xi)\,. \tag{12.103}$$

where $H_n(x)$ is the n-th Hermite polynomials and where c_n is a normalization constant chosen below. The eigenvalues are

$$\lambda_n \;=\; -\,2n, \tag{12.104}$$

As demonstrated above, the eigenfunctions of the Smoluchowski operator do not form an orthonormal basis with the scalar product (3.129) and neither do the functions $f_n(\xi)$ in (13.18). Instead, they obey the orthogonality property

$$\int_{-\infty}^{+\infty} d\xi\, e^{-\xi^2} H_n(\xi) H_m(\xi) \;=\; 2^n n!\sqrt{\pi}\delta_{nm}\,. \tag{12.105}$$

which allows one to identify a bi-orthonormal system of functions. For this purpose we choose for $f_n(\xi)$ the normalization

$$f_n(\xi) \;=\; \frac{1}{2^n n!\sqrt{\pi}}\, e^{-\xi^2}\, H_n(\xi) \tag{12.106}$$

and define

$$g_n(\xi) \;=\; H_n(\xi)\,. \tag{12.107}$$

One can readily recognize then from (13.20) the biorthonormality property

$$\langle g_n | f_n \rangle = \delta_{nm}\;. \tag{12.108}$$

The functions $g_n(\xi)$ can be identified with the eigenfunctions of the adjoint operator

$$\mathcal{L}^+(\xi) = \partial_\xi^2 - 2\xi\partial_\xi\;, \tag{12.109}$$

obeying

$$\mathcal{L}^+(\xi) g_n(\xi) \;=\; \lambda_n g_n(\xi)\;. \tag{12.110}$$

Comparing (13.18) and (13.22) one can, in fact, discern

$$g_n(\xi) \;\sim\; e^{\xi^2}\; g_n(\xi). \tag{12.111}$$

and, since $\xi^2 \;=\; fx^2/2k_BT$ [c.f. (13.9, 13.11)], the functions $g_n(\xi)$, according to (12.56), are the eigenfunctions of $\mathcal{L}^+(\xi)$.
The eigenfunctions $f_n(\xi)$ form a complete basis for all functions with the property (13.14). Hence, we can expand $q(\xi,\tau|\xi_0,\tau_0)$

$$q(\xi,\tau|\xi_0,\tau_0) = \sum_{n=0}^{\infty} \alpha_n(t) f_n(\xi)\;. \tag{12.112}$$

Inserting this into the Smoluchowski equation (13.12, 13.15) results in

$$\sum_{n=0}^{\infty} \dot{\alpha}_n(\tau) f_n(\xi) \;=\; \sum_{n=0}^{\infty} \lambda_n\; \alpha_n(\tau)\; f_n(\xi)\,. \tag{12.113}$$

Exploiting the bi-orthogonality property (13.23) one derives

$$\dot{\alpha}_m(\tau) \;=\; \lambda_m\; \alpha_m(\tau)\,. \tag{12.114}$$

The general solution of of this differential equation is

$$\alpha_m(\tau) = \beta_m\; e^{\lambda_m \tau}\;. \tag{12.115}$$

Upon substitution into (13.27), the initial condition (13.13) reads

$$\sum_{n=0}^{\infty} \beta_n\, e^{\lambda_n \tau_0}\, f_n(\xi) \;=\; \delta(\xi-\xi_0)\;. \tag{12.116}$$

Taking again the scalar product with $g_m(\xi)$ and using (13.23) results in

$$\beta_m \, e^{\lambda_m \tau_0} = g_m(\xi_0) \, , \tag{12.117}$$

or

$$\beta_m = e^{-\lambda_m \tau_0} \, g_m(\xi_0) \, . \tag{12.118}$$

Hence, we obtain finally

$$q(\xi, \tau | \xi_0, \tau_0) \, = \, \sum_{n=0}^{\infty} e^{\lambda_n (\tau - \tau_0)} \, g_n(\xi_0) \, f_n(\xi) \, , \tag{12.119}$$

or, explicitly,

$$q(\xi, \tau | \xi_0, \tau_0) \, = \, \sum_{n=0}^{\infty} \frac{1}{2^n n! \sqrt{\pi}} \, e^{-2n(\tau - \tau_0)} \, H_n(\xi_0) \, e^{-\xi^2} \, H_n(\xi) \, . \tag{12.120}$$

Expression (13.35) can be simplified using the generating function of a product of two Hermit polynomials

$$\frac{1}{\sqrt{\pi(1-s^2)}} \, \exp\left[-\tfrac{1}{2}(y^2 + y_0^2) \, \tfrac{1+s^2}{1-s^2} \, + \, 2 y y_0 \, \tfrac{s}{1-s^2} \right]$$

$$= \sum_{n=0}^{\infty} \frac{s^n}{2^n n! \sqrt{\pi}} \, H_n(y) \, e^{-y^2/2} \, H_n(y_0) \, e^{-y_0^2/2} \, . \tag{12.121}$$

Using

$$s = e^{-2(\tau - \tau_0)} \, , \tag{12.122}$$

one can show

$q(\xi, \tau | \xi_0, \tau_0)$

$$= \, \frac{1}{\sqrt{\pi(1-s^2)}} \exp\left[-\frac{1}{2}(\xi^2 + \xi_0^2) \, \frac{1+s^2}{1-s^2} \, + \, 2 \xi \xi_0 \, \frac{s}{1-s^2} \, - \, \frac{1}{2}\xi^2 \, + \, \frac{1}{2}\xi_0^2 \right] \, . \tag{12.123}$$

We denote the exponent on the r.h.s. by E and evaluate

$$\begin{aligned} E \quad &= \quad -\xi^2 \frac{1}{1-s^2} \, - \, \xi_0^2 \frac{s^2}{1-s^2} \, + \, 2 \xi \xi_0 \frac{1}{1-s^2} \\ &= \quad -\frac{1}{1-s^2} (\xi^2 \, - \, 2 \xi \xi_0 s \, + \, \xi_0^2 s^2) \\ &= \quad -\frac{(\xi - \xi_0 s)^2}{1-s^2} \end{aligned} \tag{12.124}$$

We obtain then

$$q(\xi, \tau | \xi_0, \tau_0) \, = \, \frac{1}{\sqrt{\pi(1-s^2)}} \, \exp\left[-\frac{(\xi - \xi_0 s)^2}{1-s^2} \right] \, , \tag{12.125}$$

where s is given by (13.37). One can readily recognize that this result agrees with the solution (4.119) derived in Chapter 3 using transformation to time-dependent coordinates.
Let us now consider the solution for an initial distribution $f(\xi_0)$. The corresponding distribution $\tilde{q}(\xi,\tau)$ is ($\tau_0 = 0$)

$$\tilde{q}(\xi,\tau) \;=\; \int d\xi_0 \,\frac{1}{\sqrt{\pi(1-e^{-4\tau})}}\,\exp\left[-\frac{(\xi-\xi_0 e^{-2\tau})^2}{1-e^{-4\tau}}\right]\,f(\xi_0)\;. \tag{12.126}$$

It is interesting to consider the asymptotic behaviour of this solution. For $\tau \to \infty$ the distribution $\tilde{q}(\xi,\tau)$ relaxes to

$$\tilde{q}(\xi) \;=\; \frac{1}{\sqrt{\pi}}\,e^{-\xi^2}\,\int d\xi_0\,f(\xi_0)\;. \tag{12.127}$$

If one carries out a corresponding analysis using (13.34) one obtains

$$\tilde{q}(\xi,\tau) \;=\; \sum_{n=0}^{\infty} e^{\lambda_n \tau}\,f_n(\xi)\int d\xi_0\,g_n(\xi_0)\,f(\xi_0) \tag{12.128}$$

$$\sim\; f_0(\xi)\int d\xi_0\,g_n(\xi_0)\,f(\xi_0) \quad \text{as } \tau\to\infty\;. \tag{12.129}$$

Using (13.21) and (13.22), this becomes

$$\tilde{q}(\xi,\tau) \;\sim\; \frac{1}{\sqrt{\pi}}\,e^{-\xi^2}\,\underbrace{H_0(\xi)}_{=1}\int d\xi_0\,\underbrace{H_0(\xi_0)}_{=1}\,f(\xi_0) \tag{12.130}$$

in agreement with (13.42) as well as with (12.87). One can recognize from this result that the expansion (13.43), despite its appearance, conserves total probability $\int d\xi_0\,f(\xi_0)$. One can also recoginze that, in general, the relaxation of an initial distribution $f(\xi_0)$ to the Boltzmann distribution involves numerous relaxation times $\tau_n = -1/\lambda_n$, even though the original Smoluchowski equation (13.1) contains only a single rate constant, the friction coefficient γ.

Chapter 13

The Brownian Oscillator

Contents

13.1 One-Dimensional Diffusion in a Harmonic Potential 162

The one-dimensional Smoluchowski equation , in case that a stationary flux-free equilibrium state $p_o(x)$ exists, can be written in the form

$$\partial_t p(x,t) \;=\; \frac{k_B T}{\gamma}\,\partial_x\, p_o(x)\;\partial_x\,[p_o(x)]^{-1}\;p(x,t)\;. \tag{13.1}$$

where we employed $D = \sigma^2/2\gamma^2$ [c.f. (3.12)], the fluctuation-dissipation theorem in the form $\sigma^2 = 2k_BT\gamma$ [c.f. (4.15)], the Onsager form of the Smoluchowski equation (4.18) applied to one dimension, and $p_o(x) = N\,\exp[-\beta U(x)]$. The form (13.1) of the Smoluchowski equation demonstrates most clearly that it describes a stochastic system characterized through an equlibrium state $po(x)$ and a single constant γ governing the relaxation, the friction constant. The equation also assumes that the underlying stochastic process

$$\gamma\dot{x} \;=\; k_BTp_o(x)\partial_x\ln[p_o(x)] \;+\; \sqrt{2k_BT\gamma}\xi(t) \tag{13.2}$$

alters the variable x continuously and not in discrete jumps.
One is inclined to envoke the Smoluchowski equation for the description of stochastic processes for which the equlibrium distribution is known. Underlying such description is the assumption that the process is governed by a single effective friction constant γ. For the sake of simplicity and in view of the typical situation that detailed informatiin regarding the relaxation process is lacking, the Smoluchowski equation serves on well with an approximate descsription.
The most prevalent distribution encountered is the Gaussian distribution

$$p_o(x) \;=\; \frac{1}{\sqrt{2\pi\Sigma}}\;\exp\left[-\frac{(x\,-\,\langle x\rangle)^2}{\Sigma}\right]\;. \tag{13.3}$$

The reason is the fact that many properties x are actually based on contributions from many constituents. An example is the overall dipole moment of a biopolymer which results from stochastic motions of the polymer segments, each contributing a small fraction of the total dipole moment. In such case the *central limit theorem* states that for most cases the resulting distribution of x is Gaussian. This leads one to consider then in most cases the Smoluchowski equation for an effective quadratic potential

$$U_{\rm eff}(x) \;=\; \frac{k_BT}{\Sigma}\;(x\,-\,\langle x\rangle)^2\;. \tag{13.4}$$

Due to the central limit theorem the Smoluchowski equation for a Brownian oscillator has a special significance. Accordingly, we will study the behaviour of the Brownian oscillator in detail.

13.1 One-Dimensional Diffusion in a Harmonic Potential

We consider again the diffusion in the harmonic potential

$$U(x) = \frac{1}{2} f x^2 \tag{13.5}$$

applying in the present case spectral expansion for the solution of the associated Smoluchowski equation

$$\partial_t p(x,t|x_0,t_0) = D(\partial_x^2 + \beta f \ \partial_x x)\, p(x,t|x_0,t_0) \tag{13.6}$$

with the boundary condition

$$\lim_{x\to\pm\infty} x^n\, p(x,t|x_0,t_0) = 0, \quad \forall n \in I\!N \tag{13.7}$$

and the initial condition

$$p(x,t_0|x_0,t_0) = \delta(x-x_0)\,. \tag{13.8}$$

Following the treatment in Chapter 3 we introduce dimensionless variables

$$\xi \ = \ x/\sqrt{2}\delta\,, \qquad \tau \ = \ t/\tilde{\tau}\,, \tag{13.9}$$

where

$$\delta = \sqrt{k_B T/f}\,, \qquad \tilde{\tau} \ = \ 2\delta^2/D\,. \tag{13.10}$$

The Smoluchowski equation for the normalized distribution in ξ given by

$$q(\xi,\tau|\xi_0,\tau_0) \ = \ \sqrt{2}\,\delta\; p(x,t|x_0,t_0) \tag{13.11}$$

is then again

$$\partial_\tau q(\xi,\tau|\xi_0,\tau_0) = (\partial_\xi^2 + 2\,\partial_\xi\ \xi)\, q(\xi,\tau|\xi_0,\tau_0) \tag{13.12}$$

with the initial condition

$$q(\xi,\tau_0|\xi_0,\tau_0) \ = \ \delta(\xi-\xi_0) \tag{13.13}$$

and the boundary condition

$$\lim_{\xi\to\pm\infty} \xi^n\, q(\xi,\tau|\xi_0,\tau_0) = 0, \quad \forall n \in I\!N\,. \tag{13.14}$$

We seek to expand $q(\xi,\tau_0|\xi_0,\tau_0)$ in terms of the eigenfunctions of the operator

$$\mathbf{O} = \partial_\xi^2 + 2\partial_\xi \xi\,, \tag{13.15}$$

restricting the functions to the space

$$\{h(\xi) \,|\, \lim_{\xi \to \pm\infty} \xi^n \, h(\xi) = 0\} \; . \tag{13.16}$$

We define the eigenfunctions $f_n(\xi)$ through

$$\mathbf{O} f_n(\xi) = -\lambda_n f_n(\xi) \tag{13.17}$$

The solution of this equation, which obeys (13.14), is well known

$$f_n(\xi) = c_n \, e^{-\xi^2} \, H_n(\xi) \, . \tag{13.18}$$

Here, $H_n(x)$ are the Hermite polynomials and c_n is a normalization constant. The negative eigenvalues are

$$\lambda_n = 2n, \tag{13.19}$$

The functions $f_n(\xi)$ do not form the orthonormal basis with the scalar product (3.129) introduced earlier. Instead, it holds

$$\int_{-\infty}^{+\infty} d\xi \, e^{-\xi^2} H_n(\xi) H_m(\xi) \; = \; 2^n n! \sqrt{\pi} \delta_{nm} \; . \tag{13.20}$$

However, following Chapter 5 one can introduce a bi-orthogonal system. For this purpose we choose for $f_n(\xi)$ the normalization

$$f_n(\xi) \; = \; \frac{1}{2^n n! \sqrt{\pi}} \, e^{-\xi^2} \, H_n(\xi) \tag{13.21}$$

and define

$$g_n(\xi) \; = \; H_n(\xi) \, . \tag{13.22}$$

One can readily recognize from (13.20) the biorthogonality property

$$\langle g_n | f_n \rangle = \delta_{nm} \; . \tag{13.23}$$

The functions $g_n(\xi)$ are the eigenfunctions of the adjoint operator

$$\mathbf{O}^+ = \partial_\xi^2 - 2\xi\partial_\xi \; , \tag{13.24}$$

i.e., it holds

$$\mathbf{O}^+ g_n(\xi) = -\lambda_n g_n(\xi) \; . \tag{13.25}$$

The eigenfunction property (13.25) of $g_n(\xi)$ can be demonstrated using

$$\langle g | \mathbf{O} f \rangle = \langle \mathbf{O}^+ g | f \rangle \; . \tag{13.26}$$

or through explicit evaluation.
The eigenfunctions $f_n(\xi)$ form a complete basis for all functions with the property (13.14). Hence, we can expand $q(\xi, \tau | \xi_0, \tau_0)$

$$q(\xi, \tau | \xi_0, \tau_0) = \sum_{n=0}^{\infty} \alpha_n(t) f_n(\xi) \; . \tag{13.27}$$

Inserting this into the Smoluchowski equation (13.12, 13.15) results in

$$\sum_{n=0}^{\infty} \dot{\alpha}_n(\tau) f_n(\xi) = -\sum_{n=0}^{\infty} \lambda_n \, \alpha_n(\tau) \, f_n(\xi) \, . \tag{13.28}$$

Exploiting the bi-orthogonality property (13.23) one derives

$$\dot{\alpha}_m(\tau) = -\, \lambda_m \, \alpha_m(\tau) \, . \tag{13.29}$$

The general solution of of this differential equation is

$$\alpha_m(\tau) = \beta_m \, e^{-\lambda_m \tau} \, . \tag{13.30}$$

Upon substitution into (13.27), the initial condition (13.13) reads

$$\sum_{n=0}^{\infty} \beta_n \, e^{-\lambda_n \tau_0} \, f_n(\xi) \; = \; \delta(\xi - \xi_0) \, . \tag{13.31}$$

Taking again the scalar product with $g_m(\xi)$ and using (13.23) results in

$$\beta_m \, e^{-\lambda_m \tau_0} = g_m(\xi_0) \, , \tag{13.32}$$

or

$$\beta_m = e^{\lambda_m \tau_0} \, g_m(\xi_0) \, . \tag{13.33}$$

Hence, we obtain finally

$$q(\xi, \tau | \xi_0, \tau_0) \; = \; \sum_{n=0}^{\infty} \, e^{-\lambda_n (\tau - \tau_0)} \, g_n(\xi_0) \, f_n(\xi) \, , \tag{13.34}$$

or, explicitly,

$$q(\xi, \tau | \xi_0, \tau_0) \; = \; \sum_{n=0}^{\infty} \, \frac{1}{2^n n! \sqrt{\pi}} \, e^{-2n(\tau - \tau_0)} \, H_n(\xi_0) \, e^{-\xi^2} \, H_n(\xi) \, . \tag{13.35}$$

Expression (13.35) can be simplified using the generating function of a product of two Hermit polynomials

$$\frac{1}{\sqrt{\pi(1-s^2)}} \, \exp\left[-\tfrac{1}{2}(y^2 + y_0^2) \, \tfrac{1+s^2}{1-s^2} \; + \; 2 y y_0 \, \tfrac{s}{1-s^2} \right]$$

$$= \sum_{n=0}^{\infty} \, \frac{s^n}{2^n n! \sqrt{\pi}} \, H_n(y) \, e^{-y^2/2} \, H_n(y_0) \, e^{-y_0^2/2} \, . \tag{13.36}$$

Using

$$s = e^{-2(\tau - \tau_0)} \, , \tag{13.37}$$

one can show

$q(\xi, \tau | \xi_0, \tau_0)$

$$= \frac{1}{\sqrt{\pi(1-s^2)}} \exp\left[-\frac{1}{2}(\xi^2+\xi_0^2)\,\frac{1+s^2}{1-s^2} + 2\xi\xi_0\,\frac{s}{1-s^2} - \frac{1}{2}\xi^2 + \frac{1}{2}\xi_0^2\right] . \tag{13.38}$$

We denote the exponent on the r.h.s. by E and evaluate

$$\begin{aligned} E &= -\xi^2\frac{1}{1-s^2} - \xi_0^2\frac{s^2}{1-s^2} + 2\xi\xi_0\frac{1}{1-s^2} \\ &= -\frac{1}{1-s^2}(\xi^2 - 2\xi\xi_0 s + \xi_0^2 s^2) \\ &= -\frac{(\xi-\xi_0 s)^2}{1-s^2} \end{aligned} \tag{13.39}$$

We obtain then

$$q(\xi,\tau|\xi_0,\tau_0) = \frac{1}{\sqrt{\pi(1-s^2)}} \exp\left[-\frac{(\xi-\xi_0 s)^2}{1-s^2}\right] , \tag{13.40}$$

where s is given by (13.37). One can readily recognize that this result agrees with the solution (4.119) derived in Chapter 3 using transformation to time-dependent coordinates.
Let us now consider the solution for an initial distribution $h(\xi_0)$. The corresponding distribution $\tilde{q}(\xi,\tau)$ is ($\tau_0 = 0$)

$$\tilde{q}(\xi,\tau) = \int d\xi_0 \frac{1}{\sqrt{\pi(1-e^{-4\tau})}} \exp\left[-\frac{(\xi-\xi_0 e^{-2\tau})^2}{1-e^{-4\tau}}\right] h(\xi_0) . \tag{13.41}$$

It is interesting to consider the asymptotic behaviour of this solution. For $\tau \to \infty$ the distribution $\tilde{q}(\xi,\tau)$ relaxes to

$$\tilde{q}(\xi) = \frac{1}{\sqrt{\pi}}\, e^{-\xi^2} \int d\xi_0\, h(\xi_0) . \tag{13.42}$$

If one carries out a corresponding analysis using (13.34) one obtains

$$\tilde{q}(\xi,\tau) = \sum_{n=0}^{\infty} e^{-\lambda_n \tau} f_n(\xi) \int d\xi_0\, g_n(\xi_0)\, h(\xi_0) \tag{13.43}$$

$$\sim f_0(\xi) \int d\xi_0\, g_n(\xi_0)\, h(\xi_0) \quad \text{as } \tau \to \infty . \tag{13.44}$$

Using (13.21) and (13.22), this becomes

$$\tilde{q}(\xi,\tau) \sim \frac{1}{\sqrt{\pi}}\, e^{-\xi^2} \underbrace{H_0(\xi)}_{=1} \int d\xi_0\, h(\xi_0) \tag{13.45}$$

in agreement with (13.42). One can recognize from this result that the expansion (13.43), despite its appearance, conserves total probability $\int d\xi_0\, h(\xi_0)$. One can also recoginze that, in general, the relaxation of an initial distribution $h(\xi_0)$ to the Boltzmann distribution involves numerous relaxation times, given by the eigenvalues λ_n, even though the original Smoluchowski equation (13.1) contains only a single rate constant, the friction coefficient γ.

Chapter 14

Fokker-Planck Equation in x and v for Harmonic Oscillator

Contents

Chapter 15

Velocity Replacement Echoes

Contents

Chapter 16

Rate Equations for Discrete Processes

Contents

Chapter 17

Generalized Moment Expansion

Contents

Chapter 18

Curve Crossing in a Protein: Coupling of the Elementary Quantum Process to Motions of the Protein

Contents

18.1 Introduction 175
18.2 The Generic Model: Two-State Quantum System Coupled to an Oscillator 177
18.3 Two-State System Coupled to a Classical Medium 179
18.4 Two State System Coupled to a Stochastic Medium 182
18.5 Two State System Coupled to a Single Quantum Mechanical Oscillator 184
18.6 Two State System Coupled to a Multi-Modal Bath of Quantum Mechanical Oscillators 189
18.7 From the Energy Gap Correlation Function $\Delta E[\mathbf{R}(t)]$ to the Spectral Density $J(\omega)$ 192
18.8 Evaluating the Transfer Rate 196
18.9 Appendix: Numerical Evaluation of the Line Shape Function 200

18.1 Introduction

The quintessential quantum process in biology and chemistry involves electrons switching between two states. Two examples are electron transfer reactions in proteins when an electron moves from an orbital on the donor moiety D to an orbital on the acceptor moiety A and bond formation or bond breaking in an enzyme when electrons shift from a non-bonding state to a bonding state or *vice versa*. The energy expectation values of the two states $E_1(t)$ and $E_2(t)$ vary in time due to motions along a reaction coordinate, but also due to thermal fluctuations of the remaining degrees of freedom of the combined reaction–protein system. Often the interaction energies which couple the two electronic states involved in the reaction are weak, i.e., are small compared to the temporal variations of $E_1(t)$ and $E_2(t)$. In this rather typical case the actual reaction process is confined to moments when the two electronic states become energetically degenerate $[E_1(t) = E_2(t)]$ or, to use a widely accepted phrase, when the curves E_1 and E_2 cross.

In this chapter we will discuss curve crossing specifically in a protein environment. We will study how interactions between a two-dimensional quantum system and a protein matrix affect the curve crossing process. In particular, we will demonstrate how the influence of the protein on the process can be captured succinctly through stochastic quantum mechanics. Such description allows one to separate protein dynamics and the evolution of the quantum system: a molecular dynamics simulation is carried out to characterize the motion of the protein; the results of the simulations are then employed in a stochastic quantum mechanical calculation involving only the quantum mechanical degrees of freedom. The best known and most widely studied curve crossing process, electron transfer, will serve as an example.

Three advantages arise from the suggested description. First, and most obvious, the procedure is computationally and conceptually simpler than combining a quantum mechanical and a molecular dynamics description into a single calculation. Second, and equally important, such description focusses on the essential contribution of the protein environment to the quantum system and, thereby, yields a better understanding of the reaction studied. Lastly, one can consider the molecular dynamics simulations, carried out classically, as the high temperature limit of a quantum mechanical description and use the results for a fully quantum mechanical description in which the protein matrix is represented as a bath of quantum mechanical oscillators, suitably chosen to match the results of molecular dynamics simulations.

The description provided here does not account for forces which the quantum system exerts back onto the classical system. This deficiency is insignificant in those cases in which many degress of freedom of the protein matrix are weakly coupled to the quantum process. This situation arises, for example, in electron transfer, in which case long-range Coulomb forces couple essentially the whole protein matrix to the quantum process; in this case the effect of the protein motion on the electron transfer involves many small, additive contributions such that a back-reaction of the quantum system becomes actually immaterial. However, in case that some degrees of freedom of the protein matrix are strongly affected by the quantum system such that the curve crossing event induces forces which correlate the protein motion with the evolution of the quantum system, one must resort to a description combining quantum mechanics and classical molecular dynamics. But even if such behaviour arises, which is expected to be the case only for a small number of degrees of freedom, one is left with a need to account for contributions of the remaining degrees of freedom, for which purpose one may want to resort to a description as outlined below.

First we consider the case in which the force generated by the quantum system and influencing the protein is not neglected. Representing the protein as an ensemble of harmonic oscillators permits one to solve the response of the protein. This renders a closed evolution equation for the density matrix of the quantum system which exhibits a non-linear term accounting for the effect of the quantum system onto the protein and back onto the quantum system. The latter term is neglected in the following sections and two approaches are considered. In a first approach the protein matrix is represented as a classical system which contributes time-dependent secular terms to the Hamiltonian of the quantum system [46]. We demonstrate how these terms affect the curve crossing process, resorting to the well-known Kubo theory of line shapes [21]. We show how the stochastic process which represents the time dependence of the stated secular terms can be characterized through an independent molecular dynamics simulation. We focus, in particular, on the case that the stochastic process is of the Ornstein-Uhlenbeck type, i.e., corresponds to a Gaussian equilibrium distribution of diagonal energies; in this case a simple analytical description for the quantum system can be given. In a second approach [61, 60], often referred to as the spin-boson model, we consider the case that the protein matrix is represented through a bath of quantum mechanical oscillators linearly coupled to the quantum system, but not subject to energy redistribution. We show that the overall effect of such bath depends on average quantities which, at physiological temperatures, can be

rather readily obtained from classical molecular dynamics simulations. The second approach can be shown to become equivalent to the first approach in certain limits, e.g., at high (physiological) temperatures and for line shape functions which are wide compared to the frequencies involved in energy redistribution among protein vibrational modes, limits which prevail in case of electron transfer in proteins.

18.2 The Generic Model: Two-State Quantum System Coupled to an Oscillator

The model we consider first is extremely simple, yet it encapsulates the essence of a reaction process in a protein governed by a quantum mechanical curve crossing process. The reaction process connects a state $|1\rangle$ and a state $|2\rangle$, e.g., two electronic states of a substrate. Examples are (i) an electron transfer process from a donor D to an acceptor A, where $|1\rangle$ and $|2\rangle$ represent the states before electron transfer, i.e., A D, and after electron transfer, i.e., $A^- D^+$, and (ii) bond breaking in which case $|1\rangle$ describes the electronic state corresponding to a covalent bond and $|2\rangle$ describes the electronic state corresponding to the broken bond.
In the following we adopt the representation

$$|1\rangle \;=\; \begin{pmatrix} 1 \\ 0 \end{pmatrix}, \quad |2\rangle \;=\; \begin{pmatrix} 0 \\ 1 \end{pmatrix} \tag{18.1}$$

such that the Hamiltonian of the quantum system is

$$\hat{H} \;=\; \begin{pmatrix} E_1 & v \\ v & E_2 \end{pmatrix} \tag{18.2}$$

where v denotes the coupling between the states $|1\rangle$ and $|2\rangle$ and where $E_{1,2}$ are the associated energy expectation values of these states. The essential aspect of the quantum system is that it is coupled to the protein matrix through a dependence of the elements of $\hat{H}$ on the state of the protein matrix. For the sake of simplicity we assume here that only the energies $E_{1,2}$ depend on the protein environment and that v is constant. Also, we represent presently the protein through a single harmonic oscillator. This oscillator exhibits its coupling to the quantum system through a shift of its equilibrium position in going from state $|1\rangle$ to state $|2\rangle$. Such behaviour is captured by the energy functions

$$E_1 \;=\; \frac{p^2}{2m} \;+\; \frac{1}{2} m\omega^2 q^2 \tag{18.3}$$

$$E_2 \;=\; \frac{p^2}{2m} \;+\; \frac{1}{2} m\omega^2 (q - q_o)^2 \tag{18.4}$$

Replacing the diagonal elements of the Hamiltonian in (18.2) by these expressions evidently leads to a dependence of the quantum system on the momentum and position of the Hamiltonian representing the protein environment.
Following the procedure for quantum/classical molecular dynamics simulations described, e.g., in [4] one can state the equation of motion for both the density matrix $\varrho(t)$ of the two state quantum system and of the oscillator. It holds

$$\dot{\varrho} \;=\; \frac{i}{\hbar} [\varrho, \hat{H}] \tag{18.5}$$

$$m\ddot{q} \;=\; -\,\mathrm{tr}\left(\varrho \frac{\partial}{\partial q} \hat{H} \right) \tag{18.6}$$

where (18.5) is the Pauli equation and (18.6) the Newtonian equation of motion where the force of the classical particle is evaluated according to the Hellman-Feynman theorem; tr$A$ denotes the trace of the operator A. In the following we wish to describe the situation that the quantum system is initially, i.e., at $t = 0$, in state $|1\rangle$ such that the Pauli equation (18.5) is solved subject to the initial condition

$$\varrho(0) \;=\; \begin{pmatrix} 1 & 0 \\ 0 & 0 \end{pmatrix} . \tag{18.7}$$

This initial condition implies, in particular,

$$[\varrho(t)]_{22} \;=\; 0 \,, \quad t \,\leq\, 0 \,. \tag{18.8}$$

Evaluation of the force exerted onto the oscillator, i.e., the r.h.s. of (18.6), yields

$$-\,\mathrm{tr}\left(\varrho \frac{\partial}{\partial q}\hat{H}\right) \;=\; -\,m\omega^2 q \;+\; \varrho_{22}(t)\; c \tag{18.9}$$

where we introduced the expression

$$q_o \;=\; c\,/\,m\,\omega^2 \tag{18.10}$$

and used $\varrho_{11}(t) + \varrho_{22}(t) = 1$. Inserting this into (18.6) leads to

$$\ddot{q} \;+\; \omega^2 q \;=\; \frac{c}{m}\;\varrho_{22}(t) \,. \tag{18.11}$$

Equation (18.11) describes a forced oscillator. Defining

$$\xi \;=\; \dot{q} \;+\; i\,\omega q \tag{18.12}$$

and

$$F(t) \;=\; \frac{c}{m}\;\varrho_{22}(t) \tag{18.13}$$

one can write (18.11) as a first order differential equation

$$\dot{\xi} \;-\; i\,\omega\xi \;=\; F(t) \,. \tag{18.14}$$

We note that, according to (18.8), holds $F(t) = 0$, $t \leq 0$.
We want to solve now Eqs. (18.12–18.14) in case that the harmonic oscillator, at $t \leq 0$, has not been coupled yet to the quantum system and exhibits a time-dependence

$$q(t) \;=\; A_o \sin(\omega t \,+\, \delta) \,, \quad t \,\leq\, 0 \,. \tag{18.15}$$

The corresponding form of $\xi(t)$, defined in (18.12), is

$$\xi_o(t) \;=\; \xi(0)\, e^{i\omega t} \,, \quad t \,\leq\, 0 \,, \qquad \xi(0) \;=\; \omega A_0 e^{i\delta} \,. \tag{18.16}$$

The solution of (18.14) which matches this functional behaviour is for $t \geq 0$

$$\xi(t) \;\;=\;\; \xi_o(t) \;+\; \delta\xi(t) \,. \tag{18.17}$$

$$\delta\xi(t) \;\;=\;\; \int_0^t dt' \,\frac{c}{m}\;\varrho_{22}(t')\, e^{i\omega(t-t')} \tag{18.18}$$

where $\delta\xi(t)$ describes the effect of the force (18.13) on the oscillator. This expression can be inserted into the Pauli equation (18.5). Noting

$$E_1 = \frac{1}{2}m\,|\xi(t)|^2 \tag{18.19}$$

$$E_2 = \frac{1}{2}m\,|\xi(t) - i\omega q_o|^2 \tag{18.20}$$

we obtain the non-linear evolution equation

$$\dot{\varrho} = \frac{i}{\hbar}\left[\varrho,\left(\begin{array}{cc} \frac{1}{2}m\left|\xi_o(t) + \int_0^t dt'\frac{c}{m}\,\varrho_{22}(t')\,e^{i\omega(t-t')}\right|^2 & v \\ v & \frac{1}{2}m\left|\xi_o(t) + \int_0^t dt'\frac{c}{m}\,\varrho_{22}(t')\,e^{i\omega(t-t')} - i\omega q_o\right|^2 \end{array}\right)\right] .$$

The evolution equation (18.2) accounts for the effect of the quantum system on the protein (oscillator) and its back-reaction onto the quantum system. The description provided can be generalized to a situation in which the protein is represented by an ensemble of harmonic oscillators. In this case the interaction between the quantum process and the protein matrix spreads over many degrees of freedom. For some of these degrees of freedom the coupling might be strong such that it cannot be neglected. For most degrees of freedom the coupling should be so weak that it's effect, in particular, in the concert of the overall motion of the protein, can be neglected. In the following sections we will disregard the perturbation $\delta\xi(t)$ [cf. (18.18)] on the quantum system and replace the non-linear evolution equation (18.2) by the linear evolution equation

$$\dot{\varrho} = \frac{i}{\hbar}\left[\varrho,\left(\begin{array}{cc} \frac{1}{2}m\,|\xi_o(t)|^2 & v \\ v & \frac{1}{2}m\,|\xi_o(t) - i\omega q_o|^2 \end{array}\right)\right] . \tag{18.21}$$

This equation accounts for an effect of the harmonic oscillator on the quantum system. The simplification introduced will allow us to generalize our treatment in several ways. We can replace the single oscillator by an ensemble of oscillators, in fact, even by an ensemble of quantum mechanical oscillators. We can also represent the ensemble of classical oscillators by a random process governing the time-dependent matrix elements in the Hamiltonian in (18.21). We will demonstrate further that the essential characteristics of the ensemble of oscillators representing the protein marix can be obtained from classical molecular dynamics simulations. These generalizations and the connection to molecular dynamics simulations are a most welcome feature of the theory presented below. Nevertheless, it appears desirable to include in these generalizations the back-reaction of the quantum system on the environmental dynamics as described by (18.2).

18.3 Two-State System Coupled to a Classical Medium

In this section we assume a two-state quantum system with energies (secular terms) E_1 and E_2 which depend on the conformation of the whole protein described through the vector $\mathbf{R}(t) \in \mathbb{R}^{3N}$ for the case of a protein with N atoms. The Hamiltonian reads then

$$\tilde{H}_I = \left(\begin{array}{cc} E_1[\mathbf{R}(t)] & v \\ v & E_2[\mathbf{R}(t)] \end{array}\right) . \tag{18.22}$$

We assume that the protein motion captured by $\mathbf{R}(t)$ leads to curve crossing events, i.e., to situations $t = t'$ in which $E_1[\mathbf{R}(t')] = E_2[\mathbf{R}(t')]$ holds. The matrix element v induces transitions between the two states of the quantum system. We assume in the following that v is time-independent,

an assumption made for the sake of simplicity, but which ought to be relaxed in a more complete theory. We want to assume also that the system has a finite life time τ_o in state $|2\rangle$. This property will be accounted for by an operator

$$K_I \;=\; \begin{pmatrix} 0 & 0 \\ 0 & \tau_o^{-1} \end{pmatrix} \tag{18.23}$$

which, save for a factor $\hbar$, represents an optical potential.
The goal of the theory is to determine the 2×2 density matrix $\tilde{\varrho}(t)$ which obeys

$$\partial_t \tilde{\varrho}(t) \;=\; \frac{i}{\hbar} \left[\tilde{\varrho}(t), \tilde{H}_I(t) \right]_- \;-\; [\tilde{\varrho}(t), K_I]_+ \; . \tag{18.24}$$

where $[\ ,\ ]_-$ presents the commutator and $[\ ,\ ]_+$ presents the anti-commutator. For an evaluation of $\tilde{\varrho}(t)$ it is helpful to adopt a new basis. Let $(\ \alpha(t)\ \beta(t)\ )^T$ denote the state of the quantum system at time t. One introduces the new basis through the scalar transformation

$$\begin{pmatrix} \alpha'(t) \\ \beta'(t) \end{pmatrix} \;=\; u_o(t) \begin{pmatrix} \alpha(t) \\ \beta(t) \end{pmatrix} \tag{18.25}$$

where $u_o(t)$ is a scalar function which obeys the differential equation

$$\partial_t u_o(t) \;=\; \frac{i}{\hbar} E_1[\mathbf{R}(t)]\, u_o(t) \; , \quad u_o(0) \;=\; 1 \; . \tag{18.26}$$

One can demonstrate that the density matrix in the new representation obeys a Pauli equation with Hamiltonian

$$H_I \;=\; \begin{pmatrix} 0 & v \\ v & \Delta E[\mathbf{R}(t)] \end{pmatrix} \tag{18.27}$$

and

$$\Delta E[\mathbf{R}(t)] \;=\; E_2[\mathbf{R}(t)] \;-\; E_1[\mathbf{R}(t)] \tag{18.28}$$

leaving (18.23) unmodified. The new representation yields the same values for the diagonal elements of the new density matrix $\varrho(t)$ as the density matrix $\tilde{\varrho}(t)$ in the old representation, i.e., the probabilities to find the system in state $|1\rangle$ or state $|2\rangle$ are identical in the old and new representation.
The density matrix $\varrho(t)$ obeys the Liouville equation

$$\partial_t \varrho(t) = \frac{i}{\hbar} [H_I(t), \varrho(t)]_- - [\mathcal{K}, \varrho(t)]_+ \; . \tag{18.29}$$

This equation shows that a description of the coupling between the protein matrix and the two-state quantum system can be reduced to an evaluation of the so-called energy gap function $\epsilon(t) = \Delta E[\mathbf{R}(t)]$ from a molecular dynamics simulation.
To link a molecular dynamics simulation to the quantum system, one monitors in the molecular dynamics simulation the function $\epsilon(t)$ at time instances $t = t_1, t_2, \ldots$ and employs the resulting values for an evaluation of $\varrho(t)$. Such evaluation is based on a solution of Eq. (18.29) for a *piecewise time-independent* Hamiltonian $\tilde{H}_I$

$$\varrho(t + \Delta t) = \mathcal{P}\ \varrho(t)\ \mathcal{P}^\dagger \; , \; \mathcal{P} = \exp\left[\Delta t (\frac{i}{\hbar} \tilde{H}_I - \tilde{K}_I) \right] \; . \tag{18.30}$$

Evaluating the exponential operator $\mathcal{P}$ through Taylor expansion and grouping terms of odd and even powers yields [46]

$$\varrho(t+\Delta t) = \left(\cos\Delta t\gamma\ \mathbf{1} + i\ \frac{\sin\Delta t\gamma}{\gamma}\ \mathbf{A}\right)\varrho(t)\left(\cos\Delta t\bar{\gamma}\ \mathbf{1} - i\ \frac{\sin\Delta t\bar{\gamma}}{\bar{\gamma}}\ \bar{\mathbf{A}}\right)\ e^{-\Delta t/\tau_o} \tag{18.31}$$

where $\mathbf{1}$ stands for the identity matrix, $\bar{\gamma}$, $\bar{A}$ denote the complex conjugate of γ, A, and the abbreviations

$$\gamma = \sqrt{\Omega^2+\omega^2}\ ,\ \omega = V/\hbar\ ,\ \Omega = \frac{1}{2\hbar}(\Delta E_{MD} - \frac{i\hbar}{\tau_o})\ ,\ \mathbf{A} = \begin{pmatrix} \Omega & \omega \\ \omega & -\Omega \end{pmatrix} \tag{18.32}$$

are used. Corresponding calculations have been carried out in [46]. The fluctuations of the energy gap $\epsilon(t)$ as a controlling factor for the rate of electron transfer in the photosynthetic reaction center had been studied by means of molecular dynamics simulations as soon as the structure of this protein had been discovered [53, 54]. A further molecular dynamics analysis in terms of the Marcus theory of electron transfer [26, 25] (see also below) has been provided in [52].

In case of electron transfer reactions in proteins the interaction matrix element v in (18.1, 18.22, 18.27) accounts for the electronic tunneling between electron donor and electron acceptor moieties. To evaluate the density matrix $\varrho(t)$ one carries out a classical molecular dynamics simulation which provides one with the vector $\mathbf{R}(t)$ describing the momentaneous protein conformation. One determines then the corresponding energy gap $\Delta E[\mathbf{R}(t)]$ for which purpose one obviously needs to know the expressions for the energies $E_1[\mathbf{R}(t)]$ and $E_2[\mathbf{R}(t)]$. For example, in case of an electron transfer reaction state $|1\rangle$ describes an electron configuration AD and state $|2\rangle$ an electron configuration A^-D^+ where A and D are electron acceptor and donor moieties in the protein. Knowing the atomic partial charges corresponding to AD and to A^-D^+ one can evaluate $E_1[\mathbf{R}(t)]$ and $E_2[\mathbf{R}(t)]$ as the Coulomb energies of the acceptor and donor moieties with the protein matrix, to which one adds the redox energies of the states AD and A^-D^+. Unfortunately, a particular molecular dynamics simulation leading to a particular history of $\mathbf{R}(t)$–values is not necessarily representative and one needs to average either over the dynamics started with many different initial conditions (ensemble average) or carry out a suitable time average.

The situation, which we wish to describe, starts from the quantum system in state $|1\rangle$, i.e., from [c.f. (18.7)]

$$\varrho(0)\ =\ \begin{pmatrix} 1 & 0 \\ 0 & 0 \end{pmatrix} \tag{18.33}$$

The system will transfer to state $|2\rangle$ in which state it decays with life time $\tau_o/2$ such that, ultimately, state $|1\rangle$ will be completely depleated. In case that τ is sufficiently short and $\Delta E[\mathbf{R}(t)]$ is random one expects that the population of state $|1\rangle$ exhibits an approximate exponential decay

$$\varrho_{11}(t)\ \approx\ \exp(-k_{\rm cl}\,t)\ . \tag{18.34}$$

The decay constant $k_{\rm cl}$ may be evaluated through

$$[\,k_{\rm cl}\,]^{-1}\ \approx\ \int_0^\infty dt\,\varrho_{11}(t)\ . \tag{18.35}$$

18.4 Two State System Coupled to a Stochastic Medium

A difficulty of the description outlined in Sect. 18.3 is the need to average the density matrix $\varrho(t)$ over many histories of the energy gap function $\Delta E[\mathbf{R}(t)]$. In this section we link the molecular dynamics simulations to the quantum system through an interpretation of $\Delta E[\mathbf{R}(t)]$ as a stochastic process. In this case one can describe the evolution of the quantum system to second order in v, as defined in (18.22, 18.27), averaged over all possible histories of the protein. Beside being eminently useful in applications the description provided in this section makes it also transparent which characteristics of the fluctuations of $\Delta E[\mathbf{R}(t)]$ are essential for the control of the quantum system by the protein.
We consider here the simplest case that the properties of $\epsilon(t) = \Delta E[\mathbf{R}(t)]$ can be captured by a so-called Ornstein-Uhlenbeck process [55, 10]. This stochastic process is characterized through three properties. The first characteristic property is the average value

$$\langle \epsilon \rangle \;=\; \frac{1}{N_t} \sum_{j=1}^{N_t} \epsilon(t_j) \; . \tag{18.36}$$

The second characteristic property implies that the distribution of values $\epsilon(t_1)$, $\epsilon(t_2)$ ... is Gaussian such that the distribution is completely characterized through the root mean square deviation σ defined through

$$\sigma^2 \;=\; \frac{1}{N_t} \sum_{j=1}^{N_t} \epsilon^2(t_j) \;-\; \langle \epsilon \rangle^2 \; . \tag{18.37}$$

The third characteristic property is related to the normalized correlation function of the energy gap

$$C_{\epsilon\epsilon}(t) \;=\; \frac{1}{\sigma^2} \left(\langle \epsilon(t)\epsilon(0) \rangle \;-\; \langle \epsilon \rangle^2 \right) \; . \tag{18.38}$$

This function is conventionally evaluated through

$$C_{\epsilon\epsilon}(t) \;=\; \frac{1}{\sigma^2} \frac{1}{M} \sum_{\alpha=1}^{M} \left(\langle \epsilon(t+t_\alpha)\epsilon(t_\alpha) \rangle \;-\; \langle \epsilon \rangle^2 \right) \tag{18.39}$$

for, e.g., $M = 100$, where t_j denotes time instances along the simulations which are spaced far apart, e.g., 10 ps. Obviously, $C_{\epsilon\epsilon}(t)$ captures the dynamic properties of $\epsilon(t)$. The present description in terms of an Ornstein-Uhlenbeck process assumes that $C_{\epsilon\epsilon}(t)$ is well described by a single exponential decay, i.e., by

$$C_{\epsilon\epsilon}(t) \;\approx\; \exp(-t/\tau) \tag{18.40}$$

such that the dynamics is presented sufficiently through a single decay time τ.
A quantity which conforms to the three characteristics of the Ornstein-Uhlenbeck process is distributed according to a probablity distribution $p(\epsilon, t)$ which obeys the Fokker-Planck equation

$$\partial_t \; p(\epsilon, t) = \mathcal{L} \; p(\epsilon, t) \; , \;\; \mathcal{L} = \frac{\sigma^2}{2\tau} \; \partial_\epsilon p_0(\epsilon) \partial_\epsilon \; [p_0(\epsilon)]^{-1} \; . \tag{18.41}$$

where

$$p_o(\epsilon) = \frac{1}{\sqrt{2\pi\sigma}} \exp\left[-(\epsilon - \langle \epsilon \rangle)^2 / 2\sigma^2 \right] \; . \tag{18.42}$$

The assumption that $\epsilon(t)$, as monitored in a simulation, obeys an Ornstein-Uhlenbeck process is made here mainly for the sake of simplicity. The general framework of the theory presented allows other stochastic processes to represent the coupling of the protein matrix to the quantum system. We note that the Ornstein-Uhlenbeck process actually describes a Brownian harmonic oscillator [10].
By employing the theory in [5, 34] one can express the density matrix

$$\varrho(t) \;=\; \int d\Delta E'\, \mathcal{I}(\Delta E')\varrho_o(\Delta E'|t) \tag{18.43}$$

where

$$\varrho_o(\Delta E'|t) \;=\; \exp\left[-\frac{it}{\hbar}\begin{pmatrix} 0 & v \\ v & \Delta E' - i\hbar/\tau \end{pmatrix}\right]\begin{pmatrix} 1 & 0 \\ 0 & 0 \end{pmatrix}\exp\left[\frac{it}{\hbar}\begin{pmatrix} 0 & v \\ v & \Delta E' + i\hbar/\tau \end{pmatrix}\right]$$

Here $\varrho_o(\Delta E'|t)$ represents the density matrix for a Hamiltonian (18.24) with a *time-independent* energy term $\Delta E'$, i.e., it can be evaluated by means of (18.31, 18.32), applying these formulas for arbitrary dt. $\mathcal{I}(\Delta E')$ is the Kubo line shape function [21]

$$\mathcal{I}(\Delta E') = \frac{1}{\pi} Re \left\langle 0 \left| \frac{1}{\frac{i}{\hbar}(u - \Delta E') - \mathcal{L}} \right| 0 \right\rangle \;. \tag{18.44}$$

Expressions (18.43-18.44) yield an approximation, accurate to third order in v, for the diagonal elements of $\varrho(t)$. However, the approximation includes all orders of v in order to conserve the trace of the density matrix and to ascertain convergence to the exact $\varrho(t)$ in the limits of slow or fast stochastic motion measured on a time scale $\hbar/v$ [21]. A method for the evaluation of the line shape function (18.44) is described in the appendix. Other computational strategies are decribed in [45, 5, 6, 38, 39]. A systematic approximation to matrix elements of the inverse of Fokker-Planck operators is provided by the generalized moment expansion. This approach is described systematically in [31] where it is considered, however, for real operators; a generalization to complex operators, as they occur in (18.44), is straightforward.
The aim of the present theory is to determine the time-dependence of the occupancy of state $|1\rangle$ which is initially populated, i.e., to determine $[\varrho(\Delta E'|t)]_{11}$. As in the description in Sect. 18.3 this state eventually should become completely unpopulated and we assume a behaviour described by a mono-exponential decay

$$[\varrho(\Delta E'|t)]_{11} \;\approx\; \exp[\,-k_{cl}^{ST}(\Delta E')\,t\,)] \;. \tag{18.45}$$

We assume the same approximation for the (1,1) element of $\varrho_o(\Delta E'|t)$, i.e.,

$$[\varrho_o(\Delta E'|t)]_{11} \;\approx\; \exp[\,-k_o(\Delta E')\,t\,] \tag{18.46}$$

and can establish then $k_o(\Delta E')$ through

$$[k_o(\Delta E')]^{-1} \;\approx\; \int_0^\infty dt[\varrho_o(\Delta E'|t)]_{11} \tag{18.47}$$

which applies if (18.46) holds exactly. Note that we do not define the rates through the time derivative of the density matrix element itself since, of course, this derivative vanishes at $t = 0$. One can conclude then from Eq. (18.43)

$$\exp[\,-k_{cl}^{ST}\,t\,] \;\approx\; \int d\Delta E'\, \mathcal{I}(\Delta E') \exp[\,-k_o(\Delta E')\,t\,] \;. \tag{18.48}$$

Differentiating both sides at $t = 0$ yields

$$k_{cl}^{ST} \approx \int d\Delta E' \, \mathcal{I}(\Delta E') \, k_o(\Delta E') \; . \tag{18.49}$$

In the present case three parameters determine the operator $\mathcal{L}$ in (18.44, 18.41) and, hence, the functional form of $\mathcal{I}(\Delta E')$, namely, $\langle\epsilon\rangle$, σ^2, and τ defined in (18.36), (18.37) and in (18.40, 18.41), respectively. $\langle\epsilon\rangle$ determines the center of $\mathcal{I}(\Delta E')$ on the $\Delta E'$ axis. The parameter σ^2 can be absorbed into the scale of the $\Delta E'$–axis. The corresponding line shape function is then, using $u' = u/\sigma$, $\Delta\epsilon = \Delta E'/\sigma$,

$$\mathcal{I}(\Delta\epsilon) \sim Re \left\langle 0 \left| \frac{1}{i(u' - \Delta\epsilon) - \rho \, \partial_{u'} p_o(u') \partial_{u'} [p_o(u')]^{-1}} \right| 0 \right\rangle \tag{18.50}$$

which expresses the line shape function in dimensionless variables. Here,

$$\rho = \frac{\hbar}{2\tau\sigma} \tag{18.51}$$

is the single dimensionless parameter which describes the dynamic effect of fluctuations in $\Delta E(t)$, large ρ values corresponding to rapid fluctuations. Since the effect of $< \epsilon >$ and σ can be absorbed through shift and scaling of the ΔE–axis, the parameter ρ constitutes the only parameter which determines the shape of $\mathcal{I}(\Delta E)$ and, hence, the effect of the protein matrix on the quantum system. In case of the photosynthetic reaction center of *Rhodopseudomonas viridis* studied in [46] a value $\rho = 0.03$ was determined which is so small that a motional narrowing of the distribution $\mathcal{I}(\Delta E')$ relative to the wide equilibrium distribution of ΔE can be neglected, i.e., $\mathcal{I}(\Delta E')$ is described well assuming that the protein matrix is characterized solely through an equilibrium distribution of all of its degrees of freedom. We will study a respective model for the protein matrix in the next two sections. However, in case of a narrow equilibrium distribution of ΔE, i.e., with a width of the order of $\hbar/\tau$ or smaller, one would expect that the fluctuations of $\Delta E(t)$ will modify $\mathcal{I}(\Delta E)$ significantly.

Applications The theory outlined in this and in the previous Section has been applied in the framework of molecular dynamics studies of the photosynthetic reaction center of *Rh. viridis* [34, 46]. Figure 18.1 compares the resulting electron transfer rates. The theory in the present Section has also been applied to describe the dynamics of radical pairs connected through a polymer chain which mediates a time-dependent exchange interaction [45, 5]. In the latter case the polymer folding motions, analyzed through molecular dynamics simulations, induces a stochastic variation of the exchange interaction. The theory has been applied also to magnetic resonance imaging microscopy [38, 39, 3]. In this case the spins of water protons, diffusing in a magnetic field gradient, experience a stochastic separation of their spin-up and spin-down states. This leads to an NMR spectrum which depends on the diffusion space and on the Brownian motion of water; the spectrum, in a proper analysis, reveals the geometry of the diffusion space. In [45, 5, 38, 39] the Kubo line shape function had been evaluated numerically through a discretization of the operator $\mathcal{L}$ in (18.44). The algorithm presented there, e.g., in [39], can be applied to a class of stochastic processes governed by a so-called Smoluchowski equation. These processes cover Gaussian and non-Gaussian equilibrium distributions $p_o(\epsilon)$.

18.5 Two State System Coupled to a Single Quantum Mechanical Oscillator

The goal in the following is to describe a two state quantum system coupled to a bath of quantum mechanical harmonic oscillators. We begin with the case that the bath contains only a single

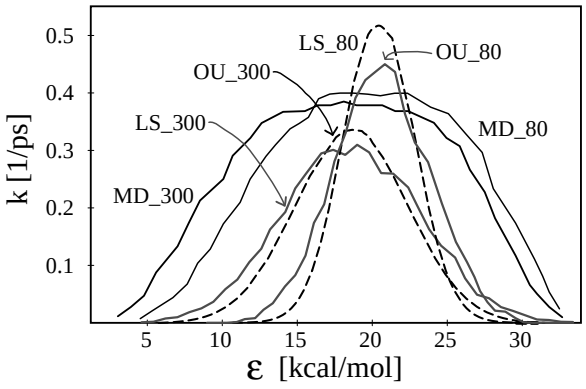

Figure 18.1: Electron transfer rates $k_{cl}(\epsilon)$ evaluated by means of molecular dynamics simulation and the theory in Sect. 18.3 at 300 and at 80 K. In the calculations the redox energy $E = \epsilon$ was varied as shown on the horizontal axis. The corresponding rate constants are labelled MD_300 and MD_80. The figure shows also rate constants evaluated according to the theory in Sect. 18.3, except that the data for the energy gap ΔE were generated by means of an Ornstein-Uhlenbeck process employing random numbers. The corresponding rates are labelled OU_300 and OU_80. A third set of rate constants k_{cl}^{ST}, labelled ST_300 and ST_80, has been calculated according to the theory in Sect. 18.4, i.e., according to Eq. (18.49) (dashed lines).

oscillator. Such situation is decribed by the Hamiltonian

$$\hat{H}_{\rm qo}^{(s)} = \begin{pmatrix} \hat{H}_r^{(s)} & v \\ v & \hat{H}_p^{(s)} + E \end{pmatrix} \tag{18.52}$$

where

$$\hat{H}_r^{(s)} = \frac{\hat{p}^2}{2m} + \frac{1}{2}m\omega^2 q^2 \tag{18.53}$$

$$\hat{H}_p^{(s)} = \frac{\hat{p}^2}{2m} + \frac{1}{2}m\omega^2 \left(q - \frac{c}{m\omega^2}\right)^2 \tag{18.54}$$

denote harmonic oscillator Hamiltonians of the *reactant* and *product* states. The additive energy term E denotes here a shift of the zero energy of the product state relative to the reactant state, e.g., denotes the redox energy difference between states AD and A^-D^+; *E will be considered a variable in the following*. If one wishes to describe a process going from the product (A^-D^+) state to the reactant (AD) state the sign of E in (18.52), representing the redox energy difference, needs to be reversed. This property will be envoked below when we consider both processes, i.e., AD $\rightarrow$ A^-D^+ and $A^-D^+ \rightarrow$ AD.

The eigenstates and eigenvalues of the Hamiltonians (18.53, 18.54) are well-known from elementary

quantum mechanics; they are

$$\langle q|n\rangle^{(\mathrm{r})} \;=\; \phi_n^{(\mathrm{r})}(q) \;=\; \left(\frac{\lambda}{\pi}\right)^{\frac{1}{4}} (2^n n!)^{-\frac{1}{2}} H_n(\sqrt{\lambda}q)\, e^{-\frac{1}{2}\lambda q^2} \tag{18.55}$$

$$\epsilon_n^{(\mathrm{r})} \;=\; \hbar\omega(n+\frac{1}{2}) \tag{18.56}$$

$$\langle q|n\rangle^{(\mathrm{p})} \;=\; \phi_n^{(\mathrm{p})}(q) \;=\; \left(\frac{\lambda}{\pi}\right)^{\frac{1}{4}} (2^n n!)^{-\frac{1}{2}} H_n(\sqrt{\lambda}(q-\frac{c}{m\omega^2}))\, e^{-\frac{1}{2}\lambda(q-c/m\omega^2)^2} \tag{18.57}$$

$$\epsilon_n^{(\mathrm{p})} \;=\; \hbar\omega(n+\frac{1}{2}) \tag{18.58}$$

where

$$\lambda \;=\; m\omega/\hbar \tag{18.59}$$

and where $H_n(y)$, $n = 0, 1, 2\ldots$ denote the Hermite polynomials. The reactant states describe an oscillator centered around $q = 0$, the product state an oscillator centered around [c.f. (18.10)]

$$q_o \;=\; c/m\omega^2\,. \tag{18.60}$$

The propagator for the harmonic oscillator is well known. In case of the reactant state the propagator is

$$\begin{aligned}\langle q'|e^{-iH_r^{(s)}(t-t_o)/\hbar}|q\rangle \;&=\; \left[\frac{m\omega}{2i\pi\hbar\,\mathrm{sin}\omega(t-t_0)}\right]^{\frac{1}{2}} \times \\ &\exp\left\{\frac{im\omega}{2\hbar\,\mathrm{sin}\omega(t-t_0)}\,\left[\,(q'^2+q^2)\,\mathrm{cos}\omega(t-t_0)\,-\,2\,q'\,q\,\right]\right\}\,.\end{aligned} \tag{18.61}$$

This is equivalent to

$$\begin{aligned}\langle q'|e^{-iH_r^{(s)}(t-t_o)/\hbar}|q\rangle \;&=\; \left[\frac{\lambda}{2\pi\,\mathrm{sinh}\xi}\right]^{\frac{1}{2}} \times \\ &\exp\left\{-\frac{\lambda}{4}\left[\,(q'+q)^2\,\mathrm{tanh}\frac{\xi}{2}\,+\,(q'-q)^2\,\mathrm{coth}\frac{\xi}{2}\,\right]\right\}\,.\end{aligned} \tag{18.62}$$

$$\xi \;=\; i\,\omega(t-t_o)\,. \tag{18.63}$$

In case of the product state, the same expression applies after replacing $q \to q - q_o$ and $q' \to q' - q_o$. The reactant states (18.55) are occupied in thermal equilibrium with probability

$$p_n^{(\mathrm{r})} \;=\; x^n(1-x)\,, \quad x \;=\; e^{-\hbar\omega/kT}\,, \tag{18.64}$$

a result which is well-known from elementary statistical mechanics. The corresponding equilibrium state density matrix of the reactant state oscillator $\rho_o^{(\mathrm{r})}$ has the matrix elements

$$\left[\hat{\rho}_o^{(\mathrm{r})}\right]_{mn} \;=\; p_n^{(\mathrm{r})}\,\delta_{nm}\,. \tag{18.65}$$

The density matrix can also be written

$$\hat{\rho}_o^{(\mathrm{r})} \;=\; 2\,\mathrm{sinh}\,(\hbar\omega/2kT)\;e^{-H^{(\mathrm{r})}/kT}\,. \tag{18.66}$$

The transitions from reactant to product states are induced through the matrix elements v in (18.52). In case of electron transfer in proteins, the coupling is induced through electron tunneling between prosthetic groups in the protein. The corresponding energy values v are very small, usually of the order of 10^{-4} eV. As a result, reactant states $|n\rangle^{(\mathrm{r})}$ and product states $|m\rangle^{(\mathrm{p})}$ couple only when they are essentially degenerate. The overall rate of transfer from reactant states R to product states P is then

$$k_{qo}(R \to P) \;=\; \frac{2\pi}{\hbar^2}\, v^2 \mathcal{S}_{qo}(E) \tag{18.67}$$

where

$$\mathcal{S}_{qo}(E) \;=\; \sum_{n,m=0}^{\infty} p_n^{(\mathrm{r})}\, |{}^{(\mathrm{r})}\langle n|m\rangle^{(\mathrm{p})}|^2\, \delta\left(\frac{E \,+\, \epsilon_m^{(\mathrm{p})} \,-\, \epsilon_n^{(\mathrm{r})}}{\hbar}\right) \tag{18.68}$$

is the so-called spectral line shape function.
We seek to express the line shape function (18.68) in a more compact form. For this purpose we use the identity

$$\delta\left(\frac{E \,+\, \epsilon_m^{(\mathrm{p})} \,-\, \epsilon_n^{(\mathrm{r})}}{\hbar}\right) \;=\; \frac{1}{2\pi}\int_{-\infty}^{+\infty} dt\; e^{itE/\hbar}\; e^{-it\epsilon_n^{(\mathrm{r})}/\hbar}\; e^{it\epsilon_m^{(\mathrm{p})}/\hbar}\;. \tag{18.69}$$

Employing the definition of the density matrix (18.65) one can write (18.68)

$$\mathcal{S}_{qo}(E) \;=\; \frac{1}{2\pi}\int_{-\infty}^{+\infty} dt\; e^{itE/\hbar} \sum_{n,m=0}^{\infty} {}^{(\mathrm{r})}\langle n|\, \hat{\rho}_o^{(\mathrm{r})}\, e^{-it\hat{H}_r^{(s)}/\hbar}\, |m\rangle^{(\mathrm{p})(\mathrm{p})}\langle m|\, e^{it\hat{H}_p^{(s)}/\hbar}\, |n\rangle^{(\mathrm{r})} \tag{18.70}$$

or, equivalently, using (18.66)

$$\mathcal{S}_{qo}(E) \;=\; \frac{1}{2\pi}\int_{-\infty}^{+\infty} dt\; e^{itE/\hbar}\; 2\sinh\frac{\hbar\omega}{2kT}\; \mathrm{tr}\left(e^{-\hat{H}_r^{(s)}/kT}\, e^{-it\hat{H}_r^{(s)}/\hbar}\, e^{it\hat{H}_p^{(s)}/\hbar}\right)\;. \tag{18.71}$$

Expressing the trace as an integral over q' we conclude that the spectral line shape function is

$$\begin{aligned} &\mathcal{S}_{qo}(E) \quad = \qquad\qquad\qquad\qquad\qquad\qquad\qquad\qquad\qquad\qquad\qquad\qquad (18.72)\\ &\frac{1}{2\pi}\int_{-\infty}^{+\infty} dt\; e^{itE/\hbar}\; 2\sinh\frac{\hbar\omega}{2kT}\int_{-\infty}^{+\infty} dq \int_{-\infty}^{+\infty} dq'\, \langle q'|\, e^{-i(t\,-\,\hbar/kT)\hat{H}_r^{(s)}/\hbar}|q\rangle\langle q\, e^{it\hat{H}_p^{(s)}/\hbar}|q'\rangle\;. \end{aligned}$$

The propagator (18.62) allows one to evaluate the line shape function (18.72). One employs

$$\begin{aligned} \langle q|\, e^{it\hat{H}_p^{(s)}/\hbar}|q'\rangle \quad &= \quad \left[\frac{\lambda}{2\pi\sinh\eta_1}\right]^{\frac{1}{2}} \;\times \qquad\qquad (18.73)\\ &\qquad \times\exp\left\{-\frac{\lambda}{4}\left[\,(q' \,+\, q \,-\, 2q_o)^2\tanh\frac{\eta_1}{2} \,+\, (q' \,-\, q)^2\coth\frac{\eta_1}{2}\,\right]\right\}\;. \\ \eta_1 \quad &= \quad -\,i\omega t\;. \qquad\qquad (18.74) \end{aligned}$$

and, displacing time into the complex plane to account for the equilibrium (temperature T) density matrix,

$$\begin{aligned} \langle q'|\, e^{-i(t\,-\,\hbar/kT)\hat{H}_r^{(s)}/\hbar}|q\rangle \quad &= \quad \left[\frac{\lambda}{2\pi\sinh\eta_2}\right]^{\frac{1}{2}} \;\times \qquad\qquad (18.75)\\ &\qquad \times\exp\left\{-\frac{\lambda}{4}\left[\,(q' \,+\, q)^2\tanh\frac{\eta_2}{2} \,+\, (q' \,-\, q)^2\coth\frac{\eta_2}{2}\,\right]\right\}\;. \\ \eta_2 \quad &= \quad i\omega t - \hbar\omega/kT\;. \qquad\qquad (18.76) \end{aligned}$$

Inserting (18.73–18.76) into (18.72) results in the expression

$$\mathcal{S}_{qo}(E) \;=\; \frac{1}{2\pi}\int_{-\infty}^{+\infty} dt\; e^{itE/\hbar}\; \frac{\lambda \sinh\!\left(\frac{\hbar\omega}{2kT}\right)}{\pi\sqrt{\sinh\eta_1\,\sinh\eta_2}}\; I(t)\;. \tag{18.77}$$

where

$$I(t) \;=\; \int_{-\infty}^{+\infty} dq \int_{-\infty}^{+\infty} dq' \exp\left[-\alpha\,(t)(q\,+\,q')^2\;-\;\beta\,(q\,+\,q'\,-\,2q_o)^2\;-\;\gamma\,(q\,-\,q')^2\right] \tag{18.78}$$

$$\alpha \;=\; \frac{\lambda}{4}\tanh\frac{\eta_2}{2} \tag{18.79}$$

$$\beta \;=\; \frac{\lambda}{4}\tanh\frac{\eta_1}{2} \tag{18.80}$$

$$\gamma \;=\; \frac{\lambda}{4}\left(\tanh\frac{eta_1}{2}\;+\;\tanh\frac{\eta_2}{2}\right) \tag{18.81}$$

Expression (18.77–18.81) for the spectral line shape function played an important role in the theory of spectral transitions of so-called F-centers in solids as reviewed in [28]. The expression can be further simplified [28]. For this purpose one transforms to new integration variables $u = q + q'$ and $u' = q - q'$. Noting that for the Jacobian holds $\partial(u,u')/\partial(q,q') = 2$, the integral (18.78) reads

$$I(t) \;=\; \frac{1}{2}\int_{-\infty}^{+\infty} du \int_{-\infty}^{+\infty} du' \exp\left[-\alpha\,(t)u^2\;-\;\beta\,(u\,-\,2q_o)^2\right]\,\exp\left[-\,\gamma\,u'^2\right]\;. \tag{18.82}$$

Completion of the square in the first exponent results in the expression

$$\begin{aligned} I(t) \;&=\; \frac{1}{2}\exp\left[-4q_o^2\left(\beta\,-\,\frac{\beta^2}{\alpha+\beta}\right)\right]\;\times \\ &\quad\times\int_{-\infty}^{+\infty} du' \exp\left[-\,\gamma\,u'^2\right]\,\int_{-\infty}^{+\infty} du \exp\left[-(\alpha\,+\,\beta)\,(u\,-\,s)^2\right]\;. \end{aligned} \tag{18.83}$$

where

$$s \;=\; 2\beta q_o\,/\,(\alpha\,+\,\beta)\;. \tag{18.84}$$

Since $\mathrm{Re}(\gamma) > 0$ and $\mathrm{Re}(\alpha+\beta) > 0$ the Gaussian integrals can be evaluated in a straightforward way and one obtains

$$I(t) \;=\; \frac{\pi}{2\sqrt{\gamma(\alpha+\beta)}}\exp\left[-4q_o^2\left(\beta\,-\,\frac{\beta^2}{\alpha+\beta}\right)\right]\;. \tag{18.85}$$

We note here that this expression and, hence, $\mathcal{S}_{qo}(E)$ do not depend on the sign of q_o. This is to be expected due to the reflection symmetry of the harmonic oscillator potential. This behaviour implies, however, that a description of a process going from product states to reactant states does not require a change in the sign of q_o, even though that such change appears to be intuitively necessary.

Using definitions (18.79–18.81) and the properties of hyperbolic functions one can show

$$\frac{\lambda \sinh\!\left(\frac{\hbar\omega}{2kT}\right)}{2\sqrt{\sinh(\eta_1)\,\sinh(\eta_2)\,\gamma(\alpha+\beta)}} \;=\; 1 \tag{18.86}$$

One can also simplify the exponent in (18.85). One obtains

$$\beta \;-\; \frac{\beta^2}{\alpha \,+\, \beta} \;=\; \frac{\lambda}{4}\left(\tanh\frac{\eta_1}{2} \;-\; \frac{\tanh^2\frac{\eta_1}{2}}{\tanh\frac{\eta_1}{2} \,+\, \tanh\frac{\eta_2}{2}}\right) \;=\; \frac{\lambda}{4}\,\frac{\tanh\frac{\eta_1}{2}\tanh\frac{\eta_2}{2}}{\tanh\frac{\eta_1}{2} \,+\, \tanh\frac{\eta_2}{2}}\;. \tag{18.87}$$

Using $\tanh\alpha \,+\, \tanh\beta \,=\, \sinh(\alpha+\beta)/\cosh\alpha\cosh\beta$ the latter expression can be further rewritten

$$\begin{aligned}
\beta \;-\; \frac{\beta^2}{\alpha \,+\, \beta} \;&=\; \frac{\lambda}{4}\,\frac{\sinh\frac{\eta_1}{2}\sinh\frac{\eta_2}{2}}{\sinh(\frac{\eta_1}{2}+\frac{\eta_2}{2})} \;=\; \frac{\lambda}{4}\,\frac{-\sinh\left(\frac{i\omega t}{2}\right)\,\sinh\left(\frac{i\omega t}{2}+\frac{\hbar\omega}{2kT}\right)}{\sinh\left(\frac{\hbar\omega}{2kT}\right)} \\
&=\; \frac{\lambda}{4}\,\frac{-\sinh\left(\frac{i\omega t}{2}\right)\,\left[\sinh\left(\frac{i\omega t}{2}\right)\,\cosh\left(\frac{\hbar\omega}{2kT}\right) \,+\, \sinh\left(\frac{\hbar\omega}{2kT}\right)\,\cosh\left(\frac{i\omega t}{2}\right)\right]}{\sinh\left(\frac{\hbar\omega}{2kT}\right)} \\
&=\; \frac{\lambda}{4}\left[\sin^2\frac{\omega t}{2}\coth\frac{\hbar\omega}{2kT} \;-\; i\cos\frac{\omega t}{2}\sin\frac{\omega t}{2}\right]
\end{aligned} \tag{18.88}$$

which yields

$$\beta \;-\; \frac{\beta^2}{\alpha \,+\, \beta} \;=\; \frac{\lambda}{8}\left[(1 \,-\, \cos\omega t)\coth\frac{\hbar\omega}{2kT} \;-\; i\sin\omega t\right] \tag{18.89}$$

Combining Eqs. (18.60, 18.77, 18.85, 18.86, 18.89) results in the final expression

$$\mathcal{S}_{qo}(E) \;=\; \frac{1}{2\pi}\int_{-\infty}^{+\infty} dt\,\exp\!\left[\,itE/\hbar \;-\; \frac{c^2}{2m\hbar\omega^3}\coth\frac{\hbar\omega}{2kT}\,(1-\cos\omega t) \;+\; i\,\frac{c^2}{2m\hbar\omega^3}\sin\omega t\right]$$

We note here that the rate for the reverse process, i.e., for going from the product state P to the reactant state R, is given by

$$k_{qo}(P\to R) \;=\; \frac{2\pi}{\hbar^2}\,v^2\mathcal{S}_{qo}(-E) \tag{18.90}$$

which differs from (18.67) solely through the sign of E.
The integral in (18.5) can be carried out and the line shape function expressed as a series of regular, modified Bessel functions $I_k(x)$ [28]. The result is

$$\mathcal{S}_{qo}(E) \;=\; \frac{e^{-\Lambda(1+2n_o)}}{\omega}\left(\frac{n_o+1}{n_o}\right)^{s_j/2}\;\sum_{k=-\infty}^{\infty}\;\delta\left(k-s(E)\right)\;I_k\left(2\Lambda\sqrt{n_o(n_o+1)}\right) \tag{18.91}$$

where $\Lambda \,=\, \frac{1}{2}m\omega^2 q_o^2/\hbar\omega \,=\, c^2/2m\hbar\omega^3$ is the so-called reorganization energy in units of vibrational quanta $\hbar\omega$, $n_o = e^{-\hbar\omega/kT}/(1-e^{-\hbar\omega_j/kT})$ is the average number of quanta thermally excited in the oscillator, and $s(E) = (E-\frac{1}{2}\hbar\omega)/\hbar\omega$ counts the number of oscillator levels up to energy E. The summation in (18.90) is over integers k such that one and only one term in the sum contributes anytime that $s(E)$ assumes an integer value. As mentioned above, expression (18.90) was originally developed to describe optical transitions in solids [28]; it was introduced for the description of thermal electron transfer by Jortner [18, 11].

18.6 Two State System Coupled to a Multi-Modal Bath of Quantum Mechanical Oscillators

In case of a two state quantum system coupled to a bath of harmonic oscillators the Hamiltonian (18.52–18.54) above is replaced by

$$\hat{H}_{\rm qb} \;=\; \begin{pmatrix} \hat{H}_{\rm r} & v \\ v & \hat{H}_{\rm p} \,+\, E \end{pmatrix} \tag{18.92}$$

where

$$\hat{H}_r \;=\; \sum_j \left(\frac{\hat{p}_j^2}{2M_j} \;+\; \frac{1}{2} M_j \omega_j^2 q_j^2 \right) \tag{18.93}$$

$$\hat{H}_p \;=\; \sum_j \left(\frac{\hat{p}_j^2}{2M_j} \;+\; \frac{1}{2} M_j \omega_j^2 \left(q_j \;-\; \frac{c_j}{M_j \omega_j^2} \right)^2 \right) \tag{18.94}$$

The Hamiltonians $\hat{H}_r$ and $\hat{H}_p$ describe here the same situation as in case of the Hamiltonian (18.52–18.54), except that the coupling is to an ensemble of oscillators which represent the protein matrix. One can absorb the masses M_j in the definition of the positions q_j of the oscillators such that we assume in the following

$$M_j \;=\; 1 \qquad \forall\, j \;. \tag{18.95}$$

The eigenstates of the Hamiltonians (18.93, 18.94) are denoted by $\langle \boldsymbol{q} | \boldsymbol{n} \rangle^{(\mathrm{r})}$ and $\langle \boldsymbol{q} | \boldsymbol{m} \rangle^{(\mathrm{p})}$, respectively, where $\boldsymbol{q} = (q_1, q_2, \dots)^T$ collects the coordinates describing the protein matrix and where $\boldsymbol{n} = (n_1, n_2, \dots)$ denotes the set of quantum numbers n_j of the individual oscillators. We assume that all degrees of freedom of the protein matrix are harmonic. The eigenstates and eigenvalues are explicitly

$$\langle \boldsymbol{q} | \boldsymbol{n} \rangle^{(\mathrm{r})} \;=\; \prod_j \langle q_j | n_j \rangle^{(\mathrm{r},j)} \;=\; \prod_j \left(\frac{\lambda_j}{\pi} \right)^{\frac{1}{4}} (2_j^n n_j!)^{-\frac{1}{2}} H_{m_j}(\sqrt{\lambda_j} q_j)\, e^{-\frac{1}{2}\lambda q_j^2} \tag{18.96}$$

$$\epsilon_{\boldsymbol{n}}^{(\mathrm{r},j)} \;=\; \sum_j \hbar \omega_j (n_j \;+\; \frac{1}{2}) \tag{18.97}$$

$$\begin{aligned} \langle \boldsymbol{q} | \boldsymbol{m} \rangle^{(\mathrm{p})} \;&=\; \prod_j \langle q_j | m_j \rangle^{(\mathrm{p},j)} \\ &=\; \prod_j \left(\frac{\lambda_j}{\pi} \right)^{\frac{1}{4}} (2_j^m m_j!)^{-\frac{1}{2}} H_{m_j}(\sqrt{\lambda_j}(q_j - \frac{c_j}{\omega_j^2}))\, e^{-\frac{1}{2}\lambda_j (q_j - c_j/\omega_j^2)^2} \end{aligned} \tag{18.98}$$

$$\epsilon_n^{(\mathrm{p},j)} \;=\; \sum_j \hbar \omega_j (m_j \;+\; \frac{1}{2}) \tag{18.99}$$

where

$$\lambda_j \;=\; \omega_j / \hbar \tag{18.100}$$

The overall rate of transfer from reactant states to product states can be written again in the form

$$k_{qb}(R \to P) \;=\; \frac{2\pi}{\hbar^2} v^2 \mathcal{S}_{qo}(E) \tag{18.101}$$

where, according to (18.68, 18.69), the line shape function is

$$\mathcal{S}_{qb}(E) \;=\; \frac{1}{2\pi} \int_{-\infty}^{+\infty} dt\; e^{itE/\hbar} \prod_j \left(\sum_{n_j, m_j = 0}^{\infty} p_{n_j}^{(\mathrm{r,j})}\, e^{-it\epsilon_{n_j}^{(\mathrm{r},j)}/\hbar} |^{(\mathrm{r},j)} \langle n | m \rangle^{(\mathrm{p},j)}|^2\, e^{it\epsilon_{m_j}^{(\mathrm{p},j)}/\hbar} \right) . \tag{18.102}$$

with

$$p_n^{(\mathrm{r},j)} \;=\; x_j^n(1\,-\,x_j)\;,\quad x_j \;=\; e^{-\hbar\omega_j/kT}\;, \tag{18.103}$$

Each of the factors on the r.h.s. of (18.102) corresponds to the single respective term in (18.70), i.e., to a term which has been evaluated above [c.f. (18.5)]. Comparision with (18.5) allows one then to evaluate (18.102) as well. This leads to the expression [9, 8, 23]

$$k_{qb}(R\to P) \;=\; \frac{v^2}{\hbar^2}\int_{-\infty}^{+\infty} dt\; e^{itE/\hbar}\; e^{iQ_1(t)/\pi\hbar}\; e^{-Q_2(t)/\pi\hbar} \tag{18.104}$$

where

$$Q_1(t) \;=\; \frac{\pi}{2}\sum_j \frac{c_j^2}{\hbar\omega_j^3}\sin\omega_j t \tag{18.105}$$

$$Q_2(t) \;=\; \frac{\pi}{2}\sum_j \frac{c_j^2}{\hbar\omega_j^3}\coth\frac{\hbar\omega_j}{2kT}\,[1-\cos(\omega_j t)]\;. \tag{18.106}$$

One can express the rate for the backward reaction by reversing the sign of E in this expression [23]

$$k_{qb}(P\to R) \;=\; \frac{v^2}{\hbar^2}\int_{-\infty}^{+\infty} dt\; e^{-itE/\hbar}\; e^{iQ_1(t)/\pi\hbar}\; e^{-Q_2(t)/\pi\hbar}\;. \tag{18.107}$$

A kinetic system with two states R and P is described by the vector $\boldsymbol{p}(t) \;=\; (p_R(t),\, p_P(t))^T$ where the components $p_R(t)$ and $p_P(t)$ account for the probability to observe, at time t, the states R and P, respectively. $\boldsymbol{p}(t)$ obeys the rate equation

$$\frac{d}{dt}\begin{pmatrix} p_R(t)\\ p_P(t)\end{pmatrix} \;=\; \begin{pmatrix} -k_{qb}(R\to P) & k_{qb}(P\to R)\\ k_{qb}(R\to P) & -k_{qb}(P\to R)\end{pmatrix}\begin{pmatrix} p_R(t)\\ p_P(t)\end{pmatrix} \tag{18.108}$$

which needs to be solved for some initial condition. In the present case we consider a system starting in state R, i.e., the initial condition is $\boldsymbol{p}(0) \;=\; (1,\,0)^T$. The corresponding solution of (18.108) is

$$\begin{pmatrix} p_R(t)\\ p_P(t)\end{pmatrix} \;=\; \frac{1}{k_{qb}(R\to P)\,+\,k_{qb}(P\to R)}\left[\begin{pmatrix} k_{qb}(P\to R)\\ k_{qb}(R\to P)\end{pmatrix} + \right. \tag{18.109}$$

$$\left. +\;\begin{pmatrix} k_{qb}(R\to P)\\ -k_{qb}(R\to P)\end{pmatrix}\exp\{-\,[k_{qb}(R\to P)\,+\,k_{qb}(P\to R)]\}\right]\;.$$

Accordingly, the state R decays with a rate $k_{qb}(R\to P)\,+\,k_{qb}(P\to R)$ to an equilibrium mixture of the states R and P, i.e., the relaxation rate k_{rel} of the initial state R, according to (18.104, 18.107) is

$$k_{\mathrm{rel}} \;=\; 2\frac{v^2}{\hbar^2}\int_{-\infty}^{+\infty} dt\,\cos(-itE/\hbar)\; e^{iQ_1(t)/\pi\hbar}\; e^{-Q_2(t)/\pi\hbar}\;. \tag{18.110}$$

Since $Q_1(t)$, according to (18.105), is an odd function of t we note that in

$$e^{iQ_1(t)/\pi\hbar} \;=\; \cos(Q_1(t)/\pi\hbar)\;+\;i\sin(Q_1(t)/\pi\hbar) \tag{18.111}$$

the real part is an even function of t and the imaginary part is an odd function of t. Since, according to (18.106) $Q_2(t)$ and, hence, also $\exp(-Q_2(t)/\pi\hbar)$ is an even function of t, the time integral involving $\sin(Q_1(t)/\pi\hbar)$ vanishes and one is left with the expression [23]

$$k_{\rm rel} \;=\; \frac{2v^2}{\hbar^2}\int_0^{+\infty} dt\,\cos(-itE/\hbar)\,\cos(Q_1(t)/\pi\hbar)\,e^{-Q_2(t)/\pi\hbar}\;. \tag{18.112}$$

The result obtained, at first sight, appears to be of little value since evaluation of the functions $Q_1(t)$ and $Q_2(t)$, according to (18.105, 18.106), requires knowledge of the quantities $c_j^2/\hbar\omega_j^3$ for the ensemble of oscillators. Fortunately, it is possible to achieve the evaluation in case that the spectral density

$$J(\omega) \;=\; \frac{\pi}{2}\sum_j \frac{c_j^2}{\omega_j}\,\delta(\omega\,-\,\omega_j) \tag{18.113}$$

is known. In fact, one can express

$$Q_1(t) \;=\; \int_0^{\infty} d\omega\,\omega^{-2}J(\omega)\,\sin\omega t \tag{18.114}$$

$$Q_2(t) \;=\; \frac{\pi}{2}\int_0^{\infty} d\omega\,\omega^{-2}J(\omega)\,\coth\frac{\hbar\omega}{2kT}\,(1-\cos\omega t)\;. \tag{18.115}$$

We want to demonstrate in the next section that the density $J(\omega)$ can be determined from molecular dynamics simulations in which the function $\epsilon(t) \,=\, \Delta E[\mathbf{R}(t)]$, as defined in (18.28), is monitored. In fact, $J(\omega)$ is the spectral density of $\Delta E[\mathbf{R}(t)]$.

18.7 From the Energy Gap Correlation Function $\Delta E[\mathbf{R}(t)]$ to the Spectral Density $J(\omega)$

In this section we will derive a relationship which connects, in the limit of high temperature, $J(\omega)$ and the auto-correlation function $C_{\epsilon\epsilon}(t)$ of the energy gap function[61], introduced in Section 18.4. We start from definition (18.38) of $C_{\epsilon\epsilon}(t)$ and express, according to (18.94),

$$\epsilon(t) \;=\; \hat{H}_p \;-\; \hat{H}_r \;+\; E \tag{18.116}$$

where the Hamiltonian operators will be interpreted as Hamiltonian functions of classical bath oscillators, an identification which holds at high temperatures. One obtains

$$\epsilon(t) \;=\; -\sum_j c_j q_j(t) \;+\; \sum_j \frac{1}{2}\,\omega_j^{-2}c_j^2\;. \tag{18.117}$$

The time average of $\epsilon(t)$ *in the reactant state*, i.e., for $\langle q_j\rangle_R \,=\, 0$, is

$$\langle\epsilon\rangle_R \;=\; \sum_j \frac{1}{2}\,\omega_j^{-2}c_j^2\;. \tag{18.118}$$

In the product state holds $\langle q_j\rangle_P \,=\, c_j/\omega_j$ and, hence, the corresponding average of $\epsilon(t)$ is

$$\langle\epsilon\rangle_P \;=\; -\sum_j \frac{1}{2}\omega_j^{-2}c_j^2 \;+\; E\;. \tag{18.119}$$

We want to evaluate now the equilibrium correlation function $C_{\epsilon\epsilon}(t)$ for the protein in the reactant state R. For this purpose we start from the expression

$$C_{\epsilon\epsilon}(t) \;=\; \frac{\langle\,(\epsilon(t)\,-\,\langle\epsilon\rangle)\,(\langle\epsilon(0)\,-\,\langle\epsilon\rangle)\,\rangle}{\langle\epsilon(0)\,-\,\langle\epsilon\rangle\,\rangle^2} \tag{18.120}$$

The quantity $\delta\epsilon(t) \,=\, \epsilon(t) \,-\, \langle\epsilon\rangle$ which enters here is, using (18.118),

$$\delta E(t) \;=\; -\,\sum_j c_j q_j(t)\;. \tag{18.121}$$

In the high temperature limit the motion of the bath oscillators is described by

$$q_j(t) \;=\; A_j\,\cos(\omega_j t \,+\, \varphi_j)\;. \tag{18.122}$$

The numerator $C_1(t)$ of the r.h.s. of (18.120) can then be written

$$\begin{aligned} C_1(t) \;&=\; \langle\delta\epsilon(t)\,\delta\epsilon(o)\rangle \\ &=\; \left\langle \left(\sum_j c_j\,A_j\cos(\omega_j t\,+\,\varphi_j)\right)\,\left(\sum_j{}' c_{j'}\,A_{j'}\cos\varphi_{j'}\right)\right\rangle \\ &=\; \frac{1}{4}\,\langle\sum_{j,j'} c_j\,c_{j'}\,A_j\,A_{j'}\,\left[\exp\left(i\,(\omega_j t\,+\,\varphi_j\,+\,\varphi_{j'})\right)\,+\right. \\ &+\exp\left(-i\,(\omega_j t\,+\,\varphi_j\,+\,\varphi_{j'})\right)\,+\,\exp\left(i\,(\omega_j t\,+\,\varphi_j\,-\,\varphi_{j'})\right)\,+ \\ &\left.+\exp\left(-i\,(\omega_j t\,+\,\varphi_j\,-\,\varphi_{j'})\right)\right]\,\rangle \end{aligned} \tag{18.123}$$

where the initial phases φ_j and $\varphi_{j'}$ are uniformly distributed in the interval $[0,\,2\pi)$.
In carrying out the averages in (18.123) we follow Rayleigh [40, 41] and note that for the averages over the phases holds

$$\langle\exp\left(i\,(\varphi_j\,+\,\varphi_{j'})\right)\rangle \;=\; 0\,; \qquad \langle\exp\left(i\,(\varphi_j\,-\,\varphi_{j'})\right)\rangle \;=\; \delta_{jj'}\;. \tag{18.124}$$

This yields

$$C_1(t) \;=\; \frac{1}{2}\,\sum_j c_j^2\,\langle\,A_j^2\,\rangle\cos\omega_j t\;. \tag{18.125}$$

Using the well-known fact that the average energy of a harmonic oscillator is $k_B T$, i.e.,

$$\frac{1}{2}\,\omega_j^2\,\langle\,A_j^2\rangle \;=\; k_B\,T\;, \tag{18.126}$$

one concludes

$$C_1(t) \;=\; \sum_{j=1}^{N} c_j^2\,\frac{k_B T}{\omega_j^2}\cos\omega_j t\;\;. \tag{18.127}$$

This can be expressed, employing the definition (18.113) of $J(\omega)$,

$$C_1(t) \;=\; \frac{2k_B T}{\pi}\,\int_0^\infty \mathrm{d}\omega\,\frac{J(\omega)}{\omega}\,\cos\omega t\;. \tag{18.128}$$

Noting $C(t) = C_1(t)/C_1(0)$ one obtains finally

$$C_{\epsilon\epsilon}(t) \;=\; \frac{\int_0^\infty \mathrm{d}\omega\; J(\omega)/\omega\, \cos\omega t}{\int_0^\infty \mathrm{d}\omega\; J(\omega)/\omega}\;, \tag{18.129}$$

a relationship which has been stated before [42, 2].
We want to express $J(\omega)$ through $C_{\epsilon\epsilon}(t)$. Fourier's theorem yields

$$\frac{2}{\pi}\int_0^\infty dt\cos\omega t\;\left[\int_0^\infty d\omega'\,\frac{J(\omega')}{\omega'}\cos\omega' t\right] \;=\; \frac{J(\omega)}{\omega} \tag{18.130}$$

and, hence, one can state

$$\frac{J(\omega)}{\omega} \;=\; \frac{2}{\pi}\left[\int_0^\infty d\omega\,\frac{J(\omega)}{\omega}\right]\;\int_0^\infty dt\, C_{\epsilon\epsilon}(t)\cos\omega t\;. \tag{18.131}$$

The integral $\int_o^\infty d\omega J(\omega)/\omega$ can be expressed in terms of the variance $\sigma^2 = \langle\epsilon^2\rangle - \langle\epsilon\rangle^2$. For this purpose we consider first a subset of N_j bath oscillators with identical frequencies ω_j. We designate these oscillators by a second (beside j) index α. $\delta E(t)$, according to (18.121), is

$$\delta E(t) \;=\; -\sum_j\sum_\alpha c_{j\alpha}\,A_{j\alpha}\cos\left(\omega_j t \,+\, \varphi_{j\alpha}\right)\;. \tag{18.132}$$

In this expression appear the quantities

$$U_{j\alpha} \;=\; c_{j\alpha}\,A_{j\alpha}\cos\left(\omega_j t \,+\, \varphi_{j\alpha}\right) \tag{18.133}$$

$$U_j \;=\; \sum_\alpha U_{j\alpha} \tag{18.134}$$

which will be characterized further; specifically, we seek to determine the distribution of U_j.
The distribution of the quantity (18.134) for oscillators in thermal equilibrium has been provided by Rayleigh [40, 41]. Following his procedure one notes

$$\begin{aligned} U_j \;&=\; \sum_\alpha c_{j\alpha}\,A_{j\alpha}\cos\left(\omega_j t \,+\, \varphi_{j\alpha}\right) \\ &=\; \cos\left(\omega_j t\right)\,\sum_\alpha c_{j\alpha}\,A_{j\alpha}\cos\varphi_{j\alpha} \;-\; \sin\left(\omega_j t\right)\,\sum_\alpha c_{j\alpha}\,A_{j\alpha}\sin\varphi_{j\alpha} \\ &=\; \gamma_j\cos\left(\,\omega_j t \,+\, \vartheta_j\,\right) \end{aligned} \tag{18.135}$$

where

$$\gamma_j \;=\; \sqrt{\left(\sum_\alpha c_{j\alpha}\,A_{j\alpha}\cos\varphi_{j\alpha}\right)^2 \,+\, \left(\sum_\alpha c_{j\alpha}A_{j\alpha}\sin\varphi_{j\alpha}\right)^2} \tag{18.136}$$

$$\tan\vartheta_j \;=\; \left(\sum_\alpha c_{j\alpha}A_{j\alpha}\sin\varphi_{j\alpha}\right)\;\Big/\;\left(\sum_\alpha c_{j\alpha}A_{j\alpha}\cos\varphi_{j\alpha}\right)\;. \tag{18.137}$$

Rayleigh has shown [41] that γ_j and ϑ_j are randomly distributed for large N_j. The distribution $p_j(\gamma_j)$ of γ_j is

$$p_j(\gamma_j) \;=\; \frac{2}{\delta_j^2}\,\gamma_j\exp\left(-\frac{\gamma_j^2}{\delta_j^2}\right)\;,\quad \delta_j \;=\; \sum_\alpha c_{j\alpha}^2\,A_{j\alpha}^2\;. \tag{18.138}$$

The distribution of the phase angles ϑ_j is immaterial as the derivation below will show. According to the above calculations U_j behaves like a *single* oscillator with randomly distributed amplitudes γ_j and randomly distributed phases ϑ_j.
Let us consider now a particular oscillator of this ensemble, described by fixed γ_j and ϑ_j,

$$U_j(t) \;=\; \gamma_j \cos\left(\omega_j t \,+\, \vartheta_j\right) \;. \tag{18.139}$$

Sampling such $U_j(t)$ at many time points $t = t_1, t_2, \ldots$ leads to a distribution [50]

$$\hat{p}_j(U_j) \;=\; \begin{cases} \frac{1}{\pi\sqrt{\gamma_j^2 - U_j^2}} & \text{for } U_j \,\leq\, \gamma_j \\ 0 & \text{for } U_j \,>\, \gamma_j \;. \end{cases} \tag{18.140}$$

For a large ensemble of oscillators with a distribution of γ_j and ϑ_j values as described above the distribution of U_j can be determined now in a straightforward way. For the oscillator (18.139) all ensemble elements with $\gamma_j \,\geq\, U_j$ contribute. The distribution $\tilde{p}(U_j)$ for the whole ensemble of bath oscillators is, therefore,

$$\begin{aligned} \tilde{p}(U_j) \;&=\; \int_{U_j}^{\infty} d\gamma_j \, p_j(\gamma_j)\, \hat{p}_j(U_j) \\ &=\; \int_{U_j}^{\infty} d\gamma_j \; \frac{2}{\delta_j^2}\, \gamma_j \exp\left(-\frac{\gamma_j^2}{\delta_j^2}\right) \; \frac{1}{\pi\sqrt{\gamma_j^2 \,-\, U_j^2}} \;. \end{aligned} \tag{18.141}$$

The integral can be evaluated analytically. For this purpose we introduce the variable $y \,=\, \gamma_j^2 - U_j^2$. Using

$$\int_0^{\infty} dy \, \frac{1}{\sqrt{y}}\, e^{-\lambda y} \;=\; \frac{\sqrt{\pi}}{\lambda} \tag{18.142}$$

one obtains

$$\tilde{p}(U_j) \;=\; \frac{1}{\sqrt{\pi\tilde{\sigma}^2}} \exp\left(-\frac{U_j^2}{\tilde{\sigma}_j^2}\right) \;, \tag{18.143}$$

i.e., a Gaussian distribution.
According to (18.132–18.134) holds $\delta E \,=\, \sum_j U_j$. Since each of the terms in this sum is Gaussian–distributed, the distribution of δE is Gaussian as well, namely,

$$p(\delta E) \;=\; \frac{1}{2\pi\sigma^2} \exp\left(-\frac{(\delta E)^2}{2\sigma^2}\right) \tag{18.144}$$

$$\sigma^2 \;=\; \frac{1}{2}\sum_j \sigma_j^2 \;=\; \frac{1}{2}\sum_{j,\alpha} c_{j\alpha}^2\, A_{j\alpha}^2 \;. \tag{18.145}$$

In the classical, i.e., high temperature, limit holds at equilibrium

$$\sigma^2 \;=\; \frac{1}{2}\sum_{j,\alpha} c_{j\alpha}^2 \,\langle A_{j\alpha}^2 \rangle \;=\; \frac{1}{2}\sum_{j,\alpha} \frac{2\, k_B\, T^2}{\omega_j}\; c_{j\alpha}^2 \tag{18.146}$$

where we have used (18.126). One can then express the sum over the coefficients $c_{j\alpha}^2$ through $J(\omega)$ using the definition of the latter, i.e., (18.113), and, hence, one can conclude

$$\sigma^2 \;=\; \frac{2k_B T}{\pi} \int_0^{\infty} d\omega \; \frac{J(\omega)}{\omega} \;. \tag{18.147}$$

We can finally provide the desired expression of $J(\omega)$. Employing (18.147) in (18.131) yields

$$\frac{J(\omega)}{\omega} \;=\; \frac{\sigma^2}{k_B\,T}\,\int_0^\infty dt\,C(t)\cos\omega t\;. \tag{18.148}$$

Accordingly, $J(\omega)$ can be determined from a molecular dynamics simulation which records the fluctuations of $\epsilon(t) = \Delta E[\mathbf{R}(t)]$ and determines then the energy gap correlation function (18.120). In case that the gap correlation function obeys a simple exponential decay (18.40) one can evaluate (18.148) further and obtains

$$\frac{J(\omega)}{\omega} \;=\; \frac{\eta\,\omega}{1\,+\,\omega^2\tau^2}\;,\quad \eta \;=\; \frac{\sigma^2\tau}{k_BT}\;, \tag{18.149}$$

a form of $J(\omega)$ known as the Debey function.

18.8 Evaluating the Transfer Rate

We want to discuss now the evaluation of the relaxation rate $k_{\rm rel}$. The evaluation is based on Eqs. (18.112, 18.114, 18.115) and requires knowledge of the spectral density $J(\omega)$ given by (18.149). For this purpose the material properties σ, τ and $\langle\epsilon\rangle$ are required as determined through a molecular dynamics simulation. Typical values of σ and τ are 3.9kcal/mol and 94 fs, determined for electron transfer at $T = 300$ K in the photosynthetic reaction center in *Rhodopseudomonas viridis* [46]. The value of $\langle\epsilon\rangle$ is difficult to determine precisely and one may rather determine the rate $k_{\rm rel}$ as a function of E and shift $k_{\rm rel}(E)$ along the energy axis according to available experimental information. $k_{\rm rel}(E)$, at physiological temperatures, assumes a maximum value for a given E–value and one may argue that in a given protein the rate process has been optimized through adapting the additive contributions $\langle\epsilon\rangle$ and redox energy difference E.
In case of $J(\omega)$, given by the Debye function (18.149), one can determine $Q_1(t)$ defined in (18.114)

$$Q_1(t) \;=\; \int_0^\infty d\omega\,\frac{\eta\,\sin\omega t}{\omega\,(\,1\,+\,\omega^2\tau^2\,)} \;=\; \frac{\eta\pi}{2}\,\left[\,1\,-\,\exp\left(\,-\frac{t}{\tau}\,\right)\right] \tag{18.150}$$

Using $1-\cos\omega t \;=\; 2\sin^2(\omega t/2)$ one can write (18.112)

$$\begin{aligned} k_{\rm rel}(E,T) \;\;&=\;\; \left(\frac{2v}{\hbar}\right)^2\,\int_0^\infty dt\cos\left(\frac{Et}{\hbar}\right)\,\cos\left[\,\frac{\eta}{2\hbar}\left(1\,-\,e^{-t/\tau}\right)\right]\,\times \\ &\qquad \times\,\exp\left[\,-\frac{2\eta}{\pi\hbar}\int_0^\infty d\omega\,\frac{\sin^2\left(\frac{\omega t}{2}\right)}{\omega\,(\,1\,+\,\omega^2\tau^2\,)}\coth\left(\frac{\beta\hbar\omega}{2}\right)\right]\;. \end{aligned} \tag{18.151}$$

To simplify this expression we define $x = t/\tau$, $y = \omega\tau$, and $\gamma = \eta/h$ which yields

$$\begin{aligned} k_{\rm rel}(E,T) \;\;&=\;\; \left(\frac{2V}{\hbar}\right)^2\,\tau\,\int_0^\infty dx\cos\left(\frac{E\tau}{\hbar}\,x\right)\,\cos\left[\,\gamma\pi\,\left(\,1\,-\,e^{-x}\right)\right]\,\times \\ &\qquad \times\,\exp\left[\,-4\gamma\int_0^\infty dy\,\frac{\sin^2\left(\frac{xy}{2}\right)}{y\,(\,1\,+\,y^2\,)}\coth\left(\,\frac{\hbar}{2k_B\tau}\cdot\frac{y}{T}\,\right)\right]\;. \end{aligned} \tag{18.152}$$

A typical numerical value for $V/\hbar$ is 5 ps^{-1} [46].

A straightforward numerical evaluation of (18.152) is time consuming since it involves a double integral. One can use a more convenient, albeit approximate, expression for the $\exp[\cdots]$ factor in the integrand of (18.152). We define for this purpose

$$q_2(x) \;=\; \int_0^\infty dy\, \frac{\sin^2\left(\frac{xy}{2}\right)}{y\,(1\,+\,y^2)}\, \coth\left(\alpha y\right)\;,\quad \alpha \;=\; \frac{\hbar}{2k_B\tau T}\;. \tag{18.153}$$

As demonstrated in [61], $q_2(x)$ is a monotonously increasing function of x. The main contribution to (18.153) stems from the region of small x. One may employ an expansion of $q_2(x)$ which holds for small x

$$q_2(x) \;\approx\; \frac{x^2}{4}\,\left[\,f(\alpha)\;-\;\ln x\,\right] \tag{18.154}$$

where

$$f(\alpha) \;=\; \int_0^\infty \frac{y\,dy}{1\,+\,y^2}\,\left[\coth(\alpha y)\;-\;1\right]\;. \tag{18.155}$$

Since $q_2(x)$ is E–independent one can use the same numerical approximation for all E–values considered. Hence, for a given temperature obtaining $k(E,T)$ at all different E values requires one to evaluate $q_2(x)$ only once. Then (18.152) is evaluated using

$$k_{appr}(E,T) \;=\; \left(\frac{2V}{\hbar}\right)^2 \tau \int_0^\infty dx \cos\left(\frac{E\tau}{\hbar}\,x\right)\,\cos\left[\,\gamma\pi\,\left(1\;-\;e^{-x}\right)\,\right]\,e^{-4\gamma q_2(x)} \tag{18.156}$$

with $q_2(x)$ given by (18.154, 18.154).

High Temperature Limit In the limit of high temperature the expression (18.112) of the electron transfer rate can be evaluated by the method of steepest descent. This approximation is based on a quadratic expansion of $Q_2(t)$ around its minimum at $t \;=\; 0$. The procedure requires one to determine the quantity

$$\mu \;=\; \frac{d^2}{dt^2}\,Q_2(t)\Big|_{t=0} \tag{18.157}$$

The expression for $Q_2(t)$ in (18.151) yields

$$\mu \;=\; \int_0^\infty d\omega J(\omega)\coth\left(\frac{\beta\hbar\omega}{2}\right)\;. \tag{18.158}$$

Unfortunately, for many choices of $J(\omega)$ this expression diverges and the steepest descent method cannot be applied. However, we note that the divergence of (18.158) is due to $\omega \;\to\; \infty$ contributions to the integral over $J(\omega)$. Since the number of modes in a protein are finite, the divergence in (18.158) is due to an artificial analytical form of $J(\omega)$. If one would assume a cut-off frequency ω_c, i.e., replace $J(\omega)$ by $J(\omega)\,\theta(\omega\;-\;\omega_c)$, a divergence would not arise in (18.158). One may, hence, assume that the second derivative (18.157) actually exists, approximate

$$Q_2(t) \;\approx\; \frac{1}{2}\,\mu\,t^2\;, \tag{18.159}$$

and employ this in a steepest descent method.

At a sufficiently high temperature, contributions to the integral in (18.112) arise only in a vicinity of $t = 0$ where (18.159) is small. In this case, one can approximate $Q_1(t)$ in (18.151) linearly around $t = 0$

$$Q_1(t) \approx \nu\, t\,; \quad \nu = \frac{d}{dt} Q_1(t)\Big|_{t=0} \tag{18.160}$$

where

$$\nu = \int_0^\infty d\omega \, \frac{J(\omega)}{\omega} \,. \tag{18.161}$$

By using the approximations (18.159) and (18.160) in (18.112), if E is not close to 0, one obtains [14, 35, 61]

$$k_{\rm rel}(E,T) \approx \frac{2\pi V^2}{\hbar} \frac{1}{\sqrt{2\pi\delta^2}} \exp\left[-\frac{(E - E_m)^2}{2\delta^2} \right] \,. \tag{18.162}$$

where

$$\delta^2 = \frac{\hbar\mu}{\pi} = \frac{\hbar}{\pi} \int_0^\infty d\omega \, J(\omega) \, coth\left(\frac{\beta\hbar\omega}{2}\right) \tag{18.163}$$

$$E_m = \frac{\nu}{\pi} = \frac{1}{\pi} \int_0^\infty d\omega \, \frac{J(\omega)}{\omega} \,. \tag{18.164}$$

At a high enough temperature, i.e., for $T > 100$ K, according to our numerical calculations, one can show further [61]

$$\delta = \sigma\,; \quad E_m = \frac{\sigma^2}{2k_BT} \,. \tag{18.165}$$

According to (18.164), E_m is actually temperature independent. Hence, one can rewrite (18.162) into a form which agrees with the rate as given by the classical Marcus theory

$$k_M(\epsilon,T) = \frac{2\,\pi\,V^2}{\hbar} \frac{1}{\sqrt{2\pi f k_B T q_o^2}} \exp\left[-\frac{(\epsilon - \frac{1}{2} f q_o^2)^2}{2k_BT f q_o^2} \right] \tag{18.166}$$

where

$$f\, q_o^2 = 2\,\epsilon_m = \frac{\sigma^2}{k_BT}\Big|_{T=300K} \,. \tag{18.167}$$

Low Temperature Limit At low temperatures, one can employ (18.155) for $\alpha = \hbar/2\tau k_BT \to \infty$, to approximate $q_2(x)$ further. It can be verified

$$\lim_{\alpha\to\infty} f(\alpha) = \frac{\pi^2}{12\alpha^2} \,. \tag{18.168}$$

The value of the integral in (18.156) results mainly from contributions at small x. Accordingly, at low temperatures one can assume the overall integrand to be dominated by the interval in which $\gamma\pi^2x^2\,/12\alpha^2$ is small. Therefore, one can apply (18.154) to expand the exponential part of (18.156),

$$\begin{aligned} e^{-4\gamma q_2(x)} &= \exp\left(\gamma x^2 \ln x - \frac{\gamma\pi^2x^2}{12\alpha^2} \right) \\ &= \exp\left(\gamma x^2 \ln x \right) \left[1 - \left(\frac{\gamma\pi^2x^2}{12}\right) \left(\frac{2k_B\tau T}{\hbar}\right)^2 \right] \,. \end{aligned} \tag{18.169}$$

Then the electron transfer rate at $T \to 0$ can be expressed

$$k(E,T) \approx k(E,0) - k_1(E) \left(\frac{2k_B\tau T}{\hbar}\right)^2 , \tag{18.170}$$

where

$$k_1(E) = \left(\frac{2V}{\hbar}\right)^2 \tau \int_0^\infty dx \cos\left(\frac{E\tau}{\hbar}\, x\right) \cos\left[\gamma\pi\,\left(1 - e^{-x}\right)\right] \left(-\frac{\gamma\pi^2 x^2}{12}\right) \exp\left(\gamma x^2 \ln x\right) . \tag{18.171}$$

From (18.170), one concludes that at low temperatures, the electron transfer rate is actually changing very slowly with temperature. This behavior has been found in many observations [12, 32].

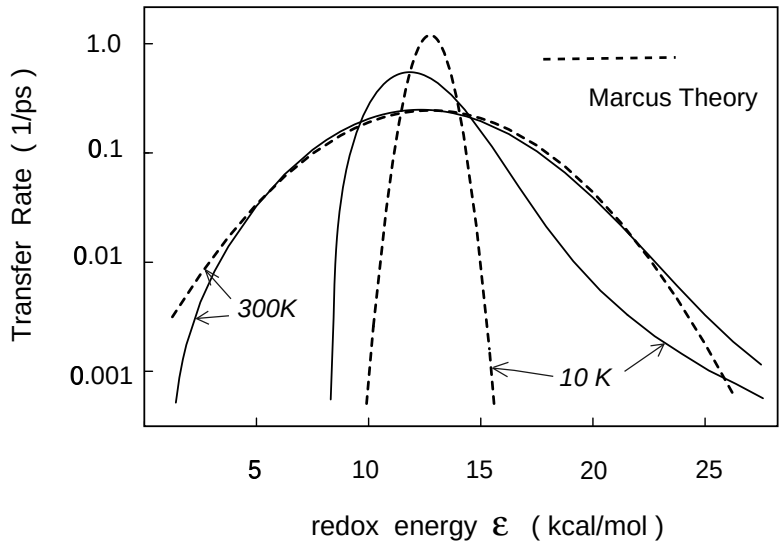

Figure 18.2: Comparison of electron transfer rates $k(\epsilon, T)$ shown as a function of ϵ evaluated in the framework of the spin–boson model (solid lines) and by Marcus theory (dashed lines) at temperatures 10 K and 300 K. The functions are centered approximately around ϵ_m. From [60].

Results In Fig. 18.2 we present calculated electron transfer rates $k_{\rm rel}(E,T)$ as a function of the redox energy difference E for temperatures $T = 10$ K and $T = 300$ K, and compare the results to transfer rates predicted by the Marcus theory, e.g., by Eq. (18.166, 18.167). One can observe that at physiological temperatures, the rate evaluated from the Marcus theory in a wide range of E–values, agrees well with the rate evaluated from the spin–boson model at $T = 300$ K, a behavior which is expected from the high temperature limit derived above. However the Marcus theory and the spin–boson model differ significantly at $T = 10$ K. At such low temperature the rate as a function of E for the spin–boson model is asymmetrical. This result agrees with observations reported in [15] which show a distinct asymmetry with respect to E_m at low temperatures. Such asymmetry is not predicted by the models of Marcus and Hopfield [27, 49, 17].
If one makes the assumption that biological electron transfer systems evolved their E-values such that rates are optimized, one should expect that electron transfer rates in the photosynthetic reaction center are formed through a choice of $E \to E_{max}$, such that $k(E_{max})$ is a maximum. In Fig. 18.3 we present corresponding maximum transfer rates, $k(E_{max})$ as well as $k(E,T)$ for non-optimal values of $E = E_m \pm \delta$, where $\delta = 2.5$ kcal/mol. Experimental data of electron

transfer processes in the photosynthetic reaction center show increases similarly to those presented in Fig. 18.3 [7, 29, 19, 32]. However, Fig. 18.3 demonstrates also that electron transfer at E-values slightly off the maximum position can yield a different temperature dependence than that of $k(E_m, T)$, namely temperature independence or a slight decrease of the rate with decreasing temperature. Such temperature dependence has also been observed for biological electron transfer [32]. As Nagarajan et al. reported in [32] the temperature dependence of the transfer rate resembles that of $k(E_m, T)$ in photosynthetic reaction centers of native bacteria and in (M)Y210F-mutants with tyrosine at the 210 position of the M–unit replaced by phenylalanine. However, a replacement of this tyrosine by isoleucine [(M)Y210I-mutant] yields a transfer rate which decreases like $k(E_m - \delta, T)$ shown in Fig. 18.3. This altered temperature dependence should be attributed to a shift of the redox potentials, i.e., $E_m \rightarrow E_m - \delta$.

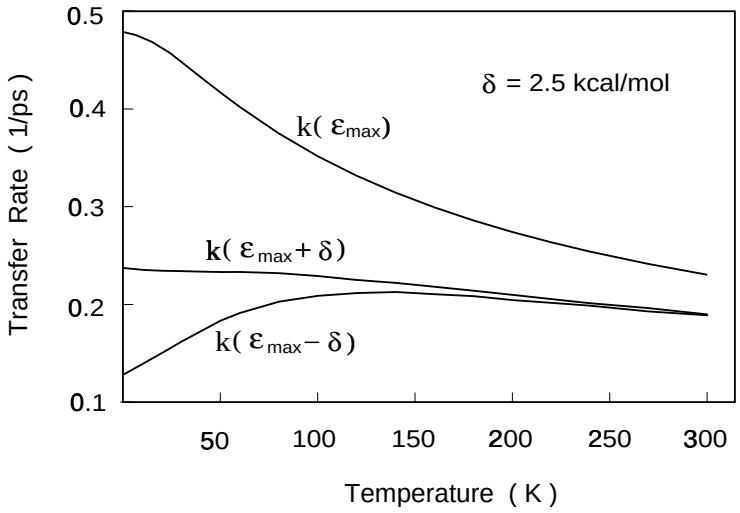

Figure 18.3: Comparison of the temperature dependence of the maximum transfer rate of $k(\epsilon_m)$ and off-maximum value $k(\epsilon_{max} \pm \delta)$, where $\delta = 2.5$ kcal/mol. $k(\epsilon_{max}, T)$ represents the fastest transfer rate of the system, the rates $k(\epsilon_{max} \pm \delta, T)$ are slower since their E–values deviate from the optimal value ϵ_{max}. From [60].

The combination of simulation methods and analytical theory outlined in this lecture has proven to be a promising approach to describe redox processes in proteins. Neither approach by itself can be successful since, on the one hand, proteins are too heterogeneous and ill understood to be molded into simple models, on the other hand, simulation methods are blind, leaving one with too much information and as a result, with none. The present example, connecting a single simulated observable, the medium redox energy contribution $\Delta E(t)$, with a model of the quantum system, avoids superfluous or undetermined parameters and can be extended readily to other curve crossing processes in proteins. We like to mention, finally, that there have been numerous similar investigations of biological electron transfer [57, 56, 59, 62].

18.9 Appendix: Numerical Evaluation of the Line Shape Function

We want to provide here an algorithm for the evaluation of the line shape function (18.44). The algorithm suggested is based on an expansion in terms of the right $[(u|m\rangle]$ and left $[\langle\tilde{n}|u)]$ eigenfunctions of the operator $\mathcal{L} = D\ \partial_u\ p_0(u)\ \partial_u\ [p_0(u)]^{-1}$ given in the Fokker-Planck Eq. (18.41).

These eigenfunctions are in the present case

$$(u|n\rangle = \frac{1}{\sqrt{\pi}}\frac{2^{-n}}{n!}e^{-u^2}H_n(u)\ , \quad \langle\tilde{m}|u) = H_m(u) \tag{18.172}$$

where H_m denotes the Hermite polynomial. We assume in the following $\sigma = 1$, i.e. measure u in units of σ and D in units of σ^{-2}. In general, the eigenfucjtions and eigenvalues of the stochastic operator are not available in analytical form and an evaluation of the line shape function is based on discretization of the coordinate u and of the operator $\mathcal{L}$. The eigenfunctions form a bi-orthogonal system [1] , i.e., defining $\langle\tilde{m}|n\rangle = \int_{-\infty}^{+\infty} du \angle m|u)\,(u|n\rangle$, the following property applies

$$\langle\tilde{m}|n\rangle = \frac{1}{\sqrt{\pi}}\frac{2^{-n}}{n!}\int_{-\infty}^{+\infty} du\ H_m(u)e^{-u^2}H_n(u) = \delta_{mn}\ . \tag{18.173}$$

One can show that the function spaced spanned by the eigenfunctions is complete, i.e., any element of $\{f(u), u\ \in\ ]-\infty,\infty[,\ f$ continuous$\}$ can be expanded. The eigenvalues of $\mathcal{L}$ follow from the property [1]

$$\mathcal{L}|n\rangle = -2mD|n\rangle\ ,\ \langle\tilde{m}|\mathcal{L}^\dagger = -2mD\langle\tilde{m}|\ . \tag{18.174}$$

According to [1] holds

$$(u|n+1\rangle = 2u(u|n\rangle - 2n\,(u|n-1\rangle\ ,\ \langle\tilde{m}|u|n\rangle = \frac{1}{2}\delta_{mn+1} + n\delta_{mn-1}\ . \tag{18.175}$$

From this and Eq. 18.174 we obtain

$$\langle\tilde{m}|i(u-u') - \mathcal{L}|n\rangle = (2nD - iu')\delta_{mn} + \frac{i}{2}\delta_{mn+1} + i\,n\delta_{mn-1} \equiv B_{mn}(u') \tag{18.176}$$

where B is an infinite-dimensional, tri-diagonal matrix. Obviously

$$(u|0\rangle = p_o(u),\ \langle\tilde{0}|u) = 1 \tag{18.177}$$

Equation (18.44) yields then

$$\mathcal{I} = \frac{1}{\pi}Re\left[B^{-1}(u')\right]_{00}\ . \tag{18.178}$$

In order to evaluate $\left[B^{-1}(u')\right]_{00}$ we start from

$$\left(\begin{array}{ccc} 1 & 0 & \dots \end{array}\right) B^{-1}(u') \left(\begin{array}{c} 1 \\ 0 \\ \vdots \end{array}\right) = \left[B^{-1}(u')\right]_{00} \tag{18.179}$$

which can be written as

$$\left(\begin{array}{c} 1 \\ 0 \\ \vdots \end{array}\right) = B(u') \left(\begin{array}{c} y_0 \\ y_1 \\ \vdots \end{array}\right),\ y_0 = \left[B^{-1}(u')\right]_{00}\ . \tag{18.180}$$

The latter equation together with Eq. (18.176) can be written in matrix notation

$$\begin{pmatrix} -iu' & \frac{i}{2} & 0 & \dots & & & \\ i & 2D-iu' & \frac{i}{2} & 0 & \dots & & \\ 0 & 2i & 4D-iu' & \frac{i}{2} & 0 & \dots & \\ \vdots & \ddots & \ddots & \ddots & \ddots & \ddots & \dots \\ 0 & \dots & 0 & 2ni & 2nD-iu' & \frac{i}{2} & \dots \\ \vdots & \vdots & \dots & \ddots & \ddots & \ddots & \ddots \end{pmatrix} \begin{pmatrix} y_0 \\ y_1 \\ y_2 \\ \vdots \\ y_n \\ \vdots \end{pmatrix} = \begin{pmatrix} 1 \\ 0 \\ 0 \\ \vdots \\ 0 \\ \vdots \end{pmatrix} \tag{18.181}$$

For the numerical solution a finite dimension $N = 2000$ is assumed for the matrix B.
The ensuing problem has been discussed in [36], albeit for a real matrix B. The use of a finite-dimensional matrix B can only be justified for $u' \ll N$.

Bibliography

[1] M. Abramowitz and I.A. Stegun. *Handbook of Mathematical Functions*. Dover, New York, 1972.

[2] J. S. Bader, R. A. Kuharski, and D. Chandler. Role of nuclear tunneling in aqueous ferrous-ferric electron transfer. *J. Chem. Phys.*, 93:230–236, 1990.

[3] Daniel Barsky, Benno Pütz, Klaus Schulten, J. Schoeniger, E. W. Hsu, and S. Blackband. Diffusional edge enhancement observed by NMR in thin glass capillaries. *Chem. Phys. Lett.*, 200:88–96, 1992.

[4] H. Berendsen and J. Mavri. Quantum simulation of reaction dynamics by density matrix evolution. *J. Phys. Chem.*, 97:13464–13468, 1993.

[5] Robert Bittl and Klaus Schulten. Length dependence of the magnetic field modulated triplet yield of photogenerated biradicals. *Chem. Phys. Lett.*, 146:58–62, 1988.

[6] Robert Bittl and Klaus Schulten. A static ensemble approximation for stochastically modulated quantum systems. *J. Chem. Phys.*, 90:1794–1803, 1989.

[7] Mordechai Bixon and Joshua Jortner. Coupling of protein modes to electron transfer in bacterial photosynthesis. *J. Phys. Chem.*, 90:3795–3800, 1986.

[8] A. O. Cardeira and A. J. Leggett. Path integral approach to quantum brownian motion. *Physica A*, 121:587–616, 1983.

[9] A. O. Cardeira and A. J. Leggett. Quantum tunnelling in a dissipative system. *J. Ann. Phys.(N.Y.)*, 149:374–456, 1983.

[10] S. Chandrasekhar. *Rev. Mod. Phys.*, 15:1, 1943.

[11] D. DeVault. *Quantum-mechanical tunneling in biological systems*. Cambridge University press, Cambridge, UK, 1984.

[12] G. R. Fleming, J. L. Martin, and J. Breton. Rate of primary electron transfer in photosynthetic reaction centers and their mechanistic implications. *Nature*, 333:190–192, 1988.

[13] C. W. Gardiner. *Handbook of Stochastic Methods*. Springer, New York, 1983.

[14] Anupam Garg, José Nelson Onuchic, and Vinay Ambegaokar. Effect of friction on electron transfer in biomolecules. *J. Chem. Phys.*, 83:4491–4503, 1985.

[15] J. R. Gunn and K. A. Dawson. *J. Chem. Phys.*, 91:6393, 1989.

[16] A. L. Hodgkin and A. F. Huxley. *J. Physiol.*, 117:500–544, 1952.

[17] J. J. Hopfield. Electron transfer between biological molecules by thermally activated tunneling. *Proc. Natl. Acad. Sci. USA*, 71:3640–3644, 1974.

[18] J. Jortner. *J. Chem. Phys.*, 64:4860–4867, 1976.

[19] C. Kirmaier and D. Holten. Temperature effects on the ground state absorption spectra and electron transfer kinetics of bacterial reaction centers. In J. Breton and A. Vermeglio, editors, *The Photosynthetic Bacterial Reaction Center: Structure and Dynamics*, pages 219–228, New York and London, 1988. Plenum Press.

[20] D. E. Knuth. *Seminumerical Algorithms*, volume 2 of *The Art of Computer Programming*. Addison-Wesley, Reading, MA, 2nd edition, 1981. page 116.

[21] R. Kubo. *Adv. Chem. Phys.*, 15:101, 1969.

[22] Gene Lamm and Klaus Schulten. Extended Brownian dynamics: II. Reactive, nonlinear diffusion. *J. Chem. Phys.*, 78:2713–2734, 1983.

[23] A.J. Leggett, S. Chakravarty, A.T. Dorsey, M.P.A. Fisher, A. Garg, and W. Zwerger. Dynamics of the dissipative two-state system. *Rev. Mod. Phys.*, 59:2–86, 1987.

[24] J. Marcienkiewicz. *Math. Z.*, 44:612, 1939.

[25] R. A. Marcus. Electrostatic free energy and other properties of states having nonequilibrium polarization. II. *J. Chem. Phys.*, 24:979–989, 1956.

[26] R. A. Marcus. On the energy of oxidation-reduction reactions involving electron transfer. I. *J. Chem. Phys.*, 24:966–978, 1956.

[27] R. A. Marcus and N. Sutin. Electron transfers in chemistry and biology. *Biochim. Biophys. Acta*, 811:265–322, 1985.

[28] J. J. Markham. Interaction of normal modes with electron traps. *Rev. Mod. Phys.*, 31:956, 1959.

[29] J. L. Martin, J. Breton, J. C. Lambry, and G. Fleming. The primary electron transfer in photosynthetic purple bacteria: Long range electron transfer in the femtosecond domain at low temperature. In J. Breton and A. Vermeglio, editors, *The Photosynthetic Bacterial Reaction Center: Structure and Dynamics*, pages 195–203, New York and London, 1988. Plenum Press.

[30] R. E. Mortensen. Mathematical problems of modeling stochastic nonlinear dynamic systems. *J. Stat. Phys*, 1:271, 1969.

[31] Walter Nadler and Klaus Schulten. Generalized moment expansion for Brownian relaxation processes. *J. Chem. Phys.*, 82:151–160, 1985.

[32] V. Nagarajan, W. W. Parson, D. Gaul, and C. Schenck. Effect of specific mutations of tyrosine-(m)210 on the primary photosynthetic electron-transfer process in rhodobacter sphaeroides. *Proc. Natl. Acad. Sci. USA*, 87:7888–7892, 1990.

[33] Nira Richter-Dyn Narendra S. Goel. *Stochastic Models in Biology.* Academic Press, New York, 1974.

[34] Marco Nonella and Klaus Schulten. Molecular dynamics simulation of electron transfer in proteins: Theory and application to $Q_A \rightarrow Q_B$ transfer in the photosynthetic reaction center. *J. Phys. Chem.*, 95:2059–2067, 1991.

[35] José Nelson Onuchic, David N. Beratan, and J. J. Hopfield. Some aspects of electron-transfer reaction dynamics. *J. Phys. Chem.*, 90:3707–3721, 1986.

[36] W.H. Press, B.P. Flannery, S.A. Teukolsky, and W.T. Vetterling. *Numerical Recipes in C.* Cambridge University Press, Melbourne, 1988.

[37] William H. Press, Saul A. Teukolsky, William T. Vetterling, and Brian P. Flannery. *Numerical Recipes in C.* Cambridge University Press, New York, 2 edition, 1992.

[38] Benno Pütz, Daniel Barsky, and Klaus Schulten. Edge enhancement by diffusion: Microscopic magnetic resonance imaging of an ultra-thin glass capillary. *Chem. Phys. Lett.*, 183(5):391–396, 1991.

[39] Benno Pütz, Daniel Barsky, and Klaus Schulten. Edge enhancement by diffusion in microscopic magnetic resonance imaging. *J. Magn. Reson.*, 97:27–53, 1992.

[40] Lord Rayleigh. *The Theory of Sound, Vol. I, 2nd ed.* MacMillan and Company Ltd., London, 1894.

[41] Lord Rayleigh. *Scientific Papers, Vol. I, p491 and Vol. IV, p370.* Cambridge University Press, Cambridge, England, 1899–1920.

[42] Ilya Rips and Joshua Jortner. Dynamic solvent effects on outer-sphere electron transfer. *J. Chem. Phys.*, 87:2090–2104, 1987.

[43] Oren Patashnik Ronald L. Graham, Donald E. Knuth. *Concrete Mathematics.* Addison-Wesley, Reading, Massachusetts, USA, 1988.

[44] K. W. Miller S. K. Park. *Communications of the ACM*, 31:1191–1201, 1988.

[45] Klaus Schulten and Robert Bittl. Probing the dynamics of a polymer with paramagnetic end groups by magnetic fields. *J. Chem. Phys.*, 84:5155–5161, 1986.

[46] Klaus Schulten and Markus Tesch. Coupling of protein motion to electron transfer: Molecular dynamics and stochastic quantum mechanics study of photosynthetic reaction centers. *Chem. Phys.*, 158:421–446, 1991.

[47] M. V. Smoluchowski. *Phys. Z.*, 17:557–585, 1916.

[48] A. Sommerfeld. *Partial Differential Equations in Physics.* Academic Press, New York, 10 edition, 1964.

[49] H. Sumi and R. A. Marcus. Dynamical effects in electron transfer reactions. *J. Chem. Phys.*, 84:4894–4914, 1986.

[50] V. K. Thankappan. *Quantum Mechanics.* John Wiley & Sons, New York, 1985.

[51] Herbert Treutlein and Klaus Schulten. Noise-induced neural impulses. *Eur. Biophys. J.*, 13:355–365, 1986.

[52] Herbert Treutlein, Klaus Schulten, Axel Brünger, Martin Karplus, J. Deisenhofer, and H. Michel. Chromophore-protein interactions and the function of the photosynthetic reaction center: A molecular dynamics study. *Proc. Natl. Acad. Sci. USA*, 89:75–79, 1992.

[53] Herbert Treutlein, Klaus Schulten, J. Deisenhofer, H. Michel, Axel Brünger, and Martin Karplus. Molecular dynamics simulation of the primary processes in the photosynthetic reaction center of *Rhodopseudomonas viridis*. In J. Breton and A. Verméglio, editors, *The Photosynthetic Bacterial Reaction Center: Structure and Dynamics*, volume 149 of *NATO ASI Series A: Life Sciences*, pages 139–150. Plenum, New York, 1988.

[54] Herbert Treutlein, Klaus Schulten, Christoph Niedermeier, J. Deisenhofer, H. Michel, and D. Devault. Electrostatic control of electron transfer in the photosynthetic reaction center of *Rhodopseudomonas viridis*. In J. Breton and A. Verméglio, editors, *The Photosynthetic Bacterial Reaction Center: Structure and Dynamics*, volume 149 of *NATO ASI Series A: Life Sciences*, pages 369–377. Plenum, New York, 1988.

[55] G.E. Uhlenbeck and L.S. Ohrnstein. *Phys. Rev.*, 36:823, 1930. These papers are reprinted in Selected Papers on Noise and Stochastic Processes, ed. by N. Wax (Dover,New York 1954).

[56] A. Warshel, Z. T. Chu, and W. W. Parson. Dispersed polaron simulations of electron transfer in photosynthetic reaction center. *Science*, 246:112–116, 1989.

[57] Arieh Warshel and Jenn-Kang Hwang. Simulations of the dynamics of electron transfer reactions in polar solvent: Semiclassical trajectories and dispersed polaron approaches. *J. Chem. Phys.*, 84:4938–4957, 1986.

[58] Stephen Wolfram. *Mathematica, A System for Doing Mathematics by Computer*. Addison-Wesley, New York, 2 edition, 1991.

[59] Peter G. Wolynes. Dissipation, tunneling and adiabaticity criteria for curve crossing problems in the condenced phase. *J. Chem. Phys.*, 86:1957–1966, 1987.

[60] Dong Xu and Klaus Schulten. Multi-mode coupling of protein motion to electron transfer in the photosynthetic reaction center: Spin-boson theory based on a classical molecular dynamics simulation. In J. Breton and A. Vermeglio, editors, *The Photosynthetic Bacterial Reaction Center: II. Structure, Spectroscopy and Dynamics*, NATO ASI Series A: Life Sciences, pages 301–312. Plenum Press, New York, 1992.

[61] Dong Xu and Klaus Schulten. Coupling of protein motion to electron transfer in a photosynthetic reaction center: Investigating the low temperature behaviour in the framework of the spin-boson model. *Chem. Phys.*, 182:91–117, 1994.

[62] Chong Zheng, J. Andrew McCammon, and Peter G. Wolynes. Quantum simulation of nuclear rearrangement in electron transfer reactions. *Proc. Natl. Acad. Sci. USA*, 86:6441–6444, 1989.